UNIVERSITY OF SAO PAULO - USP
POLYTECHNICAL SCHOOL - POLI
DEPARTMENT OF METALLURGICAL AND MATERIALS ENGINEERING

RONALDO ADRIANO ALVARENGA BORGES

Modeling the refractory wear rate of the LD Converter using statistical techniques and self-organizing maps (SOM)

São Paulo
2023

RONALDO ADRIANO ALVARENGA BORGES

Modeling the refractory wear rate of the LD Converter using statistical techniques and self-organizing maps (SOM)

Corrected Version

Thesis presented to the Polytechnic School of the University of São Paulo to obtain the title of Doctor of Science.

Area of concentration: Metallurgical and Materials Engineering.

Advisor: Prof. Dr. Guilherme Frederico Bernardo Lenz e Silva

São Paulo

2023

Cataloging in publication
Library
Polytechnic School of USP

Este exemplar foi revisado e corrigido em relação à versão original, sob responsabilidade única do autor e com a anuência de seu orientador.

São Paulo, **04** de **Dezembro** de **2023**

Assinatura do autor: Ronaldo Adriano Alvarenga Borges

Assinatura do orientador: Guilherme Luz

Catalogação-na-publicação

Borges, Ronaldo Adriano Alvarenga
Modeling the refractory wear rate of the LD Converter using statistical techniques and self-organizing maps (SOM) / R. A. A. Borges -- versão corr. -- São Paulo, 2023.
197 p.

Tese (Doutorado) - Escola Politécnica da Universidade de São Paulo. Departamento de Engenharia Metalúrgica e de Materiais.

1.Refractories 2.LD Converter 3.Refractory Wear 4.Process Variables 5.Self Organizing Maps (SOM) I.Universidade de São Paulo. Escola Politécnica. Departamento de Engenharia Metalúrgica e de Materiais II.t.

Name: BORGES, Ronaldo Adriano Alvarenga

Title: Modeling the refractory wear rate of the LD Converter using statistical techniques and self-organizing maps (SOM)

Thesis presented to the Polytechnic School of the University of São Paulo to obtain the title of Doctor of Science.

Approved in: October 6, 2023.

Examination Board

Prof. Dr.:	Guilherme Frederico Bernardo Lenz e Silva
Institution:	EP - USP
Judgment:	Approved
Signature:	

Prof. Dr.	Antonio Malynowskyj
Institution:	Metallurgy Consultant
Judgment:	Approved
Signature:	

Prof. Dr.	Flavio Beneduce Neto
Institution:	EP - USP
Judgment:	Approved
Signature:	

Prof. Dr.	Alan Fernando Ney Boss
Institution:	PosDoc - EP
Judgment:	Approved
Signature:	

Prof. Dr.	Antonio Manuel Andre Quadros da Cunha Feteira
Institution:	(Sheffield Hallam University – SHU)
Judgment:	Approved
Signature:	

ACKNOWLEDGMENT

I would like to thank the advisor of this work, Prof. Dr. Guilherme Frederico Bernardo Lenz e Silva, for the great attention given during this trajectory.

To the professors who participated in the examining board of this thesis: Antonio Malynowskyj (Metallurgy Consultant), Flavio Beneduce Neto (EP - USP), Alan Fernando Ney Boss (PosDoc - EP), Antonio Manuel Andre Quadros da Cunha Feteira (Sheffield Hallam University - SHU).

To my wife Marcia, with love, admiration and gratitude for her understanding, affection, presence and tireless support throughout the period of preparation of this work.

To friends and workmates Natalia Piedemonte, Luccas Krotz and Danyela Cardoso for their support and great help in building the databases, analyzes and writing the Thesis.

The Polytechnic School of the University of São Paulo, for the opportunity to study a Doctorate in this respected institution.

The company USIMINAS, for allowing and encouraging this academic journey.

To Managers Silvio Henrique Chagas and Cleber Guimarães dos Santos for their support and patience during the course.

To my family and to God for always being present in my thoughts.

ABSTRACT

BORGES, R. A. A. **Modeling the refractory wear rate of the LD Converter using statistical techniques and self-organizing maps (SOM).** 2023. Thesis (Doctorate in Metallurgical and Materials Engineering – Polytechnic School of USP, University of São Paulo, São Paulo, 2023).

The increased of demand for more elaborate steels, in terms of chemical composition and internally defects free, makes the primary refining conditions of steelmaking plants severe. At the same time, the rise of time in steel manufacturing process, together with other operational variables such as quantities and types of chemical additions, bath and slag oxidation levels, dephosphorus rate, end blow temperatures, among others, make the conditions to which the refractories linings of steel production furnaces (LD Converters) are subjected to more aggressive conditions with a consequent reduction in the performance (life) and availability of equipment for producyion. Therefore, this thesis sought to build models to predict the wear rate of refractories in these furnaces as a function of process variables with the objective of greater operational control and safety. Statistical data analysis tecniques were used (time series, univariated and multivariate correlation) and Self Organization Maps (SOM) that never were used in LD Converters and with results were found similar in the two techniques. The modeling was carried out under the most critical regions of the furnaces (trunnions), in order to establish a deterministic equation for predicting the wear refractories rate of such regions and, consequently, of the furnaces. The modeling took into account data from 3 campaigns (over 12,000 heats) of one of the steelmaking LD converters of an integrated plant with a capacity of 4.5 Mt/year. The analysis showed that the main variables that impact the wear rate of the LD trunnion bricks are the MgO and CaO content of the slag, the percentages of scrap and reblowing, the binary basicity of the slag, the oxidation levels, the rate of dephosphorization and nepheline used, the temperature and the carbon at the end of the blow. The comparative analysis of data, by classical statistics and SOM, validated the possibility of using this new data analysis tool in process analysis in steelmaking plants and in the adjustment of equations for deterministic models.

Keywords: Refractories. LD Converter. Wear. Variables. SOM.

RESUMO

BORGES, R. A. A. **Modelamento da taxa de desgaste do refratário do Convertedor LD utilizando técnicas estatísticas e mapas auto-organizáveis (SOM).** 2023. Tese (Doutorado em Engenharia Metalúrgica e de Materiais – Escola Politécnica da USP, Universidade de São Paulo, São Paulo, 2023).

O aumento da demanda por aços mais elaborados em termos de composição química e limpidez interna torna as condições de refino primário das aciarias das siderúrgicas cada vez mais severas. Em paralelo, o aumento dos tempos de processo de fabricação do aço aliado às outras variáveis operacionais como quantidades e tipos de adições químicas, níveis de oxidação do banho e da escória, taxa de desfosforação, temperaturas de final de sopro, dentre outras, fazem com que as condições às quais os revestimentos refratários dos fornos de produção dos aços (convertedores LD) sejam cada vez mais agressivas com conseqüente redução do desempenho (vida) e de disponibilidade do equipamento para a produção. Logo, essa tese objetivou a construção de modelos de previsão da taxa de desgaste dos refratários destes fornos em função das variáveis de processo visando maior controle operacional e de segurança. Foram utilizadas técnicas estatísticas de análise de dados (séries temporais, correlação uni e multivariadas) e mapas auto-organizáveis SOM (*Self Organization Maps*), até então nunca utilizado em LD's e com resultados encontrados que foram similares aos estatísticos. A modelagem foi realizada sob as regiões mais críticas dos fornos (região dos munhões) de modo a estabelecer modelos de previsão da taxa de desgaste refratário e consequentemente dos fornos. O modelamento levou em consideração os dados de 3 campanhas (mais de 12.000 corridas) de um dos convertedores LD da Aciaria de uma usina integrada com capacidade de 4,5 Mt/ano. As análises mostraram que as variáveis que impactam a taxa de desgaste dos tijolos dos munhões do LD são os teores de MgO e CaO da escória, os percentuais de sucata enfornada e de ressopro, a basicidade binária da escória, os níveis de oxidação do banho metálico e da escória, a taxa de desfosforação e nefelina utilizada, a temperatura e o carbono de final de sopro. A análise comparativa dos dados via estatística clássica e SOM validou a possibilidade de utilização desta nova ferramenta em análise de processo em Aciarias e no ajuste de equações de modelos determinísticos.

Palavras Chaves: Refratários. Convertedor LD. Desgaste. Variáveis. SOM.

LIST OF FIGURES

LIST OF TABLES

LIST OF ABBREVIATIONS AND ACRONYMS

ABM	Brazilian Association of Metallurgy and Materials
ABNT	Brazilian Association of Technical Standards
BMU	Best Matching Unit
BOF	Basic Oxigen Furnace
CAC’s	Castables based on Calcium Aluminates
JIS	Japanese Industrial Standard
LD	Linz Donawitz Converter or Basic Oxygen Furnace
NBR	Regulatory Brazilian Standard
TAR	Technical Association of Refractories
SOM	Self Organization Maps

SUMMARY

1 INTRODUCTION

Traditionally, a subclass of ceramic materials known as refractory materials stands out for its intensive use in the steel industry worldwide. It is in the steelmaking shops, where steel is manufactured, that the various equipment for manufacturing, refining and transporting these steels are required under the most severe working condictions and the refractories are responsible for their internal relinings, making them structurally ready for the most diverse requests (EUROPEAN REFRACTORIES PRODUCERS' FEDERATION, 2009; LENZ e SILVA, 2007).

What makes refractories the most suitable material for the diverse and severe thermal, chemical and physical conditions that exist in these production facilities are the properties that these compounds present, such as a high melting temperature, high structural resistance at high temperatures and in a corrosive environment, stability in the face of intensive thermal variations, high resistance to mechanical shocks, among others.

A good refractory project with adequate properties to the requests imposed by the processes is essential for a good refractory life performance. However, a good refractory project is of no use without proper control of the process variables that impact the life of the refractory lining.

Therefore, the determination of deterministic models capable of predicting the wear rates of refractory structures are fundamental for the control and life performance.

In this context, this thesis aim to find a model that establishes the relationship between the refractory wear rate of critical regions of Usiminas steelmaking LD furnace and the various variables of the process using classic statistical techniques and new data analysis techniques such as self-organizing maps.

1.1 Justification

Oxygen steelmaking shops have LD converters (Linz Donawitz - LD) as their main reactor in the steel manufacturing process. The LD is a reactor (furnace) consisting basically of a metal shell lined internally with refractory bricks based on magnesia-carbon (MgO-C).

One of the factors with the greatest impact on the operational availability of the LD converter is the refractory wear during steel production operations. Not necessarily the cost of the refractory lining having the greatest impact on production costs, but the reduction of availability of this equipment during stops for projection of repair mass in the points of wear of the refractory bricks together with the stops for total change of the linned during the refractory campaigns. Not less important is the operational safety factor, which significantly depends on the capacity that the refractories are capable of withstanding, without losing their structural resistance, to the various conditions involved in the process. If the safety factor not well implemented, it can cause irreparable accidents in relation to human life.

It is worth remembering that in order to meet the increased demands in terms of steel quality, the processes and practices in the steelmaking shops have been continuously changing to meet it, implying dynamic process variables and complex wear mechanisms of refractories, which justifies a continued research and development effort in this area.

In the case of converters, the regions known as trunnions and the transition regions of the lower cone stand out as those that determine the life of the refractory lining, as they are the regions that are subjected to the most severe conditions of the process. Thus, it is necessary to determine predictive models of the wear rate of such regions in order to find which are the process variables that must be controlled to guarantee a good refractory performance of the converter. Therefore it must take into account the fact of the dynamic and joint action of the process variables, as it is this factor that will determine the prediction efficiency of the models in the face of real process situations.

This tese aim to understand which operational variables impact the life (wear rate) of the refractory of the converters of the steelmaking shop of a traditional steel plant in Brazil using traditional analysis tools such as statistics (univariate and multivariate) and tests of post-mortem of bricks at the end of the campaign, as well as the use and development of non-traditional and unfamiliar tools in this sector such as Self Organization Maps (SOM).

Subsequently, a deterministic model was be developed correlating these variables with the reafractory wear rate of these reactors in order to carry out a better performance and safety management in the use of this type of reactor.

1.2 Objectives

Build and evaluate static deterministic models by conventional statistics and using a new data analysis tool (SOM) in steelmaking processes in order to correlate the main operational variables such as the type of steel, the process temperature, the basicity, the type of slag, among others, with the wear rate (life) of the refractorie bricks lining the steel production furnaces (converters) of a LD steelmaking shop throughout its campaign. In this way, we will aim to determine a predictive model of the wear rate of the region (trunnions) that determines the life of the LD converters as a function of the process variables and, consequently, the optimization of the performance (life), the safety (final residual) of these metallurgical reactors and the implementation of a new data analysis tool in the production processes of Brazilian steelmaking shops.

1.3 Structure of the research work

This thesis was structured in six chapters, including an introductory one in which the contextualization, delimitation and definition of the objectives of the work are made. In Chapter 2, the “Bibliographic Review” is presented, to understand the main types and mechanisms of refractories wear in steelmaking furnaces and analysis methods: traditional statistics and new ones such as the SOM analysis tool. In Chapter 3, “Materials and Methods”, the procedures adopted in the construction and analysis of the database of process variables is reported, applying classical statistics and the SOM tool. In Chapter 4, “Results and Discussions”, the results of the operational data analysis are presented and the discussion about the construction of deterministic models and the refractory wear mechanism acting in the furnace through post-mortem tests on end-of-life refractory bricks is presented. In final campaign. In Chapter 5, “Conclusions”, a conclusive summary of this work is presented. In Chapter 6, “Suggestions for Future Work”, relevant themes are suggested for continuity and deepening in relevant topics of this thesis.

2 LITERATURE REVIEW

2.1 Initial considerations

The degree of development of a country can be measured indirectly by the production and consumption of steel, since it is one of the main raw materials used in the construction of buildings, manufacture of cars, machines, oil platforms, domestic utensils, among others. Considering all the existing materials on the planet, steel is the one that has the most diverse applications. Poor is a society that does not produce steel, because any form of economic development will first go through the stages of development and consolidation of a steel industry (ARAUJO, 2009; CHIAVERINI, 2005; SARKAR, 2016). However, to be produced steel with high productivity and safety, it is necessary to use refractories materials. According to Quintela (2003, p. 5)

> The steel industry is the main consumer of refractory materials, corresponding to around 70% of the world market. This represents a significant costs and has been a concern for this sector since the beginning of its activities. In addition, frequent stoppages for refractory maintenance, especially unscheduled ones, interrupt operational activities, contributing indirectly to raising steel production costs.

The dependence on the manufacture of vital materials for modern society such as steel, cement, copper and glass is linked to the extreme conditions to which the production reactors of these materials are subjected in the various production processes.

Therefore, the internal relining of these reactors with some type of refractory material with desirable properties of high resistance becomes indispensable and vital to withstand the extreme conditions of temperatures, pressures and chemical reactions operating in these systems and which would limit the performance and bring instability to the various industrial systems (EUROPEAN REFRACTORIES PRODUCERS' FEDERATION, 2009; RAAD, 2008; SARKAR, 2016).

The Technical Association of Refractory Japan (TARJ), which is traditional and globally recognized in the area of ceramic refractory materials, provides a very comprehensive definition of what such materials are (TECHINICAL ASSOCIATION REFRACTORIES JAPAN, 1998, p.1).

> Refractories are non-metallic materials that are difficult to melt at high temperatures, such as formed materials that withstand high temperatures (>1500°C), non-formed materials (generally refractory masses) and injection masses whose working temperatures are around 800°C.

In the context of the steel industry, the processes and practices of production and primary refining of steel in the steelmaking shops that have LD converters as the main reactor for the production of steel have been undergoing evolutions over time, in parallel, the compositions of the refractory bricks that relining these furnaces are becoming more and more sophisticated in order to cope with these developments. Refractory producers have been making important changes in the refractory composition of bricks such as the addition of new metallic antioxidants and boron-containing compounds, the introduction of special graphites and other forms of carbon, increasing the amount of electrofused MgO with high grain size, along with improvements in the technologies and ways of processing these materials.

The LD converter is the main metallurgical reactor for steel production in steelmaking shops. This equipment basically consists of a metallic shell internally relining with refractory ceramic bricks whose main function is to withstand the various thermal, chemical and physical stresses resulting from the metallurgical processes necessary for the production of steel.

Due to the quantity and complexity of the different chemical reactions that occur inside the converters during steel manufacturing and considering that each region of the reactor LD is exposed to different phenomena and refractory wear mechanisms, it becomes increasingly complex to define which process variables and which furnace regions determine performance (life). This complexity comes from the fact that these variables act together in industrial processes, and laboratory tests cannot reproduce all these events at the same time.

According to the company internal report the trunnion region is the most critical in terms of LD refractory performance, given the absence of the protective slag layer formed during the repair and slag protection processes.

Additionally, it is believed that the accelerated wear of the bricks in this region of the refractory lining may impact the performance of the refractories in the surrounding regions, thus limiting the life of the refractory lining for converters.

The other regions of the converters are also subject to different wear mechanisms and phenomena, such as, the scrap and pig iron impact region subject to mechanical degradation due to the impact of charge scrap with different characteristics. Mention is also made of the steel tap region in which long tap times expose the refractories in that region to aggressive erosive processes and chemical corrosion. Similarly, the junction regions are subject to erosion and chemical

corrosion phenomena due to the presence of slags with high levels of oxidation. In the bottom region, in several cases, such as converters that have combined blowing, *back attack* phenomena and others can lead to the end of the campaign for these reactors.

LD refractories bricks, whose basic chemical constitution is the carbon magnesia compound (MgO-C), have been widely used for decades in steelmaking shops as a lining for converters LD. According to Takeda *et al*. (2001), its use is due to the high resistance to corrosion by slag formed during the steel manufacturing processes and the high resistance to thermal shock, both granted, in part, by the chemical element carbon of the matrix.

However, the presence of carbon in the refractory brick can, in some situations, lead to disadvantages such as the reduction in mechanical strength due to carbon oxidation of the brick. As a countermeasure to attenuate these effects, some powder metals and special additives such as Silicon (Si), Aluminum (Al), Magnesium (Mg), some types of metallic alloys, compounds containing boron which they act to increase the mechanical strength, resistance to erosion and resistance to oxidation, although they may contribute to the formation of cracks due to thermomechanical stresses, due to the lower flexibility of the refractory resulting from these additives (QUINTELA *et al*., 2005).

In addition to the compounds listed above, the binding system of the refractory matrix of the MgO-C system is generally formed by the use of artificial resins and/or products bound to pitch. In the first case, there is a refractory structure with weaker bonds due to the isotropy of the formed phases. In the second case, a stronger connection of the structure is observed. As a third option, the combination of artificial resins with pitch-bound products may result in greater flexibility of refractory bricks due to the crystalline carbon characteristics and formation of anisotropic phases (KANNO *et al*., 1999).

Efforts for an adequate formulation of refractory systems for converters LD involve not only static considerations, but dynamic factors related to the various changes in the microstructure during its use.

All of this reveals the high level of complexity of refractory design formulations and the need for process controls both in refractory manufacturing and in the operation use of bricks. The use of different statistical techniques for analyzing

process data and *post-mortem* studying characterization is vital for the knowledge and determination of control models and determination of the refractory wear rate.

Traditional statistical techniques have been used for a long time, however, due to the number of variables operating in real process systems, it is difficult to obtain forecast results with a high degree of reliability, in addition to the exhaustive work in jointly determining which variables are or are not relevant to the system. The application of new data analysis tools, such as SOM, brings greater flexibility and speed in dealing with large amounts of process variables that act together in complex systems such as those that take place in the LD reactors of steelmaking shops.

2.2 LD converter

The 1950s represent a milestone for the world steel industry, especially for LD steelmaking shops. It was at the beginning of that decade that the first plant, in Linz, Austria, began steelmaking operations in LD converters using oxygen as a source for converting liquid pig iron into steel. According to Maia (2007, p.4)

> In 1949, Voest Linz and Alpine Donawitz attempted to oxidize hot metal by blowing with pure oxygen. For this series of tests, pig iron was transfer in ladles were first used as test vessels. The first steel factory via BOF (Basic Oxigen Furnace) went into operation in the city of Linz in the autumn of 1952, and in Donawitz in the spring of 1953, hence the use of the acronym “LD” in reference to the cities located in Austria, where the process was originally developed.

From that moment on, according to Barão *et al.* (2011), what was seen was steelmaking shops around the world using high-purity oxygen blowing in LD converter reactors as the main way of converting raw materials (liquid pig iron, scrap, fluxes and scorifiers) into steel liquid.

In Brazil, the process was quickly disseminated through Belgo-Mineira steel company at the João Monlevade city in 1957, followed by Usiminas in 1962 (Ipatinga city) and Mannesmann steel company in Belo Horizonte in 1963 followed by Cosipa (São Paulo) in 1965. The Barão de Cocais steel company shop began adopting the LD process in 1979 by a company that is part of the Siderbrás Group. Currently, practically all the large integrated steelmaking shops use this type of steel manufacturing process in their operation plants (Figure 1).

Figura 1 – Converter LD (Basic Oxygen) and the percentage distribution of the different types of steelmaking processes employed around the world

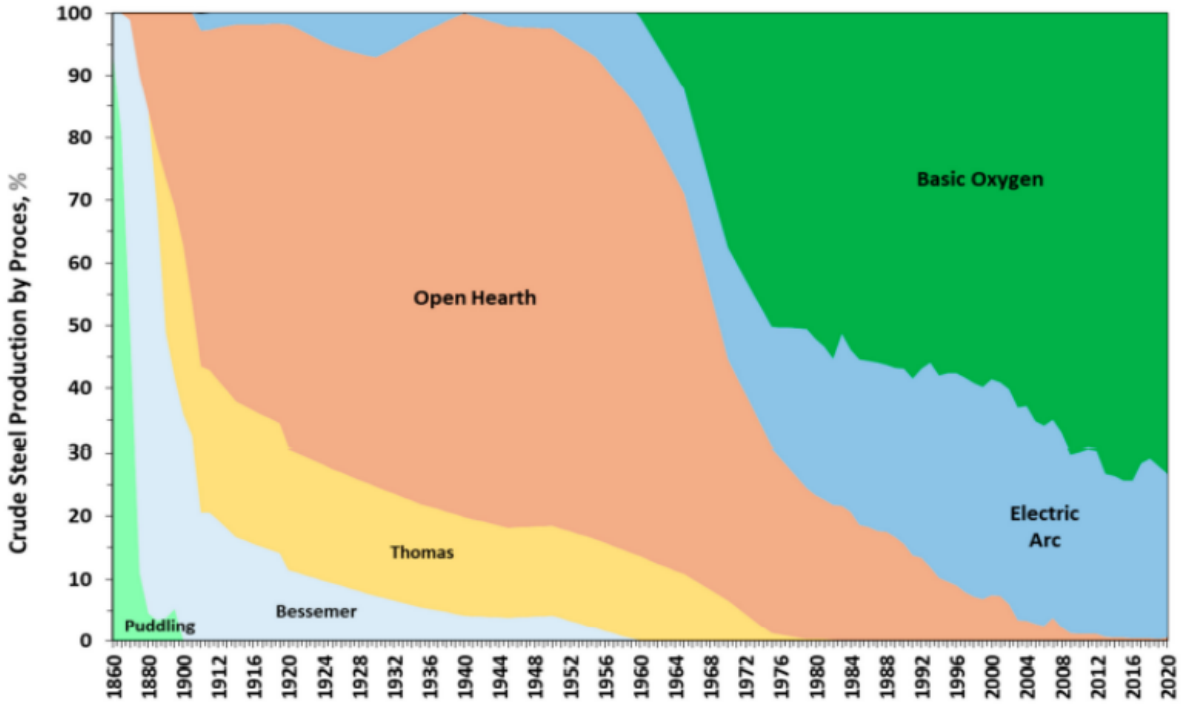

(A)

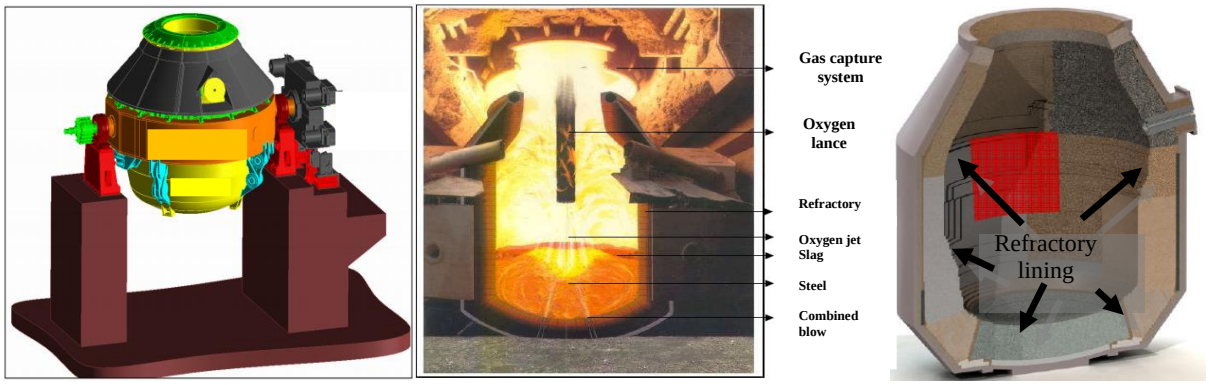

(B) (C) (D)

Source: Reference A (MALYNOWSKYJ, 2022), B (CHAVES, 2006), C (GONÇALVEZ, 2005) and D (JANSEN, 2003).

According to Chaves (2006), around 80% of steel production in Brazil is by LD converter, the other 20% being produced by electric arc furnace (EAF). This is mainly due to the characteristics of the LD process being high productivity, more adequate costs and great metallurgical flexibility. The main difference between LD and EAF is basically in the energy sources and in the composition of the metallic and non-metallic charge. These two processes, even when compared to the old steel production furnaces (Siemens-Martin), have several advantages such as, lower

investment and operating costs, improved steel quality, greater reproducibility of results and lower production costs (BARÃO et al., 2011).

For Maia (2007, p.5)

> The quickly sequence of refining operations in high-capacity steelmaking shop and the simultaneous operation of converters gives LD steel plants high productivity. On the other hand, with the application of appropriate blowing practices, almost all refining reactions can be obtained, giving the process great metallurgical versatility.

Considerable developments have been made over the years, both in the capacity of the LD furnaces, which reach 400 tons, as well as in the shape and devices for support and tilting, in the shape and number of nozzles for blowing oxygen, in the refractories quality and other process variables (MUNDIM, 1991).

2.2.1 The LD reactor

The LD converter is a reactor in which, using a supersonic oxygen blowing lance, raw materials such as liquid pig iron, scrap metal, fluxes and scorifiers are transformed into steel, slag and gases. This furnace is basically made up of a metal shell lining internally with MgO-C refractorie bricks (Figure 1).

Due to the various physical chemical reactions that occur inside the LD furnace and turbulence generated by the movement of fluids at high temperatures, there must be a structure that supports all these requests. This structure is formed by materials of ceramic origin. Basically, they are oxides and elements such as carbon, aluminum, silicon, magnesium, among others. The main characteristic of these ceramic materials known as refractories is their ability to withstand, without losing their properties, high temperatures in highly corrosive environments with intense fluid movement. According to Routschka (2004, p.1) “refractories are non-metallic ceramic materials”, for Lenz and Silva (2007) refractory compounds are basically oxides or mixtures of oxides with a high melting point and physical chemical stability, and may present other constituents such as carbon, carbides, nitrides and borides.

2.2.2 Stages of steelmaking processes in the LD converter and refractories wear phenomena

The manufacture of steel in LD furnaces begins with the charge of solid metallic (metallic scrap) through channels or scrap chutes. Subsequently, the liquid

pig iron is charge by the pelican ladle. After charging, the metallic bath (pig iron and scrap metal) is subjected to a high-flow oxygen blow with a water-cooled lance. During blowing, other raw materials are added (fluxes, scorifiers and coolants) which have the function of forming a slag in which impurities from pig iron and scrap (P, Si, others) will be retained in the form of oxides. These oxides are formed by the oxidation of the chemical elements in metallic bath with parallel formation of $CO_{(g)}$ and $CO_{2(g)}$ gases resulting from the oxidation process of the carbon in the pig iron. These gases will be captured by the LD suction system carrying particulates in general.

The entirety of this process is considered to be exothermic. The energy released has the purpose of completely melting the metallic charge and promoting the diverse chemical reactions and phase changes of the system. The goal is to obtain a liquid steel with adequate temperature and chemical composition for subsequent refining stages. According to Cho (1982), compliance with the metallurgical specifications of steel is obtained by calculating the proportions of the raw materials to be fired as a function of chemical analyzes and by controlling the height of the oxygen blow lance.

In relation to the initial phase of charging, the first phenomena of refractories wear are observed. The process begins with charging the LD furnace with the solid scrap using the so-called scrap channels by tilting the reactor at an angle of approximately 45° in relation to the vertical. The gutter basically consists of a bucket open at the top and at one end, allowing the scrap to slide when the bucket is tilted. This event is characterized as the first phenomenon of refractory wear, in which the impact of these scraps on the refractory surface within the LD can cause breakage of the refractory structure.

Subsequently, liquid pig iron is charged (by pig iron ladle) into the reactor over the scrap. In this case, when the pig iron comes into contact with the refractory surface, it causes an erosive/abrasive effect that, over time, can lead to tearing and wear of bricks or part of them on the refractory surface (Figure 2).

Figure 2 – Schematic representation of the scrap charging (A) and pig iron (B) in the converters LD

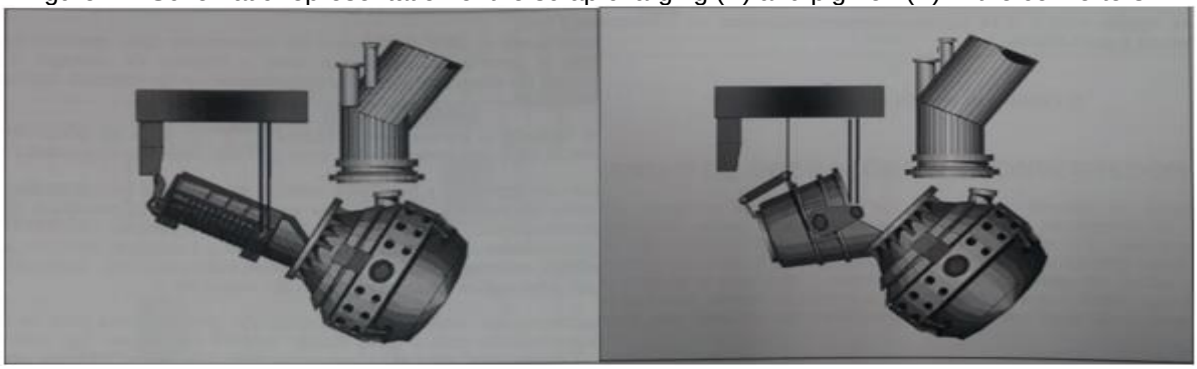

(A) (B)

Source: Borges (2016).

These effects can be minimized by placing the lighter scrap at the front of the channel so that, when charging the scrap into the furnace, the lighter scrap forms a protective mattress inside the furnace. Likewise, the advance addition of scorifiers before charging the scrap forms a protection (lining) in the scrap impact region of refractories, minimizing refractory wear in this region. Variations in charging angles throughout the operation shifts are fundamental for controlling refractories wear in this region.

The next step after charging the raw materials, with the LD in a vertical position, consists of lowering and blowing with oxygen using a lance (Figure 3). This lance is water-cooled, with supersonic oxygen output nozzles at its end. This entire process of blowing and converting the metallic charge into steel and slag is carried out according to a pattern, in which different lance heights in relation to the metallic bath are carried out in such a way that oxidation of the metallic bath occurs. This height pattern is determined by the different stages of the blowing process (MAIA, 2007).

Figure 3 – Schematic representation of the oxygen blowing in the LD during the formation of the gas-metal-slag emulsion

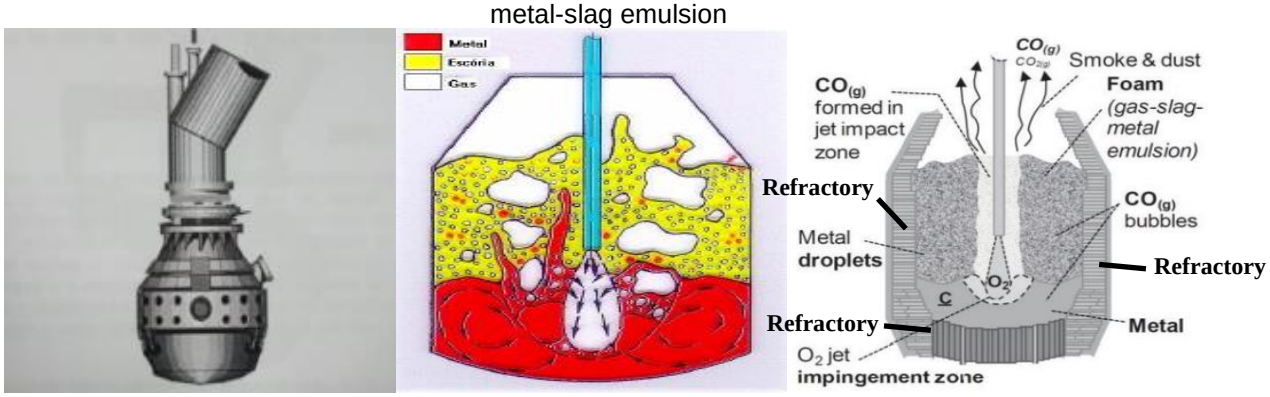

(A) (B) (C)

Source: Reference A (BORGES, 2016), B (MALYNOWSKYJ, 2004) and C (MALYNOWSKYJ, 2022).

The oxygen blowing process, which corresponds to the manufacture of steel itself, takes place according to 4 distinct stages; Ignition, slag formation, decarburization and oxidation. For each stage described above, different phenomena and wear mechanisms occur in the structure of the refractorie bricks of the LD, and these phenomena occur most of the time in a dynamic and joint manner, which makes the definition of which mechanisms and phenomena are preponderant in the wear of the refractory. In these cases, a set of control measures is adopted to minimize impacts on the furnace refractory.

The beginning of the process consists of lowering the oxygen lance to a height that allows the ignition of the metalic bath, that is, the oxidation of some element of the bath by the blown oxygen occurs (MAIA, 2007). Next, the slag formation stage begins, which lasts approximately 6 minutes. In this step, the basicity of the slag and the saturation of MgO must be controlled, since the main compound formed is SiO_2, which has an acidic characteristic and can react with the basic MgO structure of the refractory bricks. This control is done through the addition of CaO and MgO sources so that slag binary basicities vary between 3 to 4.5 and MgO saturations between 8 to 13%.

This step, also known as the first period of decarburization, is characterized by almost complete oxidation of silicon and a marked oxidation of manganese. In parallel, while the speed of decarburization increases, the contents of Si and Mn decrease in the metal bath. Knowledge of the characteristics of the slag, the refractory and the interaction between them is of fundamental importance, since the dissolution of MgO in the bricks by slag can lead to high refractories wear rate.

The evolution of the chemical composition of the metallic bath and the slag formed during the blowing process is illustrated in figure 4 according to the variation of the decarburization reaction speed.

At this point, it is worth remembering the importance of Slag Splashing and Slag Coating techniques, which, if well applied, can keep the refractory bricks covered with the slag from the previous heat, forming a physical barrier against the attack of the slag from the current heat. These techniques will be discussed in detail later in this thesis.

Figure 4 – Schematic representation of chemical composition evolution of the metalic bath and slag during oxygen blowing in the LD converter

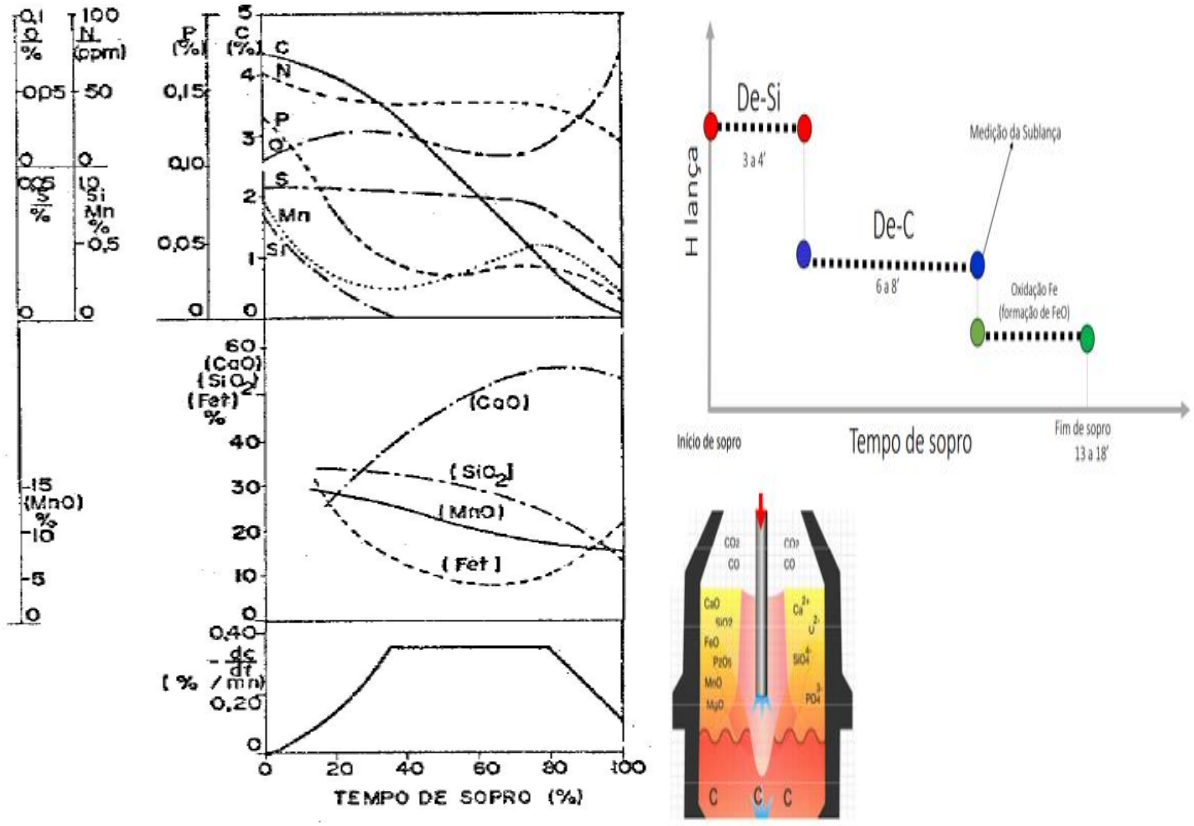

Source: Malynowskyj (2004).

The initial stage of slag formation is characterized by the addition of sources of CaO and MgO (calcitic lime, dolomitic lime and raw dolomite) traditionally known as scorifiers. These materials are added through overhead silos located above the converter. Other materials such as iron ore (sinter), used as a coolant, nepheline (slag fluidizer) may also eventually be added. The slagging materials are added during blowing, causing an increase in the percentages of CaO and MgO in the slag, with the incorporation of these basic oxides dependent on the temperature of the bath/slag and the percentages of FeO and SiO_2, the latter determining the speed of lime dissolution (MAIA, 2007).

At this stage it is essential that the slag is saturated in MgO and that there is a protective layer (coating) of slag from the previous heat on the surface of the bricks. This will physically and chemically reduce the probability of brick refractory wear (migration of MgO from the refractory brick to the slag due to the chemical gradient between the two) due to the dissolution of the refractory matrix by the process slag.

As the blowing time evolves, the main constituents of the slag are formed: CaO, SiO_2, FeO, MgO; MnO, P_2O_5, among others.

Figure 4 illustrates the evolution of decarburization of the metal bath during blowing and the decarburization rate. The second stage is mainly characterized by this oxidation of carbon, which occurs with greater intensity after the oxidation of silicon. Under such conditions, the metallic bath inside the reactor LD undergoes a considerable rise of temperature due to the decarburization reactions being exothermic. Another characteristic of this stage of the process is the existence of a metal-gas-slag emulsion that favors decarburization, with the reaction speed being determined only by the availability of oxygen. This entire step is represented by the section where –d%C/dt is constant in figure 4.

The formation of gases in this period through the oxidation reaction is evidenced by two gaseous products, CO and CO_2, with analysis varying between 55 to 70% of CO and 45 to 30% of CO_2. The generation of these gases within the metal-slag emulsion causes the foaming of the slag and the formation of the metal-gas-slag emulsion, which occupies most of the furnace volume.

In this stage, the high temperatures and the possibility of reaction of the carbon in the MgO-C matrix of the refractory bricks with the oxygen in the system, can cause a high level of oxidation and chemical corrosion of the bricks, since the formation of pores in the matrix of the refractories with consequent infiltration of slag and its subsequent reaction with the MgO in the bricks are extremely harmful to the refractory structure.

The last stage of the blow is characterized by a decreasing speed of decarburization and a gradual increase in the oxidation of manganese and iron, factors that can make the process slag highly corrosive. Furthermore, high levels of metallic bath and slag oxidation are extremely deleterious for refractories bricks. The control of carbon and temperatures in the end of blow process is essential for the preservation and reduction of the wear rate of refractories. The decrease in the generation of gases causes the gradual destruction of the emulsion, with the coalescing of the metallic particles and their return to the bath.

The period comprised by the beginning and end of the oxygen blow determines the total blowing time, which varies from 16 to 23 minutes. All these transformations that occur in the LD reactor during the blowing time lead to the transformation of the raw materials charged into liquid steel with a typical composition at the end of the blowing of 0.03 to 0.08% of carbon, around 0.17% of manganese,

0.018% phosphorus and 0.018% sulfur (all dissolved in iron), plus a slag with the following main constituents (SiO_2, Al_2O_3, FeO, Fe_2O_3, CaO, MgO, MnO, P_2O_5).

At this point, it is worth mentioning that the contact and interaction of the metallic bath and the slag with the refractories bricks are the factors in which we must act to reduce refractory wear. This is done with the appropriate practices of Slag Splashing and Slag Coating, through which the refractories bricks are covered with the slag from the previus process (heat) with the necessary corrections.

After the oxygen blowing period is over, the steel is sampled and the temperature of the metallic bath is measured. If temperature and chemical composition are in accordance with the estimated forecast for steel, the LD converter is tilted to tap liquid steel into a steel ladle. During steel tap, deoxidizing materials and alloys are added, depending on the quality of the steel to be produced. This period of steel taping is extremely important to refractory wear, as the region of the taping bed and the taphole undergoes intense corrosive and abrasive wear. For approximately 7 minutes the steel and slag are in contact with the taping refractories bed, providing contact for reactions of the slag to occur with the refractories bricks and promoting the erosive process caused by the flow of steel through the taphole. Practices for protecting the refractory with refractory mass in the taping bed and around the taphole, in addition to adding fluxes before taping, are alternatives for controlling wear in this region.

Then, the converter is tilted to tap out the slag, which takes place on the opposite side of the steel taping. This step is perhaps the most important for the process, as Slag Splashing and Slag Coating practices fundamentally depend on the amount of slag remaining in the furnace and its packaging. Slag Splashing basically consists of projecting the slag left over from the heat, duly prepared with scorifiers, onto the walls of the LD by blowing nitrogen or another inert gas with the oxygen blowing lance. There are several control parameters for the process to be effective, because the slag is projected in adequate quantity and properties for good adherence. It is this protective layer of slag that will prevent the slag and metallic bath from attacking the furnace walls in the next heat. The slag coating is very similar, however there is no inert gas blowing, only the furnace tilted and the consequent deposition of the slag on the taping refractory bed and impact bed, leaving the trunnions completely unprotected.

Finally, the converter is tilted again at an angle of 45º in relation to the vertical, where it will be prepared to receive a new metalic charge and start the cycle again. The entire LD production cycle in the steelmaking shops is governed by the sequence of movements of the converter and equipment such as oxigen lance blowing and among others. The steps described above contemplate the LD production cycle time, called process time. This time is between 38 and 40 minutes per heat.

In the case of the refractories of the converters, as the LD reactor is completely lining with this type of material, all the steps and processes described above take place and are supported by the reactor properties of this specific group of materials. It is the refractories bricks developed for this type of process and condition that determine the life and performance of these reactors. In addition, the entire issue of operational safety and availability of the equipment is in charge of the control and performance of the refractories bricks of the converters, which in turn is associated with process variables, refractory design, conditions of assembly and start-up of the equipment, it is of course, the preservation conditions of the bricks mainly linked to the standards of Slag Coating and Slag Splashing.

2.2.3 Metal bath and LD slags

The mix metallic bath, slag and gas form the set of components that will interact with each other and with the refractories bricks of the LD. Bricks need to be able to withstand the various refractory wear phenomena arising from the interactions of these components.

The metallic bath basically consists of iron, carbon, silicon, manganese, phosphorus and sulfur. Initially these compounds are dissolved in the metallic bath and later they are in the form of oxides in the slag or gases formed during the oxygen blowing process. In addition to these, at the end of the blowing, soluble oxygen is dissolved in the bath.

Another component of the system is the slag. It is basically constituted by a mixture of oxides that supernatate in the metallic bath due to its lower density. The third constituent of the system that acts on the refractories are the gases resulting from the carbon oxidation and from the system itself, such as oxygen and nitrogen.

Special attention must be given to slag due to its great importance in terms of reactivity with refractory system of the LD furnace. Basically, they are formed during the oxygen blowing process and by the addition of scorifiers. Chemically, we can say that they are solutions of positively charged ions (Mg^{+}, Ca^{2+}) and negatively charged ions (complex silicates, aluminates, phosphates) (TURKDOGAN; FRUEHAN, 1999).

The main chemical constituent is the tetrahedral silicate SiO_4^{-4}, the silicon atom being tetrahedrally surrounded by four oxygen atoms, which in turn is bonded to two silicon atoms. Electrically, this atomic system will have silicon with valence +4, oxygen −2 and the resulting silicate with valence −4 as resultant.

These silicates form a network which, during the addition of basic oxides, such as CaO and MgO, contained in the scorifiers, promotes breakage and, consequently, the depolymerization of the network (Figure 5). In practice, what happens physically in basic slag is a reduction in viscosity as the silicate chain breaks down.

$$\begin{array}{c} | \quad | \\ \text{-Si-O-Si-} \\ | \quad | \end{array} + MO = 2 \begin{array}{c} | \quad - \\ \text{-Si-O} \\ | \end{array} + M^{2+} \qquad (1)$$

Under certain conditions, Al_2O_3 may rearrange the silicate network, forming Al^{3+} cations, or certain isomorphic structures with silicon. In low concentrations of the element phosphorus in the slag, PO_4^{-3} phosphate ions may eventually be incorporated into the silicate network together with sulfur in the form of S^{2-} sulfide ions. SO_4^{2-} sulfate ions can also exist in slag at high levels of oxidation with low levels of iron or other oxidizable metal (AUAD, 2018).

$$\begin{array}{c} | \quad | \\ \text{-Si-O-Si-} \\ | \quad | \end{array} + MAlO_2 = 2 \begin{array}{c} | \quad | \quad | \quad - \\ \text{-Si-O-Al-O-Si-} \\ | \quad | \quad | \end{array} + M^{+} \qquad (2)$$

Figure 5 – Depolymerization of the silicate network through the basic oxides

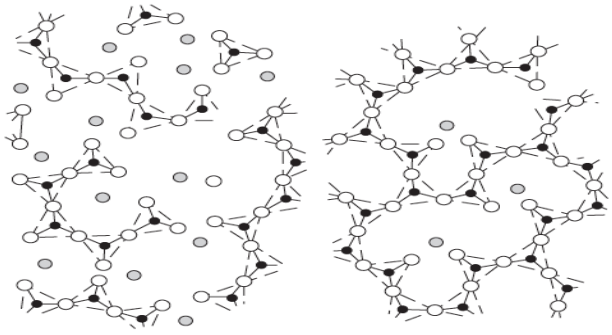

Source: Turkdogan and Fruehan (1999).

2.3 Refractories to LD Converters

The applications are the most diverse possible when talking about refractories products. Such applications are related to their properties, which in turn result from the type of microstructure and chemical composition. For a better understanding and application, we can divide the refractories according to some classes and later use them in different operating conditions.

For Freitas (1993), a classification into shaped and unmoulded can be applied to refractories products so that the group of shaped materials would be defined as refractory materials molded before their final application (bricks, plates, valves, others), and the group of unmoulded, or monolithic, materials would be those molded at the time of application (concrete, mortar, projection and molding masses).

According to Lenz and Silva (2007), a classic type of classification of refractories materials is in relation to their acid-base behavior, which can be expressed by the ability to receive and give ions (O^{2-}). This characteristic is described by the percentage ratio between CaO/SiO_2 (binary basicity) so that for this classification we would have acidic and basic refractories. This classification facilitates the understanding of the transformations, reactions and stability of the main refractory systems. Tables 1, 2 and 3 illustrate the features described above.

Table 1 – Classification of silica-based acid refractories

Refractories	Sub Group	Content of Al_2O_3 (%)
Silica		< 7%
Sílico Aluminuos	Siliceous	7 - 22%
	Silico-Aluminuos	22 - 38%
	Aluminuos	38 - 50%
High Alumina	Sillimanite	50 - 65%
	Mulita	65 - 75%
	Coridon e Bauxite	75 - 98%

Source: Lenz e Silva (2007).

Table 2 – Main groups of calcium aluminate-based concretes

Classification	Content of CaO (%)
Conventional castables (CC)	> 2,5%
Castables of low contente of cement (CBC)	1 - 2,5%
Castables of ultra low content of cement (CUBC)	0,2 - 1%
Cementless castables	< 0,2%

Source: Lenz e Silva (2007).

Table 3 – Refractories products classification

Criterion	Characteristics	
As for the presence of Clay	Clayey	Silica-aluminous, etc.
	Not Clay	Magnesia-carbon, chrome-magnesia, silica, etc
As for the type of raw material	Natural	Bauxite, graphite, Kyanite, andalusite, sillimanite, dolomite, magnesite, etc.
	Synthetic	Electrofused Magnesia, Fused mullite, silica, Silicon carbide, etc.
As for the Chemical composition majority	Aluminous	Alumina, High-Alumina
	Silico-Aluminous	Mullite, alumina-mullite, etc.
	Chrome-Magnesians	Magnesia-chrome
	Alumina-Carbon	Alumina-carbon
	Magnesia-Carbon	Magnesia-carbon
	Dolomites	Dolomite (limestone+magnesia)
	Zirconia	Zirconia (tottaly ou partially stabilized for limestone or ítria)
As for the acidity/basicity	Ácids	Silica
	Bases	Magnesia-carbon, dolomite burned, magnesia
	Neutrals	Chromia
As for the type processing/application	Formed	Bricks, insulatings bricks, valves, sleeves
	Not formed	Castables, mortar, projection masses, punching masses
	Precast	"Snorkels", gas/particulate injections lances
As for the density	Dense	Bricks, sleeves, valves, etc.
	Not Dense	insulating bricks, ceramic fiber
As for the type of chemical reaction in service	“In Situ”	Bricks and concrete with antioxidants, spinelables, etc.
	“Ex Situ”	Burned bricks
As for the type of Chemical bond	Direct bond	$MgO\text{-}Cr_2O_3$
	Rebond	$MgO\text{-}Cr_2O_3$
	Bonded by acid phosphoric	Castables
	Bonded by chromate	Mortars
	Bonded by clay	Several
As for the type of carbon source	Bonded by pitch	Dolomites, magnesia-carbon
	Bonded by Resin	Magnesia-carbon, alumina-magnesia-carbon, alumina-silico carbide-carbon, etc.
As for the type of tar	Liquid pitch	Dolomites, magnesia-carbon, etc.
	Solid pitch	Magnesia-carbon, alumina-magnesia-carbon, alumina-SiC-carbon, etc
As for the type of impregnation	Impregnated with pitch	Magnesia-carbon, alumina-carbon plates
	Not impregnated	Magnesia-carbon, alumina-carbon, alumina-Silico carbide-carbon, etc.
As for the type of application in service	Projected	Several
	Vibrated	Several
	Poured	Several
	Precast	Several, including concrete, bricks and insulators

Source: Lenz e Silva (2007).

Some groups of refractories do not fit into any of these groups and, even so, have important applications in the steel industry, such as the group of carbides applied in refractory linings of pig iron ladles. According to Lenz e Silva (2007, p.275)

> [...] when this type of refractorie classification is used, some types of refractories end up not being classified in either of these two groups, such as borides, carbides, nitrides, etc., which are classified in a group called special refractories.

During the evolution and development of refractories for steelmaking shops, the change in demand from the well-known acid chemical-based refractories to basic ones was noticeable.

Chesters (1993), mentions in his work the change with the advent of LD converters and oxygen steel production furnaces in the types of refractories used in the steel manufacturing process and as the inducing event of the change in the demand for acid refractories by the basic. For the group of basic refractories, magnesium stands out as its main constituent, with the compound magnesia as the major component, MgO, as the main oxide.

This choice for magnesium refractories is due to the high melting point (above 2800°C) and high resistance to attack by iron oxides and alkalis, which makes it an excellent option for different types of furnaces. For Lenz e Silva (2007, p.282)

> The existing variations of these oxide systems include MgO, MgO-CaO, MgO-Cr_2O_3, MgO-Al_2O_3, MgO-C, Al_2O_3-MgO-C, making the field of use of this group extend to cement furnaces linings and calcination, steel ladle lining, passing through reactors and degassers (RH, VOD, AOD), LD converters and electric arc furnaces.

In the wake of this development, we can mention the dolomitic refractories. Such a group was developed in England during the World War II as a result of studies by several research groups that were published at the Institute of Iron and Steel in 1946 (CHESTERS, 1993). According to Lenz e Silva (2007, p.285)

> This group has dolomite, calcium and magnesium carbonate ($CaMg(CO_3)_2$), as the main source of raw material for its manufacture. The decomposition of this carbonate generates Calcium (CaO) and Magnesia (MgO) which are basic compounds of dolomitic bricks.

It is common to divide dolomitic refractories into two categories, burned dolomites and pitch-bound dolomites. For Lenz e Silva (2007, p.286)

> The first class is used in cement furnace firing zones, while the second class can be considered as the precursor of modern magnesia-carbon bricks, having accompanied the entire development of primary refining processes in oxygen converters (LD converters).

The current practice that has been used is the use of dolomitic bricks in electric arc furnaces, in oxygen converters and in steel ladles. The advent of dolomitic refractory bricks was accompanied by the use of carbon in their manufacture, this group being of particular importance and widely used in the steel

industry, in particular refractories of Al_2O_3-SiO_2-C, Al_2O_3-SiO_2-SiC-C, MgO-C (BROWN; WHITE, 1986; COOPER, 1980; SAKANO; TAKAHASHI, 1988.).

Lenz e Silva (2007, p.290) reports that “the use of carbon in refractories is not new, its use was, and still is, important in dolomite-based refractories resined or bonded to pitch”. According to Lenz e Silva (2007, p.290)

> However, from the 1970’s onwards, with the use of graphite and resin in the MgO-C system and the expansion of its use to other refractory systems such as: Al_2O_3-C; Al_2O_3-MgO-C; Al_2O_3-SiC-C; Al_2O_3-MgO-SiC-C; Al_2O_3-ZrO_2-C, etc. transformed the materials: refractory oxide + carbon (graphite + organic binder) + antioxidants, into the main high-tech and high-performance composite materials, capable of withstanding increasingly aggressive and complex operating conditions.

One of the main characteristics of the chemical system (carbon/graphite + oxide/antioxidant) is modify the thermomechanical and thermochemical behavior of the refractory, modifying the surface tension and reducing the wettability of the refractories component by metals and slag. For Lenz e Silva (2007, p.291)

> In general terms, carbon/graphite changes the surface tension of the refractory, decreasing wettability by metals and liquid slag. Another important point are the reactions between the oxides + antioxidants with carbon at high temperatures (especially MgO+C) capable of reducing the porosity of the hot refractory face due to processes of reduction/oxidation of the magnesium oxide and changes in the system oxygen: refractory-slag-metal.

The main types of carbon that can be found in this type of refractory system are: graphite carbon, free carbon derived from resins and carbon formed by the reactions between antioxidants and $CO_{(g)}$ (YAMAGUCHI; ZHANG, 1996). As for the type and amount of antioxidants used in the refractory project, the in situ chemical transformations are related to structural, thermomechanical and physical-chemical changes during the refractory campaign and depend on the antioxidants used.

According to Yamaguchi (2006), the reaction of antioxidants such as aluminum (Al) and silicon (Si) with the carbon in the refractory structure forms compounds such as silicon and aluminum carbides that subsequently form a protective surface on the refractory itself, reducing porosity and increasing the resistance to corrosion.

As a negative point of refractories containing carbon, the ease with which carbon reacts with oxygen stands out, making this type of refractory easily oxidizable in environments rich in oxygen, as is the case with LD coverters. Therefore, it is necessary to use antioxidants in refractories containing carbon to avoid the corrosive process (by oxidation).

Through Table 4, it is possible to visualize the main refractories systems of the oxide + carbon + antioxidant type used in steelmaking. In addition, this table brings the various equipment used in steelmaking shops in which this type of refractories is used, among which we have the LD converters, the object of study of this thesis.

Figure 6 illustrates a typical LD converter highlighting its various regions and refractory brick structures.

Table 4 – Main oxide + carbon refractories systems used in steelmaking processes

System	Equipment
MgO-C	Steel Ladles for transport and refining (metal and/or slag line) Oxygen Converters (LD/BOF) Electric Arc Furnace (FEA)
MgO-CaO-C	Steel Ladles of the Electric Steelmaking Shops (Silico – killed steel)
MgO-Al_2O_3-C	Steel Ladles (metal line and impact region), Gate valve mechanism plates, Pig Iron transport ladle
Al_2O_3-C	Long and submerged valves, Torped cars impregnated
Al_2O_3-ZrO_2-C	Gate valve mechanism plates
Al_2O_3-SiC-C Al_2O_3-MgO-SiC-C	Torped cars, Pig iron ladles with desulfurization

BOF – Basic Oxygen Furnace; LD – Linz Donawitz; FEA – Electric Arc Furnace.
Source: reference (LENZ E SILVA, 2007)

Figure 6 – Schematic representation of the refractory structure and application in LD converter

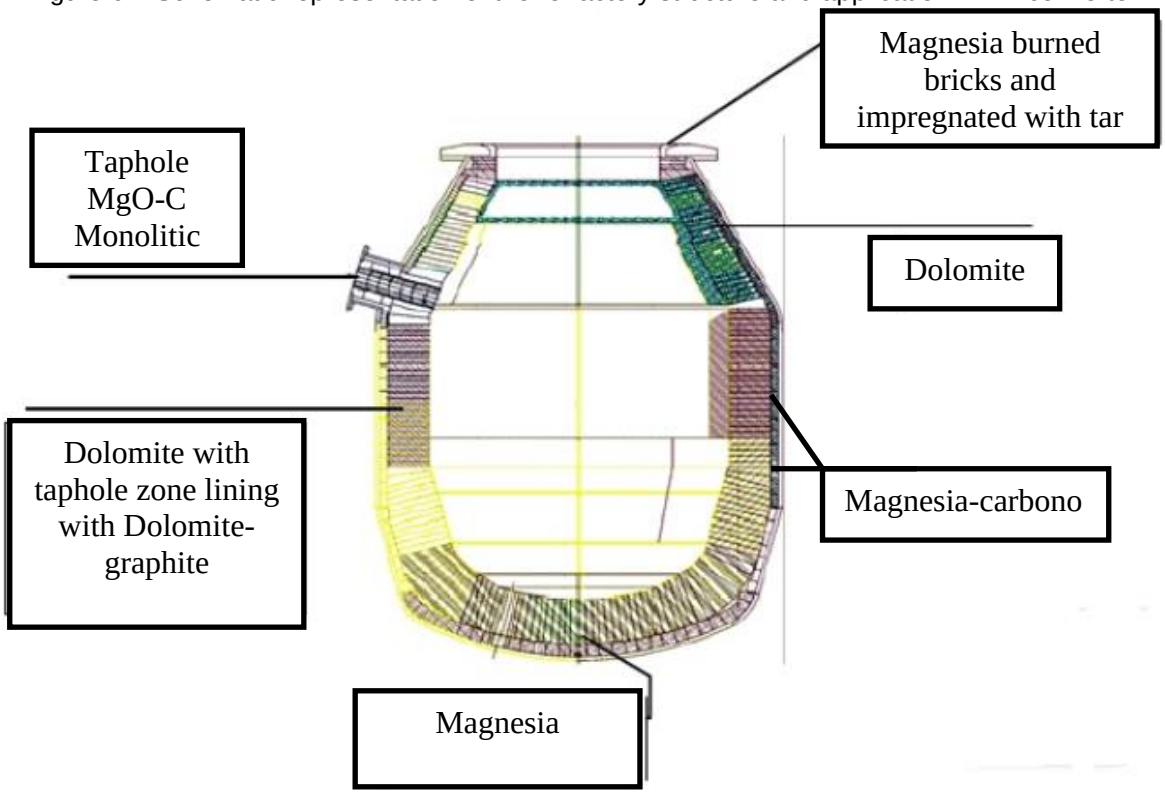

Source: https://pt.scribd.com/document/191210399/Refratarios-em-Convertedor-LD-docx, acessed in 2021/10/13).

2.4 Binding systems for converter refractories

There are differences in thinking for the use of binders in carbon-containing refractory systems. On the one hand, there are those who defend the use of binders based on mineral tar pitches, on the other hand, there are those who prefer the use of synthetic resins. While in most of Europe the use of pitch prevails, the other regions opt for phenolic resin. Such differences are related to technical and/or manufacturing issues. Both have advantages and disadvantages (WILLIAMS; TAYLOR; LEONI, 1993).

According to Yamamura *et al*. (1996), the main disadvantage of tar-derived pitch is the presence of carcinogenic compounds. Refractories manufactured with phenolic resin, on the other hand, have lower resistance to thermal shock and oxidation due to the formation of an isotropic phase of coke residue.

In addition, the resin is not considered an ideal binder due to the low amount of carbon when compared to other carbonaceous compounds, high shrinkage above 600 °C and lower ability to form graphite, which reduce the mechanical strength of the brick, the resistance to damage by thermal shock and corrosion resistance at high temperatures (Kanno *et al*., 1999).

The type of binder can be identified by gas chromatography techniques with coupled mass spectrometer, since pitch contains substances that significantly differentiate it from phenolic resins (GARDZIELLA; SUREN, 1997.). Studies and development of new binder compounds, such as carbo-resin, have been proposed to overcome the deficiencies or disadvantages of pitch or phenolic resin (BUCHEBNER; NEUBOECK, 2001).

In Brazil, refractories manufactured with phenolic resin and antioxidants prevail due to the difficulties inherent in the processing of bricks bound to pitch. A typical case is the process of mixing and hot pressing and adjustments in the refractory manufacturer's industrial facilities to meet the requirements required by environmental agencies. For Gardziella and Suren (1997), the concern with the bonding system of these materials results from the different characteristics provided by pitch or phenolic resin because during pyrolysis pitch passes through a stage of liquid mesophase to semi-coke between 400 °C to 550 °C leading to a graphitic character (molecular orientation) from 650 °C to 1000 °C.

Secondary carbon derived from traditional phenolic resin does not have a graphitic character, that is, during its formation there is no indication of long distance ordering. On the contrary, the carbon from the resin leads to a glassy carbon structure without orientation (glassy isotropic), which is easily oxidized and has greater rigidity (BUCHEBNER; NEUBOECK, 2001).

The pitch provides the refractory with superior resistance to thermal shock damage, as the residual pitch in the pores of the refractory can dissipate part of the elastic energy stored in the refractory during its pyrolysis by mesophase and graphitization states, when a strength is applied to the refractory. This greater integrity of the refractory containing pitch after the initial heat treatment, when compared to the phenolic resin bonded one, would be responsible for its superior resistance to thermal shock.

Yamamura *et al*. (1996) concluded that, although the phenolic resin has characteristics favorable to the mixing and pressing process, the carbon formed during its carbonization is amorphous, which is one of the reasons for the lower resistance to thermal shock of MgO-C bricks bonded to resin. In addition, the superior permanent expansion of the pitch in relation to the phenolic resin, favors the closing of the joints of the refractory lining, which contributes to reducing the chipping of the edges in the hot face of the bricks and to avoid possible penetration of metal in the joints and in the back part of the brick lining (BORZOV; ULBRICHT; SCHULLE, 2001). Therefore, expansion of the resin-bonded refractory resulting from the presence of antioxidants is not a concern in pitch-bonded bricks. The phenolic resin has good characteristics regarding the wettability of metallic oxides (MgO), molding and higher amount of carbon when compared to other resins, which are pointed out as advantages.

There are efforts by the industry to develop alternative binders that improve the properties of refractories and, at the same time, reducing emissions of substances harmful to health. However, both binders (resin and pitch) continue to be used due to the combination of good properties with relatively low cost. The current trend is to seek a balance between good resistance to oxidation and thermal shock. Optimizing the combination of variables such as carbon and antioxidant content, granulometry, control of the pore size distribution of the aggregate is essential to obtain a refractory design suitable for current steelmaking processes.

2.5 Antioxidants for refractories in LD Converters

The main chemical elements used as antioxidants in LD converters are aluminum (Al) and magnesium (Mg). The main objective of using these elements in refractory systems for LDs is to increase resistance to oxidation, since with the advent of the use of carbon in the refractory matrix with the advantages mentioned above, there was a sharp drop in resistance to oxidation. According to Yamaguchi (1987), in AI-C type systems it is possible to form $AIN_{(s)}$, $AI_4C_{3(s)}$ and $Al_2O_{3(s)}$ at temperatures above 700 °C.

In the AI-MgO-C system, this same researcher observed the formation of $Al_4C_{3(s)}$ and $AIN_{(s)}$ between 700 °C and 1300 °C and the disappearance of $AI_4C_{3(s)}$ above 1400 °C. Furthermore, the concentration of AI decreased significantly from 800 °C onwards, making it no longer possible to detect it as a phase at temperatures above 900 °C, although traces of this phase can be observed in the MgO-C-AI system at temperatures between 1000 °C and 1200 °C (QUINTELA *et al*., 2003; WATANABE *et al*., 1987).

Direct contact between $AI_{(l)}$ and $C_{(s)}$ or between $AI_{(g)}$ and $C_{(s)}$ can initiate the formation of $AI_4C_{3(s)}$. These possibilities may be associated with the presence of coarse AI particles in carbon-containing refractories. In this case, the surface of these particles reacts with the $C_{(s)}$ to form a layer of $Al_4C_{3(s)}$, whose melting point is approximately 2230 °C. In such cases, $AI_4C_{3(s)}$ can form a passivating layer that can inhibit the direct reaction between residual AI and $C_{(s)}$. In specific situations, $AI_{(l)}$ inside these particles coated with $AI_4C_{3(s)}$ can give rise to various gases, such as $AI_{(g)}$. This gas, through diffusion by $Al_4C_{3(s)}$ can react with neighboring carbon forming $Al_4C_{3(s)}$. Therefore, the formation of $AI_4C_{3(s)}$ is possible in any region of the refractory (ZHANG; MARRIOTT; LEE, 2001).

In the open pores of the refractory, studies by Yamaguchi, Nakano and Wang, (2000), reveal that $Al_2O_{3(s)}$ is the most stable condensed phase in the AI-O-C system (considering partial pressure of CO, Pco, of 1 atm). On the other hand, in the presence of $C_{(s)}$, at 1327 °C, $Al_4C_{3(s)}$ and $Al_2O_{3(s)}$ coexist in equilibrium under certain conditions of pressure and temperature. Such phases produced when solid can fill the open pores and consequently reduce the porosity of the refractory resulting in a denser and tighter structure reducing the probability of penetration of oxygen, slag, pig iron and steel. In their studies, Taffin and Poirier (1994) revealed the possibility

that Al particles covered by a thin layer of $Al_2O_{3(s)}$ can increase the temperature at which Al can become liquid, which would contribute to the retention of this compound in the refractory.

A relevant contribution, in the sense of increasing the mechanical strength of the refractory material, may come from the formation of $Al_4C_{3(s)}$ plates and $AlN_{(s)}$ whiskers (TAFFIN; POIRIER, 1994; YAMAGUCHI, 1987). These authors also refer to the importance of reactions up to 1100 °C in which $Al_{(l)}$ is converted into $Al_4C_{3(s)}$ crystals, generating a solid structure in the center and in the vicinity of the void left by Al, also citing the formation of spinel $MgAl_3O_{4(s)}$ around this additive by direct reaction of Al with $MgO_{(s)}$.

For temperatures above 1400 °C, studies by Taffin *et al*. (1994) reveal the formation of $MgAl_3O_{4(s)}$ crystals on the $Al_4C_{3(s)}$ plates located in the center of the voids left by Al and the reaction of $Al_4C_{3(s)}$ with $CO_{(g)}$ forming $Al_2O_{3(s)}$, which, combined with $MgO_{(s)}$ form $MgAl_3O_{4(s)}$.

Important results were obtained in ceramographic analyzes carried out by Taffin *et al*. (1994) in which the formation of $MgAl_3O_{4(s)}$ was verified through direct solid/solid and solid/gas reaction.

Above 1500 °C, $Al_4C_{3(s)}$ is no longer found, only the presence of $MgAl_3O_{4(s)}$ crystals being observed (TAFFIN; POIRIER, 1994). All the previous transformations cited have a direct effect on the mechanical strength of the MgO-C refractory. At a temperature of approximately 1100 °C, the increase in mechanical strength is attributed to the formation of $Al_4C_{3(s)}$ and at 1500 °C to the development of $MgAl_3O_{4(s)}$ crystals. When compared, $MgAl_3O_{4(s)}$ is more compact and the bond between crystals is more resistant than $Al_4C_{3(s)}$, (TAFFIN; POIRIER, 1994).

For Zhang, Marriot and Lee (2001), at high temperature Al reacts with graphite and/or nitrogen to form $Al_4C_{3(s)}$ and/or $AlN_{(s)}$, occasionally it can be oxidized directly by $CO_{(g)}$ to form $Al_2O_{3(s)}$. The $Al_4C_{3(s)}$ formed can, under certain conditions, react with nitrogen forming whiskers of $AlN_{(s)}$ and/or with $CO_{(g)}$ forming $Al_2O_{3(s)}$ which, in turn, when combined with $MgO_{(s)}$ will form $MgAl_3O_{4(s)}$. Thermodynamic calculations suggest that after $Al_4C_{3(s)}$ disappears, $AlN_{(s)}$ will react with $CO_{(g)}$ to form $Al_2O_{3(s)}$, which combines with $MgO_{(s)}$ to form $MgAl_3O_{4(s)}$.

Regarding the gaseous species, for example $Al_{(g)}$, its explain the different morphologies of the reaction products, such as $AlN_{(s)}$ (whiskers) and $MgAl_3O_{4(s)}$ (precipitated on the surface of the large MgO aggregate). The amount of $MgAl_3O_{4(s)}$

at 1200 °C is relatively small. At a temperature of 1500 °C, the reaction between $MgO_{(s)}$ and $C_{(s)}$ becomes significant and contributes to the process of formation of $MgAl_3O_{4(s)}$. Therefore, in addition to the solid/gas reaction, there is a contribution of the gas/gas reaction to the formation of $MgAl_2O_{4(s)}$.

Some mechanisms are proposed in an attempt to understand the morphology and formation mechanisms of $Al_4C_{3(s)}$ and $Al_2O_{3(s)}$, such as those proposed by Quintela (2003) and Zhang; Marriott; Lee, (2001). One of these mechanisms would be, in the surface region of the AI particles, this would be transformed into the compound $AI_4C_{3(s)}$, in parallel, there is a growth towards the center of the AI particle. If $Al_4C_{3(s)}$ is not quickly oxidized by $CO_{(g)}$, the AI will be converted to an $Al_4C_{3(s)}$ particle.

In situations where the surface layer of $Al_4C_{3(s)}$, which contains AI in its interior, is rapidly oxidized by $CO_{(g)}$, a considerable volume expansion will occur (approximately 93.5%) which may result in a layer of $Al_2O_{3(s)}$ which may contain cracks and micropores. Another possibility is carbon condensation, in this situation it can occur when the oxidation frontier reaches the $AI_{(l)}$ included in the $AI_4C_{3(s)}$ layer, the $AI_{(g)}$ will evaporate and escape through the cracks and micropores of this AI_2O_3 layer(s) leaving a pore in the center of the particle.

According to Quintela (2003), it is possible that $Al_4C_{3(s)}$, $Al_2O_{3(s)}$ and $Al_{(l)}$ coexist in MgO-C-AI systems after coking at 1000 °C for 5 hours (Figure 7). It can then be inferred that, with the oxidation of said $Al_4C_{3(s)}$ layer, part of the resulting $C_{(s)}$ has reacted with the residual $Al_{(l)}$ inside the particle, forming $Al_4C_{3(s)}$ again.

A second option would be the formation of the $Al_2O_{3(s)}$ layer on the AI particle, a mechanism very similar to the previous one, since this $Al_2O_{3(s)}$ envelope would also not be dense and could contain some cracks or micropores due to the large volume expansion that accompanies the reaction of AI with $CO_{(g)}$.

It is also possible that the expansion of the other components of the refractory would also have a great influence on these mechanisms and morphologies of the generated phases.

Figure 7 – Photomicrographs of the general (A) and field (B), and microanalyses of the present phases (C) and (D) of the MgO-C-Al brick coque at 1000 °C for 5 hours

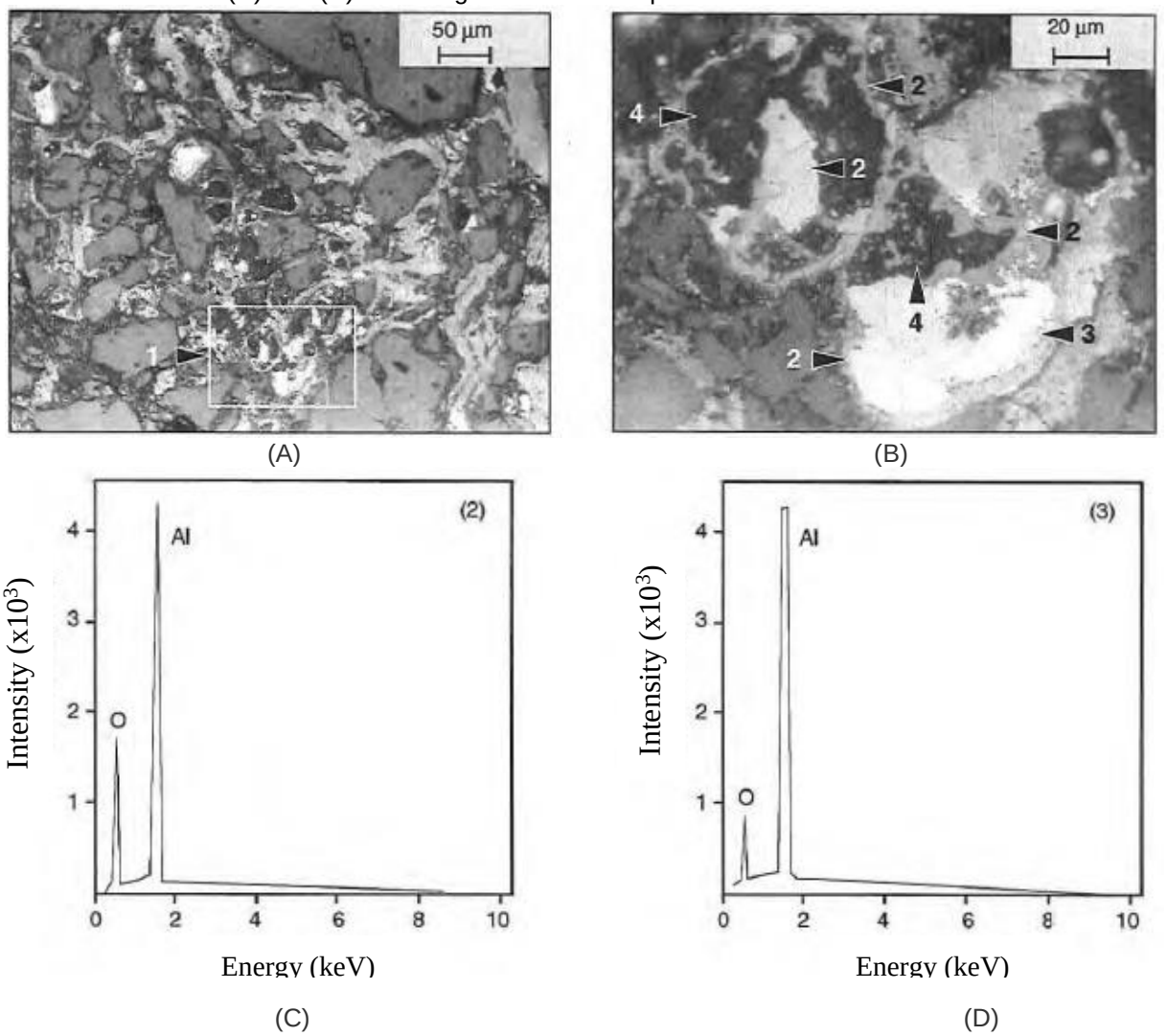

Source: Quintela *et al*. (2003).

Other possibilities of $MgAl_3O_{4(s)}$ formation processes for the MgO-C-Al system were proposed by Toritani *et al*. (1985).

There are indications that the atmosphere inside the refractory may vary locally, becoming more oxidizing towards the hot face (ZHANG; MARRIOTT; LEE, 2001). Considering the brick from the cold face to the hot face, we would have a variation from reducing to oxidizing from the atmosphere and a substantial amount of $Mg_{(g)}$ that could be produced and, more pronounced, above 1500 °C (YAMAGUCHI, 1993; ZHANG; MARRIOTT; LEE, 2001). In this case, the $Mg_{(g)}$ formed normally migrates towards the slag layer and upon reaching the interface between the decarburized layer and the layer containing slag, due to the more oxidizing atmosphere, it reoxidizes, forming $MgO_{(s)}$ (YAMAGUCHI, 1984; ZHANG; MARRIOTT; LEE, 2001). This would be one of the hypotheses of the mechanism that would lead

to the formation of the dense layer of $MgO_{(s)}$, which inhibits the oxidation of carbon, through a physical barrier, reducing the access of external gases and slag liquids in deeper layers of the refractory. Furthermore, the continued formation of this layer is favored by the presence of high basicity slag and slag containing iron oxide. It is believed that this layer and the mechanisms mentioned above can substantially contribute to reducing the heat transfer rate in the refractory lining in the intervals between heats or stops for maintenance and repairs.

Good preservation and integrity of this dense layer is obtained when its formation rate is greater than or equal to its dissolution rate in the slag. Assuming that the slag is composed of CaO and SiO_2, the CaO/SiO_2 ratio of the slag which delays or reduces the dissolution of MgO must be investigated. A good example would be the determination of the amount of liquid phase that can be formed by the reaction of MgO and slag (CaO and SiO_2) in different % of these chemical compounds, at temperatures around 1600 °C (Figures 8 and 9). The isothermal section (1600 °C) of the thematic $CaO\text{-}MgO\text{-}SiO_2$ system illustrates these effects well.

Figure 8 – Isothermal section at 1600 °C of the ternary system $CaO\text{-}MgO\text{-}SiO_2$

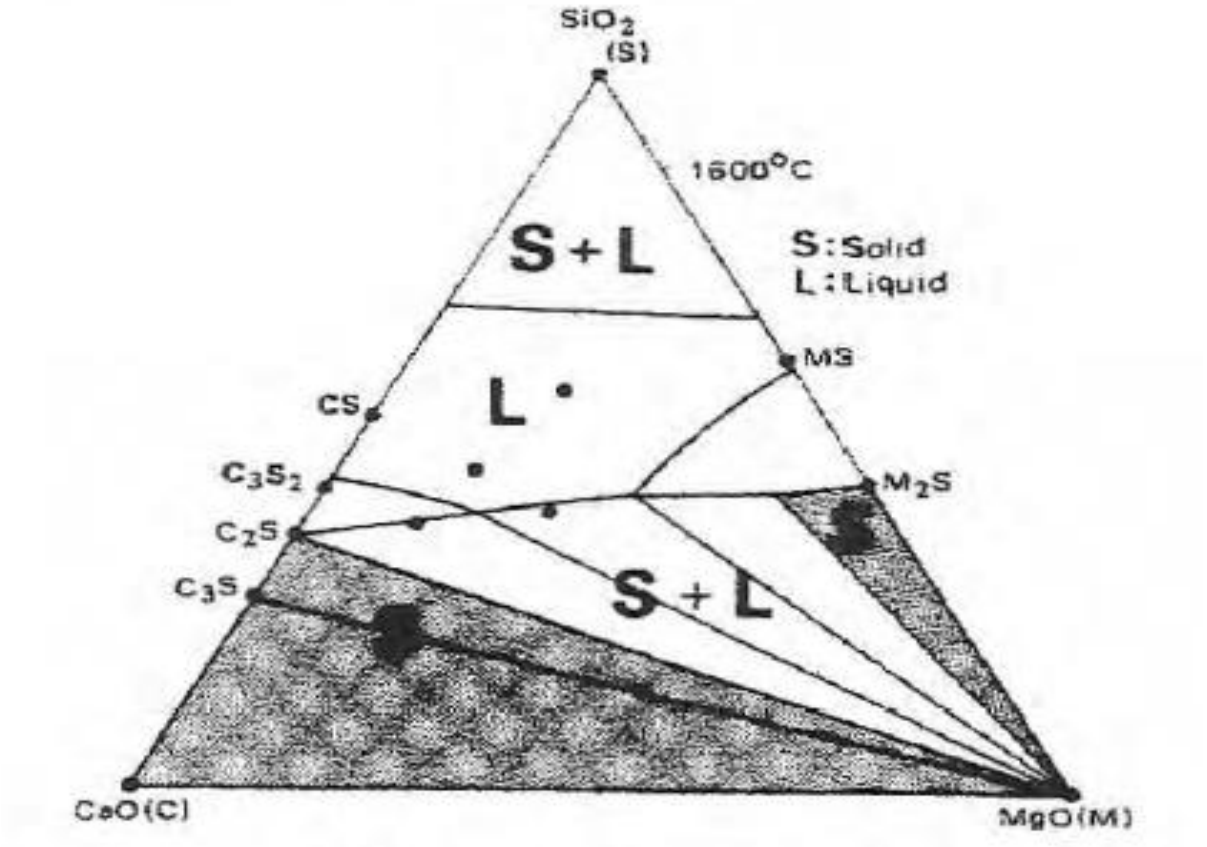

Source: Quintela (2003).

Figure 9 – Amout of liquid generated by reaction between MgO and CaO-SiO_2 fron the slag at 1600°C

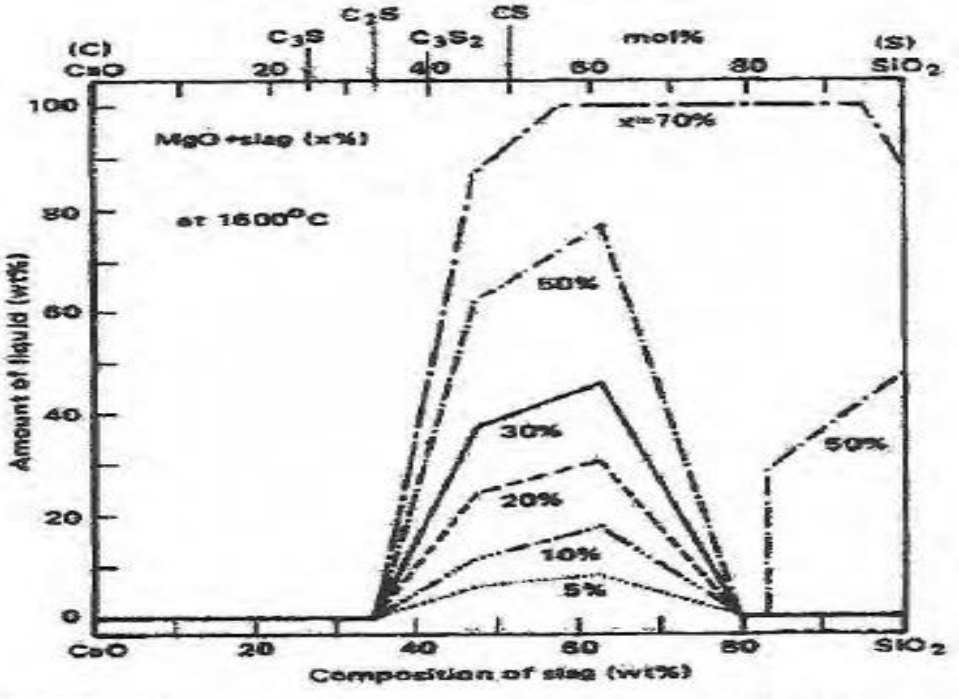

Source: Quintela (2003).

From the analysis of the figures above, it is possible to verify that, for a CaO/SiO_2 ratio (binary basicity) greater than 2, the slag does not react with MgO. For basicity lower than 2, there is the possibility of formation of a liquid phase and consequent reaction between the slag and the MgO. However, the fact that the slags contain other components, such as iron oxides and MnO that contribute to the dissolution process and enable the MgO to be dissolved in the slag for any composition, may contribute to the increased dissolution of the MgO layer. Therefore, it appears that slags containing a high CaO/SiO_2 ratio are less aggressive and dissolve MgO at relatively lower rates. Furthermore, if MgO is dissolved in the slag, the dissolution rate of MgO from the dense layer (brick) is likely to be lower due to the smaller chemical gradient between the brick and the slag.

An intriguing issue that draws attention is the fact that the dense layer of MgO is continuously dissolved or removed. Assuming that the MgO layer is formed close to the hot face of the brick, providing protection to the internal structure of the refractory, and assuming that Pco (partial pressure of CO) and P_{Mg} (partial pressure of Mg) reach the equilibrium partial pressure, making the reaction in dynamic equilibrium, the dense layer of MgO would be continuously dissolved or removed. For the MgO layer to grow, it would be necessary to generate $Mg_{(g)}$, which would react with oxygen to form $MgO_{(s)}$. This fact would lead the dense layer formed to generate

a barrier to the supply of external oxygen, which would be essential for its continuous formation. This would render this model or mechanism inconsistent unless the effect of iron oxide present in the slag contributes to its formation under certain conditions. Microanalytical results of a dense MgO layer of a MgO-C brick, containing 21% C by weight, after slag etching (Fe_2O_3 = 33%, SiO_2 = 12%, Al_2O_3 = 2%, CaO = 46% and MnO = 3%; CaO/SiO_2 = 3.8), indicated the reduction of iron oxide from the hot face of the dense layer (Figure 10). Next to the hot face, the presence of $MgFe_2O_4$ (magnesium ferrite) was observed, inside the layer, MgO-FeO (solid solution) and, on the back face, metallic iron. Thus, it is assumed that oxygen is continuously supplied from the outer face to the inner face of the layer. In the inner part, the reduction of FeO occurs, contributing to the growth of the MgO layer and leading to the precipitation of metallic iron.

Figure 10 – Photomicrograph of a dense MgO layer next to the hot MgO-C brick face

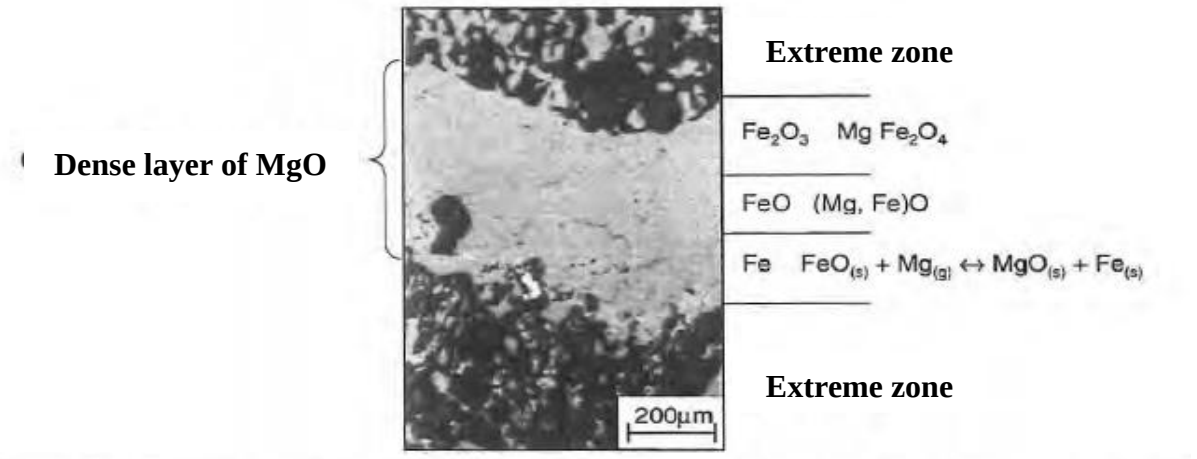

Source: Quintela (2003).

According to Takanaga (1993), a relevant and very important factor is the increase in iron content in the slag, which will produce a pronounced MgO-C refractory wear due to the increase in the solubility of MgO and the oxidation of carbon by FeO and Fe_2O_3. Considering the oxidation of the carbon in the refractory, the wettability of the refractory increases drastically as the content of this element is reduced, since there is a reduction in the surface tension of the material, which will facilitate the penetration of slag into the microstructure of the refractory and, consequently, will promote the dissolution of the MgO aggregate by the slag. A relevant factor is the increase in the fluidity of the slag in the presence of FeO and Fe_2O_3, which enhances the refractory dissolution reactions by the process slag.

2.6 Wear and life of refractories in LD Converters

2.6.1 Initial considerations on refractory wear of LD Converters

In steelmaking shops around the world, for decades, MgO-C bricks have been used in the lining of converters due to their high resistance to corrosion by basic slag and high resistance to damage by thermal shock (JANSEN; GROBE DALDRUP, 2005; QUINTELA; PESSOA; SALGADO, 2009). Such properties derive, in part, from the element carbon linked to MgO, that forms a stable structure in the face of the various demands to which these refractories are subject when used in LD converters. According to Quintela, Pessoa and Salgado (2009, p.36)

> Over the years, the durability of these bricks has been continuously improved through research and development studies, which have focused efforts on making feasible the use of nobler raw materials and formulating more sophisticated refractories, such as those containing MgO electrofused, high purity graphite, metallic (Al, Mg etc.) and intermetallic (B_4C, ZrB, SiC) antioxidants, and complex ligand systems.

In the case of LD converters, what often determines the life of the refractory lining is the bricks performance in the trunnion region. This performance is generally related to the effectiveness of the protective layer of slag formed on the bricks during the processes known as Slag Splashing and Slag Coating. Such processes are basically brick coverings using the process slag itself with its respective physical-chemical adjustment. For Quintela, Pessoa and Salgado (2009, p.36)

> Certainly, one of the great challenges in this field is to better understand the wear mechanisms of these materials, with a view to boosting the development of refractories with properties adjusted to the particularities of each steelmaking shops.

Premature wear of refractories in trunnions is mainly associated with the absence of a protective layer of slag in this region, which is due in part to the inefficiency of the traditional process known as Slag Coating in the regions corresponding to the scrap loading and taping of liquid steel (JANSEN; DALDRUP, 2003; TAKANAGA, 1993; YAMAGUCHI, 1984). This fact is explained due to the movement of the converters being exclusively tilting, hence the reason for the slag coating not coming into contact with the refractories in the region of the trunnions. Therefore, the lack of this protective layer leads to a more severe oxidation of the refractory carbon in this region, resulting in a higher rate of corrosion by slag/metal of the bricks, low mechanical resistance and low resistance to cyclic temperature variations of the decarburized layer.

2.6.2 Properties and refractory wear mechanisms of LD Converters

Different environments and operational conditions define the demands that the refractory materials are submitted and what is necessary to adapt in terms of properties to obtain a satisfactory performance and safety. According to Lenz e Silva (2007), the properties that differ refractories in terms of application and performance are:

- Density
- Porosity
- Modulus of elasticity
- Refractory
- Resistance to abrasion and erosion
- Mechanical resistance (compression and bending)
- Mechanical resistance under charge at high temperature
- Resistance to oxidation
- Resistance to flux and slag attack
- Thermal expansion and reversible dilation
- Thermal conductivity

In the case of LD converters, the adequacy of these properties is made according to the main wear mechanisms of the refractory bricks used in this equipment, which, according to Bilgiç (2005), are:

- Chemical corrosion
- Hydration
- Steel and slag infiltration
- Oxidation
- Mechanical erosion
- Wear and mechanical impact
- Thermomechanical stresses
- Thermomechanical fatigue

In order to better understand the different refractory regions that make up a LD converter and its main wear mechanisms, we can divide the converter into 6 regions,

namely: mouth, upper cone, taphole, cylinder (trunnions), low Cone and bottom. Still, there are several possibilities and types of refractories and thicknesses used in this type of metallurgical reactor, which will depend, in general, on the type of request in each region (Figure 11).

Figure 11 – Schematic representation of typical region of a LD Convert

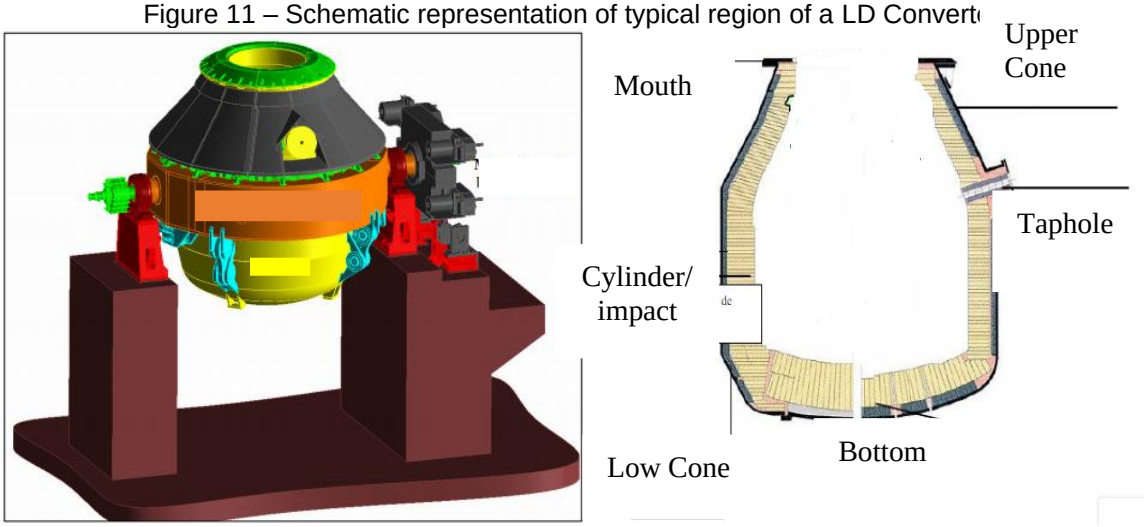

Source: Reference A (CHAVES, 2006) and B (LENZ e SILVA, 2009).

The upper region of the converter is made up of the mouth (region where scrap, pig iron, fluxes are charged and where the end-of-process slag is removed), the upper cone and the taphole (where the steel is removed from the furnace). The intermediate part is basically composed of the cylinder (region where the trunnions are), which is followed by the lower cone and the bottom, which constitute the bottom part of the converter. In the bottom there are still a porous structure through which inert gases are blown for homogenization and improvement in the metallurgical efficiency of steel manufacturing.

The main phenomena and refractory wear mechanisms of each of the regions mentioned above can be summarized as follows:

1-Mouth:

- Erosion: during the removed of the slag (fluid), there is an erosive and corrosive process resulting from the movement of the oxidized slag at temperatures above 1680 °C that passes through the mouth area. Slag with high temperatures intensifies the erosive and corrosive process of refractories in this region. However, as there is the formation, during

blowing, of a kind of “shell” in the mouth, this mechanism can be minimized. In addition, the slag itself, when in contact with the mouth, solidifies and forms a shell and, consequently, a protective layer.

- Abrasion: The movement of solid particles that pass through this region during oxygen blowing at high speeds can generate refractory degradation by abrasion.
- Mechanical removal: During the mechanical removal of the scum accumulated in the region of the mouth, there is the possibility of partial or total removal of the refractory from the mouth, since the scum is adhered to the refractory. This causes severe wear or even partial loss of the lining.
- Poorly dimensioned post-combustion processes and poorly executed mouth blowing can greatly degrade this region.

2-Upper Cone:

The upper cone has different wear processes depending on its regions. In general, the following refractory wear processes stand out:

- The tap region, close to the taphole, suffers the same wear mechanism as the taphole region in the cylinder (erosion and abrasion).
- In the region of the trunnion line in the upper cone/cylinder, the occurrence of wear due to abrasion prevails. This is due to the output of particles at high temperature and with high kinetic energy. In equipment that occurs post-combustion phenomena, high wear can occur due to the intense energy released in this type of process.

3-Taphole:

Critical region of the furnace due to the various refractory wear mechanisms that act together in this region, most of which are associated with the intense and intermittent movement of steel in this region and the taphole changes that occur due to the natural process of wear. The following main wear mechanisms are highlighted:

- Erosion.
- Oxidation.
- Corrosion.
- Thermal shock.
- Mechanical impacts during the taphole change.

4-Cylinder:

- The cylindrical region can be subdivided into four parts: Taphole bed, charging bed, trunnions and taphole slag line. The taphole bed is subjected to contact with the metal and slag, thus suffering erosion and corrosion mechanisms, mainly in it's central part and in the region adjacent to the taphole. In the charging bed, mechanical refractory wear due to the impact of scrap and pig iron stands out. The slag line is subject to carbon oxidation due to the oxygen present in FeO and MnO. As for trunnions, the predominant refractory wear mechanism is in the oxidation process.

5-Lower cone:

- The lower cone is one of the most critical regions of the furnace, as steel and slag are in contact with this region at all times. In addition to the erosive process caused by the movement of fluids, the corrosive process due to slag attack stands out.
- Erosion.
- Corrosion.

6-Bottom:

- Wear is essentially promoted on the tuyeres due to the injection of gases through the bottom of the reactor. The most important mechanism in this case is Back Attack and the refractory thermoclasing mechanism. Also noteworthy are the impacts derived from the fluid dynamics of moving fluids and the jet of oxygen.

For Bilgiç (2005), Kawashima *et al*. (1990) and Takanaga (1993), the performance of the refractory lining for a converter strongly depends on the characteristics of the equipment, metallurgical practices, process variables and types of steel. However, one can generally mention the following wear mechanisms that determine the refractory performance of converters through the following illustration (Figure 12).

Figure 12 – Schematic representation of the wear mechanisms of refractories for LD Converter

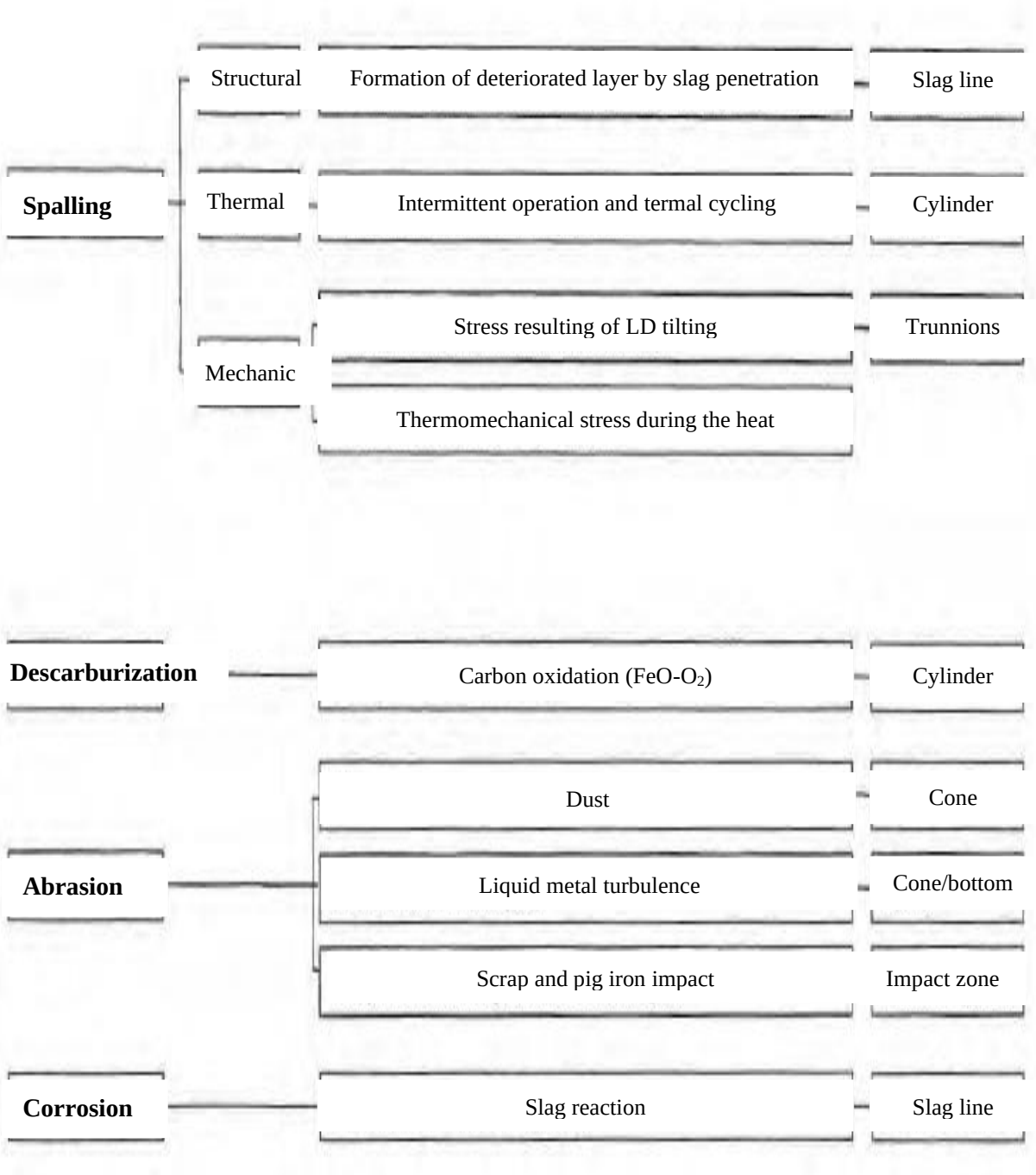

Source: Adapted fron the Kawashima *et al*. (1990).

A relevant factor is the resistance of the bricks to the propagation of cracks and fracture caused by thermal stresses. The ideal is to have bricks that, after the beginning of the formation of cracks or small fractures, manage to contain their propagation through the refractory structure. The wear mechanisms of greatest interest for this study are discussed below.

2.6.3 Refractory wear phenomena and mechanims in LD Converters

2.6.3.1 Chemical reaction of dissolution of the refractory MgO by slag generated in the processo of the LD Converters

The process of degradation and dissolution of the MgO aggregates of the refractory brick by the slag resulting from the metallurgical operations of the LD converter originates, in part, from chemical reactions and consequent dissolution by the compounds silicon (Si) of silica and CaO of lime. The theory indicates that initially the Si from the slag penetrates the grain boundary of periclase (MgO) separating and dissolving its crystals in the slag. In parallel, the FeO from the slag diffuses into the periclase crystals forming phases of low refractoriness, which are separated and dissolved in the slag. In certain situations, the refractoriness of the slag in contact with the surface of the refractory increases, increasing its viscosity. In this case, the layer of slag that adheres to the surface of the brick can function as a protective layer, inhibiting or reducing the above effects.

Therefore, a favorable balance between the formation of the slag layer and the dissolution of MgO from the refractory matrix must occur. One of the factors that favors the balance in the sense of refractory protection is the purity of the graphite (reduction of the wettability of the refractory by the slag) combined with the purity and grain size of MgO (greater grain size and purity reduces the contact surface and reactivity of MgO), besides, of course, the saturation of the slag in MgO (reduction of the chemical gradient of MgO between slag and refractory and increase of the viscosity of the slag). Thus, the rate of wear of the brick by corrosion depends on the nature of the phenomena described above.

There are some hypotheses about how the corrosion process occurs in the refractory matrix of MgO-C bricks. The most cited in the literature proposes three steps for the corrosion process considering a typical converter slag (CaO = 42%, SiO_2 = 13%, Al_2O_3 = 9%, iron oxides = 20%, MgO = 8%, MnO = 8 %, CaO/SiO_2 = 3), namely: (i) the Fe_2O_3 in the slag attacks the MgO aggregates, which causes the formation of a solid magnesium-wustite solution that is dissolved in the slag; (ii) the remaining Fe_2O_3 oxidizes the graphite in the brick matrix; (iii) the slag basicity reduces at the brick interface and accelerates the dissolution of MgO in the slag (TAKEDA *et al*., 2001).

2.6.3.2 Carbon loss from refractories bricks due to oxidation

Basically, there are 4 carbon removal reactions from the refractories bricks resulting from oxidation. This removal is by iron oxides in the slag, $O_{2(g)}$, $CO_{2(g)}$ from the ambient gas and carbon reactions with MgO.

2.6.3.2.1 Oxidation by iron oxides of the slag

The influence of the percentage of iron oxides in the slag on the wear of MgO-C bricks is illustrated in figure 13. It is believed that the refractory wear comes from the increase in the solubility of MgO in the slag with the increase in the iron content (Fe) total in the slag and the oxidation of carbon in the brick promoted by FeO and Fe_2O_3.

Figure 13 – Wear rate of MgO-C bricks as a function of the amout of total iron in the slag

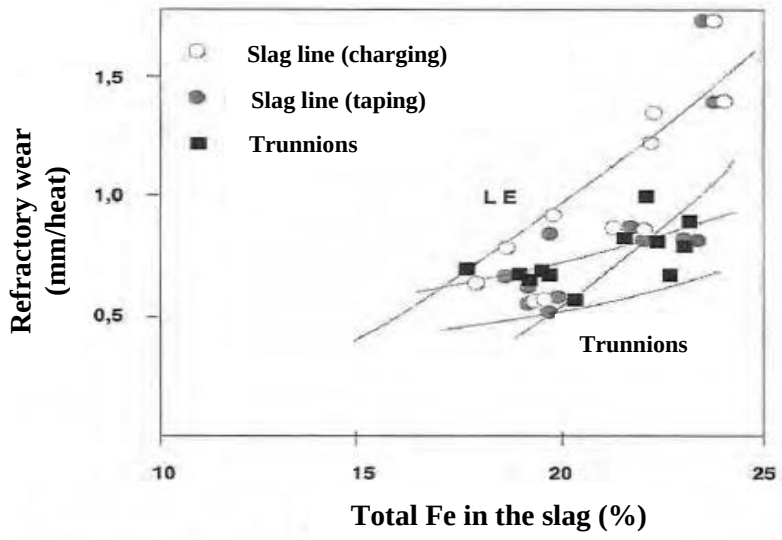

Source: Takanaga (1993).

The oxidation of carbon in the refractory matrix directly affects the wettability and open porosity of the refractory. In the case of carbon reduction, both properties increase significantly, which can lead to a significant increase in slag penetration into the refractory matrix which, in turn, will promote greater reactivity of the slag with the MgO aggregates in the refractory, resulting in phenomena such as the dissolution of the MgO matrix. According to Takanaga (1993), the trunnions region is less affected by the effects of carbon oxidation by the iron oxides of the slag if a slag layer is formed (processes where there is Slag Splashing). However, wear in the slag line is

more severe due to the dragging of the slag layer by the liquid steel jet, that is, erosion and corrosive phenomena coexist in this region.

2.6.3.2.2 Carbon oxidation by $O_{2(g)}$ e $CO_{2(g)}$

For Takanaga (1993), carbon is stable during oxygen blowing in the converter, since the partial pressure of oxygen in this step does not assume considerable values. Therefore, oxidation of the refractory by atmospheric oxygen becomes relevant after taping the steel due to the air entering the converter and not during the oxygen blow. If the refractory lining is covered by the slag layer formed by Slag Splashing and Slag Coating practices, oxidation of the carbon in the brick is not a cause for concern. In situations where this practice is not carried out or is carried out inefficiently, eventual refractory wear due to carbon oxidation can be significant. Figure 14 illustrates the effects of Slag Coating on lining refractories decarburization.

For Takanaga (1993), oxidation phenomena are rarely observed due to the beneficial effects (protection) of Slag Coating or Slag Splashing above 1000 °C, although oxidation by oxygen in the atmosphere becomes relevant when the temperature of the refractory lining reaches values below 1000 °C. For the refractory lining without the protective layer, the effects are opposite.

Figure 14 – Oxidation (decarburization) of the refractory MgO-C bricks lining as a function of temperature with and without coating by the pratice of a slag coating

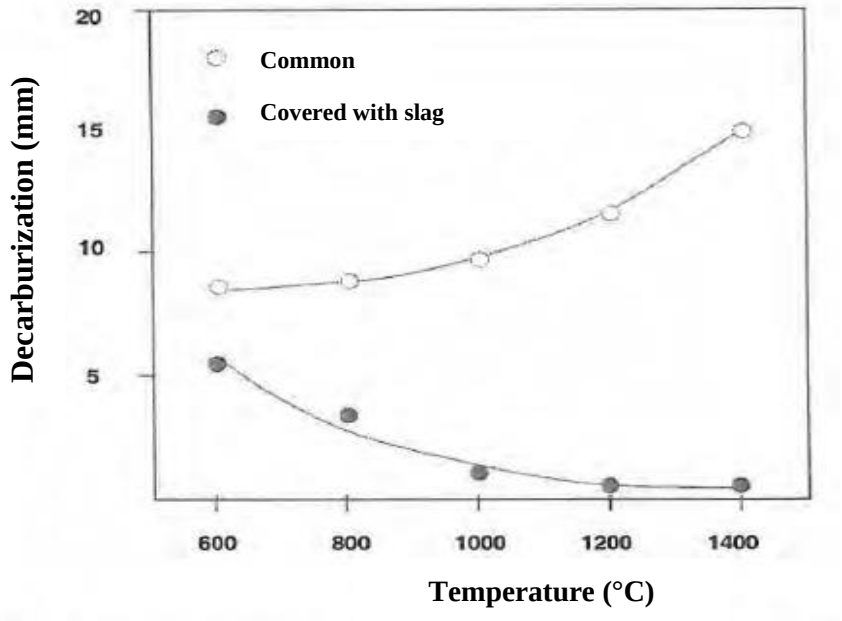

Source: Takanaga (1993).

2.6.3.2.3 Carbon oxidation by MgO of the refractory brick

An interesting and possible phenomenon is the oxidation of carbon by MgO in the refractory itself. Generally these phases (MgO and C) coexist stably at temperatures below 1400 °C. However, the reaction ($MgO_{(s)} + C_{(s)} = Mg_{(g)} + CO_{(g)}$) can occur at certain temperatures above 1400 °C. In these cases, the $Mg_{(g)}$ and $CO_{(g)}$ phases tend to migrate through the pores and escape from the refractory through its hot face, causing structural deterioration of the brick. For this degradation mechanism to be controlled, it is necessary that $Mg_{(g)}$ must be oxidized again to form a protective layer on the reaction front, thus inhibiting the continuity or speed of the process.

2.6.3.3 Refractory wear due to scrap impact and liquid pig iron jet

This type of refractory wear is characterized by the physical nature of the phenomenon, that is, the impacts caused by scrap and liquid pig iron colliding with the refractories bricks during furnace charging promote the degradation of the refractory matrix. In addition, the abrasion and erosion caused during the charging of liquid pig iron contribute to the wear process. In this case, the increase in the hot mechanical resistance of the brick contributes to significantly reduce the wear. The production of refarctories bricks with high mechanical strength is linked to the use of high-performance presses and equipment for extracting gases during brick pressing, which provide high-density structures.

Alternatives such as the addition of metallic antioxidants such as aluminum powder can bring about an increase in mechanical strength through the formation of secondary phases of high resistance, such as $Al_4C_{3(s)}$ and $MgO.Al_2O_{3(s)}$. However, there are deleterious effects of increasing the mechanical strength, such as the reduction in the total fracture energy, which can lead to the propagation of cracks in the refractory and reduced its thermal shock resistance, leading to the collapse of the structure.

2.6.3.4 Refractory wear due to impact and movement of the liquid steel jet

This type of refractory wear is totally linked to fluid dynamics resulting from the movement of steel inside the LD due to the jet of oxygen from the lance and the

blowing of inert gas through the bottom (tuyers) of the furnace. In both cases the predominant phenomenon is the erosive process due to fluid movements at high temperatures inside the LD. The control variables for this effect are linked to the flow rates of the jet of oxygen from the lance and the tuyers, together with the respective lance heights and distribution geometry of the tuyers.

2.6.3.5 Refractory wear due to TiO_2 in the LD slag

Studies carried out by Prudente, Fera and Alentini (2006) revealed possible refractories wear in the lower region of the cone and in the junction with the bottom of the LD, which may be correlated with the presence of TiO_2 in the slag. The authors suggest that the high concentration of this compound in the LD slag reduced the refractory life by approximately 20%. However, for a better understanding of this behavior, a deeper analysis is necessary, which is not the focus of this work.

Figure 15 – Refractory wear rate as a function to percentage of TiO_2 in the LD slag

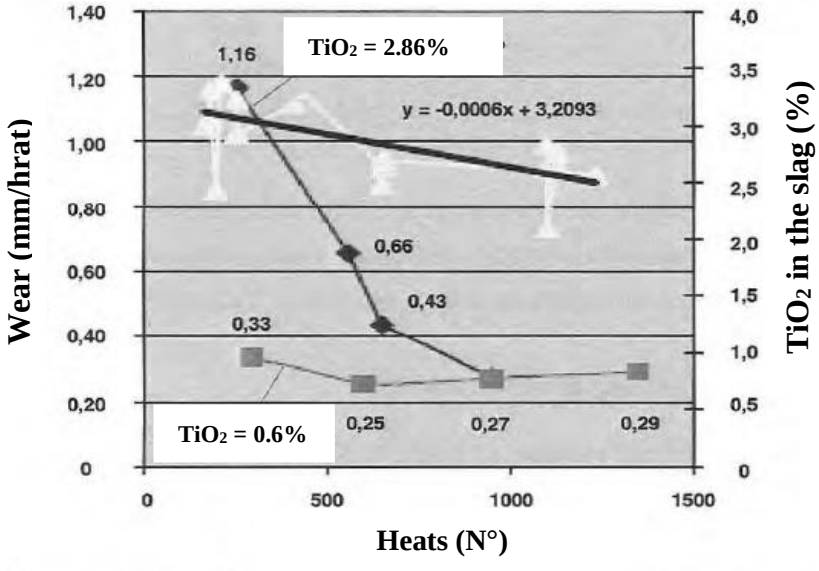

Source: Prudente, Fera and Alentini (2006).

2.6.3.6 Refractory wear due to structural thermal spalling

Takanga (1993) related the wear of LD bricks by mechanism known as Spalling to the stresses generated during successive thermal shocks and the consequent thermomechanical stresses caused by the imbalance of the structure of the refractory lining. Mechanical properties such as flexural strength, modulus of

elasticity and total fracture energy are crucial for good performance. The percentage of carbon in the bricks is added as a determining factor to reduce such wear generated by thermal variations due to oscillations in operational cycles. Refractories considered to be of satisfactory performance contain at least 10% of carbon. Values between 15% and 20% of carbon are among those with the highest performance in terms of containment of crack propagation. For Takanga (1993), spalling wear has been observed in special regions such as tuyeres and converters whose lining are subject to severe operating conditions.

2.6.3.7 Final consideration about refractory wear due to carbon oxidation

Refractory structures containing carbon under normal atmosphere (air) and high temperatures are subject to the reaction of gaseous oxygen with the carbon of the binder and with the carbon of the graphite, causing the deterioration of the chemical and physical properties of these materials (RIGAUD *et al*., 1993). In addition, refractory decarburization and, as a result, its performance generally depends on the atmosphere, temperature, operating practices of steelmaking equipment and refractory properties, which, in turn, are influenced by the purity of the raw materials, type and amount of carbon and antioxidants. A good example of these variables is the temperature range at which carbon is oxidized, which depends on whether the carbon comes from the binder or graphite. In general, the carbon in the binder oxidizes (Figure 16) at a temperature lower than that of graphite (TAKEUCHI; YOSHIDA; TSUBOI, 2003).

Figure 16 – Weigth loss of graphite and phenolic resin by oxidation in air

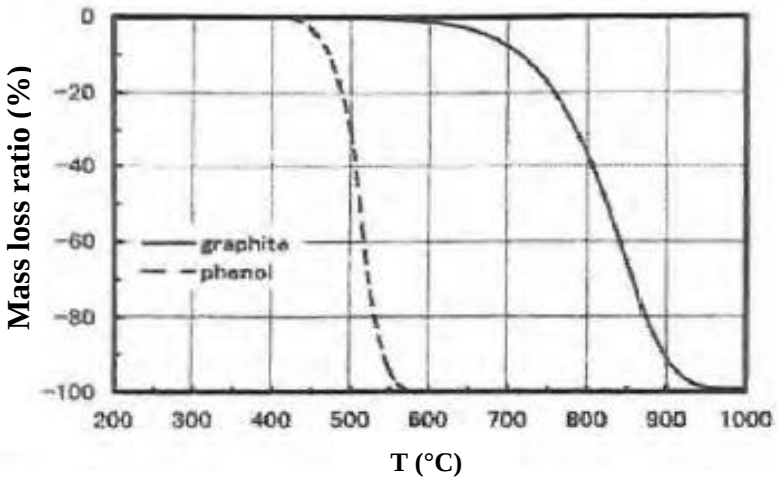

Source: Quintela (2003).

The oxidation of carbon in refractories can occur in three ways: oxidation by gaseous, liquid and solid phases. For Li, Rigaud and Palco (1993), carbon oxidation in the MgO-C system occurs mainly by direct oxidation and/or indirect oxidation according to the equations below, which depend on the temperature and system atmosphere.

$$2C_{(s)} + O_{2(g)} = CO_{(g)} \quad (3)$$
$$MgO_{(s)} + C_{(s)} = Mg_{(g)} + CO_{(g)} \quad (4)$$

For Zhang, Marriott and Lee (2001), carbon oxidation occurs through direct contact of $C_{(s)}$ in the refractory brick with $O_{2(g)}$ in the atmosphere.

$$C_{(s)} + O_{2(g)} = CO_{2(g)} \quad (5)$$

Experimentally, after testing to assess resistance to attack by slag, it was also verified that in cases where there is the presence of metallic Fe and Mn in the decarburized layer of samples of MgO-C bricks, containing antioxidants, there is the possibility of a reduction of $FeO_{(l)}$ and $MnO_{(l)}$ of the slag by the carbon of the brick.

$$C_{(s)} + x\ FeO_{(l)} = x\ Fe_{(l)} + CO_{(g)} \quad (6)$$
$$C_{(s)} + MnO_{(l)} = Mn_{(g,\,l)} + CO_{(g)} \quad (7)$$

When talking about oxidation resistance in carbon-containing refractories, temperature, oxygen partial pressure, oxygen availability and carbon reactivity are the main process variables to be controlled. The availability of oxygen to the reaction centers in the refractory structure is primarily determined by the connected porosity. For a given fixed value of temperature and partial pressure of oxygen, the most effective measure to improve the oxidation resistance is to block the pores (RIGAUD *et al*., 1993; YAMAGUCHI, 1984; YAMAGUCHI; KUN, 1984).

An effective approach to control and reduce refractory decarburization is the addition of metallic (Al, Si, Mg and Al-Si and Al-Mg alloys) and intermetallic (B_4C and CaB_6) antioxidant agents that, through different mechanisms, can inhibit carbon oxidation.

For most experts, gas phase oxidation (direct oxidation) is the most relevant mechanism for carbon loss in refractories, which has been the focus in the development of carbon-containing bricks (ICHIKAWA; NISHIO; HOSHIYAMA, 1994).

Under high thermal conditions, carbon oxidation can be much more pronounced and, in this case, the open pores become pathways for the gaseous phases to penetrate throughout the refractory structure.

An accepted mechanism for carbon oxidation would be that the carbon contained in the pore path and the carbon present in the walls are oxidized by oxygen from the air. Under multiple thermal cycling, there is an increase in refractory pore size due to continuous carbon oxidation. This mechanism can be observed on the cold face of bricks containing carbon after their industrial use, since, in this particular case, the oxidized layer of the refractory, which is fragile by nature, would not be removed.

The most relevant variables for porosity control are the technology for processing and pressing refractory bricks and the type of resin. The level of open porosity can be reached with a pressing condition, but if the decomposition of the phenolic resin occurs, between 200 °C and 800 °C, which is used as a binder, an excess of volatile materials such as $H_2O_{(g)}$, $H2_{(g)}$, $CO_{(g)}$ and $CO_{2(g)}$ will occur. The evaporation of volatile materials during the lining start-up causes the formation of fine channels in the refractory matrix, which connect the inside of the brick to its surfaces, thus increasing the initial porosity of the refractory.

Considering the decomposition of the phenolic resin at 300 °C and rapid heating at 600 °C, the volumes of gases evaporated at the respective temperatures were determined by the gas state equation. Assuming that the gases generated are ideal gases, that the gases evaporate when a given pressure (P) is reached and the volume of gases is proportional to the temperature, a greater amount of pores would be obtained for a temperature of 600 °C. Therefore, the initial heating of the lining at low temperatures to allow the gradual evaporation of the gases is of great importance in order not to negatively affect its structural integrity.

2.6.4 Refractory protection and maintenance mechanisms for LD

There are several preservation practices and refractory maintenance in LD's. Those in which repair masses are used and those that use slag from the process itself stand out. In addition, some operational practices can bring satisfactory results in order to contribute to extending the life of the refractories bricks while maintaining operational safety.

2.6.4.1 Maintenance and repair techniques for refractories in LD

In general, we consider hot and cold repair refractories techniques to be the two main practices for repairing refractory converter linings. However, due to operational and safety difficulties, we practically only use hot repair techniques on LD converters.

To the frequency of LD repairs to be low and consequently the availability of the LD furnace for production to be high, it is essential to keep the refractory bricks always covered with the process slag itself. This will reduce the wear refractory rate, as the formation of this layer of slag on the bricks known as a coat or coating will be effective against virtually all wear mechanisms such as abrasion, corrosion, erosion, oxidation and thermoclase.

The process conditions and slag adjustment are fundamental for a good formation of an adequate coat. In addition, adjusting the type of hot repair to be done will depend on the region and the prevailing wear mechanism in the specific region.

The common types of techniques used in converters can be divided into Slag Splashing, Slag Coating, poured masses and refractory mass projections. The first two are known as low-cost, fast-running maintenance techniques. The last two are known as recovery techniques that demand more execution time and have higher costs.

2.6.4.1.1 Coating as protection of the refractory in LD

The formation of a layer of highly refractory slag and/or refractory mass with high adhesion capacity in refractory bricks is the most effective method for protection against the main wear mechanisms listed above.

Covering the surface of the working refractory lining creates a physical barrier to decarburization, infiltration and reaction of lower melting point phases and acts as a barrier to abrasion and erosion of the refractory bricks.

Some authors also mention the possibility of the layer of slag and/or refractory mass forming a kind of thermal block in the sense of reducing and stabilizing the thermal gradients between the hot and cold face of the refractory bricks, which could reduce thermomechanical stresses and consequently decrease the intensity of generation of cracks and the phenomena resulting from thermoclase.

2.6.4.1.1.1 Slag Coating

As soon as the tapping of steel from the converter is completed, material (dolomite generally) is added or not (depending on the thermochemical conditions of the slag) to the slag in order to make it more suitable for protecting the refractory. A distribution of the slag can also be carried out in order to adjust its volume to the process conditions. The addition of materials and the adjustment in the volume of the slag are aimed at reducing the temperature, adjusting the fraction of solids and their viscosity to obtain phases of high refractoriness and adherence to the walls of the bricks.

Next, the converter is tilted in the direction of the steel tapping bed towards the scrap impact region so that the slag covers these regions and forms a protective layer (coating). Slag Coating can be carried out with or without Slag Splashing, but it is more appropriate to carry out it after this process, since the process slag will be in an optimal condition due to the Slag Splashing preparation process itself. If you don't have the necessary equipment for the Slag Splashing technique, the Slag Coating technique is performed in practically all heats.

2.6.4.1.1.2 Slag Splashing

The process or technique known as Slag Splashing consists of the use of blowing with the oxygen lance using an inert gas (generally nitrogen) through which the energy of the gas jet is transferred directly to the slag at the end of the process duly adjusted with additions of specific scorifiers, which leads it to be projected onto the refractory LD lining (Figure 17). When projected on the surface of the refractories bricks, if its properties are adequate, there will be the formation of a layer of slag that will cover and protect the bricks. The advantage of this technique when compared to the Slag Coating is that the entire LD will be covered with slag, not just the taping bed and scrap impact region.

In general, this is the most effective technique to reduce the refractory wear. This technique began in North America at the Indiana Harbor plant, which in 1994 reached 13,568 heats in the LD (MILLS *et al*., 2005). Basically, we have two types of Slag Splashing practices, namely: Slag Washing and Slag Ejection.

Figure 17 – Schematic representation of the Slag Splashing

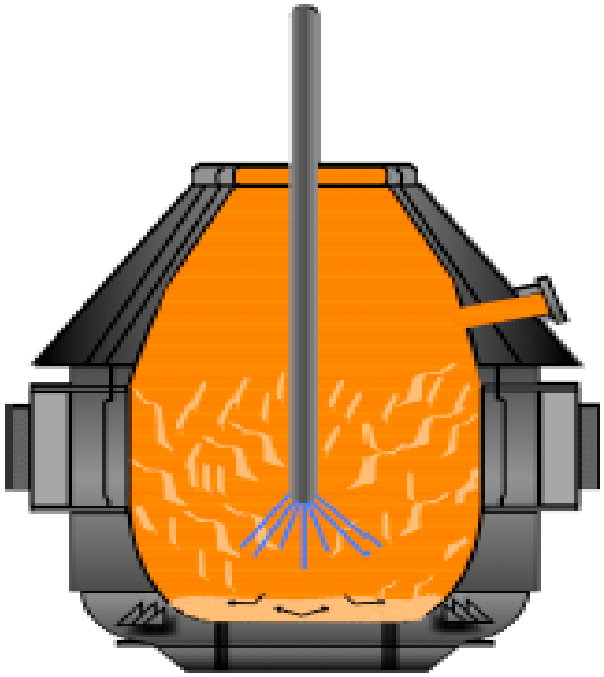

Source: Auad (2011).

Slag Washing consists of moving the slag over the converter wall, which can result in the solidification of a protective layer of slag on the furnace walls, if the slag has adequate properties (MILLS *et al*., 2005). In the Slag Ejection process, the slag is projected onto the furnace walls and, as it cool down, it forms a protective layer over the refractory structure.

Regardless of the type to be practiced, the factors that influence the refractory protection effectiveness of this technique are the blown gas flow, lance height, lance type, additions and slag properties. The speed and angle of projection of the slag define the characteristics of the jet (MILLS *et al*., 2005).

The practice of Slag Splashing, in general, occurs as follows. After tapping the steel from the converter into the ladle and after evaluating the end-of-blow parameters of the steel and slag (visual observation is also extremely important), the additions of the MgO source are added. If the volume of slag is high, this slag is partitioned in an adequate amount. During this period the furnace refractory can be evaluated if necessary. Position the converter vertically and charging the additives (dolomite) to adjust the slag, if necessary. Soon after, the oxygen blowing lance is lowered to a predetermined position and inert gas (generally nitrogen) is injected.

During blowing, adjustments to the height of this lance are desired and can be programmed in order to reach specific regions of the furnace with slag projections. The idea is to cover the entire refractory lining of the furnace or target a specific area (generally with the greatest wear). The blowing time is also predetermined and varies according to the characteristics of the slag. After the pre-established blowing time, it is interrupted and the boom is raised. It is very effective that after the blowing has ended, the converter is tipped to perform the bath with the slag remaining from the slag splashing. Then, the process ends with tipping of the converter to remove the remaining slag.

In situations where time is available, the remaining slag from the Slag Splashing process can be used to cover specific regions (such as those with high wear), such as the scrap charging region, bottom of the LD or steel tapping bed, through the practice of *Slag Coating* or simply leaving the converter stopped with the slag deposited on the specific region.

Figure 18 – Phase distribution and velocity vectors in a BOF converter. The Slag Splashing mechanisms are checked. The bue color represents the nitrogen and the red the slag

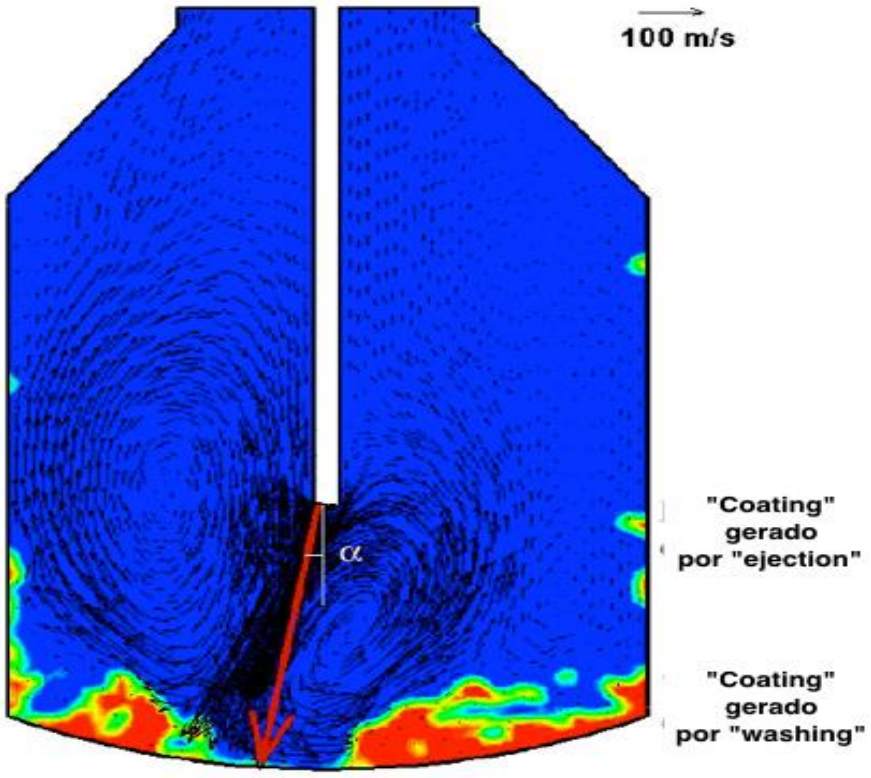

Source: Barron and Hileiro (2011).

2.6.4.2 Fundamentals of refractory protection of LDs with slag

The protection of the refractory structure through the use of slag from the process itself is based on the effectiveness of transporting the slag to the refractory and on its ability to adhere and remain on the refractories bricks. In this case, analyzing the kinetic and thermodynamic fundamentals is necessary to understand the slag adhesion mechanism at the refractory interface.

The approach taken by Yuan *et al*. (2013) describes well the kinetic aspects of the reaction liquid phase with solid phase. When the thermodynamic conditions are not impeditive for the occurrence of the process, the basic conditions for a reaction to occur from the point of view of kinetics are the transport of the material to the reaction interface, the reaction itself and the transport of the reaction products to outside the reaction interface zone, the first two being the process controllers. Therefore, it is necessary to control the penetration of the slag into the open porosities and irregularities of the hot face surface of the refractory material and the dissolution reaction of the slag with the refractory phases. An interesting fact is still the possibilities of corrosion, being active corrosion and passive corrosion that presupposes either the formation of dense phases to block the active corrosion reaction front or the formation of a coating protecting the working refractory. In the case of refractory working coatings for converters, a dense layer of MgO is formed through reduction, sublimation and subsequent oxidation of periclase and/or the formation of the coating itself.

According to Lee (2004) and Riaz, Mills and Bain (2002), it is possible to quantify the penetration rate of the slag in the refractory structure and quantifies the influence of the refractory microstructure represented by the pore size, the interfacial energy and the effect of slag viscosity, which is a function of temperature and the solid phases formed.

$$l^2 = \cos(\theta/4) * ((\Upsilon * r) / \eta)) * t \quad (8)$$

Equation 8 establishes the following parameters: depth of penetration l (m) of the slag, r is the open porosity of the refractory (m), ɳ is the viscosity of the slag (Pa.s), Ɣ is the surface tension of the slag (Nm^{-1}) and ɵ is the contact angle between the slag and the working refractory (degrees) and t is the contact time (s).

The surface tension and viscosity of the slag have a great influence on the reaction rate, since a higher surface tension and lower viscosity will imply greater penetrability of the slag and will increase the depth of penetration of the slag into the refractory structure of the working lining, which will increase the speed and area of reaction and consequent degradation of the refractory structure.

The control of these two important properties of the slag involves controlling the temperature, percentage of MgO and iron oxide in the slag. There are even optimal dissolved oxygen values for the adequacy of these slag parameters that are in balance with the FeO concentration values in the slag so that Slag Splashing and Slag Coating practices are effective (MILLS *et al*., 2005).

Figure 19 – Sensitivity analysis of viscosity variation, contact angle and interfacial tension as a function of penetration depth

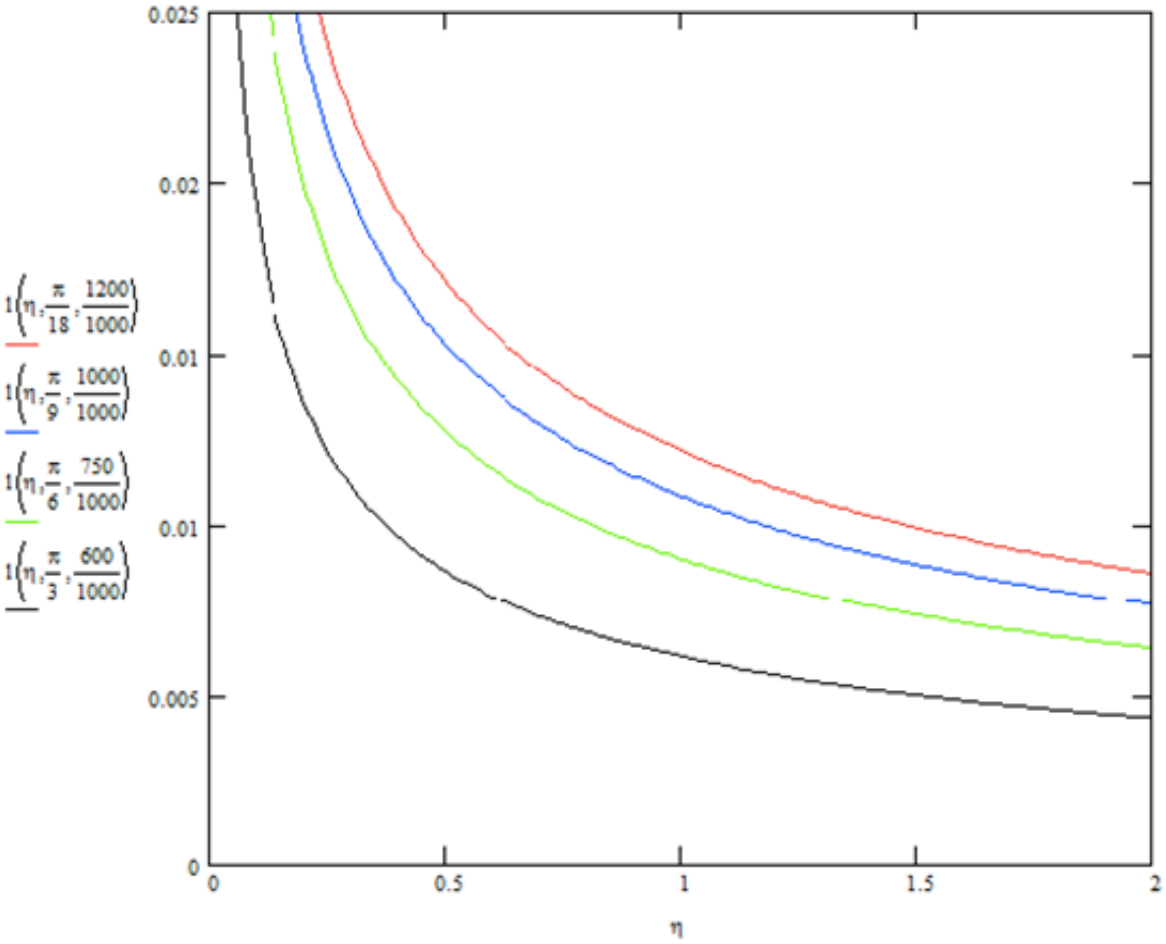

Source: Auad (2018).

According to Auad (2018), the controlling step of the process is dissolution and, in the Slag Splashing and Slag Coating processes, the controlling step is the

penetration of the slag, forming an infiltrated layer between the slag and the refractory. This author states that the infiltrated layer is in the range of 5 to 10 mm, there being an optimal range of slag property that would suit the real values.

The slag layer is formed, initially, by the mechanical transport of the slag over the refractory, followed by the adhesion of the slag to the surface of the refractory or to the surface of the previously adhered slag and subsequent hardening and solidification of the slag in the refractory lining (BARRON *et al*., 2014).

The drop in temperature of the slag together with the increase in solid phases promotes hardening with consequent solidification and adhesion on the hot face of the refractory. In this context, it is worth mentioning the importance of the slag containing a minimum percentage of liquid phases, as a slag with only solid parts would not be able to wet the refractory (YUAN *et al*., 2013).

For Auad (2018), there is the possibility of forming a layer of Fe compounds between the refractory and the slag layer, making the protective layer of slag susceptible to failure (Figure 20). Auad (2018) also reveals the possibility that slag with liquid phases has sufficient fluidity to infiltrate the pores and cause fractures inherent to the surface of the MgO-C material, generated by decarburization and/or thermomechanical processes. The ideal in these cases is the formation of a good coating that would be the formation of a layer composed of [(Mg,Mn,Fe)O)] that would favor the development/adhesion and mechanical resistance in the coating (Figure 20).

Figure 20 – Interface aspect of splashing slag slag and MgO-C refractory

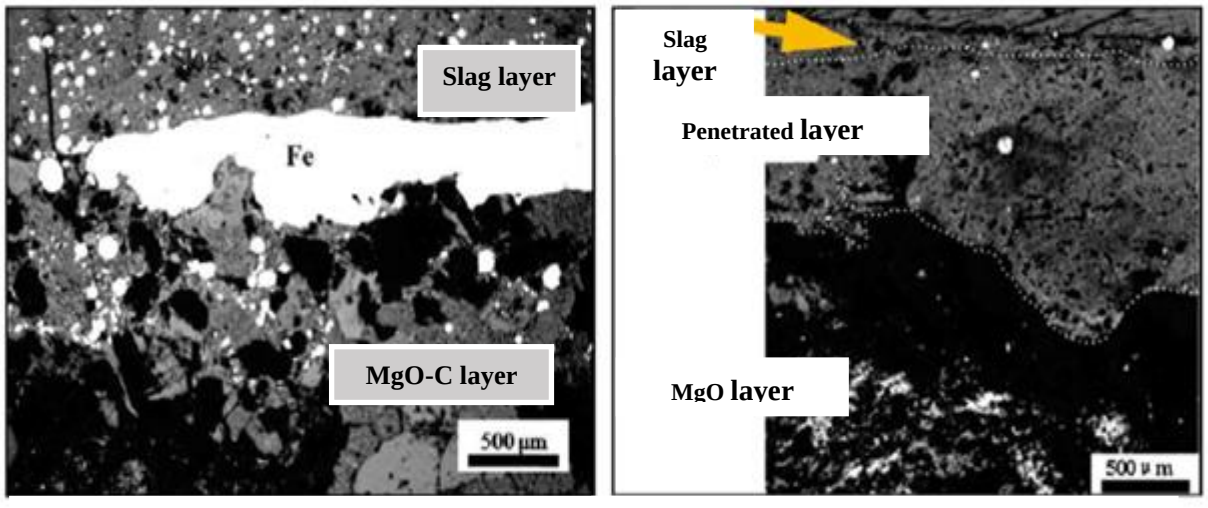

(B) Slag with 100% solid phase **(A) Slag with liquid and solid phase**

Source: Auad (2018).

For Yuan (2013), there is a time limit after which, for a given temperature, the contact angle between the slag and the refractory will stop varying. From this point on, the adherence of the coating to the refractory during the Slag Splashing process is reduced. These factors are related to time, temperature and reduction of iron oxides by carbon.

For Auad (2018), some details should be considered when using the fundamentals exposed by Yuan *et al*. (2013), such as considering a MgO-C refractory without decarburization to carry out the tests. This assumption implies that the iron oxide in the slag will be reduced by the carbon in the refractory.

This fact will probably not occur if the refractory already has a decarburized layer or if there is already slag on top of the refractory, which is closer to the actual boundary conditions. It is concluded in this case that, in addition to affecting the viscosity and the formation of solid phases, the iron oxide will determine the wettability and consequently the interfacial tension of the refractory by the slag. An important factor to be considered is how the slag properties and blowing patterns of Slag Splashing influence the volume of slag formed and projected onto the walls of the refractory structure. For Barro and Hilerio (2011), the important variables to determine the fraction of the projected slag volume are the height of the blowing lance, the jet velocity, the jet exit angle and the viscosity of the slag.

The next parameter that can affect slag characteristics for effective coating is the effectiveness of this slag/refractory contact. This effectiveness is related to the effective viscosity of the slag, and there is an optimal viscosity value that will provide the best adhesion of the projected material. It is found that a lower viscosity increases the volume of material applied over a given area and generally incurs an increase in the thickness of the penetrated layer. However, low viscosity slags perform poorly in Slag Splashing and Slag Coating, and typically have a “runny appearance” and limited durability due to melting of the layer on the next heat.

Likewise, slags with very high viscosity do not adhere in the refractory wall and normally generate an ineffective coating. The above argument is in line with the range of dissolved oxygen in steel, considering that soluble oxygen in steel is associated with iron oxide in the slag which determine the fraction of solids and consequently the viscosity of the slag.

Figura 21 – Optimum point of suitability of the slag, for the practice of Slag Splashing, due to the increase in the fraction of solids

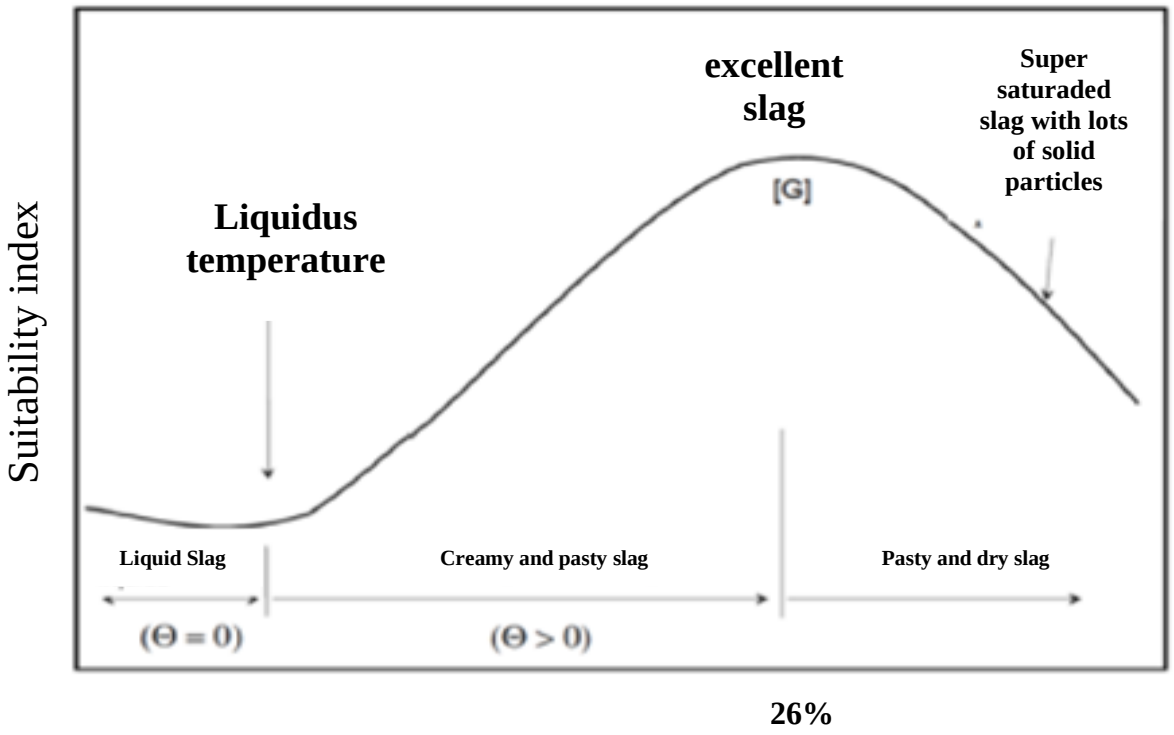

Source: Pretorius and Carlisle (1999).

Not necessarily a greater volume of slag per unit area transported to the refractory wall will be an optimal condition for Slag Splashing. In cases where the slag viscosity is low, will not have the best slag/refractory adhesion condition. Therefore, adhesion efficiency occurs under certain conditions and are dependent on the characteristics of the projected slag.

For Troiano *et al*. (2014), four regimes represent this adhesion system. The first one being represented by the adherent particle in contact with the adherent wall, the second by the non-adherent particle in contact with the adherent wall, the third by the adherent particle in contact with the non-adherent wall and the latter indicated by non-adherent particle in contact with non-adherent wall.

Figure 22 – Regimes for adhesion of particles to walls

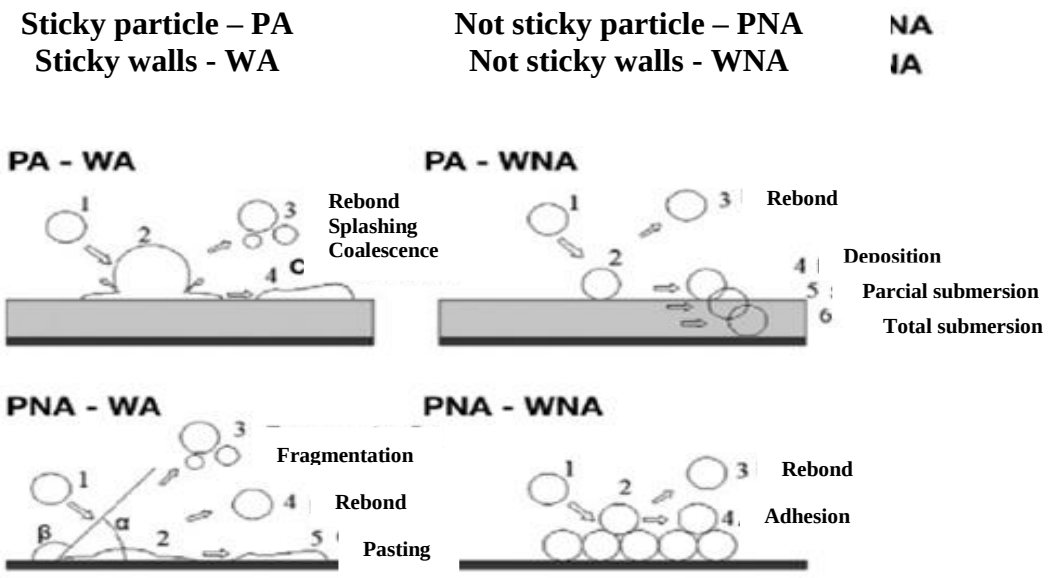

Source: Auad (2018).

The characteristics of the type of collision of the slag particles against the refractory wall will determine the effectiveness of the coating formation. Such collisions are characterized by a coefficient called coefficient of restitution (e). This parameter can be defined as the ratio of impact and rebound velocity. In numerical terms, when the coefficient (e=1) means a perfectly elastic rebound while (e=0) it means that all kinetic energy of the particle has dissipated after the impact.

Another relevant variable in adhesion efficiency is the capture velocity, in which an efficient impact is a function of particle size, density, surface energy and elastic properties of the particle and surface. At speeds higher than the capture speed, a greater proportion of rebound would occur (material that did not adhere to the refractory wall and consequently was not effective in refractory protection).

2.6.5 Materials used in slag ajustment for refractories coating processes

The three main factors that determine the best choice of slag fitting materials for Slag Coating and Slag Splashing are coating effectiveness, material cost and availability. From the metallurgical point of view, the ability to reduce the temperature and adjust the viscosity lead to the choice of materials with higher MgO contents. The following materials stand out as slag conditioners for LD (AUAD, 2018): Raw Dolomite ($CaCO_3$+$MgCO_3$), Calcitic Lime (CaO), Dolomitic Lime (CaO+MgO),

Magnesite ($MgCO_3$), Sources of high MgO content (such as materials that have expired their original function or scrap material used as briquetted bricks), Materials containing $Mg(OH)_2$.

Other ways of adjusting the slag would be the addition of materials that promote the deoxidation of the iron oxides in the slag after the end of the oxygen blow and during the depletion of the LD steel. This reduction reaction must be carried out before removing the steel to the ladle, since the liquid metal during the Slag Splashing process contributes negatively to the effectiveness of the process due to changes in the properties of the slag.

Alternative sources from recycled materials are also used, such as: leftovers from demolitions, projection rebounds from basic materials, such as (projection rebounds from RH snorkels, waste from distributors work masses, demolition of converter linings and steel ladle slag (AUAD, 2018).

For Deng and Du (2014), in relation to the comparison between dolomitic lime and raw dolomite in the slag adjustment processes for coating, the greater efficiency of raw dolomite in relation to calcined dolomite is due to the greater capacity of reducing the temperature of the slag and higher speed of CaO and MgO solubilization due to the rapid decomposition of carbonates into CaO and MgO at temperatures in the range of 1600 °C. For Auad (2018), “previously calcined materials have slower kinetics, which makes their solubilization difficult, causing a problem of slag accumulation in the LD bottom (slag built up)”. Auad (2018) also mentions the advantage of the higher density of raw dolomite (2840 kg/m^3) compared to calcined dolomite (920 kg/m^3).

In general, raw dolomite has advantages in terms of cost, handling and metallurgical efficiency when it comes to adjusting slag for coating processes. However, according to Auad (2018), “the use of carbonates (and hydroxides) has a limit in quantity, as additions above a limit can generate agitation and excessive slag foaming, leading to operational problems”. Therefore, stops must be established in addition models in order to establish limits on the amounts to be added of these materials that are normally established in a practical way.

2.7 Data Mining

One of the great challenges in obtaining and managing knowledge today is the analysis of the large volume of data generated in the most diverse areas of human knowledge. There are several sources and complexity of this data, and transforming them into useful information that can be used and generate applied knowledge is the great challenge of Data Mining tools.

For Han, Kamber and Pei (2012) Data Mining consists of the process of determining patterns and knowledge in large amounts of data, and these sources may come from the most diverse data sources.

The application of techniques and tools capable of analyzing large volumes of data is essential nowadays due to the limitation of human capacity in the face of such volume and complexity of trying to obtain knowledge that is, in a way, hidden in these large databases data.

For Fayyad *et al*. (1996), the determination of patterns, differences or similarities in large volumes of data makes the development of mining and analysis techniques the differential in the development and evolution of knowledge. Figure 23 illustrates the evolution and development of data analysis techniques and knowledge generation capabilities.

Figure 23 – Evolution of data science technology and gain in analytics

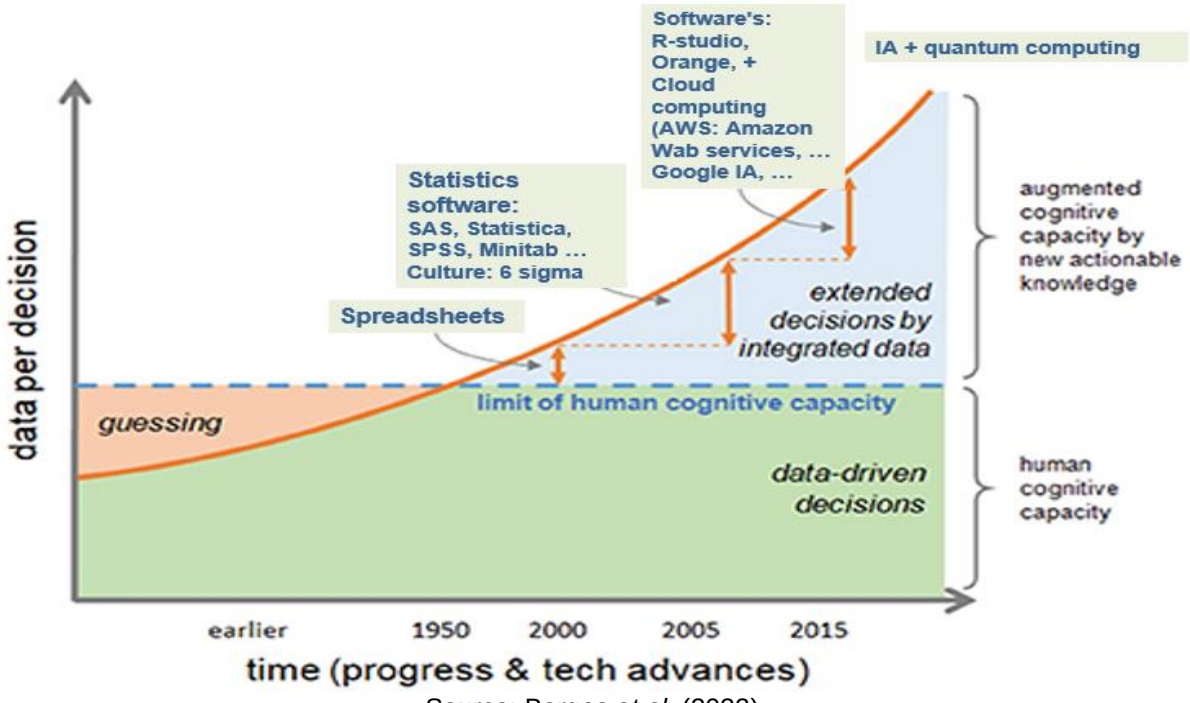

Source: Borges e*t al*. (2022).

When it is said that we are living in the information age, in fact, it would be correct to say that we are living in the data age. Virtually endless volumes of data are dumped on us every day mainly through computer networks and their various data storage devices.

Such gigantic growth in the amount of available data comes from the computerization of society and the rapid development of powerful tools and techniques for collecting and storing data. Large business groups around the world generate gigantic data sets, including transactions of the most different types such as engineering, medicine, sales, logistics, product descriptions, etc. A classic example is large stores such as Wal-Mart, which handle hundreds of millions of transactions a week in thousands of branches around the world.

Powerful and versatile tools are extremely necessary to identify valuable information from huge amounts of data and transform them into organized knowledge. All of this led to the birth of data mining. It is, therefore, a young, dynamic and promising field. Figures 24 and 25 illustrate the data mining and the evolution of data system technology.

Figure 24 – Data Mining process

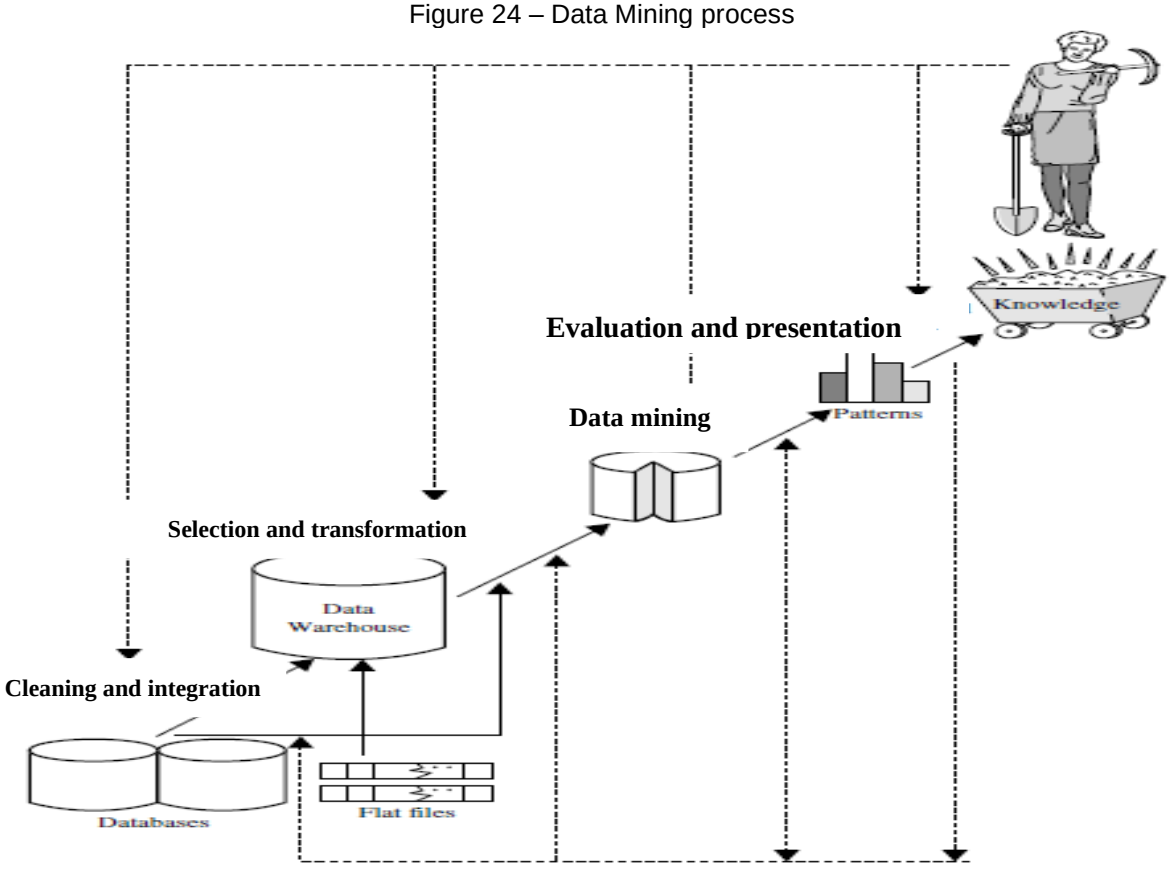

Source: Han, Kamber and Pei (2012).

Figure 25 – Evolution of data system technology

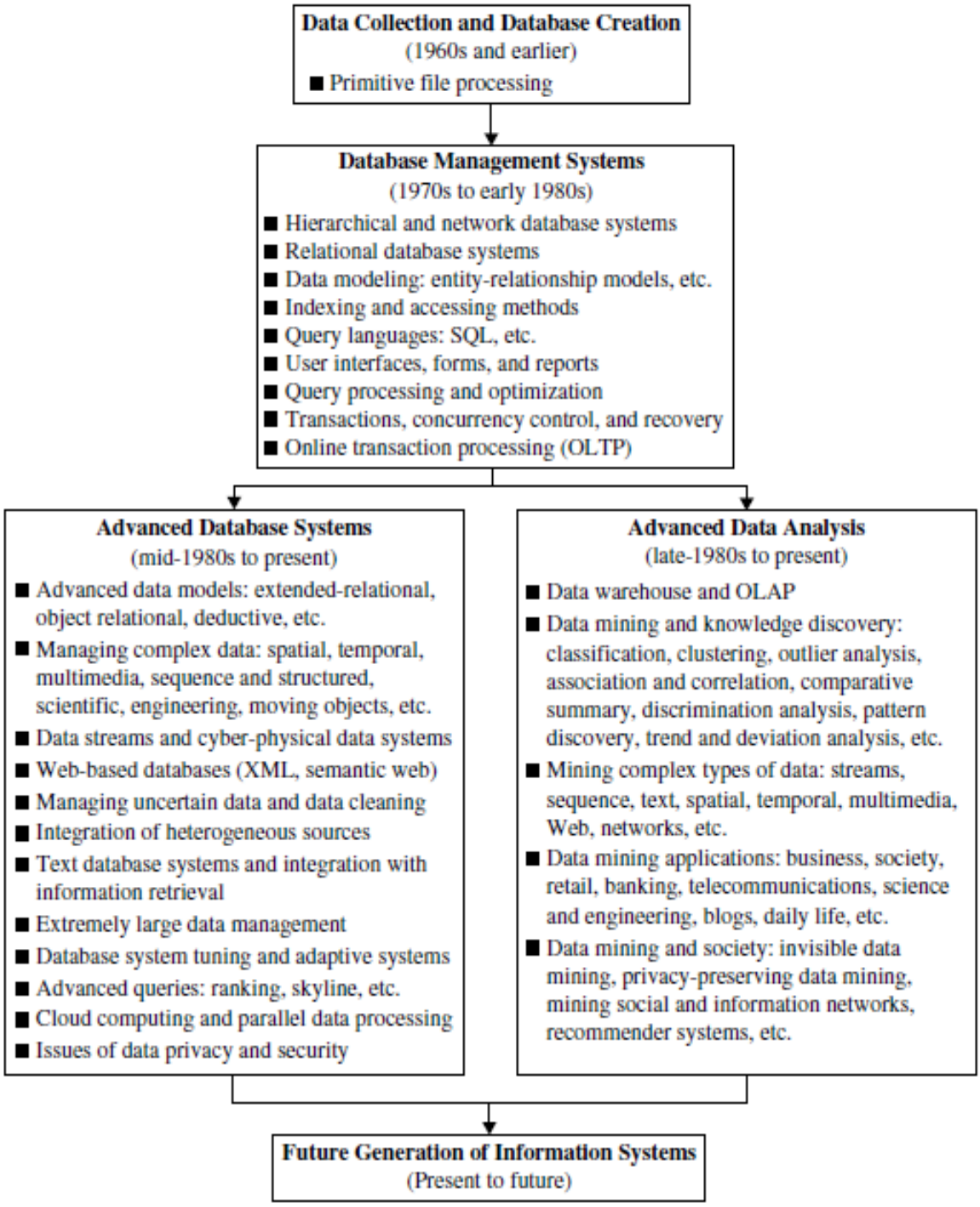

Source: Han, Kamber and Pei (2012).

The evolutionary process of data analysis tools allows us to analyze and make decisions faster, so that survival in different areas such as production, science and economics depends entirely on it. The improvement and development of techniques and tools started to give us more options than classic statistics. Tools such as Self Organization Maps (SOM), one of the objects of study in this work, expand the

capacity and speed of analysis of large volumes of data and large amounts of variables associated with a given process (Figure 26).

Figure 26 – Classical statistics versus new data analysis tools

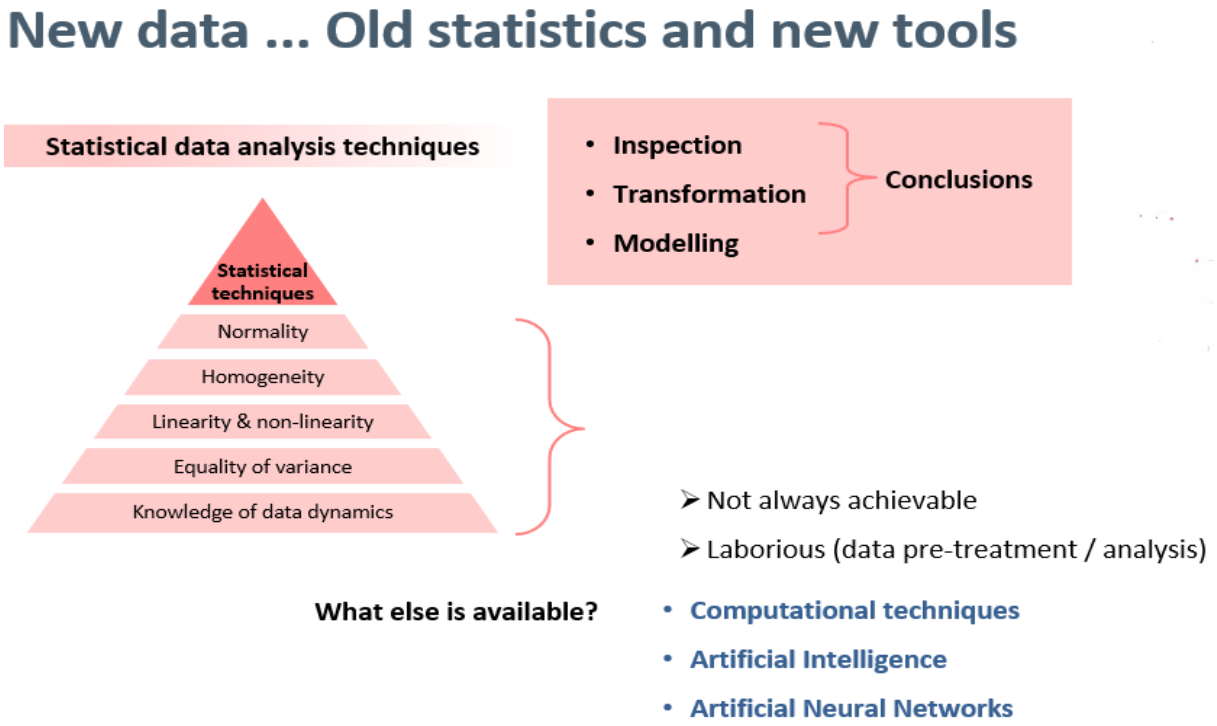

Source: Borges *et al*. (2022).

Techniques that are based on brain analysis behaviors, as well as statistical data analysis tools, play a key role. In this context, the SOM tool has great application potential, especially when talking about large amounts of variables and volume of data to be treated at the same time. For Zuchini (2003), the main characteristics that justify the application of SOM would be:

- Ability to operate with a large set of data;
- Ability to operate with data represented with a large number of characteristics (high dimensionality);
- Use of unsupervised learning;
- Ability to perform data projection;
- Ability to perform data reduction;
- Possibility of graphical evaluation of the obtained results;
- Simple and fast algorithms;
- Ability to generalize the models.

2.8 Conventional statistical analysis

It is possible, through “conventional” statistical modeling (univariate and multivariate analyses, statistical regression, etc.), to identify the main factors that influence certain parameters such as refractory wear (object of study in this work). The regression analysis aims to determine in the functional form ($y=y_0+ y_1x_1+y_2x_2+y_2x_1x_2+...+y_nx_1x_2...x_m+\varepsilon$) the relationship between the variables of interest, making it possible to make inferences about the parameters of the regression equation and estimate or predict the average response for a given input value (LENZ E SILVA, 2007).

There are several problems involving the analysis of the relationship between two or more variables. One of the classic tools used in statistics is the so-called correlation analysis. There is correlation between variables when one of them is, in some way, related to the other. In simple correlation analysis are studies the correlation between just two variables x and y, this is usually done with the aid of a scatter plot and a measure known as the correlation coefficient. The latter measures the degree of linear or non-linear association between the two variables.

The use of this technique is very wide. It ranges from visualizing how one variable is related to the other in a given process to the magnitude of the strength of this relationship. For example, in the case of LD converters, is possible to verify how the wear of the refractory bricks is correlated with factors such as process temperature, degree of acidity of the slag, oxidation of the metal bath, among others. Knowing these relationships, it is possible to build life (or wear refractory) prediction models to operational control of wear and management of process control actions.

From there, new questions must be asked, such as, how such these relationship take place? Or, what would happen to the wear of the bricks if a reduced in the LD's end-of-blow temperatures? These and new others questions can be answered through regression analyses. In this second stage, regression analysis is considered one of the most used statistical tools, as through it is possible to numerically explore the relationship between variables. In the field of regression, we mainly use simple linear regression, but as the models require more complex degrees of analysis, other types of regression such as multiple linear or non-linear regression can be used. Models like these establish the relationship between the variables x (predictor variable) and y (response variable) involved in the problem

through linear or non-linear equations. The key point of this technique is the use of the adjusted model to make predictions in order to predict future results. The traditional functional form of this type of equation can be described in the following format

$$Y = f(x) = \beta_0 + \beta_1 X + \varepsilon \quad (9)$$

Where:
Y = response variable
X = predictor variable
β_0= intercept
β_1= slope (angular coefficient)
ε = model error

The β's coefficients of the equation 9 (β_0 and β_1) are determined in order to minimize the sum of squares of the residues (difference between the values observed in the sample and the predictions made by the equation). This method is known as the Least Squares Method.

Figure 27 – Ilustration of residuals in linear regression analysis

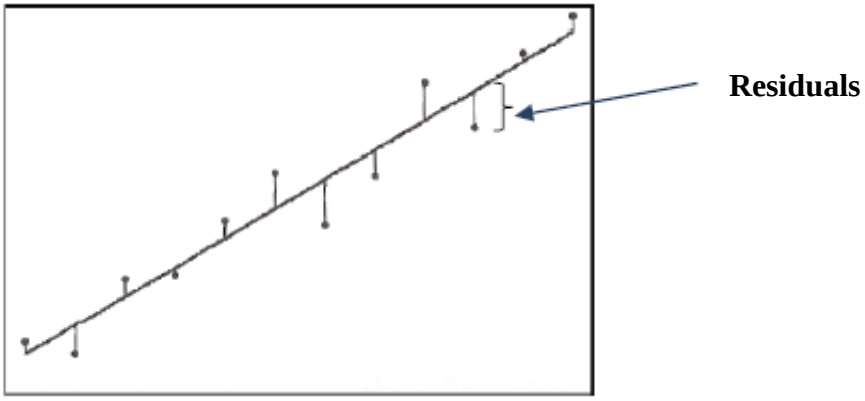

Source: Own authorship.

It is important to emphasize that in the regression analysis the cause and effect relationship between x and y may or may not exist. Therefore, what the equation shows is only the relationship between the variables, if it exists. In cases of spurious relationships, real or physical knowledge of the phenomenon is essential so that correlations without any physical meaning can be ruled out.

Another basic hypothesis to be observed is the non-negligence in the regression analysis of the analysis of the model residues, which must comply with the following premises:

1. Normality
2. Constant variation (homocedasticity)
3. Independence

From the correlation coefficient it is possible to obtain the determination coefficient known as R^2 and adjusted R^2. Such coefficients indicate the proportion of response variability explained by the model. In general, the higher the values of the coefficient of determination, the better the fit of the model to the studied phenomena. It is worth remembering that the adjusted R^2 is indicated when there is more than one predictor in the adjustment. Another important parameter is S, known as the estimate of model variance. High values of S indicate a lack of confidence in the prediction, since the dispersion of the model's prediction results can lead to results far from the true mean.

Another control parameter during modeling is the lack of fit test, as the lack of fit may imply failure to describe the relationship between the factors studied in the experiment and the response variable. Usually the absence of important factors in the final model as well as high residuals can cause this type of problem.

The hypotheses considered in the hypothesis test of lack of fit are:

H_0: The model fits the data well;

H_1: The model does not fit the data well.

Therefore, a model well adjusted to the data will present a high *p*-value and greater than the considered α.

When the relationship between the variables does not happen in a linear way, polynomial regression models come into play. Such models are used when the relationship between variables is curvilinear. Unlike linear regressions, whether simple or multiple, polynomial models can contain quadratic and/or cubic factors. In general, polynomial models have the following formats:

$$Y = f(x) = \beta_0 + \beta_1 X + \beta_2 X^2 + \varepsilon \quad (10)$$

$$Y = f(x) = \beta_0 + \beta_1 X + \beta_2 X^2 + \beta_3 X^3 + \varepsilon \quad (11)$$

Where:

Y = response variable
X = predictor variable
β_0= intercept
β_i (i=1....k) coefficients associated with predictor x
ε = model error

The cases above comprise situations of correlation and regression techniques that cover only the relationship between two variables, a predictor (x) and a response (y). However, in practice, most phenomena involve more than one predictor variable. In this case, the above methodologies can be generalized to situations where there are more than one predictor variable. In these cases, we apply correlation and multiple regression techniques, by modeling the existing relationship between a response variable y and several predictors x's at the same time.

The general representation of multiple linear regression models can be represented according to:

$$Y = f(x) = \beta_0 + \beta_1 X_1 + \beta_2 X_2 + \ldots\ldots\ldots + \beta_k X_k + \varepsilon \quad (12)$$

Where:

Y = response variable
X_i, i = 1, ..., k = predictor variables
β_0= intercept
β_i (i=1....k) coefficients associated with each predictor Xi
ε = model error

The basic assumptions for this type of model, considering the analysis of residuals, are normality, constant variation (homocedasticity) and independence of residuals.

For multiple regressions, multicollinearity is a common problem that can occur due to having multiple Xi predictors as a function of one Yi response. It usually occurs when there is a correlation between the predictor variables. In these cases, the multicollinearity makes the variance of the regression coefficients high, making its estimation imprecise, impairing the fit of the model. The identification of multicollinearity can be performed by a parameter known as VIF (Variance Inflation Factor). The Variance Inflation Factor indicates how much the variance is being increased due to correlations between the predictor variables. That is, multicollinearity can mean that part of the variance does not come from the phenomenon itself, but from induced relationships between the variables.

Typical reference values for the VIF would be:

VIF ≤ 1 (little or no increase in variance)

1 < VIF ≤ 5 (slightly to moderately increased variance)

VIF ≥ 6 (great increase in variance)

The treatment for models that present high VIF would be to remove the variable with high VIF from the model.

In general, the main criterion for evaluating the coefficients of regression models is the well-known *p*-value. The adjustments of the regression models used the *p*-value to verify the significance of the coefficients of the regression variables. A common practice is to exclude from the models the variables whose coefficients are not statistically significant through comparative use with the established *p*-value (generally $p < 0.05$). This traditional analysis technique is called Backward. Other techniques can be used, mainly with the use of specific statistical software for regression analysis. It is common to use methods such as Best Subsets, in this case the adjustment is performed considering a group of probable models in which some criteria such as R^2, Cp-Mallows and S are evaluated simultaneously. Another well-known technique is the Stepwise method, in which the fit starts with no variable in the model and then variables are automatically added one at a time at each step.

The basic assumptions to be obeyed so that the regression models can be used reliably are:

- 1st Hypothesis on the simple linear regression model
  $E(\varepsilon i) = 0$
- 2nd Hypothesis on the simple linear regression model
  The errors are normally distributed
- 3rd Hypothesis on the simple linear regression model
  $E(\varepsilon i, Xi) = 0$; Regressor variables are not correlated with the error
- 4th Hypothesis on the simple linear regression model
  $Var(\varepsilon i) = \sigma^2 =$ constant
- 5th Hypothesis on the simple linear regression model
  $E(\varepsilon i, \varepsilon j) = 0$, com $i \neq j$; Errors cannot be autocorrelated
- 6th Hypothesis on the simple linear regression model
  The Xi variables cannot be a linear combination of the other Xi variables

The purpose of this section is not to delve into the subject of correlation and statistical regression by classic models such as those mentioned above, since this subject is part of the basic approach of undergraduate and graduate courses in the areas of exact sciences and it is understood that is known to everyone. The objective was just to summarize and remember such models with their basic assumptions so that the reader has a systemic view of the subjects that underlie this thesis, namely: Build and compare models capable of showing how, which and in what quantity the process variables may jointly affect the wear of the refractory lining of the LD converters. In the case of this thesis, the idea is to model the refractory wear of the LD by classical statistics and self-organizing maps (data mining tool known as SOM) in order to have, a refractory wear model and a new tool for analysis and modeling in Aciarias LD.

2.9 Analysis by SOM (Self Organization Maps) technique

2.9.1 Initial settings

Currently, one of the great challenges faced by many professionals from the most different technological areas is to analyze in an integrated and meaningful way the enormous amounts of data generated in different industrial processes. An alternative to conventional statistical analysis is the SOM tool, which is a computational approach based on self-organized maps through which it is possible to understand and synthesize these data (BIERLEIN *et al*., 2008; FRASER; DICKSON, 2007; VATANEN *et al*., 2015). We can define SOM as an analysis technique for understanding relationships within and between disparate data sets by providing a means of analyzing and interpreting large amounts of data in a meaningful way. Figure 28 illustrates the framework of the technique and some applications.

Figure 28 – Framework of the SOM technique

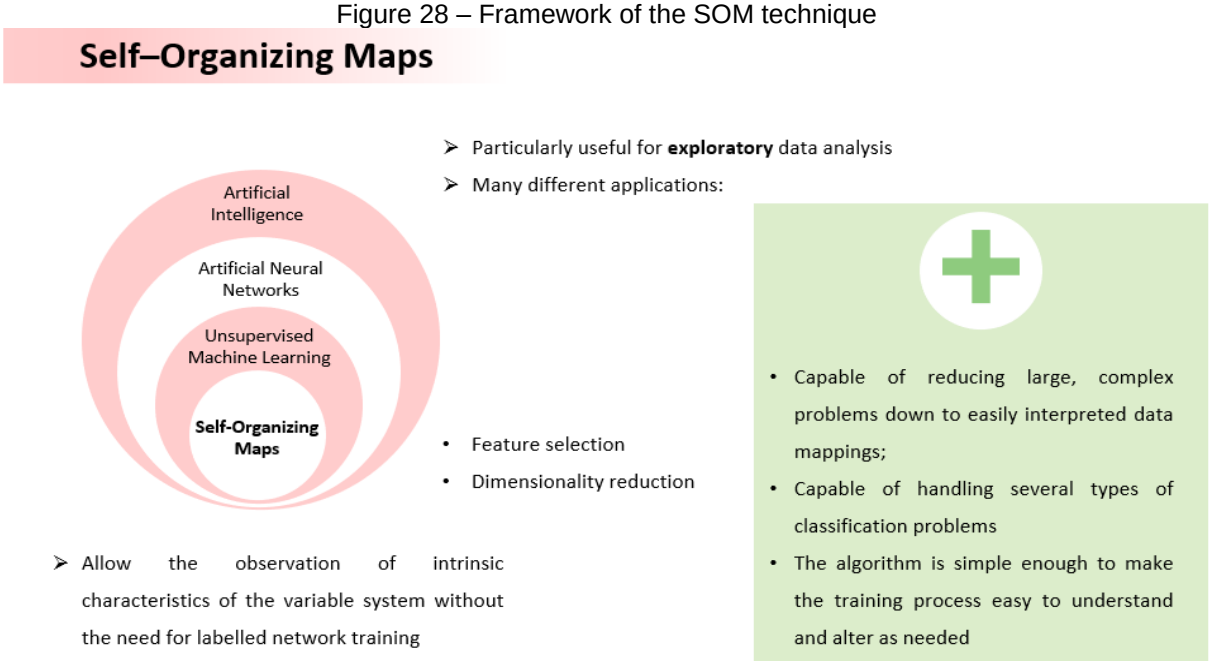

Source: Borges e*t al*. (2022).

A striking feature of this tool is the application of procedures for graphical visualization of the data, with the alternative of dimensionality reduction with preservation of the topological structure of distribution of these data, facilitating in cases where there are many variables under analysis.

According to Carneiro *et al*. (2012) and Vatanen *et al*. (2015), SOM is a data analysis and visualization tool based on vector quantification principles. In addition, the method can be used to perform various types of operations, such as function fitting, prediction or estimation, grouping, pattern recognition, noise reduction and various classifications (FRASER; DICKSON, 2007; KOHONEN, 2001).

Through this tool, based on principles of quantification and vector similarity, it is possible to better visualize, analyze and interpret data. For Kaski, Kangas and Kohonen (1998); Merja, Samuel and Teuvo (2003), Polla, Honkela and Kohonen (2007), the main feature of Kohonen maps (SOM) is having the property of organizing the vectors that represent the data points, both in relation to the underlying distribution and topologically.

This topology is generally linear, although we can have the underlying network as a grid, which makes the tool applicable in several functions. For Austudillo and Oommen (2011); Nguyen *et al*. (2015), the SOM is a data representation of a sample or population in a space whose dimension is generally smaller than that in which the initial samples are found, with their topological properties of the input space preserved.

This tool is used in different areas such as finance, industrial control, astronomy, petroleum, mining, aerospace and geochemistry (BRIQUEU *et al*., 2002; GARCIA-BERRO *et al*., 2003; KASKI *et al*., 1998; PENN, 2005; STRECKER and UDEN, 2002). Through the use of this tool, we can identify relationships between the various process variables and indirectly identify their correlations, thus establishing behavior and system control standards.

In the SOM analysis, each sample is treated as a vector in which its orientation and spatial position are determined by its variables, and vector similarity measures are used to order the input data into patterns (CARNEIRO *et al*., 2012; FRASER; DICKSON, 2007).

For example, a possible representation of the data through to the vectors could be done considering a set of vectors of the type $V = \{v_1,....,v_n)$, with $V \subset R^D$, being the vectors $V_n = [V_{n1}, ..., V_{nD}]^T$, with n (1,....,N), with $V_{nD} \in R$, D = 1,...d. A possible data entry table for analysis would be of the type below:

Table 5 – Table type for inputting data in vector form

Objects	**Attributes**			
	1	**2**	**...**	**4**
1	V_{11}	V_{12}	...	V_{1D}
2	V_{21}	V_{22}	...	V_{2D}
:	:	:		:
N	V_{N1}	V_{N2}	...	V_{ND}

Source: Zuchini (2003).

Due to the fact that this data exploratory tool is unsupervised, the patterns, borders and relationships between the variables are derived internally to the software, that is, it does not need to be trained. (FRASER; DICKSON, 2007).

2.9.2 Traditional methods of data visualization and interpretation

Traditional methods of data visualization such as graphs and mathematical calculations, when considered for small amounts of variables or data, can provide useful information and analysis. However, as the volume of data and variables increase (increase in dimensionality), new analysis techniques are needed for a more correct visualization of the relationship of these variables. Everitti (1993); Jain; Dubes (1988) and Nguyen *et al*. (2015) mention that for an efficient and effective data

mining it is necessary techniques that can reduce the dimensionality of the sample while preserving its characteristics and allowing the visualization of typical patterns in samples.

On the other hand, data grouping methods can be more useful in large volumes of data when you want to determine patterns or groups with different characteristics, but common within groups. In these cases, one or more characteristics are sought that can separate, within or between samples, groups with characteristics or some kind of common pattern. For Costa (1999), processes of this type do not necessarily need to be supervised, as the process itself should determine the optimal number of groups and the particular characteristics of these groups. In these cases, algorithms can be created to identify and separate these similar groups. Obviously, for the algorithm to be efficient in this type of classification, it is necessary to create a database in which the patterns are previously defined or it is necessary to have methods that facilitate the recognition of patterns by the algorithm (MICHAlSKI *et al*., 1998).

A third group of analysis techniques is projection. These methods are based on mapping objects that are in a certain input space (R^D) to a hyperplane (R^P) usually of smaller dimensions (Figure 29). The objective is to represent the objects, or rather, possible groupings in a dimension that can be visualized and understood. The representation of points (sample or population data) is carried out through vectors and the basic principle of similarity or possible groupings is done by vector distances (SVENSÉN, 1998). A typical example of this technique is SOM.

Figure 29 – Set of points in input R^D space mapped to a hyperplane in R^P space, where $P \leq D$

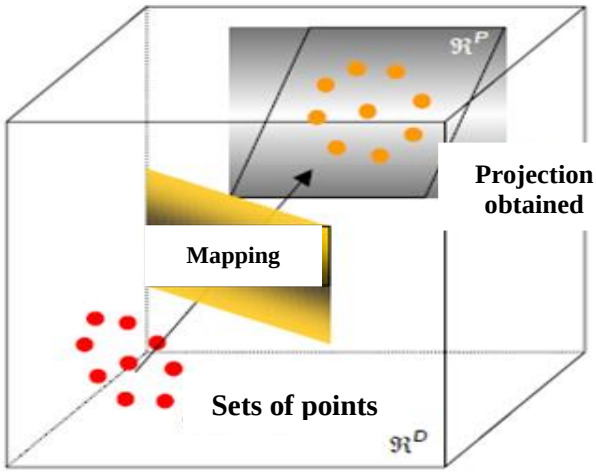

Source: adapted fron the Zuchini (2003).

Some techniques can be cited as Principal Components Analysis (PCA) that use linear operators, Multidimensional Scaling (MDS) and Sammom Projection that use nonlinear operators and Curved Components Analysis. The generative methods that use probability density complement these techniques. This introduction to the subject of data analysis methods that go beyond classical statistics has other variants and techniques that go beyond the scope of this thesis. It is worth remembering Bishop's approach (1995); Costa (1999); Duda *et al*. (2000); Jain *et al*. (1999) among others that are references in data analysis outside the scope of traditional classical statistical analysis.

2.9.3 Description and rationale for the SOM analysis tool

For Kohonen (1997) and Vatanen *et al*. (2015), SOM is a type of neural network capable of projecting a sample or a population of multidimensional data into a P-type dimension, where P=1, 2, ... n, smaller than the original input space D. Therefore, we can evaluate the input data of a database through its projections in a certain space, being determined by data vectors (neurons) and their distances. These projections are determined by an algorithm that in practice works as a neural network.

Through a rectilinear (two-dimensional) output map, SOM can show an ordered two-dimensional representation of the multidimensional system of the input data, in which it displays relationships between the input samples. More importantly, the map can also be used to show the contributions of variables related to these samples (FRASER; DICKSON, 2007).

The fundamentals of the idea of this technique of analysis are found in the fundamentals of functioning of the human brain, in which the cerebral tissues are separated according to the specific function, of the types of stimuli and linked to the corresponding regions of the body. In this way, the brain is segmented (grouped) into neurons with similar functions (characteristics). The SOM algorithm groups objects in the input space and projects them onto the requested dimensions so that data with similar behavior (features) are close to each other. This is done by vector calculus.

For Hulle (2000), the similarity between the functioning of the human brain can be transcribed in the form of an algorithm that projects an n-dimensional space of

data into projections so that we can verify clusters of data that have similar or correlated characteristics using distance comparisons vector.

These projections, also known as topological maps, can be established by various techniques or models. In particular, the most used are the gradient-based models and those based on competitive learning. *SOM* uses the second case, which has vector quantization and the previously described fundamentals as its basic foundation.

A didactic view, presented by Carneiro *et al*. (2012) and Zuchini (2003), summarizes the step-by-step SOM operating logic. Initially, a set of data represented in space by R^D vectors is randomly and repetitively presented to a network of neurons with a given array distributed vectorially with their respective weights. In the next step there will be a competition between the vectors to represent each of the data presented to the network. Vectors whose coordinates are closest to each of the data will be chosen to represent them. After this initial competition, the coordinates of the chosen vectors are even closer to the data coordinates in order to have a topological representation as close as possible. Next, the neighboring vectors of the chosen neurons are adjusted in order to be closer to the previously determined data. In the end, there is a topological network identical to the vector network of the initial data and thus it is possible to map the distribution and determine the data groupings according to criteria to be defined. The fundamental idea is that vectors close to each other represent similar data among themselves so that the representation of data in high dimensions can be represented by simpler neuron networks, however maintaining the original configuration of the data.

It is important to point out that the visualization of data clusters is only effective for a visualization of the data distribution for dimensions 1 to 3, although there is no restriction for the number of dimensions of the neuron network.

Zuchini (2003) describes modeling via SOM as follows: For a given set of input data represented by vectors of the type $V=\{v_1,....,v_n\}$ with $V \subset R^D$, each data being represented by a vector of the type $Vn = \{v_{n1}, v_{n2},.....,v_{nD},\}^T$ with R^D, with $n = (1,....,N)$ in a D dimensional space, through its D attributes, SOM can be defined by its i neurons, where $i = 1,...,Q$ arranged in an arrangement that defines the neighborhood of each neuron (Figures 29 and 30).

Figure 30 – Different array configurations for the SOM in R^2, in A the rectangular neighborhood, in B the array with hexagonal neighborhood

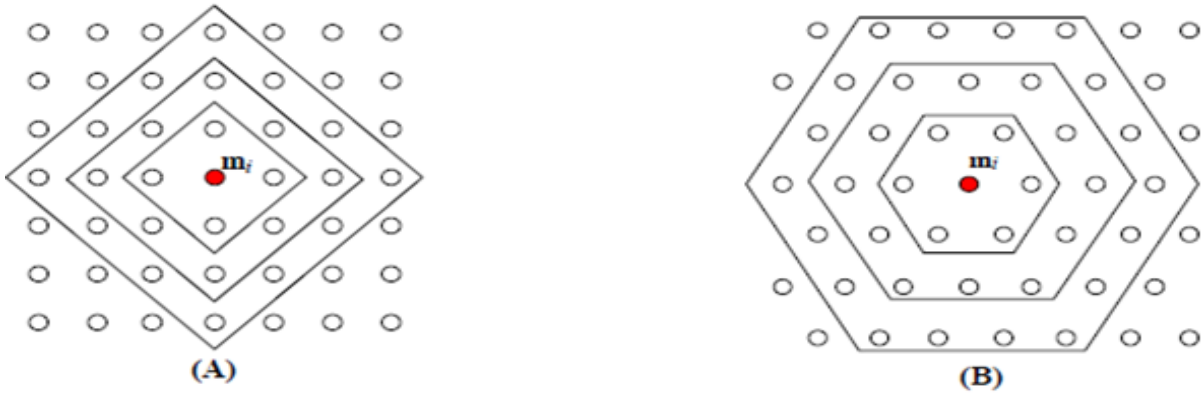

Source: Zuchini (2003).

In this case, each neuron i is represented by a vector to which weights can be assigned and are represented in the form $mi = [mi_1, ... mi_D]^T \epsilon R^D$. The input data is connected to all neurons i in order to establish a competition between them to represent such input data. For example, for a given set of data to be analyzed by SOM, so that each data in this set is represented by a vector of spatial coordinates as a function of its attributes, the vector distance between the neurons and the input data of so that, the closer they are, the greater the chance of choosing that neuron to represent the data.

The main metric used to calculate vector distances is the well-known Euclidean distance represented by the equation below:

$$d(m_i, v_n) = |m_i - v_n| = \sqrt{\sum_{j=1}^{D} |m_{ij} - vn_j|^2} \quad (13)$$

Where:

v_n: vector;

m_{ij}: weight assigned to vector.

After determining the vector distances, the weight vector that is closest to the data is chosen, which is chosen within the network and identified as Best Matching Unit (BMU). The metric used to choose the BMU can be given by:

$$C = \arg\min \{|m_i - v_n|\} \quad (14)$$

According to Kohoen (1997), in addition to the BMU, the neighboring neurons are also adapted (adjusted) to compose the network with the BMU so that all its neighborhood represents the input data and forms the data representation map. For this, the learning of the network is done using synaptic weights so that in each neuron, at time t+1, a new synaptic weight is used by the following metric:

$$m_i(t+1) = m_i(t) + \alpha(t) * h_{ci}(t) * [m_i(t) - v_n(t)] \quad (15)$$

Where:

t: time;

m_i: weight assigned to vector;

α(t): learning rate;

h_{ci}: neighborhood function;

There are several ways to estimate the neighborhood function, traditionally the h_{ci} function is estimated by a Gaussian function

Figure 31 – Ilustration of adapting the weights of a SOM for the presentation of a single pattern in R^2

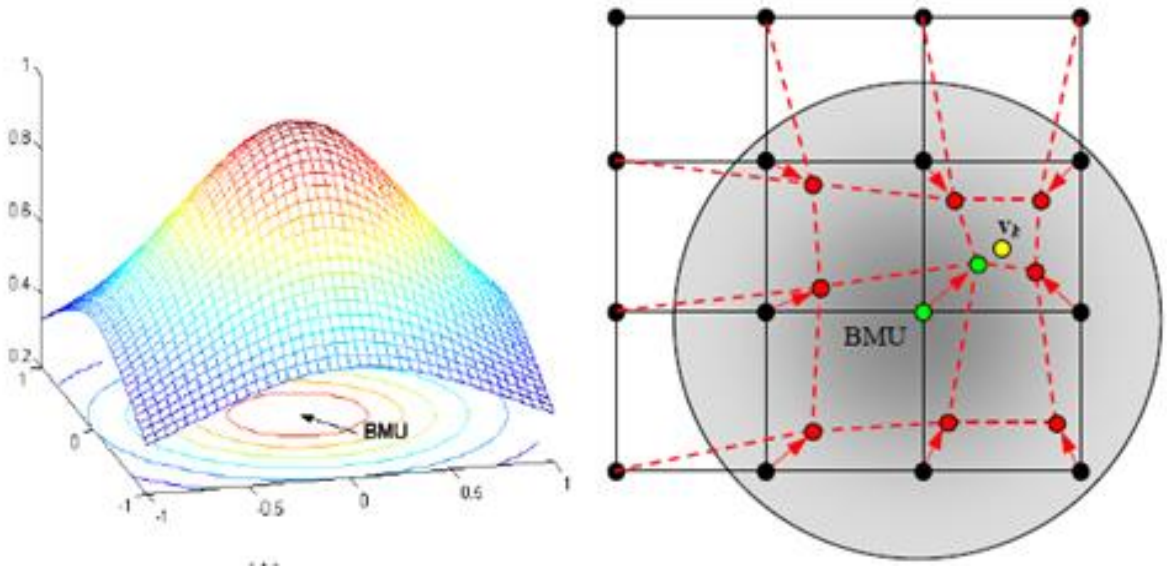

Source: Zuchini (2003).

When using SOM, everything happens as if the neurons that represent the input data were in a grid or network, in which the adaptations of the neurons to adjust to the input data were made through movements within the network, time stretching, sometimes contracting, sometimes distorting their positions due to this better adaptation to the data. An essential consideration of neuron movements within the

network is the fact that compressed regions represent a high density of neurons and the extended regions represent a low concentration of them. For the interpretation of the input data, this is fundamental, since the similar characteristics of a group of data will tend to visualize regions of high concentration.

The vectors have been trained to represent the structure of the input data (now called node vectors), all original input samples closest to this node-vector are represented by this node in the output 2D map. Using a regression it is possible to map from nD space to the 2D rectilinear representation. The main characteristic of this mapping is the relative preservation of the relationships (topology) between the node-vectors. That is, node vectors that are close together in nD space have nodes that are close together in the 2D map. According to Fraser and Dickson (2007, p. 908)

> The original input samples are now represented by nodes in the self-organized map, and these can form a group or cluster. However, if a node is close to other nodes on the "map", these nodes may be a subset of a larger group of similar samples formed by all samples belonging to locations close to the nodes. The self-organized "map" is an ordered 2D representation of a complex multi-parameter dataset. It is an ideal framework for subsequent viewing and interpretation. The "Unified Distance Matrix" and component plots are two examples of such views.

2.9.4 SOM implementation algorithm

There are basically two usual ways of implementing the algorithm. The most usual form is the one in which the training algorithm is updated (neuron weights) every time an input data item is presented to the network (incremental type algorithm).

The other form differs from the first one because that the update is performed only when all items in the input set are presented to the network.

For the first case, the great advantage would be not having all the input data at the start. It is common, in the analysis of certain systems, to carry out a previous research and not all the information of the system under study is known. In this case, it is necessary to evaluate data by data until all of them are available for analysis. For these cases, the algorithm is simpler and cheaper, requiring even less memory for its use.

The basic implementation sequence of the incremental type algorithm follows the following steps:

1-Initialization of the weight vector;

2-Selection of an input data vector;

3-BMU vector selection;

4-Update of the BMU and its neighbors

5-Make t=t+1 and return to item 2;

6-Increase the number of interactions until the number of interactions has reached the pre-established number.

2.9.5 Types, analysis and interpretation of SOM maps

The results of implementing SOM in databases can be interpreted through topographic maps of one, two or more dimensions. Determining the quantity of dimensions to be used will depend on the objectives of the analyses, and its efficiency will be determined by the most appropriate choice.

2.9.5.1 SOM maps types

2.9.5.1.1 One dimensional arrays

According to Erwin *et al*. (1992), one-dimensional shapes, despite being little used, have ways of proving convergence of this type of model. Applications like the one presented by Aras *et al*. (1999) can be used for practical use of one-dimensional models. A classic example of the application of this type of model is the case of the traditional traveling salesman problem that needs to determine the optimal path to be taken between different cities, in which the algorithm is initially formed by only 2 neurons inserted so that they are close to each other and in the center of mass of a region that forms a group of cities. The model is developed in 2 stages, the first called the attraction stage and the second repulsion stage.

In the attraction stage, the neurons that represent the data of the closest cities are identified by geometric calculations and, from there, the other neighbors are attracted in order to represent the network of the points with greater density. The repulsion stage is then formed by the neurons that were not classified because they

have greater distances in relation to the BMU and, in this case, are moved away from the others. The sets of neurons must be positioned in such a way that the properties of the input data set are kept constant (mean data and data variance).

In the case mentioned above two versions of the SOM could be used, a traditional one and an adapted version (Knies). In the two cases a satisfactory results to the optimal path between the cities could be found.

2.9.5.1.2 Two dimensional arrays

For two-dimensional arrays, 4 main types are used, rectangular, hexagonal, cylindrical and toroid. The first two are the most common. Figures below illustrates the most used types of two-dimensional arrays.

Figure 32 – Examples of two dimensional arrays of the rectangular and hexagonal type

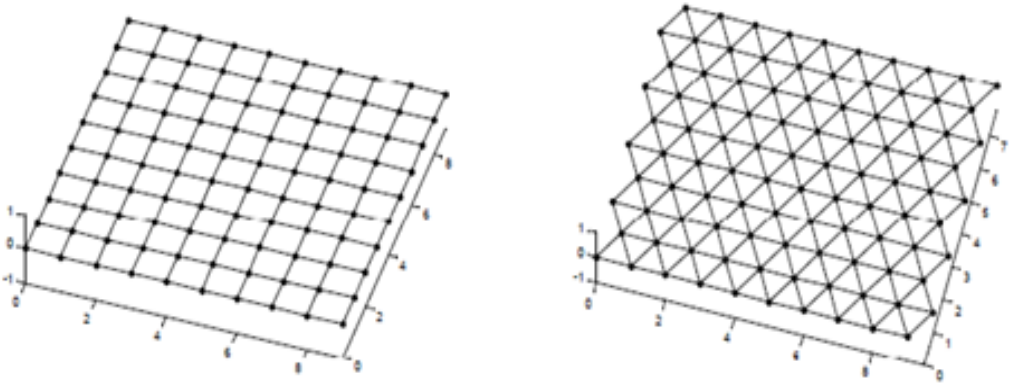

Source: Zuchini (2003).

Figure 33 – Examples of two dimensional cylindrical and toroidal type

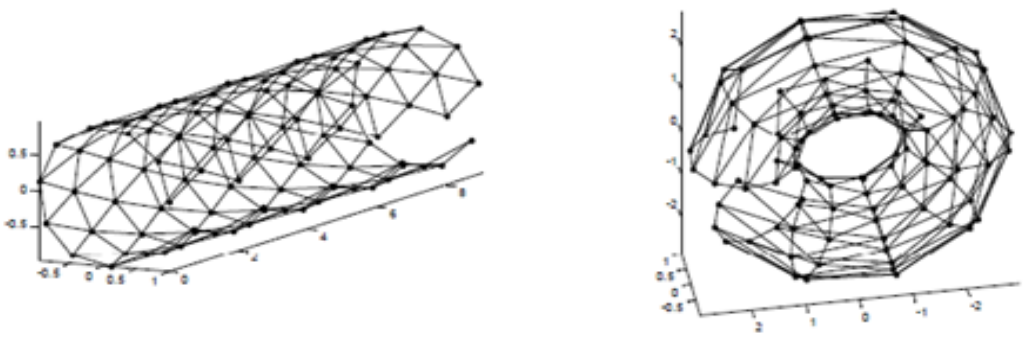

Source: Zuchini (2003).

For the treatment of data through clusters, according to Ulstch and Siemon (1989), a technique widely used by SOM is the U matrix, also known as the unified

distance matrix. The analysis of clusters can be done using this type of matrix so that the distances between neurons can be inserted in the matrix in rectangular and hexagonal formats. Figure below illustrates the format and type of the U matrix.

Figure 34 – Examples of matrix U in a rectangular array (A) and hexagonal array in (B)

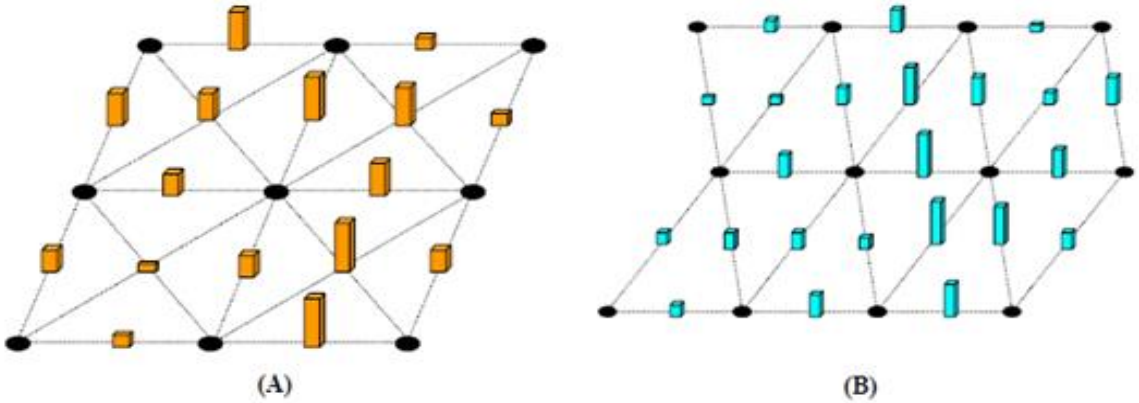

Source: Zuchini (2003).

The U matrix can be constructed considering two dimensions L and C, for example, and the final matrix will have 2L-1 by 2C-1 if a rectangular array is considered. The structure of the matrix is based on the arithmetic mean of the distance between the weight vector and its neighbors. For Vesanto *et al*. (2000); Livarinen *et al*. (1994) such constructions are feasible for a visualization in which the matrix will be represented by a level surface in which the valleys will represent conglomerates of points close to each other forming clusters and separated by elevations of low concentration of points.

2.9.5.1.3 N-dimensional arrays

N-dimensional arrays are those in which N variables are inserted. The great advantage would be the power of data analysis in a multivariate way. The biggest difficulty would be the non-direct visualization of the data since this feature is limited to up to two dimensions. There are methods and tools developed that allow evaluating the results when the number of dimensions is greater than 2, but the implementation is complex and more expensive from a computational perspective. Proposals like the one suggested by Costa (1999) would be possibilities to be discussed and implemented in N-dimensional cases.

2.9.5.2 Other types of SOM tools approach

It is possible to find in the specialized literature some variants or some models derived from the SOM. According to Kohonen (1997), it is possible to build models using the basic principles of SOM. Such constructions must be based on choosing and updating the BMU and determining the arrangement of neighboring neurons. For Hulle (2000), the implementation of numerous variant models of the SOM tool is possible as long as the determination of the BMU and the adjustment of neighboring neurons are carried out by efficient metrics and choices of networks appropriate to the type and objective analysis of the input data. Also according to Hulle (2000) and Kohonem (1997), the main aspects that can be modified in the construction of models derived from the SOM would be: 1- way of choosing the metric to determine the BMU, 2- criterion for determining the neighborhood (more cases common are rectangular and hexagonal), 3-invariant data characteristics, 4-hierarchical data structure. Regarding item 1, other possibilities, in addition to the Euclidean metric, widely used in situations where there is no initial information about the input data, are described in the table below.

Table 6 – Types of metrics used to calculate distances, in addition to Euclidean

Metric	Application	Reference
$d_\lambda(x,y) = \lvert x-y\rvert_\lambda = \sqrt[\lambda]{\sum_{i=1}^{D}\lvert x_i-y_i\rvert^\lambda}$, $\lambda \in R$	Recognition of patterns that undergo linear transformation	Minkowsky's metric
$d_T(x,y) = \lvert x-y\rvert_T = (x^T*y)/(x^T*X+y^T*y-x^T*y)$	Used for text pattern recognition	Tanimoto's metric
$d_M(x,y) = \lvert x-y\rvert_M = \sqrt{[(x-y)^T\ cov^{-1}(x-y)]}$	Used in data that have correlation with each other (not independent)	Mahalanobis's
$d_{ATW}(v,m) = \sqrt{\sum_{j=1}^{D}[\omega^2_{ij}(v_j-m_{ij})^2]}$	Used for input data with very different variances	Adaptive Tensorial Weighting (ATW)

Source: Zuchini (2003).

Regarding item 2, in situations where the initial data have elongated clusters or different classical patterns, the applied rectangular or hexagonal geometries are

not the best ways to represent the neighborhood data. In these cases, the literature suggests some options like the one described by Kansas *et al*. (1990), in which the distances between neurons are defined during training and not rigidly as the previous ones. For this model, the length of the arcs is defined by the Euclidean distances between the neurons in the array.

An important contribution was made by Martinetz and Schulten (1991) through a model in which the neurons do not have a pre-established neighborhood region (rigid) for updating the weights. In this model, the neighborhood is defined as each input data is presented to the structure of the network. An abstraction of this model could be visualized as a sequence of data and neurons trying to fit sequentially into the network structure in order to obtain a spatial arrangement consistent with the patterns of the input data. known as NG (Neural Gas) or adapted versions such as the one proposed by Fritzke (1995a) called GNG (Growning Neural Gas), this model like the MST (Minimum Spanning Tree) does not guarantee topological ordering, but it is possible to analyze through its data similarity issues.

Proposed by Fritzke (1991), the GCS (Growing Cell Structure) is a model in which a 2D array has neurons connected to each other forming a kind of triangular structure, with each vertex corresponding to a neuron in which the BMU and its neighbors are updated. for each data entry. The main difference of this model is the insertion of new nodes as large representation errors are found in neurons. The evolution of this model proposed by the same author would be an array structure formed by hypertetrahedrons promoting a more effective recovery of the original structure.

An important proposed variant of the GCS model was the Growing Grid (GG), in which the model is built in order to obtain the best possible arrangement in dimensional terms from a basic initial construction formed by 4 initial neurons and new neurons are inserted and adjusted in rows and columns in the initial network after the initial data entry starts.

Other proposed models such as the IGG (Incremental Grid Growing) by Blackmore and Miikkulaine (1995), or the GSOM by Alahakoon *at al*. (2000), have characteristics that solve the typical problems of the GCS and NG models, such as those with high dimensionality and difficult visualization. Such models have flat formats which improve the visualization, but restrict the analysis to flat structures.

A variant of hierarchical maps was implemented by Cho (1997), in which 4 neurons in a 2x2 array are trained according to classic SOM patterns. After the initial training, there is an analysis of patterns on the neurons so that non-representative neurons are removed from the network. In the end, a form of hierarchical map is obtained in which each chosen neuron can represent one or more classes.

There are other variants of the SOM model, but with the same final objectives, which is to have a more flexible arrangement and a larger number of neurons. The level of complexity, visualization difficulties and computational costs are the main factors that will define the type of variant to be used or the classic forms of SOM.

2.9.5.3 Data interpretations and analysis through SOM maps

The visualization, interpretation and analysis of the information extracted from the databases of the systems under study can be obtained via SOM through the so-called U-Matrix and the arrangements and networks from the groupings of neurons. The unified matrix (U-Matrix), is a matrix in which the input samples are analyzed according to their similarities in relation to the other samples, so that similar samples were close to each other or separated by nodes of cold colors like blue.

In contrast, the dissimilar samples were far from each other or separated by nodes of warm colors such as red (FRASER; DICKSON, 2007; ULTSCH, 1993; ULTSCH; VETTER, 1994). Figure below illustrates the previous data.

Figure 35 – Example of SOM maps for a dataset of 220 geochemical samples for igneous rocks (NE Queensland) each with 32 analysis variables. (A) Representation of the U matrix with withe hexagons sized proportionally to the number of samples falling at each node. (B) node color coding

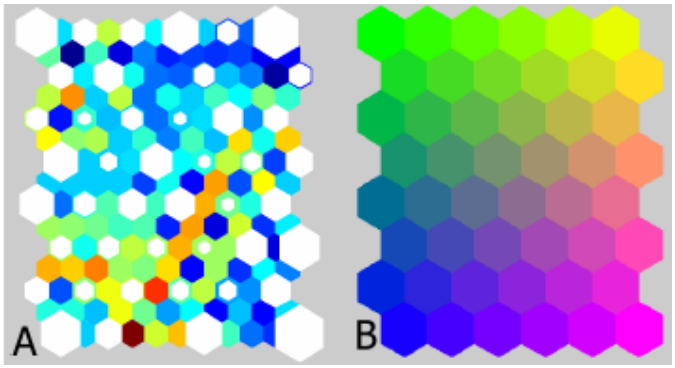

Source: Fraser and Dickson (2007).

Another type of visualization and analysis that can be obtained by SOM are the so-called "Component Graphs". Through these graphs it is possible to visualize

the contribution of each node to a particular variable, and display the values again using a color temperature scale so that low values (of the variable in question) are displayed in blue and high in red. It is also possible to use standard image processing procedures, such as principal component analysis, to determine relationships and trends between these images (FRASER; DICKSON, 2007). Figure 36 illustrates a type of component graph.

Figure 36 – Example of component plots for SiO_2, CaO, Ba eTh. Th e SiO_2 have similar behavior, since Ca is different from SiO_2 and Ba

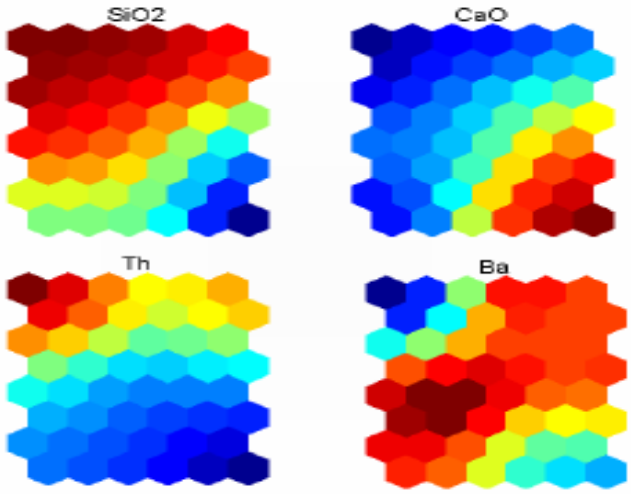

Source: Fraser, Dickson (2007).

Another use of the SOM tool is the color mapping of map nodes in scatterplots. Since SOM is a segmentation technique, scatterplots constructed from it can show linear or non-linear relationships and trends that are difficult to observe in the input data (FRASER; DICKSON, 2007).

Figure 37 – Example scatter plot of Th versus Ba showing the different trends in Ba and Th due to fractional crystallization

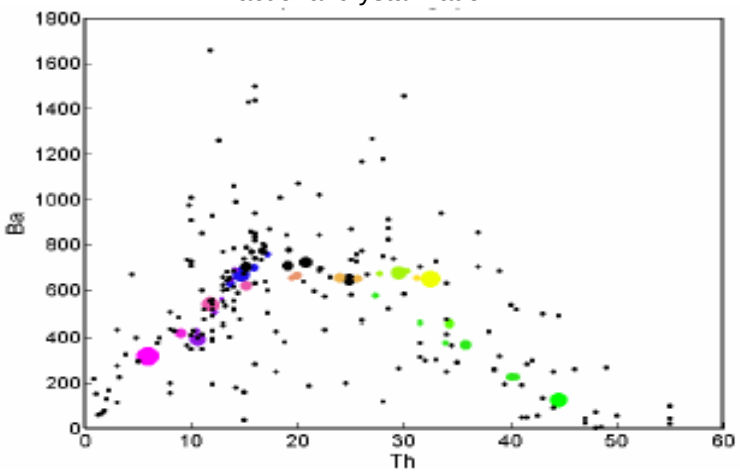

Source: Fraser, Dickson (2007).

According to figure 37 is possible to verify the possibility of determining correlations between the various process variables and, in the case of the analysis of wear and life of the refractories of LD converters, it is possible to identify which variables or groups of variables have greater or lesser relevance to such a process.

The characterization of what is “hidden” behind the input data can be identified, in general, by the following parameters: 1- Effectiveness of the projection carried out by the SOM of the input data in R^D to the space in R^P, 2-Capacity of detection of data clusters with associated characteristics, 3-Efficiency in determining which vectors will be considered as a function of the ratio of the percentage of attributes found in the input data, 4- Capacity to differentiate extreme data from sparse data.

The big question asked about SOM concerns the guarantee of map convergence, as there is great difficulty in establishing error functions for generic situations. Models proposed by Cheng (1999), Erwin *et al*. (1992) and Kohonen (1982b), illustrate some alternative convergence models for topological maps.

In Kashi (1997) a good model proposal is found for the error equation that should be minimized and for the choice of the BMU. In addition to the error minimization parameter, two metrics are used for modeling via SOM. The first is the Mean Quantization Error (QE) which calculates the average of the distances between each data vector and the corresponding weight vector of the BMU neuron. The second metric is the so-called topographic error (TE), which estimates the efficiency of the map to represent the topography of the input data.

The use of the two metrics mentioned above must be done with some care, such as checking phenomena such as overfitting, in which a kind of overlapping occurs. This occurs in situations of low values for QE and TE, which may cause loss of SOM capacity.

The reverse phenomenon, underffitng, can have negative effects on the efficiency of the analysis. If the number of neurons is too small to represent a large number of input data or if the radius of the function is greater than 1, the SOM map will lose flexibility in adjusting to the input data, becoming unrepresentative of the actual physical arrangement of the neurons. data. This phenomenon can be monitored when high EQ and low TE values occur, keeping in mind that these indices should be used as a reference and not as absolute parameters for determining the SOM in cases of statistical analysis of model generalization.

In this case, the proposal by Kashi and Lagus (1996) can be used to better define whether the model presented by SOM can or cannot be used for a given set of input data. In this proposal, a combination of QE and TE Metrics is used in a single measure, in which the distance between an object and its BMU and its second BMU are used together, considering the shortest path of the first BMU. The idea would be to identify possible discontinuities in the topological map.

2.9.6 Analysis of SOM control metrics

SOM control for use as a data analysis tool involves choosing parameters such as those for defining the structure to be used, dimensional parameters, determining the neighborhood and arrangements, radius and the neighborhood function (ZUCHINI, 2003). In addition to these parameters, those of the network training, such as definition by batch, incremental, or in two phases.

The determination of which parameters to use and their values are performed by heuristics based on the behavior of the maps and on the statistics explained above. On the other hand, the adjustment of the maps can be done using heuristics such as visualization methods capable of revealing global data structures in order to define dimensions of the arrangements. Kohonen (1997) mentions Sammon's projection, for example. As for the calculation of the number of neurons, Kaski (1997) says that it can be given by the number of input data if this value is less than or equal to 1000. SOM itself has a tool called Toolbox in which $Q=5\sqrt{N}$ is used, where N equals the number of input data. The array with hexagonal neighborhood and neighborhood function in Gaussian format is preferable for better visualization of the clustering structure in U-type matrices. batch algorithm option a better choice. Ideally, several configuration tests should be done on the SOM before making specific map choices.

2.10 Short descrption of the problem

The problem to be solved is how to jointly identify and model the main process variables that impact the performance (life) of LD converters using classical modeling by conventional statistics and self-organizing maps (SOM). The determination of a predictive model of the wear rate of the refractory of the LD trunnions in function of the process variables is necessary for the proper operational and safety control, in addition, of course, to the planning and management of the refractory supply structure of the steelmaking shop.

The search for new analysis tools in refractories of LD converters is necessary, given that classical statistics has its limitations such as those previously discussed (data normality, non-collinearity, homoscedasticity, etc.). The effort with SOM seeks exactly this objective, that is, in procedural dynamics in which classical statistics cannot predict possible results with certain security and reliability, SOM can be applied in order to help and even determine more accurate results.

Obviously, a good mathematical model involves a physicalchemical foundation in which possible hypotheses about the physical and chemical mechanisms that act in the system under study and consequently determine the causes of the problem under study (refractory wear) can be identified. In this case, a post-mortem laboratory analysis of the refractory bricks was carried out and possible hypotheses were formulated about the main mechanism of wear. Furthermore, the proposed mathematical equations and the results found by the statistical analysis and by the SOM were based on such hypotheses.

Therefore, this thesis is based on the triad: classical statistics, SOM analysis and post-mortem study for modeling the wear of the refractory bricks of the trunnions of LD converters.

3 METHODS AND MATERIALS

The realization of this thesis was conducted, basically, in 7 stages, namely:

1. Survey of operational data (process variables that are related to the wear process of the LD refractories bricks according to the literature and operational observation);
2. Realization and compilation of wear maps by laser scanning of the LD using FERROTRON equipment with specific software for determining wear refractories rates as a function of process variables;
3. Construction and correlation analysis of wear refractories rates versus process variables using conventional classical statistics (Time series, Uni and multivariate analysis by MINITAB statistical software);
4. Construction and correlation analysis of wear refractories rates versus process variables using SOM methodology by R software;
5. Comparison of methodologies and applicability of data analysis techniques (classical statistics versus SOM);
6. Post-mortem analysis of LD trunnions refractories bricks aiming to physically and chemically substantiate the analyzes obtained from process data and wear refractories rate;
7. Construction of a final wear model for the LD trunnions based on classical statistical analysis techniques and new tools (SOM), both based on post-mortem analyzes of the refractory bricks of the trunnions.

The detailed description of each step and the considerations that were adopted are described in the following sections.

3.1 Step 1

Step 1 was carried out by building a real process database for the period from January/2014 to December/2018 (5 years) in which the main operational variables (temperature, basicity, oxidation, process times, among others) that are related to the wear process of refractories in the LD4 converter of steelmaking shop 02 at the Ipatinga Plant of Usiminas. There were 30 variables analyzed (APPENDIX E).

This survey was carried out using Microsoft Access software, in which data were obtained from three campaigns with different lifetime performances, one campaign with a lifetime considered low (< 4,000 heats), a campaign with a lifetime considered medium (approximately 4,000 heats) and a campaign of life considered high (above 4,000 heats).

The objective is to have a table that has the average data of the process variables for each interval between measurements of the thickness of the refractory bricks. In this case, in the interval between thickness measurements (and consequent calculation of thickness reduction) also have the average value of the process variable. Thus, it was possible to verify possible correlations between operational fluctuations and the percentage or rate of reduction of the refractory thickness (wear refractory rate).

Table 7 – Illustrative example of the operational data entry table and the wear rate built fron the LD laser meansurement and the survey of process variable values during the thickness measurement intervals

Wear refractory rate (mm/heat)	**Process variable**			
	MgO in the slag	Metal bath oxidation	Average temperature	Others
(Previous thickness – Current thickness) / (Number of measurement interval heats) = 0,18	10%	800 ppm	1670°C	etc
(Previous thickness - Current thickness) / (Number of measurement interval heats) = 0,21	9%	700 ppm	1665°C	etc

Source: Own authorship.

3.2 Step 2

Step 2 was carried out through laser scanning with FERROTRON equipment, which, randomly, is carried out through laser measurement of the thickness of the LD bricks throughout the campaigns (Figure 38 A). This thickness measurement is represented through a color map by the software installed in the FERROTRON equipment. The map indicates, through different colors, the thickness values of the bricks. “Cold” colors such as blue and gray indicate regions with greater thicknesses (above 750 mm). “Warm” colors such as yellow and red represent the smallest thicknesses (below 300 mm). The greenish hue indicates regions of intermediate thickness (between 300 and 700 mm).

Figure 38 – Laser scan image of a converter throughout a campaign showing the wear profiles over time through the color map (thickness of the bricks)

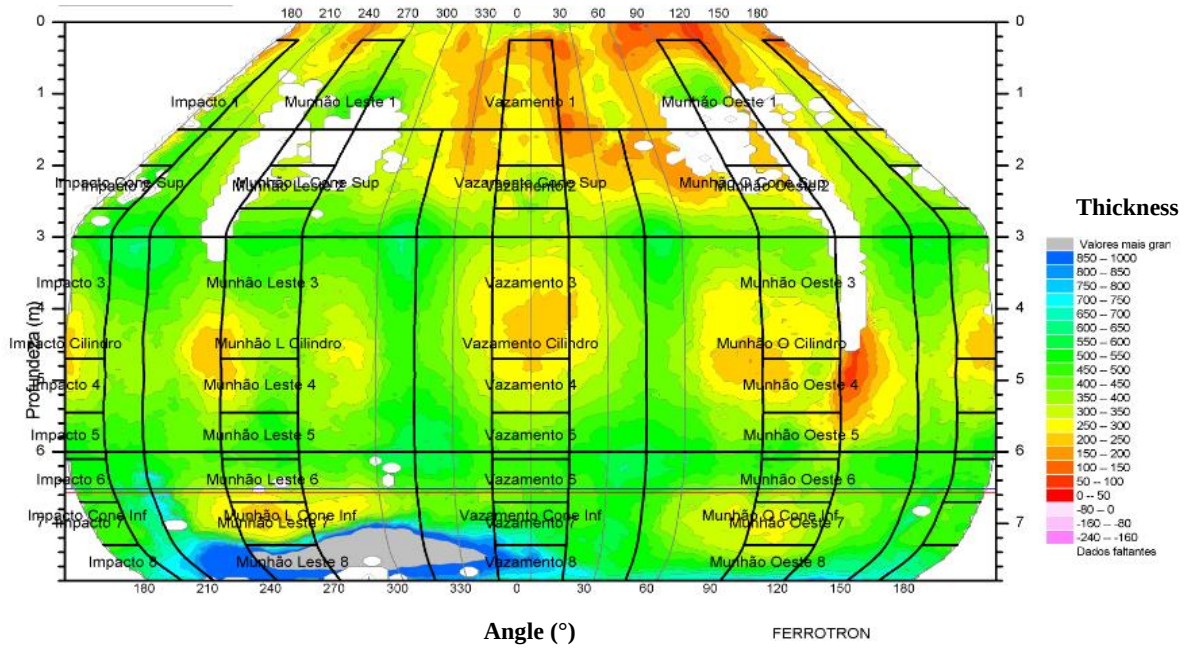

(A)

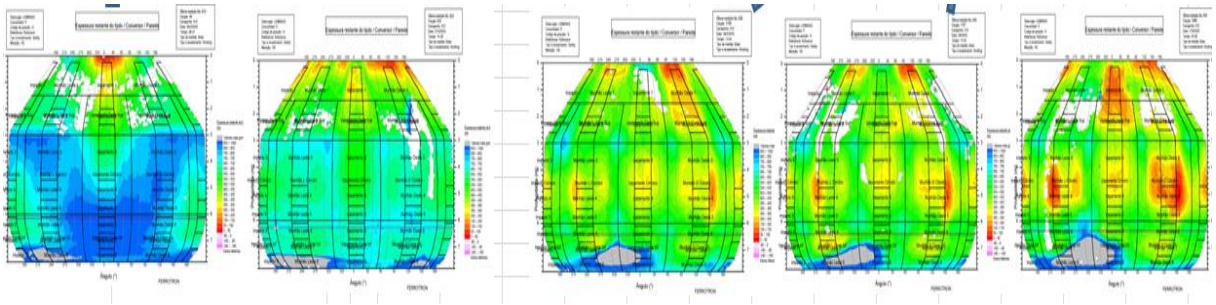

(B) (C) (D) (E) (F)

Source: Own authorship.

Figure 38 (B, C, D, E and F) illustrates five scans performed in five different periods (increasing from B to F). The evolution of the refractory wear is verified through the evolution of the shades from blue to red regions (practically with total wear of the working brick). It is clearly to notice how the regions of the trunnions are the ones that are most quickly wear and, therefore, are the regions that determine the life of the lining (region object of study and modeling in this thesis).

From these measurements, it was possible to calculate the wear rates between measurement periods, which are basically given by the difference in the measured value of the previous thickness reduced from the current thickness value and divided by the number of heats in that measurement interval (Table 7). The unit of measure for this wear rate is millimeters of wear per heat (mm/heat).

For each measurement interval of this wear rate, the mean values of the process variables for the corresponding period were calculated (Table 7). Therefore, it was possible to verify how the increase or decrease in the wear rate is influenced (correlated) by the increase or decrease in the average values of the process variables.

3.3 Step 3

Step 3 was performed through statistical modeling of the wear refractory rate as a function of process variables using the MINITAB software. Univariate and multivariate correlation models were built and analysis through time series of these parameters sought to determine which variables are relevant (the criteria for choosing is in APPENDIX E) for the control of refractory wear of the LD trunnions. In addition, deterministic models were built to predict the wear rate as a function of process variables for each analyzed campaign.

The main statistical criteria adopted are not discussed in this section due to the fact that they have already been discussed in the bibliographic review of section 2.8 and because they are common knowledge of classical statistics adopted in scientific studies, but the main methodology was to minimize the sum of squares of the residues.

Specific criteria for analysis and acceptance of parameters are addressed throughout the analysis of results and the determination of deterministic equations found through data analysis.

3.4 Step 4

In step 4, the SOM data analysis technique was applied, through which correlations between process variables and wear refractory rate were identified, identifying the most relevant control parameters in refractory performance. The same database used in the statistical analyzes was used by SOM so that the results could be compared and validated.

Figure 39 illustrates a SOM result in which the refractory wear rate is correlated with the percentage of MgO compound in the LD slag of one of the campaigns. It appears that there is a negative correlation between these two variables, showing that for higher levels of MgO in the LD slag will have a possible reduction in the refractory wear rate. This identification of the correlation is seen through the color map of figure 39, in which the regions with the lowest wear rate (cluster of blue colors) are in the same position as the region with the highest MgO contents of the slag (cluster of red colors and Yellow). The run scale represents the values of the variables going from the lowest ("cold" runs to the highest "hot" runs). The values of the ruler (axis) to the right of the map indicate the values of the respective correlated variables (wear rate and MgO content in the slag).

Figure 39 – Images by SOM showing the correlation between the wear refractory rate and the percentagem of MgO in the LD slag

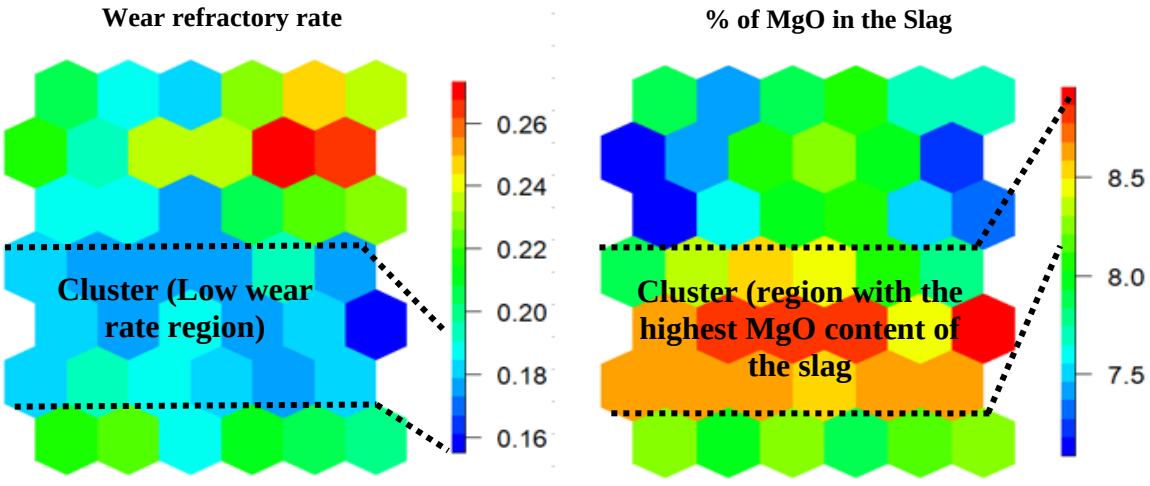

Source: Own authorship.

To perform the analysis by SOM, an algorithm was built using the R software and its programming interface called RStudio. The input data was fed into the program through matrices and cleared of any empty columns or rows. Then, the data

were normalized to take into account different magnitudes in the data, and randomized, to ensure an unbiased selection of entries during processing. The SOM analysis was performed considering a hexagonal and toroidal space with 42 nodes, Gaussian neighborhood function and Euclidean object distance. The resulting 2D map is renormalized and brought back to the original data magnitude.

For good statistical accuracy, the complete SOM learning process may require a substantial number of steps. The available sample itself was used repeatedly in training, feeding it several times into the algorithm, as a bootstrap technique. The minimum number of steps indicated in the bibliographic references is 500 times the number of network units. For this job-specific dataset, convergence was found at about 33,600 steps.

3.5 Step 5

In step 5, a comparison was made between the analysis techniques (SOM and classical statistics) implemented in this thesis to verify the efficiency and complementarity of such different techniques applied in modeling refractory wear in LD converters. In the case of the steelmaking shop, the SOM tool presents itself as an innovation in process analysis of this type, in particular, in the analysis of refractory wear in LD, since there is no reference for the application of this analysis technique in processes like this.

The results found in the statistical analyzes were compared to those identified using the SOM analysis. A comparative analysis of the effects of the process variables in relation to the refractory wear rate was carried out, as well as the characterization of the complementarity between such different tools. Therefore, the validation of the application of the SOM tool was carried out by comparing the two methodologies.

3.6 Step 6

In step 6, a post-mortem analysis of refractory bricks from the regions of the trunnions was carried out in order to verify and validate the mechanisms and phenomena of wear found in samples of bricks and to verify if the parameters found in the data analysis make physical sense, that is, are related to the actual

degradation processes of the bricks. In particular, the validation of the next step can be verified through this step 6.

This step was carried out by comparing analyzes samples of trunnion bricks in three different period. The first period is related to samples from a campaign prior to the databases of this thesis and carried out in studies carried out by Usiminas in order to verify possible refractory failures. The second period is related to refractory samples from a contemporary campaign to the data analyzed in this thesis. The third period is related to the campaign carried out after the period of the analyzed data. The aim was not only to verify the current wear phenomena and mechanisms, but also to verify if these phenomena are recurrent over time. That is, can the proposed models be applied in periods different from those of the databases?

Furthermore, the analysis was carried out with two different suppliers. Therefore, it was possible to map the three main elements in the refractory wear of trunnions, namely:

1. the process variables;
2. the temporal dynamics;
3. the supplier (material).

The post-mortem analyzes on the refractory brick samples were carried out considering the following tests and characterizations:

1. Photographs of longitudinal cuts to identify internal cracks and surface chipping;
2. Chemical analysis to identify the chemical compounds and their percentages in the brick (by X-ray fluorescence spectrometry);
3. Analysis of the carbon content along the thickness of the brick to identify the degree of decarburization (oxidation);
4. Microstructural analysis by X-ray diffraction to identify the main phases present in the brick and its possible transformations throughout the campaign;
5. Density;
6. Porosity;
7. Compression strength to verify the drop in refractory strength throughout the campaign;
8. Average pore size.

Items 5, 6 and 8 concern the investigation of the possible degree of reactivity of the refractory gases, metals and slag throughout the campaign.

3.7 Step 7

In the final step 7, deterministic models were built to predict the wear rate of the refractories of the LD trunions as a function of the process variables. Such models were built using the MINITAB software, considering as important variables for determining the models the results found in the statistical analyses, in the SOM results and in the hypotheses of the mechanisms and phenomena of wear whose foundation came from the post-mortem analyses.

The possibility of adjusting the parameters (variables) of the deterministic equations based on the responses found in the SOM maps is highlighted. Therefore, such a tool, combined with statistical tools, can better guide the choice of which variables should compose the forecast models.

Finally, all the results and analysis found were modeled in order to establish a more effective management process for the purchase contracts of refractories for LD furnaces, the operational management of the life of the refractory lining through the control of the most relevant process variables in the process refractory wear, better planning of stoppages for changing campaigns and greater control over the operational safety of LD converters. For such purposes, it is necessary to establish an efficient model to predict refractory life as a function of the various process variables.

Table 8 summarizes the various phases and stages planned and executed for the realization of this thesis.

Table 8 – Planning and execution of activities and actions carried out – 5W1H

Activities	What?	When?	Where?	Why?	Who?	How?
Database construction	Historical data collection of operational variables	Construction -18/08 to 19/2 Validation – 19/03 to 19/04 Usage – 19/05 to 22/12	In the Steelmaking shop database and management reports	To carry out the analyzes statistics and the SOM tool	The author of the thesis	Through Access software and by Excel
Statistical analysis	Perform uni, multivariate and time series analysis on the data	After construction and validation of the database – 19/05 to 22/12	In the historical data raised in the previous item	Determination of correlations and construction of the wear rate prediction model	The author of the thesis	Software Statistical (Excel and Minitab)
SOM analysis	Perform the analysis of historical data	After construction and validation of the database – 19/05 to 22/12	In the historical data raised in the previous item	Determine the relationships of process variables and the rate of wear	The author of the thesis	Software SOM
Comparison and validation of the SOM technique in Steelmaking	compare the two analysis techniques and validate the SOM	After the previous 3 stages – 19/05 to 22/12	In the historical data raised in the previous item	Compare analysis tools and validate SOM application	The author of the thesis	Comparison of tool responses
Post-mortem analysis of trunnion bricks	Carry out analyzes of the characteristics of the bricks after the end of the campaign	21/01 to 22/06	At the industrial plant and at USP Laboratories	Identify wear mechanisms and phenomena. Physically validate statistical and SOM analysis	The author of the thesis	Tests, analysis and laboratory tests
Construction of a deterministic model and comparison between the 2 analysis techniques	Build a prediction model for the wear rate of LD converters	22/01 to 22/08	Usiminas/USP	Furnace life forecast	The author of the thesis	By MINITAB and SOM

Source: Own authorship.

4 RESULTS AND DISCUSSIONS

In this chapter, the results found in the analysis of the databases by classical statistics and using the SOM data analysis tool are presented and discussed. At the same time, deterministic models for estimating the wear refractory rate are presented as a function of the process variables whose statistical and SOM analyzes identified as relevant in the refractory wear process of the LD converter trunnions. In addition, discussions were made of the correlations found of the deterministic models built and a comparison between the analysis tools used.

Subsequently, the analyzes of the results obtained in the tests and post-mortem tests carried out on the samples of the refractory bricks from the region of the trunnions of the LD are discussed, in order to physically substantiate the models and results of the statistical and SOM analyses, as well as the deterministic models. The idea is to carry out a comparison of these models for the three selected campaigns and later a global analysis joining the three campaigns. Correlations of operational variables were also analyzed in the form of time series that, in principle, could be affecting the wear of the converter's refractory (life) as a function of the wear rate of the bricks.

4.1 Comparative analysis of the refractory wear profile in the east cylinder (trunnion) regions of the LD converter in the 3 campaigns analyzed using classical statistics and self-organizing maps (SOM)

For the analysis and modeling of the refractory wear rate of the LD converter, the region of the cylinder known as trunnion was considered, since it is this region that most often defines the life of the LD and the number of stops for refractory maintenance (availability of the active for production) during the useful life (campaign) of the furnace as discussed in the previous sections.

Due to symmetry considerations and the large amount of analyzes involved, the modeling was handled for only one of the LD regions (east side) as a similar behavior is expected for the west side because there are no differences in the design of converters between the two sides.

To carry out the analysis, three campaigns with very different life performances were considered. Campaign A with the best performance (above 4,000

heats), campaign B with approximately 4,000 heats considered intermediate performance and campaign C with the worst performance (below 4,000 heats).

This choice dynamic aims to obtain a sample that contemplates totally different spectrums in terms of performance and at the same time that it covers most of the company's real cases. Basically the range of heats for these three campaigns (samples) was 3,500 to 4,500 heats.

4.1.1 Analysis of the refractory wear profile in the trunnion region east cylinder of campaign A using classic statistical tools

The analysis and modeling of the wear refractory profile of the cylindrical region (trunnion) east of the converter was initially carried out through laser scanning of this region during the three campaigns, in which, at each given time interval (interval between heats), the measure thickness of refractory bricks was given (by scanning laser) to a certain life of the LD.

For better accuracy and safety of the analysis, the region with the smallest measurement of the area in question was considered (the scanner maps the entire region and indicates the failure, when it occurs, it is determined by the point of greatest wear (smallest thickness).

Figure 40 illustrates the wear refractory profiles of the three campaigns: campaign A (life greater than 4,000 heats considered a long campaign), campaign B (life of approximately 4,000 heats considered a medium campaign) and campaign C (life less than 4,000 heats considered a short campaign).

Figure 40 – Wear profile of refractory thickness curves over the service life of the LD obtained by laser scanning, fron the 3 campaigns under analysis, fron the trunnion region of the east cylinder with their respective regression equations

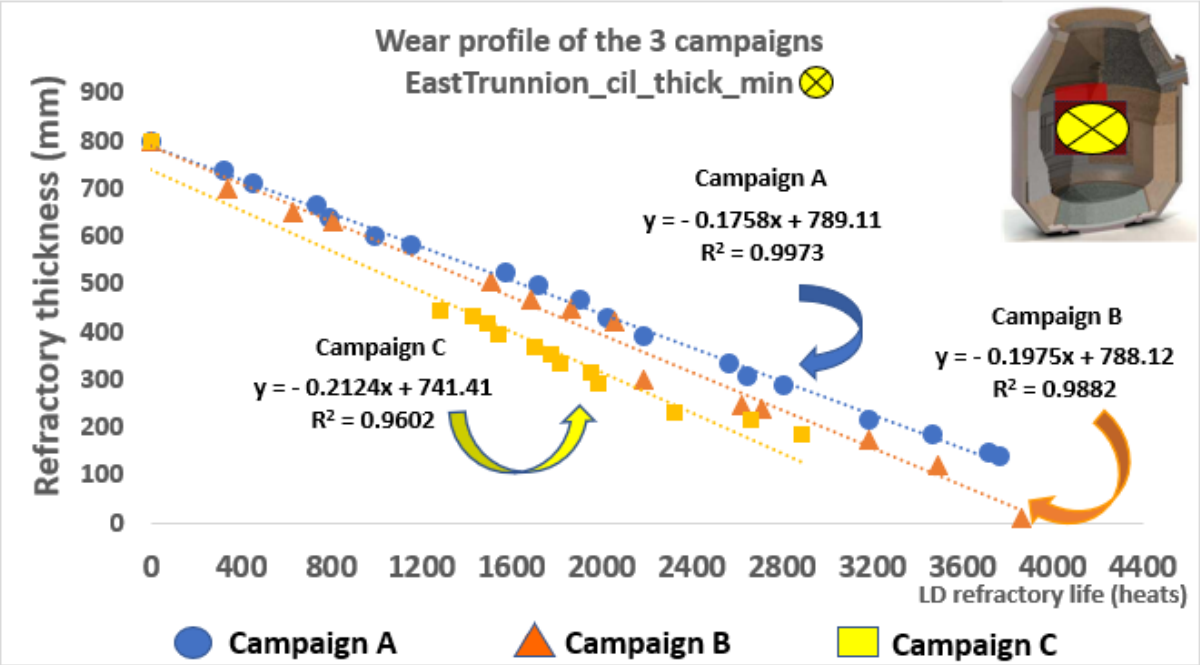

The analysis of figure 40 indirectly reveals the average refractory wear rates through the regression coefficients of the equations. For the campaign with the longest life (A) it have the lowest negative value for the coefficient (-0.1758), showing the lowest slope of the curve and consequently the lowest refractory wear and longest life of the LD furnace. For the other campaigns, intermediate and of shorter life, the values of the coefficients were -0.1975 and -0.2124, respectively. For the purpose of measuring units, these rates are considered as millimeters of wear per heat (mm/heat).

As the refractory design for the LD was the same for the three campaigns and there was no time interval between the campaigns that could justify any relevant technological updates in the equipment, it appears that the differences in performance come from the different process conditions (process variables). Therefore, all the modeling and identification of the refractory wear variables was carried out considering the variables indicated by the literature and by the professional experience of the people who work in the operational area of the steelmaking shop. For such modeling, 33 process variables were considered.

Due to the large number of variables and the high level of correlation between them, in addition to the different conflicting ways in which they can act in the process, it was decided to carry out a serial analysis over time to identify the most relevant

variables and their direction of action in the refractory wear rate of the LD. This analysis was carried out for each of the three campaigns, highlighting within each campaign the fluctuations of the most important variables in the refractory wear process (33 variables were mapped and analyzed for each of the three campaigns, however, only those that proved to be relevant in the wear process was used to modeling, as it would be very tedious and extremely useless to discuss variables with little or no relevant impact on the wear rate).

The average variations of the process variables were identified between each stretch of refractory thickness laser measurement (sections from 2 to 16 indicated in the following figures) and was possible to identify their effects on the wear refractory rate measured between each interval measurement with the scanner. The following figures illustrate the main effects identified in the refractory wear rate of Campaign A, as well as their direction (increase or reduction in the wear rate).

Figure 41 – Evolution of the refractory wear rate of the east trunnion in campaign A as a function of the fluxes and scorifiers, the condiction of slag and the percentage of heats with reblow in the LD converter process.

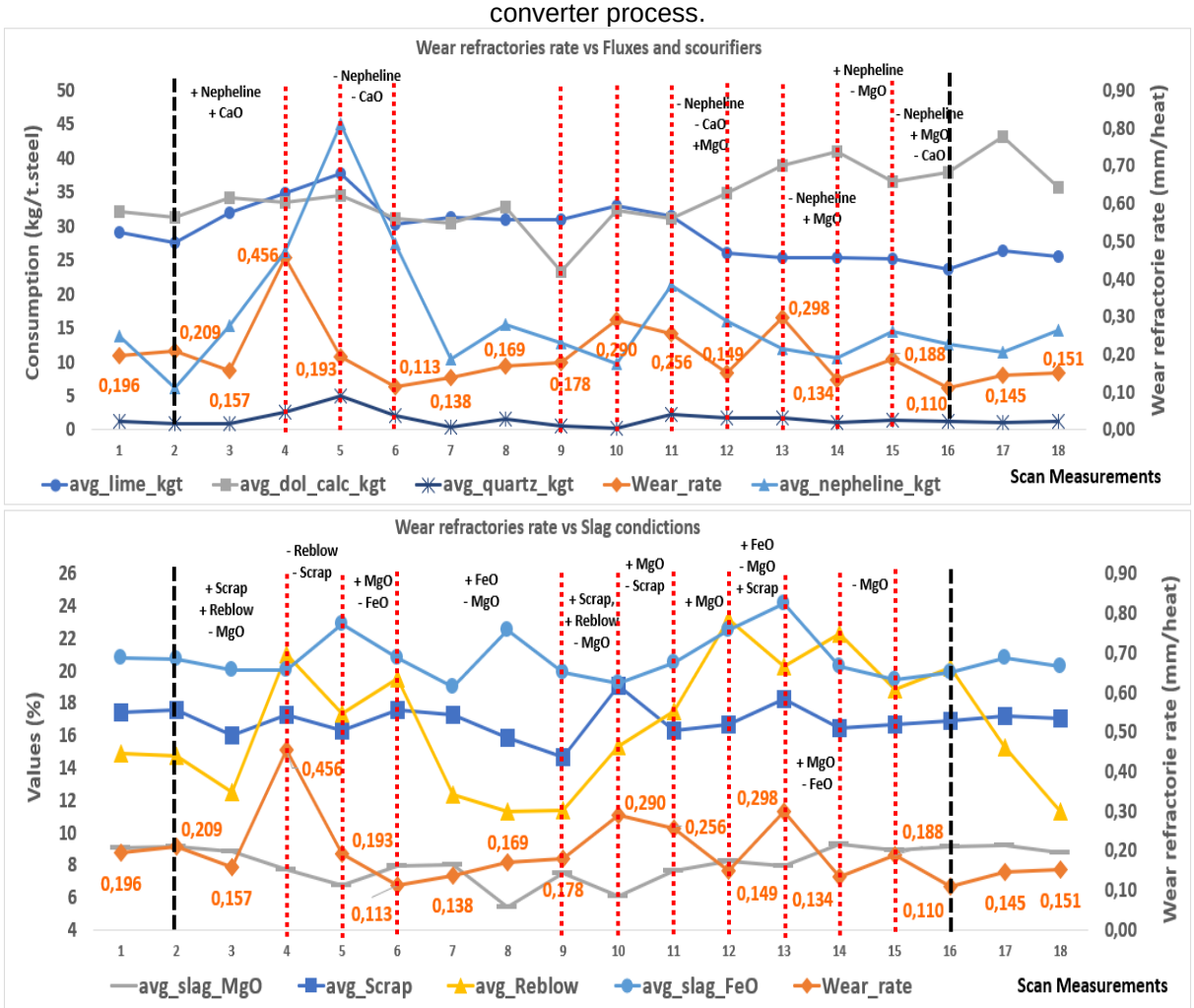

Figure 41 illustrates, through the two superimposed graphs, the effects of fluxes and scorifiers added during the steelmaking process, the chemical conditions of the slag and the percentage of heats with reblow on the refractory wear rate of the LD trunnion in campaign A. The effect of fluxes and scorifiers is verified through the influence of their compounds represented here by the variables lime (avg_lime_kgt), calcined dolomite (avg_dol_calc_kgt), quartz (avg_quartz_kgt) and nepheline (avg_nepheline_kgt) on the refractory wear rate (Wear_rate) of the trunnion. Where is see positive signs (+) it indicates an increase in the amount of these compounds, where is see negative signs (-) the opposite occurs, that is, the reduction. Figure 41 must be read together and between the measurement sections (2 to 16) indicated on the x axis, as events and phenomena occur simultaneously and can act by adding to each other (if they are in the same direction of wear) or canceling each other out (if they go in opposite directions). This dynamic of action of the variables is what makes the system of high level of complexity of analysis and control.

Figure 41 shows the effects towards increasing the refractory wear rate When is increase the additions of nepheline (source of Na, K and Si) and lime (source of CaO). The increase in calcined dolomite (source of MgO) produces the opposite effect, that is, a decrease in the refractory wear rate. In the first case, nepheline is a powerful slag fluidizer with a high power to reduce the melting temperature of the compounds, making the slag more corrosive and increasing the wear rate of the trunnions. Lime, on the other hand, has a harmful effect from certain values, since the basicity control is carried out through the addition of this compound. However, above certain values, excess CaO (from lime) in the slag ends up diluting other important compounds in wear control, such as MgO from calcined dolomite. Another factor that could be an explanation is the fact that high levels of CaO in the slag have the power to increase its melting point (the so-called dry slag), making it difficult for the slag to absorb P_2O_5 and, consequently, to dephosphorize inside the furnace. which would imply higher levels of oxidation of the metallic bath to obtain the desired final phosphorus in the steel.

Now, regarding the conditions of the slag, amount of scrap charged in the furnace and the percentage of heats with reblow, it is possible to verify from figure 41 its main effects on the trunnion wear rate. It is evident that the higher the FeO content of the slag (avg_slag_FeO), the greater the rate of reblown heats (avg_Reblown) and the greater the amounts of scrap used (avg_Scrap), the greater the rate of wear in

the furnace. These three variables are linked to higher levels of oxidation of steel and slag (as will be shown in the following figures), which makes the furnace environment completely corrosive for MgO-C bricks.

Furthermore, figure 41 illustrates that refractory wear rates are reduced for higher percentages of MgO dissolved in the slag (avg_slag_MgO), which is in agreement with the type of refractory brick used (MgO-C). In this case, the saturation of the slag in MgO is essential so that chemical gradients between the slag and the brick do not occur, reducing or even preventing the transfer of MgO from the refractory structure to the slag and, consequently, the degradation of the refractory structure of the LD furnace.

Figure 42 – Evolution of the refractory wear rate in the east trunnion of campaign A as a function of oxygen volume using during the reblow and the carbon content (indirectly from oxidation) in the metallic bath at the end blowing of the heats in the LD converter process

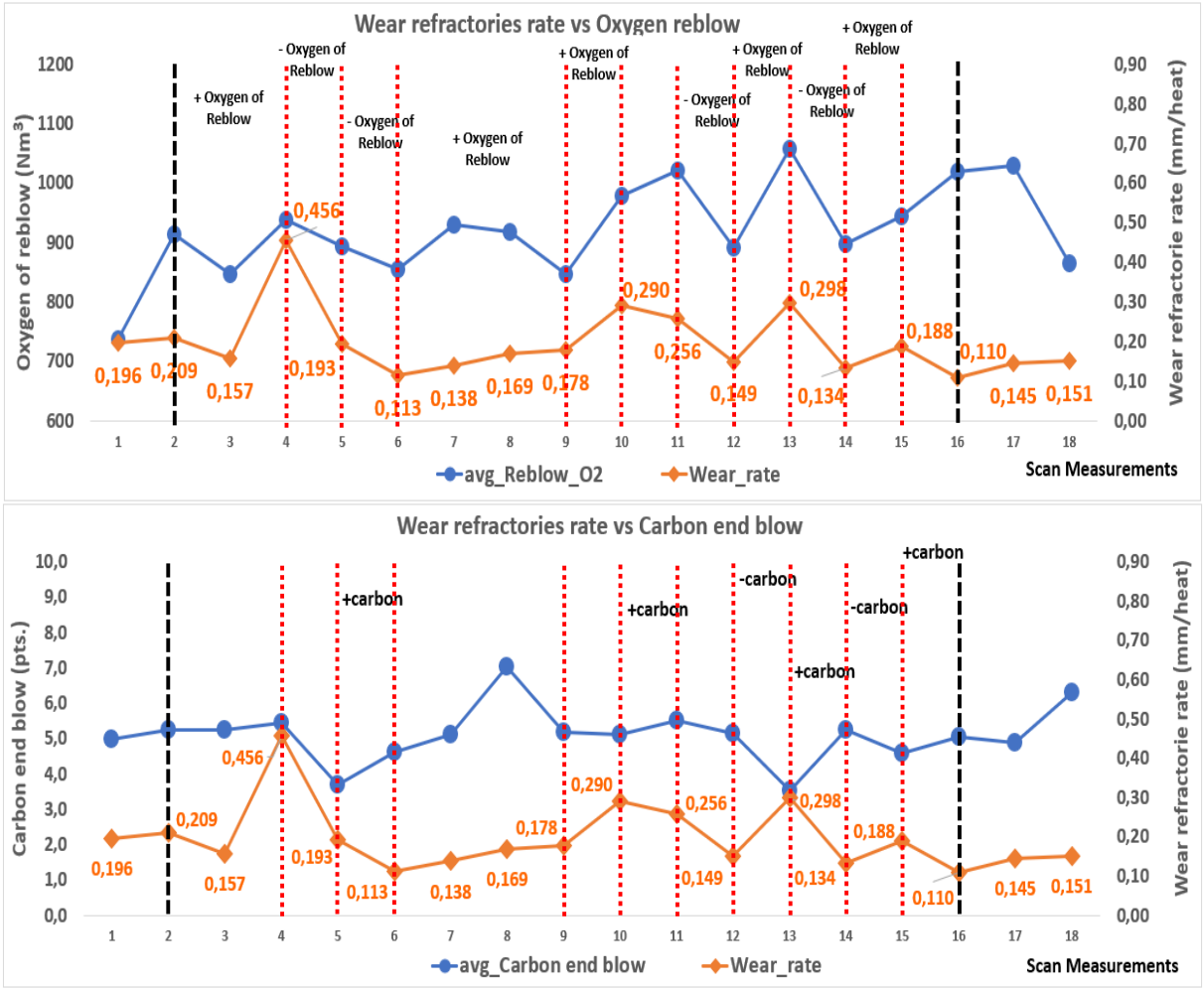

The reblow of the heat is a condition in which, after the end of the process blow in the heat, an additional blowing step was required, resulting in a high level of

oxidation of the slag and metallic bath. This condition is one of the most aggressive for the refractory brick, because in addition to carbon oxidation in the refractory bricks, the excess of iron oxides in the slag makes the slag highly reactive. In these cases, not only the percentage of reblow heats (as shown in figure 41), but the value of the volume of oxygen reblowing in the heat (avg_Reblow_O2) has a direct influence on the refractory wear rate and, consequently, on the level of aggressiveness of the reblow. Figure 42 makes it clear that the wear rate increases when this volume of blown oxygen increases in the reblow.

Regarding the carbon content of the metallic bath at the end of blowing, figure 42 reveals in several sections such as 5 to 6, 10 to 11, 12 to 13 and 13 to 14 that the highest carbon at the end of blowing (avg_carbon end blow) contributes favorably to the drop in the refractory wear rate. This is explained by the lower oxidation of the metallic bath and slag for higher end-of-blow carbon values and consequent lower corrosive effect on the refractory. Obviously, as the refractory is made of MgO-C, higher levels of bath oxidation (lower carbon at the end of the blow) and slag promote oxidation of the refractory carbon, which leads to greater refractory wettability by metals and slag and the formation of voids (pores) in the structure with consequent infiltration and corrosion by the slag also rich in oxygen and drop in the refractory mechanical resistanse.

Figure 43 – Evolution of the east trunnion refractory wear rate of campaign A as a function of the dephosphorization rate in the metallic bath of the LD converter process

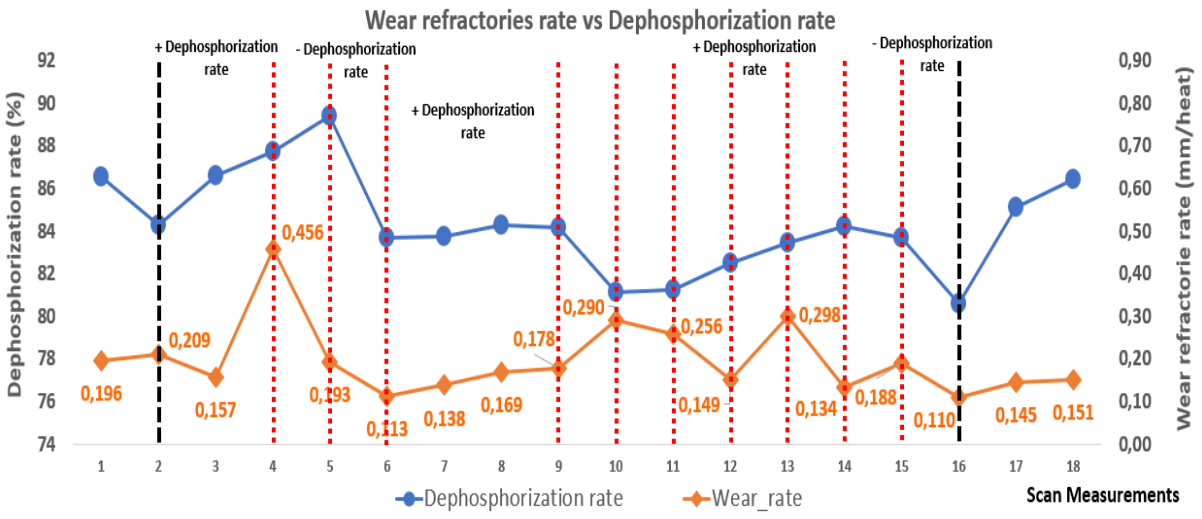

The effect of the dephosphorization rate (Dephosphorization rate) in the LD furnace is very evident in the seven sections shown in figure 43, the

dephosphorization rate was calculated considering the initial phosphorus in the raw materials (pig iron) and the phosphorus of the steel at the end of the blowing process. This variable is closely related to the levels of oxidation of the metal bath and slag, which need to be high to obtain high rates of dephosphorization of the metal bath, an extremely deleterious situation for the refractory, as previously described.

Figure 44 – Evolution of the refractory wear rate in the east trunnion of campaign A as a function of the silicon content in the pig iron and the average process time in the LD converter

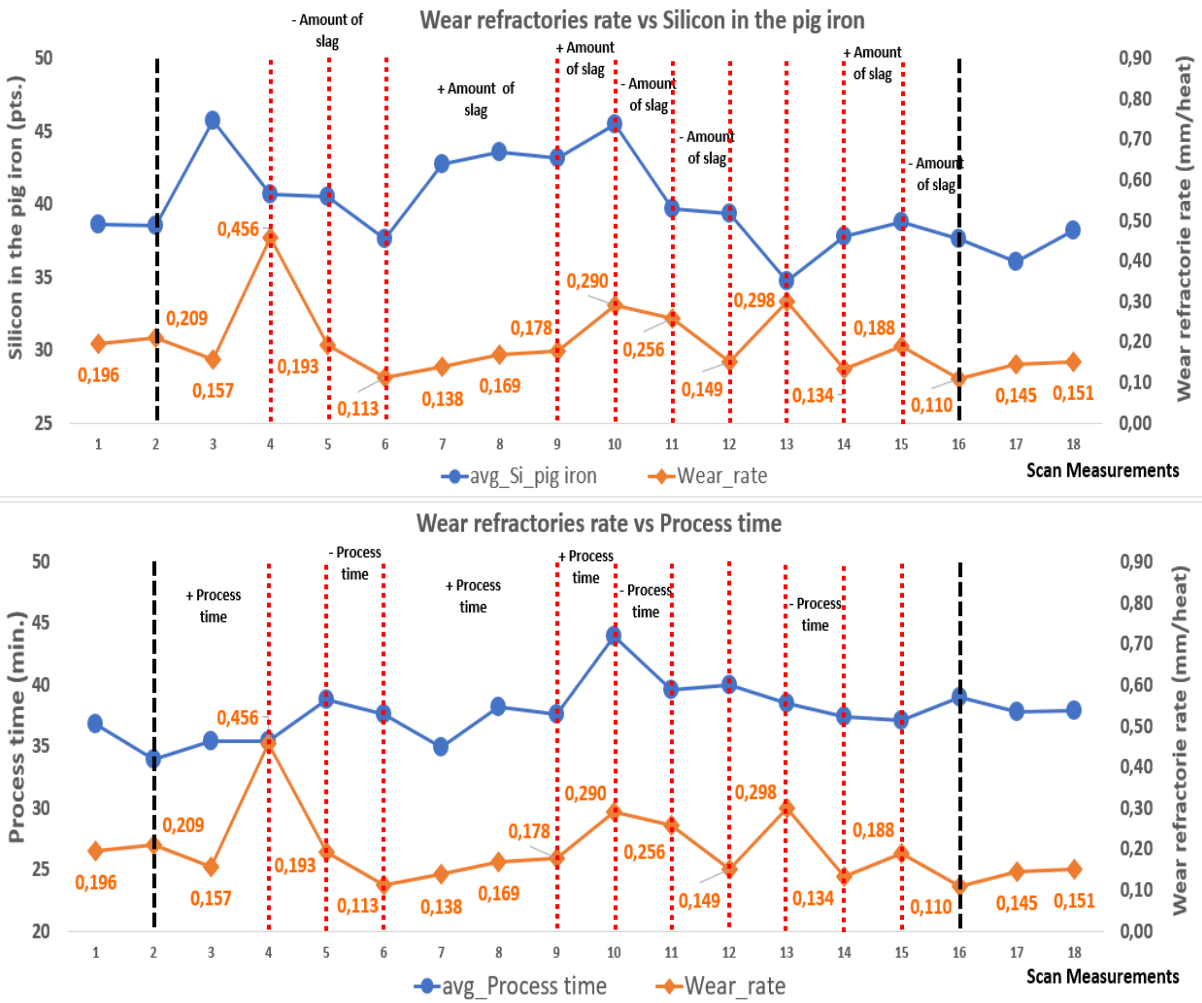

The percentage of silicon in the pig iron (avg_Si_pig iron) can influence the refractory wear rate, especially when its values oscillate far outside the average. In the case of excessive increase, for the same basicity of the LD furnace, a high amount of slag is obtained in the LD due to the addition of CaO added by lime to neutralize the SiO_2 formed in excess by the increase in silicon in the pig iron. If this slag is not in proper condition, an increase in the wear rate may occur. In addition,

there are several operational problems related to the high volume of slag, mainly operational stops to control furnace foaming. When these stops are constant within the blowing process in the LD, the process conditions are more aggressive, such as, for example, the increase in the percentage of reblowing in the heats due to reactions at the end of the blowing, temperature drops, among others. Figure 44 shows that the wear rate increases when the percentage of silicon in the pig iron also increases.

Another impact of the increase in silicon in the pig iron would be the effect of greater oxidation of the bath and slag, since the removal of the silicon element from the pig iron is done by oxidation of the silicon itself by the blow of oxygen. Therefore, higher volumes of oxygen blown are expected in heats with higher silicon content in the pig iron.

The opposite effect, of silicon reduction with reduction of the wear rate is also observed, evidencing its possible direct correlation. Obviously, very low values of silicon (this was not the case observed in figure 44) could have deleterious effects due to the lack of thermal input and consequent excess oxidation of the metallic bath at the end of the blowing process.

The process time (avg_Process time) shown in figure 44 was also representative of the refractory wear rate, it can be seen that the wear rate increases for longer process times. Longer process times of a heat indicate longer contact times between the refractory bricks with the metallic bath and the slag, generating greater exposure to the various chemical reactions of refractory dissolution, in addition, to greater exposure to the thermal conditions of the process.

The two variables, pig iron silicon and process time, seem to be correlated betwen then as shown in figure 44 (same highlights for each variable). In fact, for higher silicon contents in the pig iron, the probability of occurrence of events that end up causing some kind of stoppage in the process (excessive foaming, for example) increases. Therefore, the analysis of figure 44 leads to directly associate refractory wear with these two process variables.

Figure 45 shows two variables (end blow temperature and binary basicity) that, in principle, would be expected to correlate strongly with refractory wear rate. However, this has not been identified. Despite this, it is relevant to comment and discuss the reason for this result given the relevance of these two variables.

Figure 45 – Evolution of the east trunnion refractory wear rate of campaign A as a function of end blow temperature and binary basicity in the LD converter process

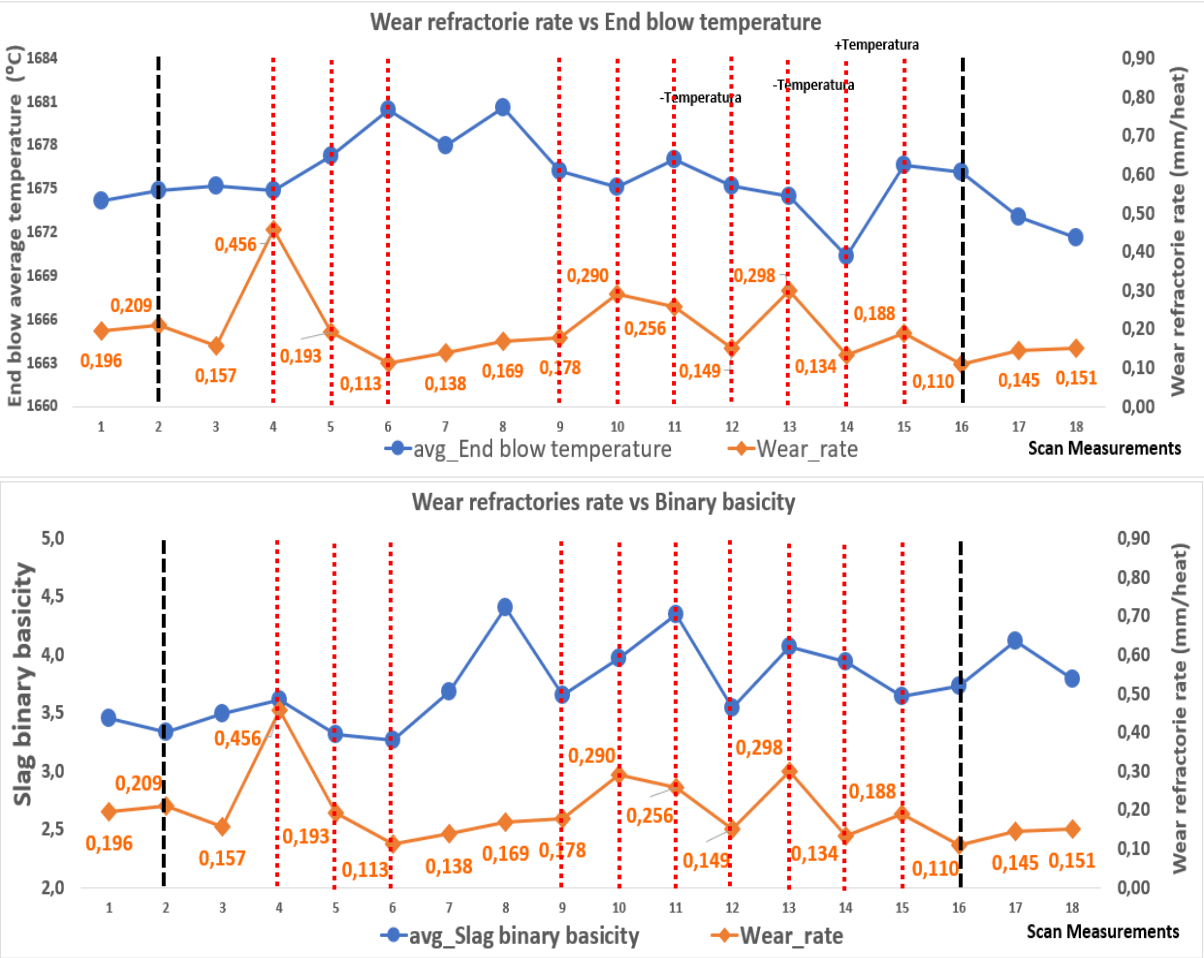

The effect of the end blow temperature (avg_End blow temperature) can be noticed more at the end of the campaign (figure 45). It is expected that the increase in average process temperature causes an increase in the refractory wear rate. However, these increases are only verified in practice when process temperatures exceed certain prohibitive values, for example, temperatures above 1690 °C. Variations within average values (1660 °C, 1670 °C, 1680 °C) do not imply variations in the wear rate that are relevant in operational practice. This may be the explanation for the lack of evidence of correlation shown above in figure 45.

With regard to the basicity of the slag, a totally unexpected effect is evident. It is observed in the graph of figure 45 that the basicity increases are accompanied by increases in the refractory wear rate. As the refractory bricks are basic, an opposite effect was expected, that is, the reduction of the wear rate with the increase in the basicity of the slag. One explanation for this phenomenon would be that, starting from certain values of basicity, the effect on the increase in the melting temperature of the

slag due to the high levels of lime added to neutralize SiO_2 and raise the basicity would make the slag “dry” and make it difficult to protection of this slag during Slag Splashing (as it would greatly increase the viscosity of the slag).

Another explanation would be the fact that increases in basicity are accompanied by increases in the amount of lime (CaO) added to the slag with consequent dilution of MgO, obviously, provided that this is not adjusted. A phenomenon that could also be occurring would be the difficulty of dissolving MgO in the slag rich in CaO from lime, as this compound would increase the liquid temperature of this slag, making the dissolution of MgO difficult. In both cases, the possibility of non saturation of the slag with MgO could lead to the dissolution of MgO from the refractory to the slag in order to balance the chemical gradient between them.

Two summary tables (tables 9 and 10) were built based on the analysis of the figures above showing the main variables that acted in the sense of increasing and reducing the refractory wear rate of the trunnion along campaign A of the LD converter. In these tables, all the complexity of analyzing systems like the one described above can be seen, in which a series of variables act at the same time. The greatest difficulty in analyzing this type of system is the fact that certain variables that would act in a certain direction on the refractory wear rate may not be being visualized (translated) in this way. For example, in certain stretches in which the oxidation of the heats is higher and an increase in the wear rate would be expected, it may not be reflected if other variables are acting in the sense of reducing the wear rate in that same stretch of analysis.

The reading of tables 9 and 10 is done considering that the first line indicates the variations in the refractory wear rate in relation to the previous section (points 2 to 16 in the figures above), for example, a Δrate indicated by + (118%) indicates that in relation to the previous section (point 2 for example) there was an increase of 118% in the wear rate to compare with point 4, in the case of an indication of – (58%) there was a reduction of 58% in the wear rate compared to the previous segment. The second line indicates the stretches (measurement intervals of the process variables). From the third line onwards are the positive (+) and negative (-) variations of the variables, in this case the respective increases and reductions.

Table 9 – Summary influence of the main variables that impacted the refractory wear rate in the east trunnion of the LD in campaign A (sections 2 to 11)

ΔRate + (118%)	ΔRate - (58%)	ΔRate - (41%)	ΔRate + (58%)	ΔRate + (63%)	ΔRate - (12%)
2 → 4	4 → 5	5 → 6	6 → 9	9 → 10	10 → 11
+Nepheline		-Nepheline			
+CaO		-CaO			
+Reblow	-Reblow			+Reblow	
		-FeO	+FeO		
-MgO		+MgO	-MgO	-MgO	+MgO
+O_2/Reblow	-O_2/Reblow	-O_2/Reblow	+O_2/Reblow	+O_2/Reblow	
		+End carbon			+End carbon
+Dephosphory rate		-Dephosphory rate			
		-Slag volume	+Slag volume	+Slag volume	-Slag volume
		-Process time	+Process time	+Process time	-Process time
+Scrap					-Scrap

Table 10 – Summary influence of the main variables that impacted the refractory wear rate in the east trunnion of the LD in campaign A (sections 11 to 16)

ΔRate - (42%)	ΔRate + (100%)	ΔRate - (55%)	ΔRate + (40%)	ΔRate - (41%)
11 → 12	12 → 13	13 → 14	14 → 15	15 → 16
- Nepheline		- Nepheline	+ Nepheline	- Nepheline
-CaO				
	+FeO	-FeO		
+MgO	-MgO	+MgO	-MgO	
-O_2/Reblow	+O_2/Reblow	-O_2/Reblow	+O_2/Reblow	
	-End carbon	+End carbon	-End carbon	+ End carbon
	+ Dephosphory rate			- Dephosphory rate
			+Slag volume	
		-Process time		
-Temperature		-Temperature	+Temperature	
	+Oxidation	- Oxidation		
	+Scrap			

4.1.2 Multivariate statistical analisys of the refractory wear rate in the east cylinder region (trunnion) of the LD of campaign A

Through multivariate statistical modeling, a deterministic equation was built through which the refractory wear rate can be estimated as a function of process variables. Equation 16 was obtained using the same database as the previous analyzes of campaign A. Acceptance criteria for the regression coefficients (*p*-value < 0.05 and 1 < VIF < 2) and the residuals (normality, homoscedasticity and independence see APPENDIX A).

$$\text{Wear rate} = -4.809 - 0.01868 * \text{dol\_calc} + 0.0772 * \text{scrap} + 0.02879 * \text{CaO\_slag} + 0.1864 * \text{BB\_slag} + 0.01320 * \text{reblow} + 0.02770 * \text{txdp} \quad (16)$$

$$R^2 = 88.81 \quad R^2(\text{aj}) = 82.70$$

Where:
Wear rate: Average refractory wear rate of bricks (mm/heat);
dol_calc: Average value of calcined dolomite for heat (kg/t. steel);
scrap: Percentage of scrap added for heat (%);
CaO_slag: Percentage of CaO in the slag (%);
BB_slag: Slag binary basicity (CaO/SiO_2 ratio), dimensionless;
reblow: Percentage of heats that reblow (%);
txdp: Average dephosphorization rate in the heats (%).

From equation 16, it can be seen that the refractory trunnion wear rate in campaign A is mainly influenced by the amount of average calcined dolomite added in the heats, by the percentage of scrap in the LD furnace metal charged, by the percentage of CaO compound in the slag, by the basicity slag binary, by the percentage of average heats reblown in the LD and by the converter's dephosphorization rate.

The first variable, calcined dolomite (dol_calc), according to equation 16, has an inverse relationship with the refractory wear rate. That is, higher average amounts added per heat reduce the refractory wear rate of the LD trunnion. The basic explanation is the increase in the MgO compound in the process slag, as calcined dolomite is the main source of addition of this compound in the LD process. As the

refractory bricks are basic and based on MgO-C, greater saturation of MgO in the process slag balances the chemical gradient between the MgO in the slag and in the refractory, causing this compound not to be dissolved by the process slag (or that the dissolution rate is reduced).

The second variable indicated by equation 16 was the percentage of scrap in the LD's metal charge (scrap). Scrap, in addition to being a source of metallic iron, is responsible for the furnace's thermal balance. In low percentages it can be beneficial to the LD. However, above certain values, scrap becomes deleterious to the refractory wear process, since the greater the amount of scrap used in the LD process, the greater the amount of blown oxygen will be necessary for the complete melting of this solid material (depending, of course, on the temperature of the charged liquid pig iron). Therefore, higher percentage amounts of scrap from certain values increase the final oxidation of the heat and the volume of oxygen blown into the furnace. Both events cause a greater oxidation of the carbon in the refractory structure, leading the furnace to higher refractories wear rate. Both the oxidation by the jet of oxygen from the lance, the post blow furnace environment and the oxidation by the metal bath and slag facilitate this reaction with the carbon in the refractory. In this case, the equation is coherent with the literature and operational practice.

The third variable, percentage of CaO in the slag (CaO_slag), has an interesting evaluation. Therefore, this compound is necessary to balance the basicity of the slag rich in SiO_2 and initially acidic, which would be highly harmful to the refractory (basic) structure. However, for certain percentages of CaO in the slag, this compound starts to dilute the added MgO, making the refractory preservation effect contrary and harmful to the refractory. If added in large amounts, dilution of MgO can cause an imbalance between MgO in the slag and MgO in the refractory. A chemical potential difference could induce the dissolution of MgO from the brick to the slag, causing a significant increase in refractories the wear rate, as indicated by the multivariate equation.

The fourth control variable was slag basicity. This was the most controversial variable, as the furnace having a basic refractory, it is expected that the more basic the slag, the lower the wear rate. However, it was not found. This variable was positively related to the wear rate. A possible explanation would be the fact that the high basicities of the furnace would make the highly viscous slag “dry”, in order to make processes such as metallic bath dephosphorization and decaburization of the

furnace difficult, in addition to the fact that it increases the volume of slag and causes the well-known reactions of end of blowing that absorb energy from the converter and cause an increase in the percentage of reblow in the heats. In the three cases, the reblow index and the longer time the steel remains inside the LD could bring about this indirect increase in the rate of wear of the bricks. Another explanation would be the fact that highly viscous slags could lose some of their adhesion efficiency to the LD walls during the Slag Splashing process. One possibility of adjustment to the equation would be the introduction of a binary variable in the equation, through which the basicity would enter in a positive and negative way at the same time for different ranges of this parameter.

The fifth variable of the equation, reblowing, showed a direct relationship with the refractory wear rate, that is, heats in which, after the end of the normal oxygen blowing process, for some reason, they have to be reblown tend to have a higher wear rate. In this case, the literature indicates a direct correlation with the refractory wear rate, as the level of metallic bath and slag oxidation increases in cases of reblow heats, which makes the environment in contact with the bricks highly corrosive. In addition to the fact of the direct oxidation of the carbon with the jet of oxygen from the lance and with oxygen from the furnace environment. Other impacts would be the fact that reblown heats acquire extremely high temperatures and slag with high fluidity, which facilitates the reaction kinetics between the medium and the refractory bricks and a low efficiency of adhesion of the Slag Splashing on the walls bricks of the LD.

The sixth and last variable, metallic bath dephosphorization rate, was directly correlated to the wear rate. This variable considers the levels of reduction of the element phosphorus charged in the raw materials and the level of phosphorus in the final steel produced in the LD. For this, the process conditions such as volume and basicity of the slag, amount of dissolved CaO, process temperature and oxidation level, must be well adjusted. The phosphorus element is removed from the metallic bath by its transformation (oxidation) to P_2O_5, which requires high levels of oxidation of the heats and consequently high levels of refractory wear. Other important variables such as the addition of nepheline (a powerful slag fluidizer) and long process times are indirectly associated with this rate of dephosphorization.

4.1.3 Analysis of the refractory wear rate in the east cylinder region (trunnion) in the LD of campaign A through the SOM

In parallel to the statistical analyzes previously carried out, a correlation analysis of the process variables with the refractory wear rate of the LD trunnion was carried out using the SOM data analysis technique using the same database used in the previous statistical analyses. In addition, the comparison of results between very different methodologies (SOM and classical statistics) was verified in order to implement the application of SOM in studies of this type.

Such analysis techniques can still act in the sense of complementarity between them, since variables that apparently were not relevant in one technique due to factors such as multicollinearity between parameters can be relevant in the other data analysis technique.

As with statistical analyses, and for the same reasons, only the most relevant results and some specific cases of behavior that deserve to be highlighted will be presented and discussed. For the same database of variables analyzed in the previous items, the SOM tool was applied with the following results.

Figure 46 – SOM analysis, refractory wear rate vs amount of nepheline used. East trunnion of campaign A of the LD converter. Direct relationship between variables (some positions in the clusters)

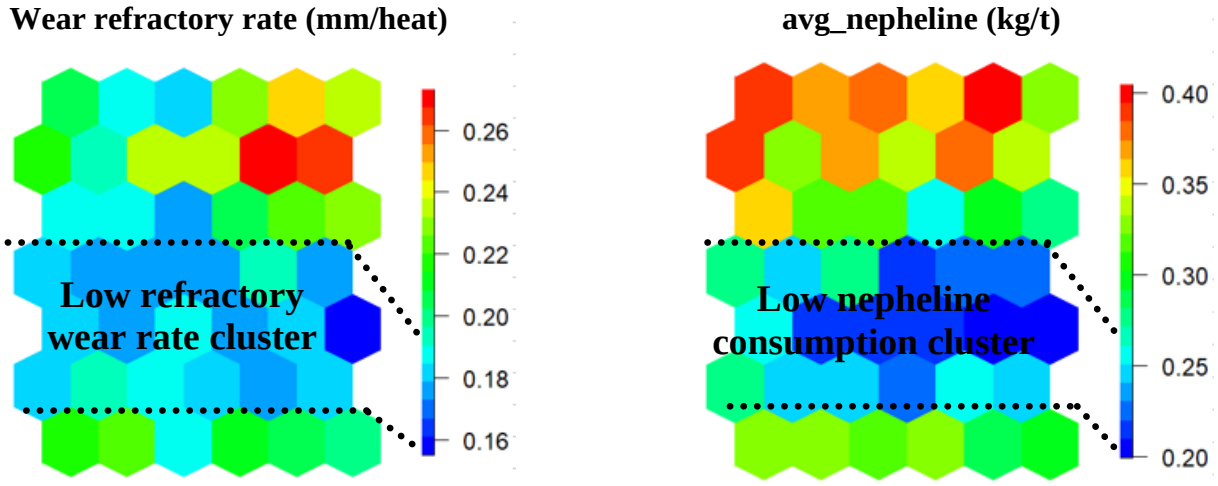

According to images in figure 46 obtained through the application of the SOM technique in the database, it can be seen that there is a direct correlation (same positioning of the clusters) between refractory wear rate and the amount of nepheline added (avg_nepheline). Note that the location of clusters with low wear rate is similar

to the location of clusters with low nepheline consumption, in the same way that places with higher wear rate coincide with those with higher consumption. This result is in agreement with the literature and with the statistical analyzes performed previously for campaign A in the time series. Nepheline, as previously discussed, is a slag fluidizer and therefore makes it highly aggressive to refractories, facilitating the penetration and dissolution of the refractory matrix by the slag from the LD process.

Figure 47 – SOM analysis, refractory wear rate vs Amount of lime used and percentage of MgO in the slag. East trunnion of campaign A of the LD converter

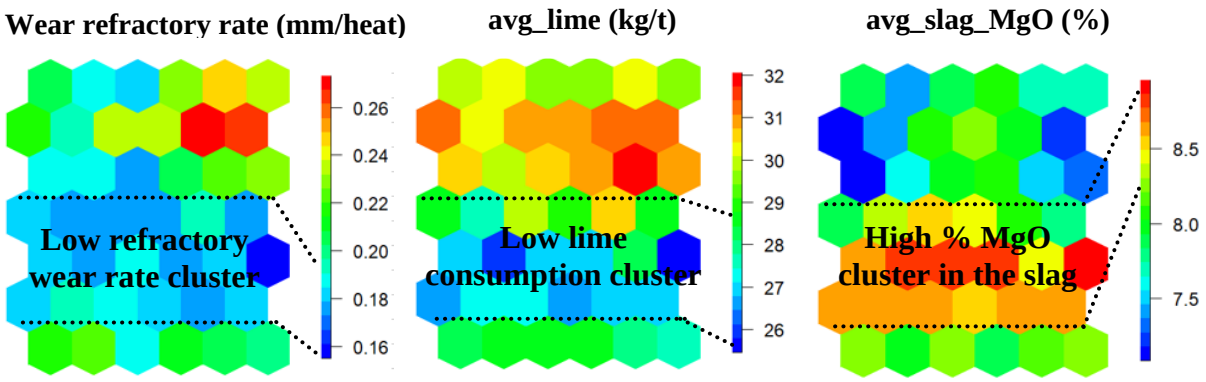

Figure 47 shows the direct relationship between the refractory wear rate and the amount of added lime (avg_lime) and inversely with the slag MgO content (avg_slag_MgO). Both results are in line with the statistical analyzes obtained and with the literature.

In the case of lime, what may be happening for large quantities added would be the dilution of the MgO in the slag itself, which would lead to the non saturation of this compound in the slag and, consequently, the dissolution of the MgO in the refractory brick to equalize the chemical gradient between the slag and refractory brick.

The inverse relationship between slag MgO and wear rate is a direct consequence of the chemical constitution of MgO based bricks. Interestingly, these variables also appeared in the previously developed multivariate equation presented in the previous section. Therefore, the results found by SOM analysis are consistent with those identified in the time series and multivariate analysis.

Figure 48 – SOM analysis, refractory wear rate vs percentage of heats with reblow and percentage of scrap charged. East trunnion of campaign A of the LD converter

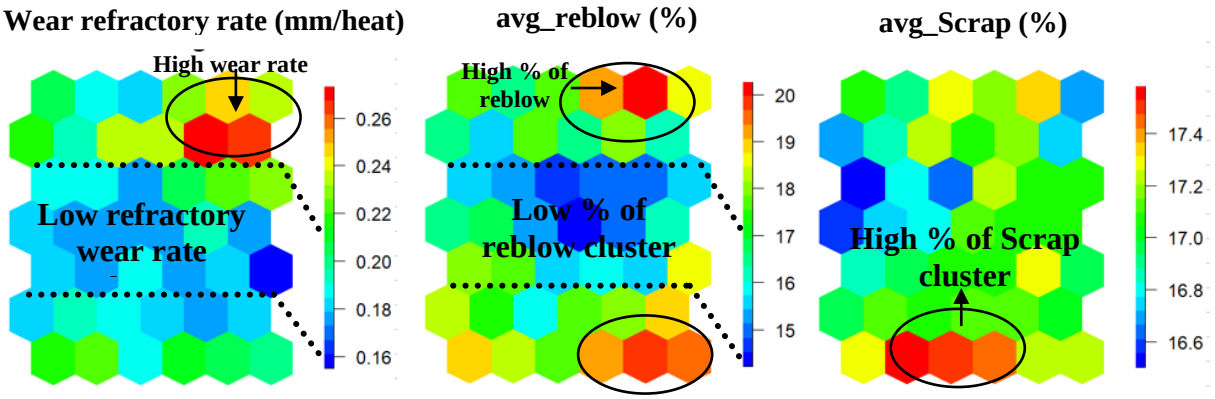

The images in figure 48 reveal the direct relationships with the wear rate of both variables, percentage of heats with reblow (avg_reblow) and percentage of scrap charged in the metal bath (avg_Scrap).

These variables, when in high values, are directly related to the levels of oxidation of the metallic bath and slag, making the refractory conditions more aggressive, as already discussed in the previous sections.

In situations with a high percentage of heats with reblow, post blow temperatures are generally higher than normal, which can accelerate refractory wear reactions. The SOM results are in agreement with the statistical analyzes and the multivariate wear equation presented above.

Figure 49 – SOM analysis, refractory wear rate vs dephosphorization rate and slag binary basicity. East trunnion of campaign A of the LD converter

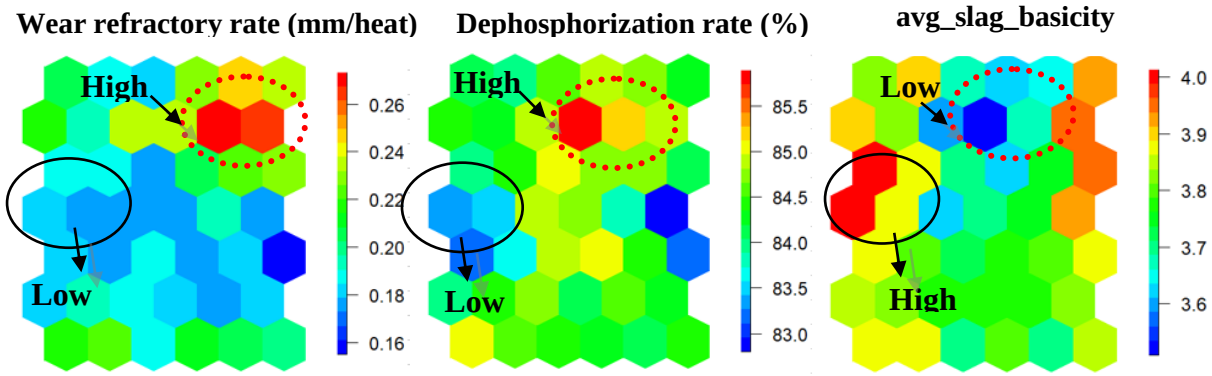

Figure 49 shows the relationships found for the refractory wear rate with the dephosphorization rate and the slag binary basicity (avg_slag_basicity). Results similar to the statistical analyzes and with the multivariate deterministic equation can

be seen in figure 49. The metallurgical considerations regarding the understanding of these variables in relation to the refractory wear rate are identical to those previously described in the statistical analyses.

Figure 50 – SOM analysis, refractory wear rate vs end blow carbon and temperature. East trunnion of campaign A of the LD converter

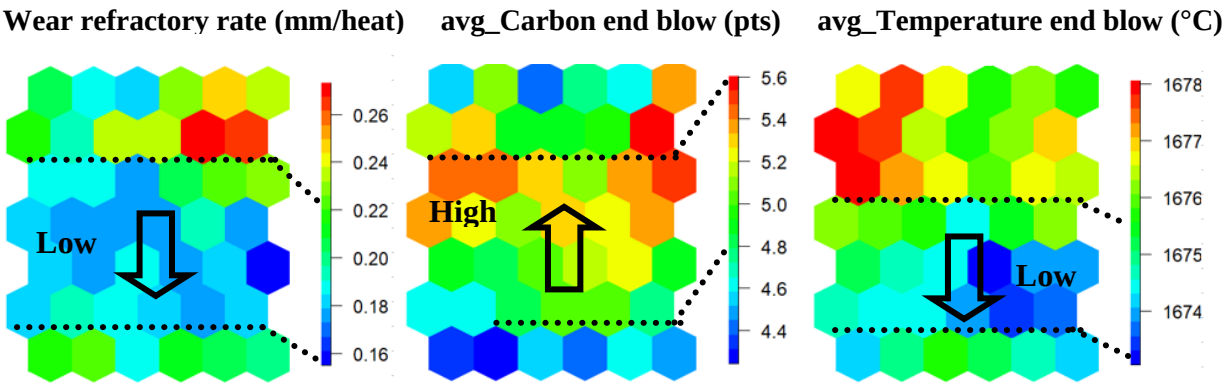

Figure 50 shows the inverse correlation of the end blow carbon (avg_Carbon end blow) with refractory wear rate and the direct correlation of the end blow temperature (avg_Temperature end blow) with wear rate.

In the first case, the higher the carbon at the end of the blowing of the metallic bath in the LD process, the lower the oxidation level of the heat and, consequently, the lower the expected wear rate. In the second case, for higher temperatures at the end of the blow, the speed of reaction between slag and brick would be greater, in addition, of course, to the greater fluidity of this slag, which would lead to greater penetration into the pores of the refractories bricks, causing higher levels of wear. Therefore such results above are also metallurgical and ceramic coherent.

It is noteworthy that the temperature variable had not been identified as relevant (within this specific range) in the statistical analyses. However, through the SOM, this variable starts to have its degree of relevance in the wear process, showing that this technique can also serve as a complementary technique in statistical analyzes in specific situations like this.

Figure 51 – SOM analysis, refractory wear rate vs iron content in the slag and process time. East trunnion of campaign A of the LD converter

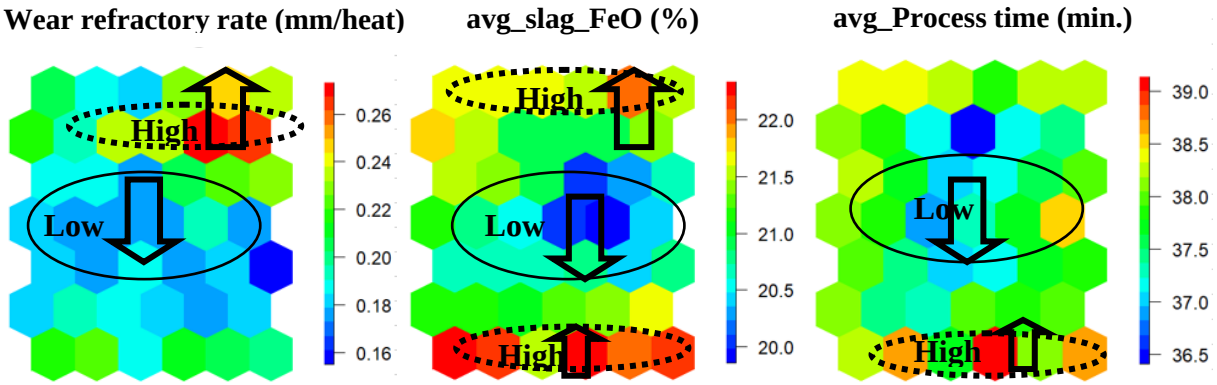

The two final variables indicated in figure 51 show the adherence of the SOM results with the other statistical analyzes and with the operational observations. The first, which is the percentage of iron oxide in the slag (avg_slag_FeO), indicates a higher rate of refractory wear for higher values of this compound in the slag. For the second variable, process time (avg_Process time), the correlation was direct with the wear rate. Higher iron content in the slag means that there was a greater oxidation of iron in the metallic bath and, consequently, migration in the form of oxide to the slag. This situation is one of the most aggressive for the refractory, since the iron oxide reduces the melting temperature of most of the slag and refractory brick constituents, and the formation of magnesiowustite is also facilitated in this condition. According to the literature and observations in the operational area, this condition greatly increases the refractory wear rate. For the process time variable, it is quite evident that longer process times mean longer contact times between the metallic bath and the slag with the refractory bricks, which will consequently cause a higher rate of wear.

4.1.4 Analysis of the refractory wear profile in the east cylinder region (trunnion) of the LD campaign B using classic statistical tools

In the same way that the analyzes were carried out for campaign A, the analysis was carried out for campaign B, which had an intermediate life performance according to figure 40. The objective is to verify and compare the effects and refractory wear models between campaigns, and, If the same variables that were relevant in one campaign are also relevant in the others.

Furthermore, by analyzing campaigns with different performances (keeping the same refractory project) we are ensuring a larger and more representative sample size.

Figure 52 – Evolution of the refractory wear rate in the east trunnion of campaign B as a function of fluxes, scourifiers and slag conditions used in the LD converter process

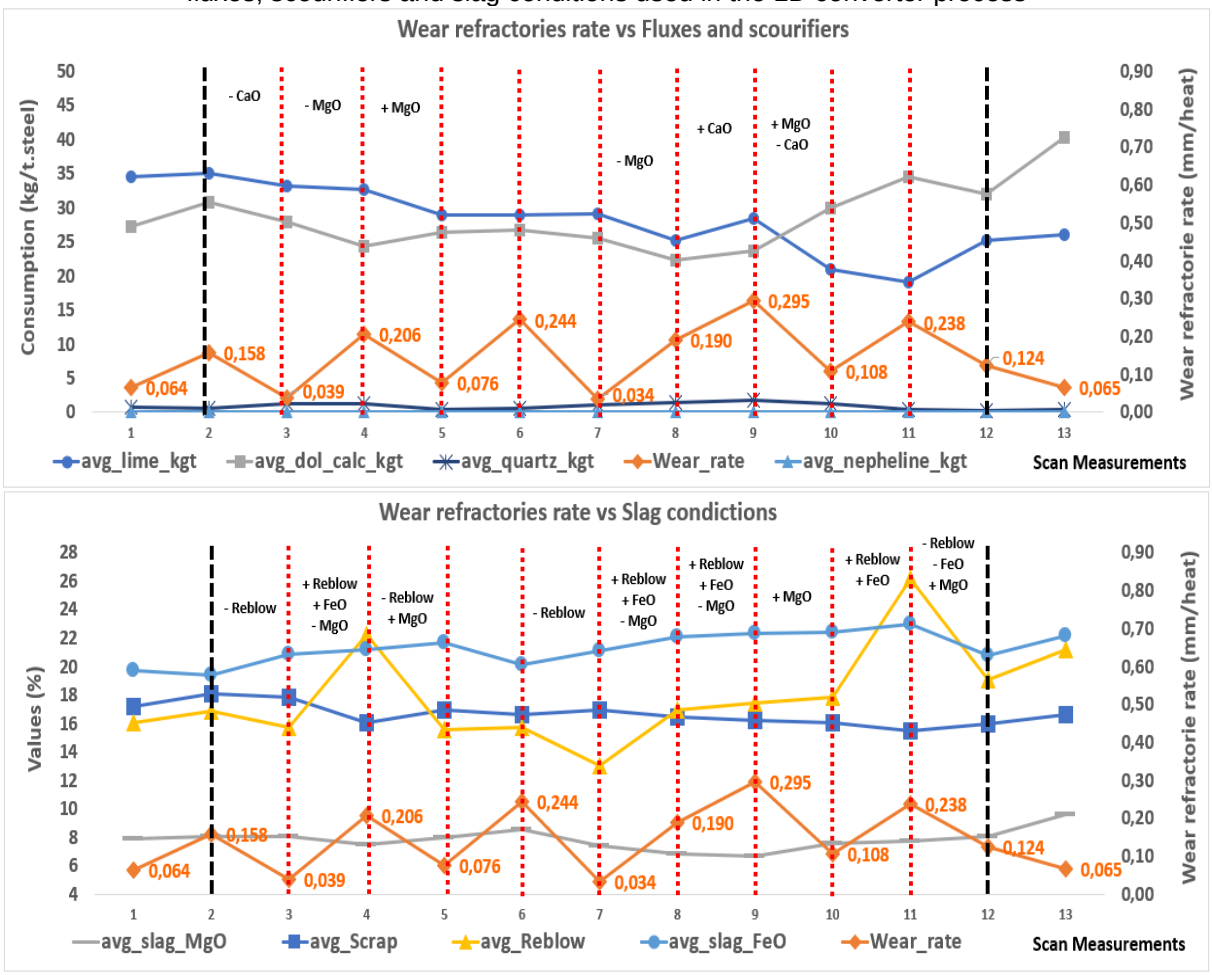

Figure 52 shows the effect of the variables lime (avg_lime_kgt), calcined dolomite (avg_dol_calc_kgt), quartz (avg_quartz_kgt) and nepheline (avg_nepheline_kgt) on the refractory wear rate (Wear_rate) of the east trunnion of the LD converter in campaign B. Where we see the signs positive (+) indicates the increase in the contents of this compound, where we visualize the negative signs (-) the opposite occurs, that is, the reduction. Figure 52 shows in some sections the effects towards an increase in the refractory wear rate when reduce the additions of calcined dolomite (source of MgO) and reductions in the wear rate when increase the additions of this compound. The explanation for this phenomenon based in the fact that MgO is present in the dolomite, as this chemical compound acts to increase the saturation of MgO in the slag, which results from the equalization of the chemical

gradient between the MgO in the slag and in the refractory (the driving force of the process of migration and dissolution of MgO from the refractory by the slag), reducing or preventing the dissolution of MgO aggregates from the refractory bricks by the slag.

With regard to CaO, the opposite effect to that of MgO is verified. In this case, increases in CaO in the slag tend to dilute the other components, such as, for example, MgO. In this case, increases in CaO in a certain proportion can promote an increase in the refractory wear rate.

Through figure 52, it is possible to observe the main slag constituents that impact refractory wear, together with the amounts of scrap charged in the LD and the reblow index of the manufactured heats. It is evident that the higher the FeO content of the slag and the higher the reblown rate, the higher the refractory wear rate, since these two variables are linked to higher levels of oxidation of steel and slag, which makes the environment fully corrosive furnace for MgO-C bricks.

Furthermore, figure 52 reveals that refractory wear rates are reduced for higher percentages of MgO dissolved in the slag, which is in agreement with the type of refractory brick employed (MgO-C). In this case, the saturation of the slag in MgO is essential so that chemical gradients between the slag and the brick do not occur, reducing or even preventing the transfer of MgO from the refractory structure to the slag and, consequently, the degradation of the refractory structure of the furnace. Such results found for campaign B are in line with those observed for campaign A.

Figure 53 – Evolution of the refractory wear rate in the east trunnion of campaign B as a function of dephosphorization rate of the metallic bath of LD converter process

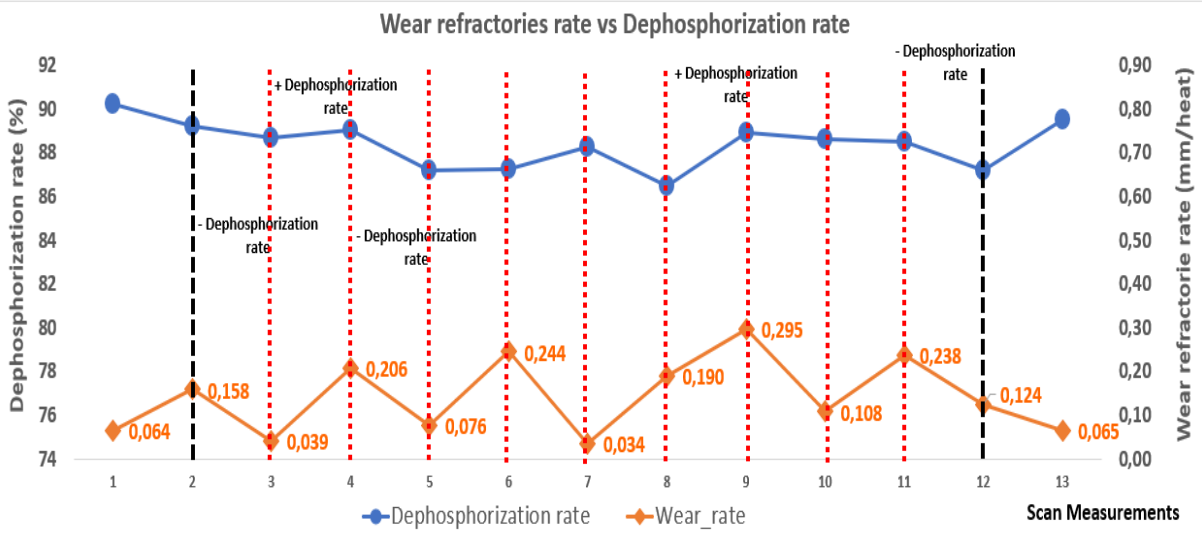

The effect of the dephosphorization rate in the LD furnace is show in the five sections of the figure 53. This variable is extremely relevant, as the high levels of oxidation resulting in the metallic bath and in the slag to obtain lower percentages of phosphorus in the final steel are extremely deleterious for the refractory structure, mainly due to the oxidation of the carbon in the refractory.

Figure 54 – Evolution of the refractory wear rate in the east trunnion of campaign B as a function of silicon content of the pig iron and the process time in the LD converter process

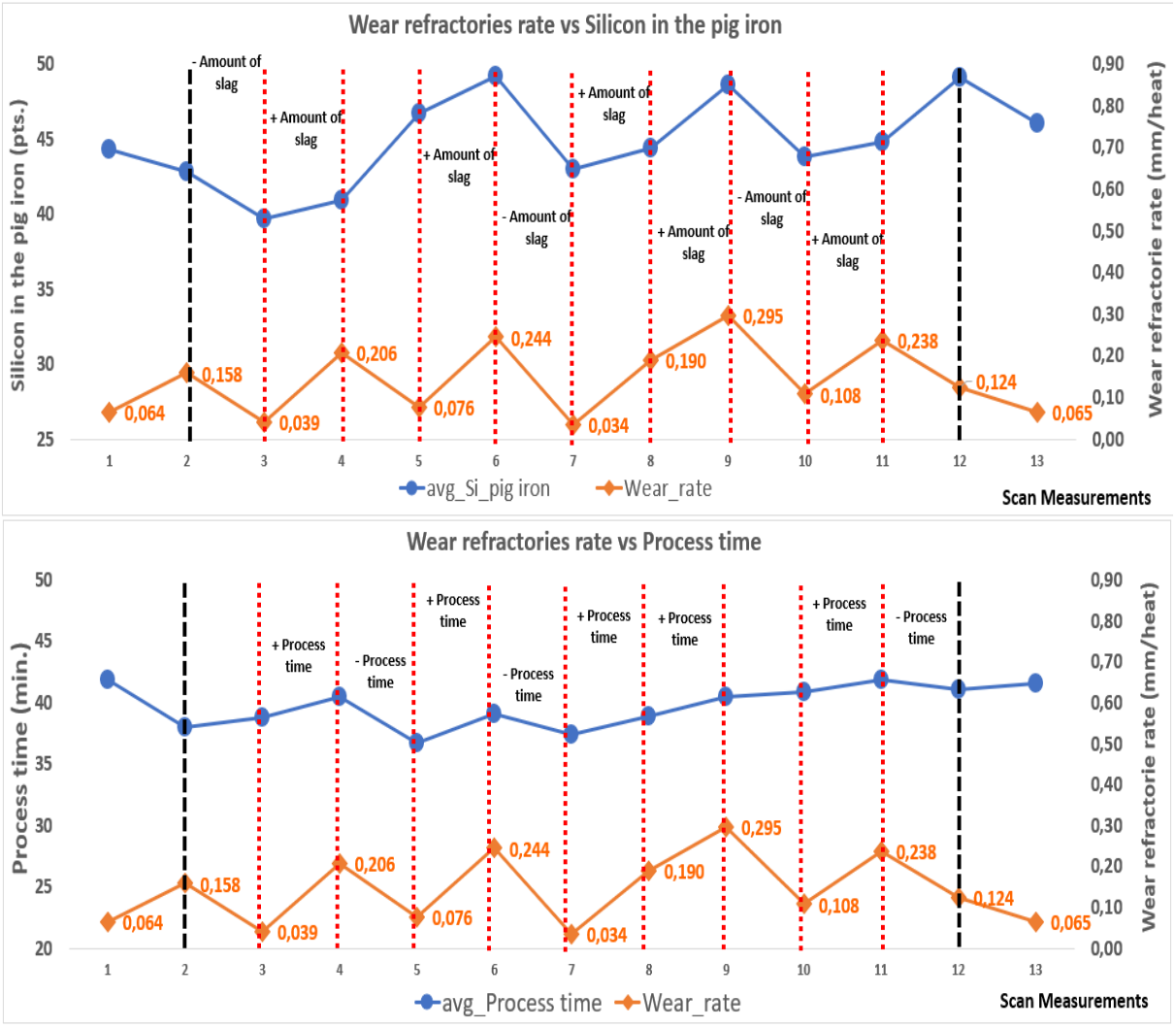

The percentage of silicon in the pig iron can influence the wear rate, especially when its values oscillate far outside the average. In case of excessive increase, for the same basicity of the furnace, a high amount of slag is obtained in the LD. If this slag is not in adequate condition, an increase in the refractory wear rate may occur. There are several operational problems related to the high volume of slag, mainly operational stoppages to control foaming (excess projections of slag and steel) in the

furnace. Generally, when these stops are constant within the blow, the process conditions are more aggressive, such as, for example, the increase in the percentage of reblow in the heats due to reactions at the end of the blow, temperature drops, among others. It can be seen from figure 54 that the refractory wear rate increases when the silicon percentage also increases. The opposite effect, of silicon reduction with reduction of the wear rate is also observed, evidencing its possible direct correlation. Obviously, very low levels of silicon in the pig iron can have deleterious effects on refractory wear due to thermal input issues and, consequently, the thermal balance and excess oxidation of the metallic bath in the LD.

The process time (avg_Process time), shown in figure 54, is directly correlated with refractory wear rate, it can be seen that the wear rate increases for longer process times. Longer process times for the same heat indicate longer contact times between the refractory bricks with the metallic bath and the slag, in addition, of course, to greater exposure to the thermal conditions of the process and oxidation of the LD.

Figure 55 – Evolution of the refractory wear rate in the east trunnion of campaign B as a function of the binary basicity of slag in LD converter process

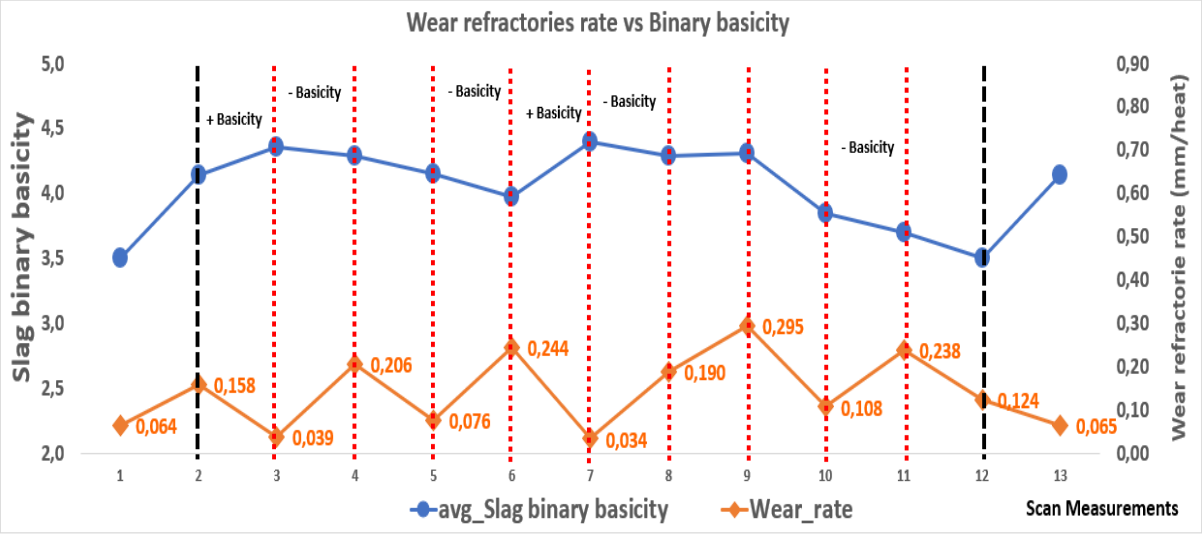

It is observed in the graph of figure 55 that the increases in basicity are accompanied by reductions in the refractory wear rate, whereas the reductions in basicity are accompanied by increases in the rate of wear. As the refractory bricks are basic, a reduction in the wear rate is expected with the increase in the basicity of the slag. Acidic or less basic slags chemically attack the basic structure of MgO-C bricks.

Two summary tables (Tables 11 and 12) were constructed based on the analysis of the figures above, showing the main variables that acted in the sense of increasing and reducing the refractory wear rate of the LD trunnion throughout campaign B of the converter. The reading and interpretation of these tables follows the same line of reasoning as tables 9 and 10 of campaign A constructed in the previous sections.

Table 11 – Summary of the influence of the main variable that impacted the refractory wear rate of the east trunnion of the LD in campaign B (sections 2 to 8)

ΔRate - (75%)	ΔRate + (428%)	ΔRate - (63%)	ΔRate + (221%)	ΔRate - (86%)	ΔRate +(458%)
2 ➡ 3	3 ➡ 4	4 ➡ 5	5 ➡ 6	6 ➡ 7	7 ➡ 8
-Reblow	+Reblow	-Reblow		-Reblow	+Reblow
	+FeO				+FeO
	-MgO	+MgO			-MgO
-Dephosphory rate	+Dephosphory rate	-Dephosphory rate			
-Slag volume	+Slag volume		+Slag volume	-Slag volume	+Slag volume
	+Process time	- Process time	+Process time	-Process time	+Process time
+Binary basicity	- Binary basicity		-Binary basicity	+Binary basicity	-Binary basicity

Table 12 – Summary of the influence of the main variable that impacted the refractory wear rate of the east trunnion of the LD in campaign B (sections 8 to 12)

ΔRate + (55%)	ΔRate - (63%)	ΔRate + (120%)	ΔRate + (48%)
8 ➡ 9	9 ➡ 10	10 ➡ 11	11 ➡ 12
	-CaO		
+Reblow		+Reblow	-Reblow
+FeO		+FeO	-FeO
-MgO	+MgO		+MgO
+ Dephosphory rate			- Dephosphory rate
+Slag volume	-Slag volume	+Slag volume	
+ Process time		+ Process time	- Process time
		- Binary basicity	

4.1.5 Multivariate statistical analysis of the refractory wear rate in the east cylinder region (trunnion) of the LD campaign B

Through multivariate statistical modeling, a deterministic equation was constructed in which the refractory wear rate can be estimated as a function of process variables. Equation 17 was obtained using the same database as the previous analyzes of campaign B. Acceptance criteria for the regression coefficients (*p*-value < 0.05 and 1 < VIF < 2) and the residuals (normality, homoscedasticity and independence see APPENDIX B).

$$\text{Wear rate} = -8.139 - 0.02447 * \text{dol\_calc} + 0.1387 * \text{CaO\_slag} + 0.07370 * \text{reblow} + 0.001837 * \text{avg\_vol\_}O_2 + 0.000373 * \text{avg\_OX3} \quad (17)$$

$$R^2 = 99.12 \quad R^2 \text{ (aj)} = 98.57$$

Where:
Wear rate: Average refractory wear rate of bricks (mm/heat);
dol_calc: Average value of calcined dolomite for heat (kg/t. steel);
CaO_slag: Percentage of CaO in the slag (%);
reblow: Percentage of heats that reblow (%);
avg_vol_O_2: Average volume of oxygen blow in the reblow (Nm^3);
avg_OX3: Oxidation in the metallic bath at the end of blow (ppm).

From the equation above, it can be seen that the refractory wear rate of the LD trunnion in campaign B is strongly influenced by the average amount of calcined dolomite added in the heats, by the percentage of CaO compound in the slag, by the average percentage of heats that are reblow in the LD, by the volume of oxygen blown in the reblow and by the final oxidation level of the metallic bath (and consequently of the slag). By classical multivariate analysis, these 5 variables can determine the rate of wear of the bricks and consequently the life of the furnace.

The first variable, calcined dolomite, according to equation 17, has an inverse relationship with the refractory wear rate. The explanation of the effects of this variable have already been made in previous sections.

The second variable, percentage of CaO in the slag, is necessary to balance the basicity of the slag rich in SiO_2 and initially acidic, which would be highly harmful

for the refractory structure. However, for certain percentages of CaO, this compound starts to dilute the added MgO in the slag, making the refractory preservation effect contrary and harmful to the refractory. The explanation of the effects of this variable have already been made in previous sections.

The third and fourth variables of the equation 17, reblow and volume of oxygen in the reblown respectively, indicate a direct relationship between the wear rate and the average percentage of these variables. In this case, as the level of oxidation of the metallic bath and slag is increased with the increase of this two variable, the environment in contact with the bricks becomes highly corrosive. Another impact would be the fact that reblown heats and, in particular, those with high volumes of oxygen, acquire extremely high temperatures, which facilitates the reaction kinetics between the medium and the refractory bricks. There is also an increase in the process time when there is a reblow of the heats, which leads to a longer contact time per heat of the refractory with the slag and the metallic bath.

The fifth variable, final oxidation level of the metallic bath (and consequently of the slag) was directly correlated to the wear rate. This variable considers the oxidation levels of the heat and, as a consequence, high levels of refractory wear due to the oxidation of the carbon in the bricks. The loss of carbon (mass) and the consequent formation of pores in the refractory structure would facilitate the permeability of the slag inside the bricks, promoting the complete dissolution of the MgO aggregates by the FeO rich slag and, consequently, the drop in the mechanical strength of the refractory bricks.

4.1.6 Analysis of the refractory wear rate in the east cylinder region (trunnion) in the LD of campaign B by SOM

In parallel to the statistical analyzes carried out above, an analysis of the correlation of the process variables with the refractory wear rate was carried out using the SOM data analysis technique for campaign B. Among the objectives of this analysis is the identification and comparison between methodologies as different aiming at results that physically should be similar.

In addition, these techniques can act in the sense of complementarity between them, since variables that apparently were not relevant in one technique due to factors such as multicollinearity between variables, can be relevant in the other data

analysis technique. In addition, of course, verify the applicability of SOM in the analysis of refractory wear in campaign B. Therefore, for the same database of the variables analyzed in campaign B, the SOM tool was applied with the following results.

Figure 56 – SOM analysis, refractory wear rate vs percentagem of MgO in the slag and amount of granulated slag used. East trunnion of campaign B of the LD converter

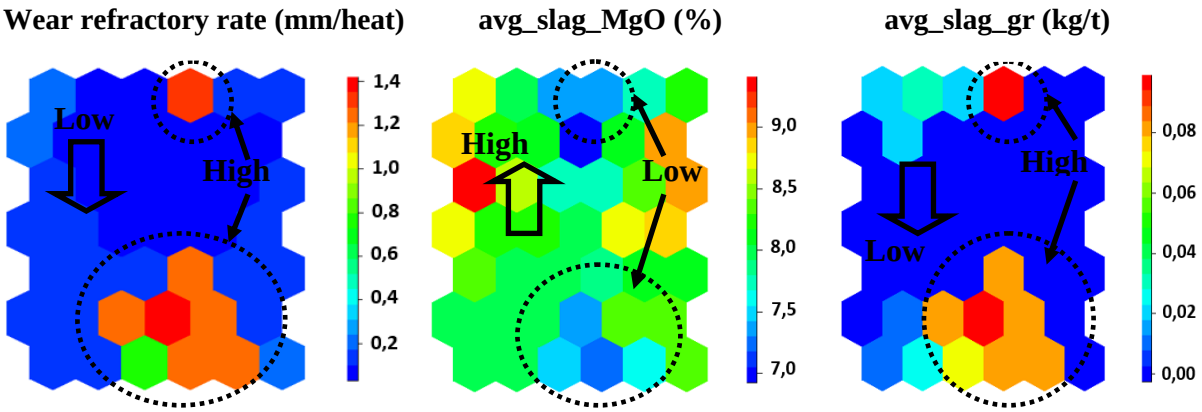

Figure 56 shows the inverse relationship between the refractory wear rate and the MgO content of the slag (avg_slag_MgO) and the direct relationship with the amount of granulated slag added (avg_slag_gr). Both results are in line with the statistical analyzes carried out for campaign B and the literature. In the case of MgO, the inverse relationship with the wear rate is a direct consequence of the chemical constitution of the MgO based bricks. The more saturated the slag is in MgO, the smaller the chemical gradient of this compound between the slag and the refractory brick. Therefore, the expected wear rate will be lower. The direct relationship with granulated slag may be related to the chemical composition of this material, which is rich in silicon (Si). Higher silicon contents tend to increase the process slag volume and reduce basicity (increase in slag acidity through SiO_2 formed). As the bricks are basic, this could cause an increase in the refractory wear rate.

Another effect regarding the amount of slag formed would be the dilution of MgO in the system and/or problems related to lack or excess of thermal input, since the use of granulated slag aims to correct the silica content of the liquid pig iron in the charge metallic.

Excessive oxidation may be a direct consequence of low silicon content in the pig iron to compensate for the thermal balance at the end of the LD furnace. On the other hand, excess Si in the pig iron can cause longer process times due to operational stops to perform double slag or excess projections in the furnace.

Figure 57 – SOM analysis, refractory wear rate vs percentage of the heats with reblow and oxygen volume blow in reblow. East trunnion of the campaign B of LD converter

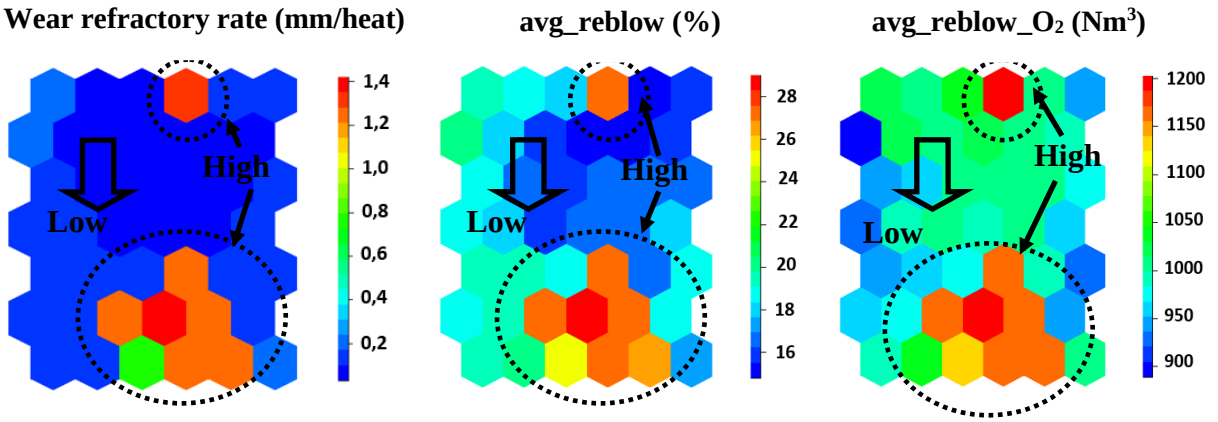

The images in figure 57 shows the direct relationships with the refractory wear rate of both variables, reblow (avg_reblow) and volume of oxygen blown from the reblow. In both cases, the variables are directly related to the oxidation levels of the metallic bath and slag, which makes the process conditions more aggressive to the refractory. The worsening of the reblow condition is greater if the volume of oxygen reblowed is high. Also, in situations with a high percentage of reblow in the heats and the volume of oxygen reblowed, the temperatures are generally much higher than normal for this type of furnace, which in turn accelerate refractory wear reactions. Furthermore, for these two variables, the SOM results are also in full agreement with the serial statistical analyzes and with the multivariate equation to the wear rate previously presented for campaign B.

Figure 58 – SOM analysis, refractory wear rate vs carbon and oxidation of the metallic bath in the end of blow. East trunnion of the campaign B of LD converter

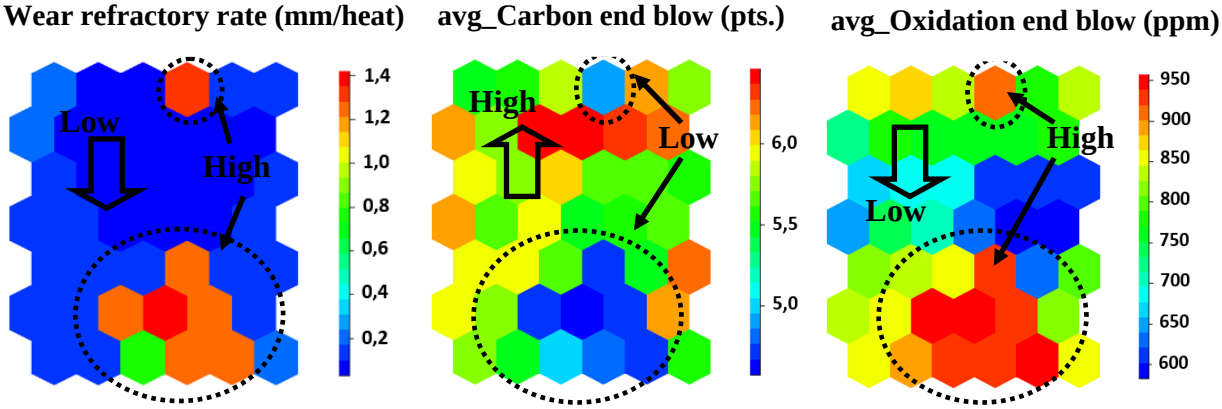

Figure 58 shows the inverse correlation of the carbon (mettalic bath) in the end of blow (avg_Carbon end blow) with refractory wear rate and, consequently, the

direct correlation of oxidation of the metallic bath at end of blow (avg_Oxidation end blow) with wear rate. In the first case, the higher the end of blow carbon, the lower the oxidation level of the heat and, consequently, the lower the wear rate. In the second case, for higher levels of oxidation of the metallic bath and slag at the end of the blow, the more intense the oxidation reactions of the carbon and of the refractory matrix of the bricks will be. A relevant contributing factor in the case of higher levels of oxidation is the greater fluidity of the slag, which would lead to greater penetration into the pores of the bricks, causing higher levels of wear. Therefore such results above are also metallurgical and ceramic coherent.

Figure 59 – SOM analysis, refractory wear rate vs percentage of heats with Slag Splashing and the silicon in pig iron. East trunnion of the campaign B of LD converter

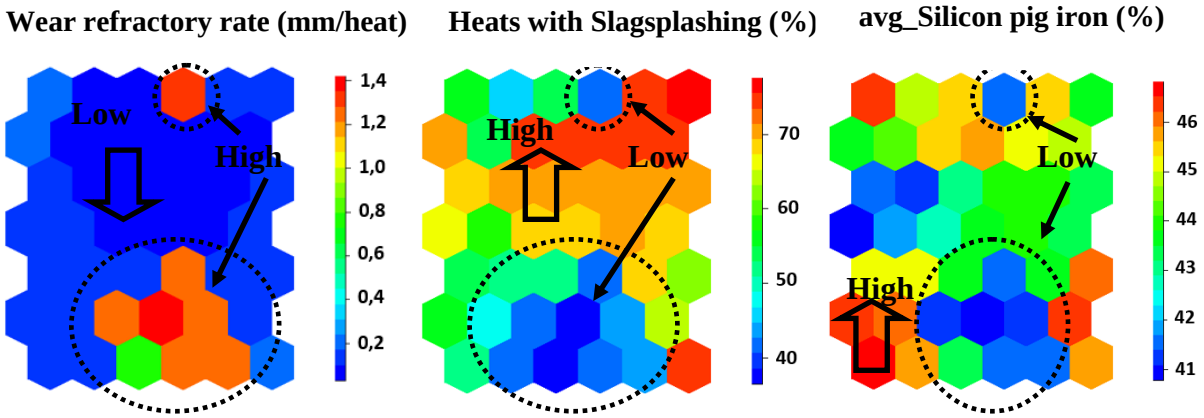

Regarding the practice of Slag Splashing (Heats with Slagsplashing) indicated by the percentage of heats in which this practice was carried out in relation to the total number of heats produced in the campaign and the silicon content (points) of the pig iron (avg_Silicon pig iron), there is a relationship inverse in both cases.

The main function of Slag Splashing is to cover the surface of the refractory bricks with a layer of slag saturated in MgO. In addition to the physical blockage of this layer preventing contact between the metallic bath and the oxidized slag with the refractory, the slag layer forms a thermal barrier reducing thermal gradients between the hot face and the cold face of the bricks. This gradient reduction is accompanied by reductions in thermomechanical stresses in the bricks, thus reducing the possibility of cracking and spalling. Obviously, a good protective layer reduces the oxidation of carbon in the bricks and the penetration of slag into the refractory matrix, which would explain the inverse relationship of this parameter with the refractory wear rate.

Regarding the silicon content of pig iron, this is the main thermogenic element of pig iron. Low silicon contents are accompanied by imbalances in the thermal balance of the system (LD), which in most cases are compensated by excess oxidation of the iron contained in the metallic bath. If this occurs, the slag will be extremely oxidized in FeO, which will lead the system to a highly corrosive chemical state for the refractories.

Figure 60 – SOM analysis, refractory wear rate vs average FeO in the slag and steel tapping time. East trunnion of campaign B of the LD converter

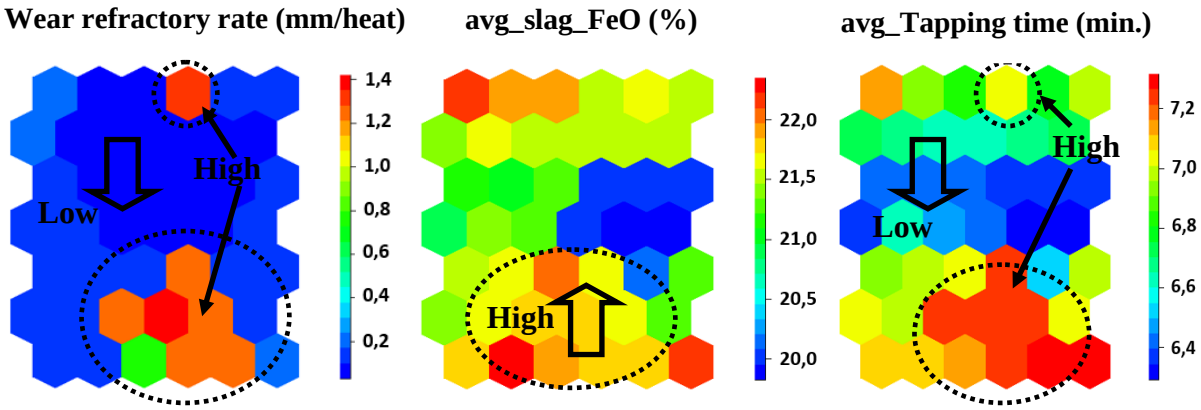

As a direct consequence of the oxidation levels of the metallic bath and slag resulting from high volumes of oxygen blown in the heats or from high percentages of reblown and volume of oxygen blown in the reblow, high levels of FeO in the slag is show in figure 60. Extremely oxidized slag promotes a more intense oxidation and dissolution of the refractory bricks, increasing the refractory wear rates as indicated in figure 60. In addition, high steel tapping times (avg_Tapping time) promote a longer contact time of the steel/slag with the refractory and consequently increase the rate of wear.

4.1.7 Analysis of the refractory wear profile in the east cylinder region (trunnion) of the LD of campaign C using classic statistical tools

Figure 61 – Evolution of the refractory wear rate in the east trunnion of campaign C as a function of fluxes, scourifiers and slag condictions used in the LD converter process

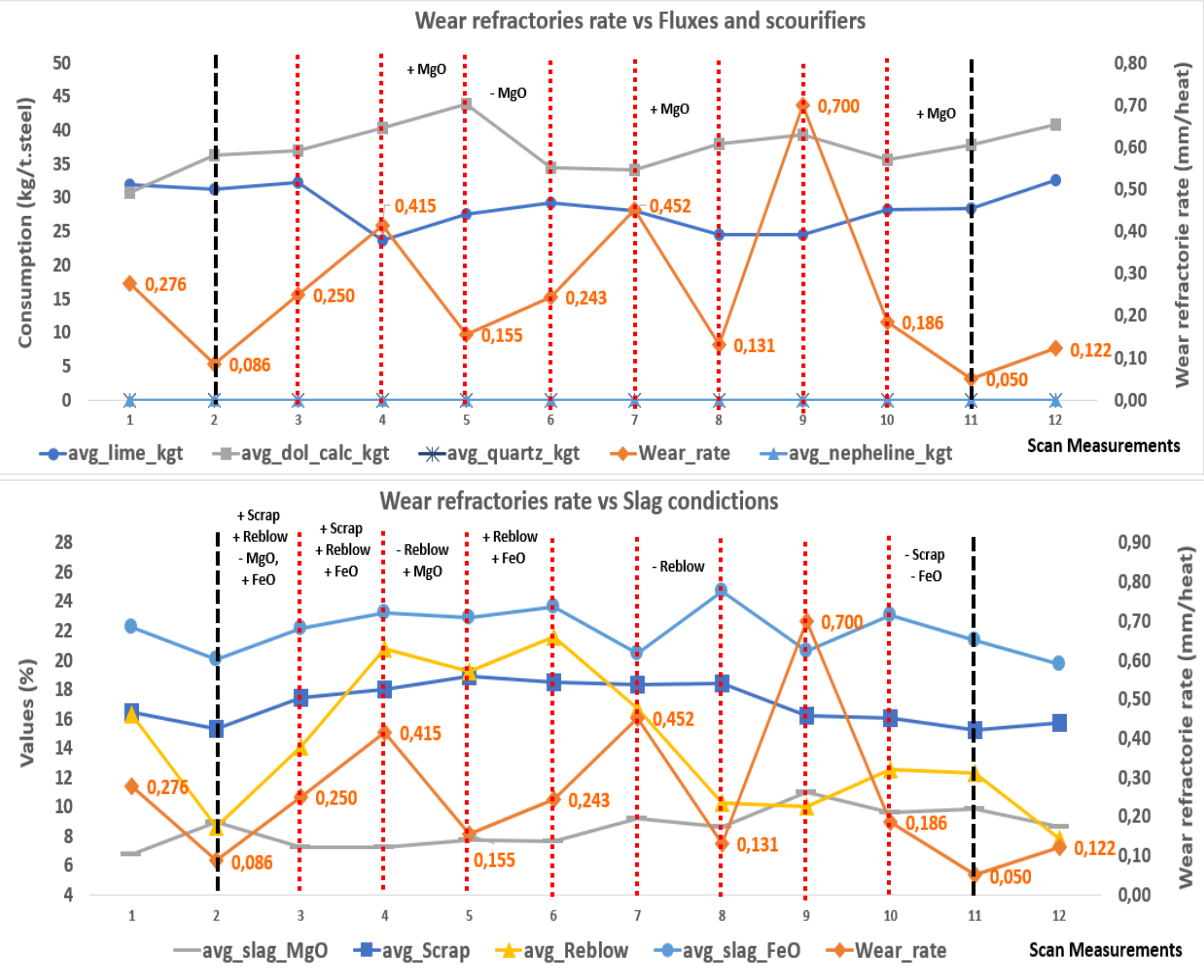

Figure 61 illustrates the effect of the variables lime (avg_lime_kgt), calcined dolomite (avg_dol_calc_kgt), quartz (avg_quartz_kgt) and nepheline (avg_nepheline_kgt) on the refractory wear rate (Wear_rate) of the trunnion of the LD converter in campaign C. Figure 61 shows the increase in the wear rate when reduce the additions of calcined dolomite (source of MgO) according to explanation in previuos sections. Still, in figure 61, observe the main constituents of the slag that impact the refractory wear, together with the amounts of scrap charged in the furnaces and the reblow index of the manufactured heats. It is evident that the higher the FeO content of the slag and the higher the rate of reblown heats, the greater the wear rate of the furnace, since these two variables are linked to higher levels of steel /slag oxidation, which makes the LD furnace environment corrosive for MgO-C bricks.

Furthermore, the figure illustrates that refractory wear rates are reduced for higher percentages of MgO dissolved in the slag, which is in agreement with the type of refractory brick used (MgO-C). In this case, the saturation of the slag in MgO is essential so that chemical gradients between the slag and the brick do not occur, reducing or even preventing the transfer of MgO from the refractory structure to the slag and, consequently, the degradation of the refractory structure of the furnace. Once again, the analyzes between campaigns A, B and C are similar, but with different impacts.

As can be seen from figures 61 and 62, the level of oxidation of the metallic bath and consequently of the slag at the end of the LD converter blow is directly related to the wear rate of the trunnion refractories. The explanation lead in the possibility of both the oxidation of the carbon in the brick and the dissolution of the MgO aggregates by a slag rich in FeO and a metallic bath rich in dissolved oxygen.

Figure 62 – Evolution of the refractory wear rate in the east trunnion of campaign C as a function of carbon and oxidation levels in the metallic bath at the end blow of heat in the LD converter process

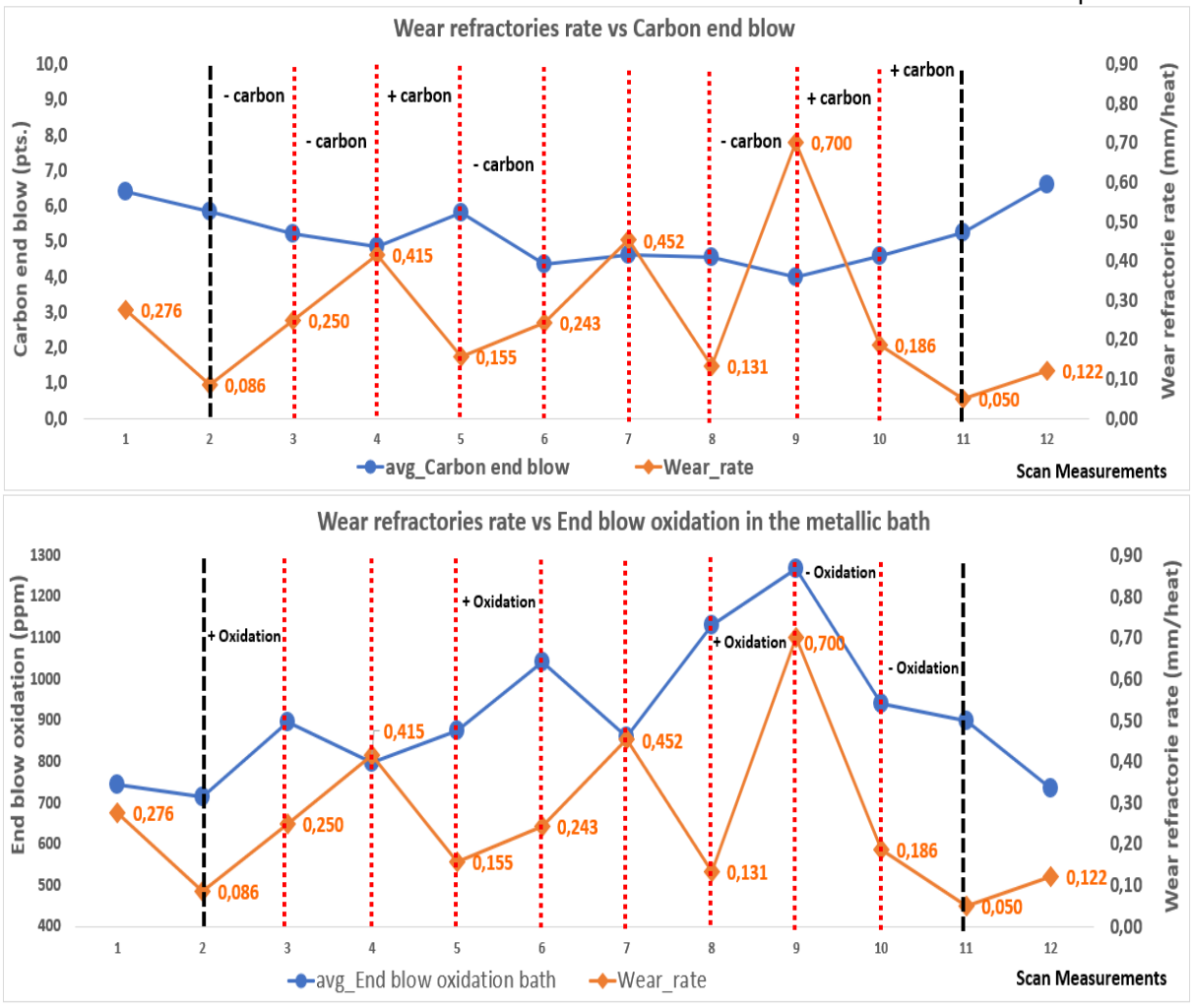

Figure 62 reveals that the higher carbon in the metallic bath at the end of the blow contributes to the drop in the refractory wear rate. This is explained by the lower oxidation of the bath and consequent lower corrosive effect of the slag.

An relevant identification is the wear rate peak observed in point 9 of figure 62. This high wear rate is correlated with the oxidation of the metallic bath at the end of the blowing, showing the relevance of this variable for the refractory wear control of the LD.

The process time (avg_Process time) and the silica content of the pig iron (avg_Silicon in pig iron), shown in figure 63 below, are also representative at some specific moments in the wear rate.

Figure 63 – Evolution of the refractory wear rate in the east trunnion of campaign C as a function of the silicon content at the pig iron and the process time of LD converter

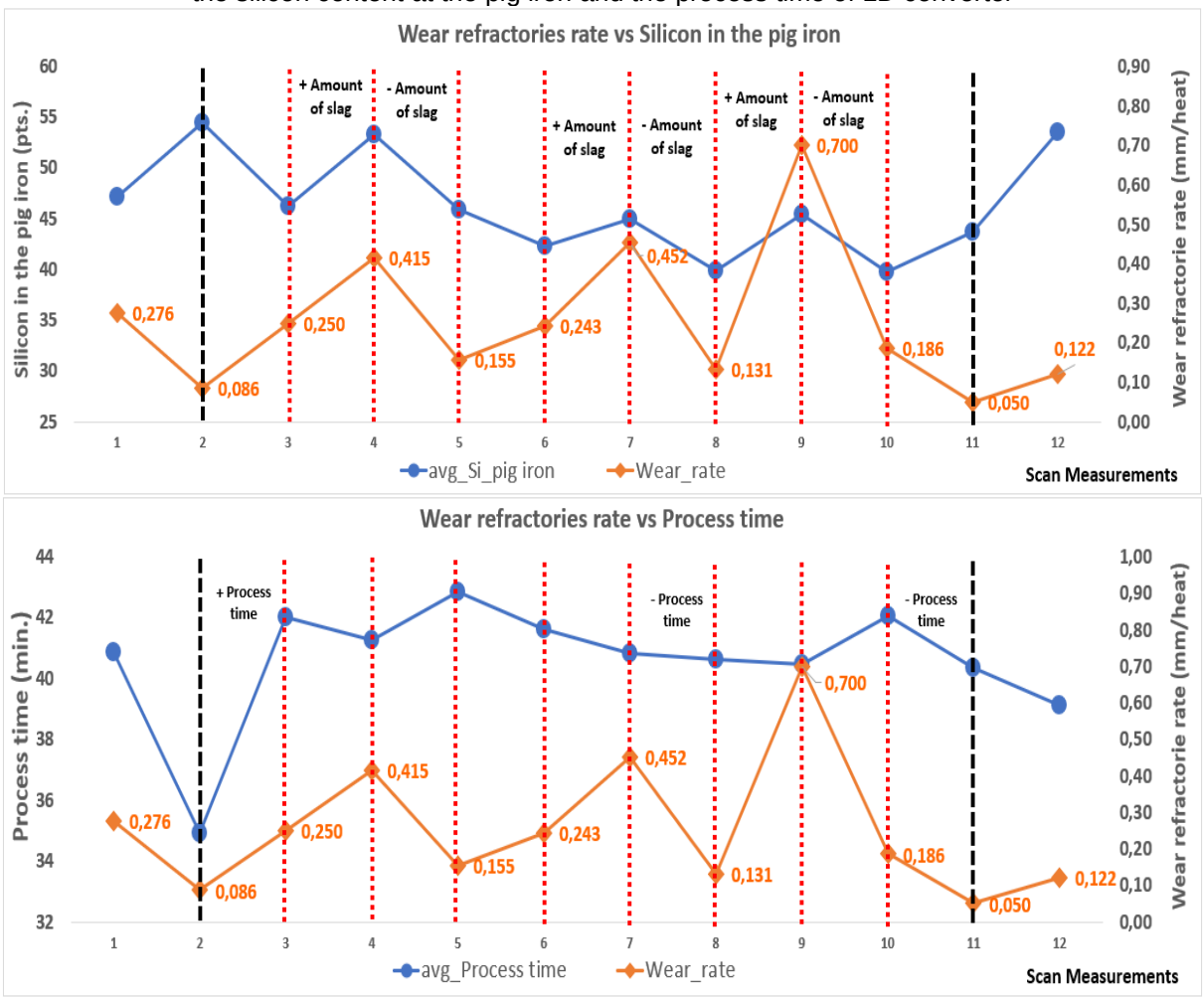

The percentage of silicon in the pig iron can influence the refractory wear rate, especially when its values oscillate far outside the average. In case of excessive increase, for the same basicity of the furnace, a high amount of slag is obtained in

the LD. If this slag is not in proper condition, an increase in the wear rate may occur. There are several operational problems related to the high amount of slag, mainly operational stoppages to control furnace foaming. Generally, when these stops are constant within the blow, the process conditions are more aggressive, such as, for example, the increase in the percentage of reblow in the heats due to reactions at the end of the blow, temperature drops, among others. It can be seen from figure 63 that the wear rate increases when the percentage of silicon also increases.

The opposite effect, of silicon reduction with reduction of the wear rate is also observed, evidencing its possible direct correlation. In some very specific situations, such as those with a very low silicon value, this effect can be inverse and harmful, since the lack of thermal input can lead to excess oxidation of the bath to reach a certain temperature at the end of the blow.

Note that the refractory wear rate increases for longer process times and for higher silicon content in the pig iron (higher volumes of slag in the furnace). The explanation is, longer process times for the same heat indicate longer contact times between the refractory bricks with the metallic bath and the slag, in addition, of course, to greater exposure to the thermal conditions of the process.

Figure 64 – Evolution of the refractory wear rate in the east trunnion of campaign C as a function of the slag binary basicity in the LD converter process

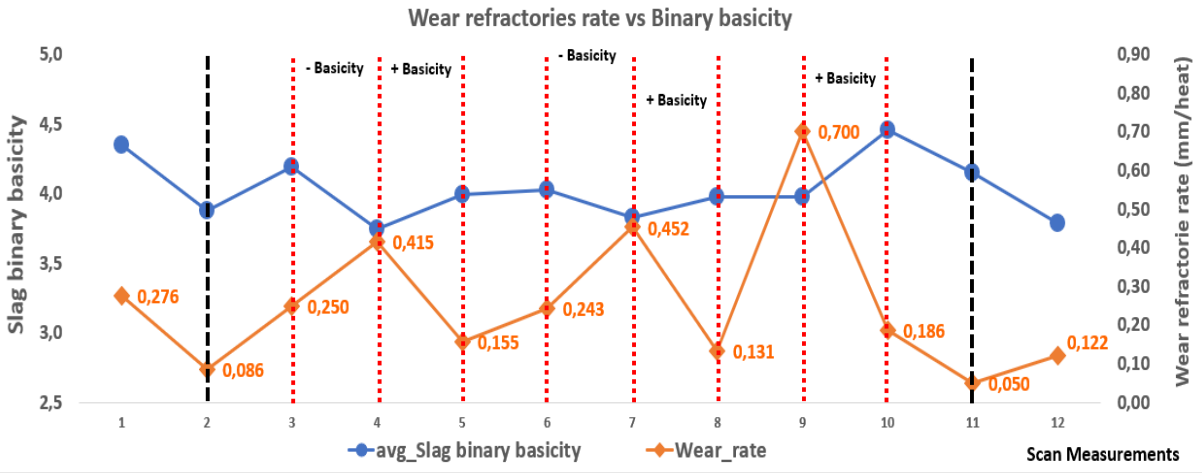

It can be seen in the graph of figure 64 that basicity increases are accompanied by reductions in the refractory wear rate, whereas basicity reductions are accompanied by increases in the wear rate. As the refractory bricks are basic, a reduction in the wear rate is expected with the increase in the basicity of the slag. Acidic or less basic slags chemically attack the basic structure of MgO-C bricks.

As for campaigns A and B, two summary tables were built (tables 13 and 14) based on the analysis of the figures above showing the main variables that acted towards increasing and reducing the refractory refractory wear rate of the trunnion throughout campaign C of the LD converter. Reading the tables is done in the same way as those constructed for the other campaigns.

Table 13 – Summary of the influence of the main variables that impacted the refractory wear rate of the east trunnion of the LD in campaign C (sections 2 to 8)

ΔRate + (191%)	ΔRate + (66%)	ΔRate - (63%)	ΔRate + (57%)	ΔRate + (86%)	ΔRate - (71%)
2 ➡ 3	3 ➡ 4	4 ➡ 5	5 ➡ 6	6 ➡ 7	7 ➡ 8
+Reblow	+Reblow	-Reblow	+Reblow		-Reblow
+FeO	+FeO		+FeO		
-MgO		+MgO	-MgO		+MgO
-End carbon	-End Carbon	+End Carbon	-End Carbon		
	+Slag volume	-Slag volume		+Slag volume	-Slag volume
+Oxidation			+Oxidation		
+Scrap	+Scrap				
	-Binary basicity	+Binary basicity		-Binary basicity	+Binary basicity
+Process time					-Process time

Table 14 – Summary of the influence of the main variables that impacted the refractory wear rate of the east trunnion of the LD in campaign C (sections 8 to 11)

ΔRate + (434%)	ΔRate - (73%)	ΔRate - (73%)
8 ➡ 9	9 ➡ 10	10 ➡ 11
		-FeO
		+MgO
-End carbon	+End carbon	+End carbon
+Slag volume	-Slag volume	
+Oxidation	-Oxidation	-Oxidation
		-Scrap
	+Binary basicity	
		-Process time

4.1.8 Multivariate statistical analysis of the refractory wear rate in the east cylinder region (trunnion) of the LD of campaign C

Through multivariate statistical modeling, a deterministic equation was constructed in which the refractory wear rate was estimated as a function of process variables. Equation 18 was obtained using the same database as the previous analyses. Acceptance criteria for regression coefficients (*p*-value < 0.05 and 1 < VIF < 2) and residuals (normality, homoscedasticity and independence).

$$\text{Wear rate} = -4.29 - 0.0235 * \text{dol\_calc} + 0.0512 * \text{Process\_time} + 0.000565 * \text{avg\_OX3} + 0.2750 * SiO_2\text{\_slag} \quad (18)$$

$$R^2 = 69.71 \quad R^2(aj) = 52.40$$

Where:
Wear rate: Average refractory wear rate of bricks (mm/heat);
dol_calc: Average value of calcined dolomite for heat (kg/t. steel);
Process_time: Average process time for heat (min.);
SiO_2_slag: Percentage of SiO_2 in the slag (%);
avg_OX3: Oxidation in the metallic bath at the end of blow (ppm).

From the equation 18, it can be seen that the refractory wear rate is strongly influenced by the amount of average calcined dolomite added in the heats, by the average process time of the heats, by the final oxidation level of the metallic bath (consequently of the slag) and by the percentage of the compound SiO_2 from the slag. By classical multivariate analysis, these 4 variables can define the direction of the rate of wear of the bricks and consequently the life of the LD.

The first variable, calcined dolomite, according to equation 18, has an inverse relationship with the refarctory wear rate. Higher amounts added per heat reduce wear rate. The basic explanation has already been disccused in the previuos sections.

The second variable, process time, is directly related to the wear rate. Longer process times are related to longer contact times between metallic bath/slag and refractory, therefore, longer reaction times for heat.

The third variable, final oxidation level of the metallic bath (and consequently of the slag) was directly correlated to the wear rate, as expected. This variable considers the oxidation levels of the heat and, as a consequence, high levels of refractory wear due to the carbon oxidation of the bricks. The loss of carbon (mass) and the consequent formation of pores in the refractory structure would also facilitate the permeability of the slag inside the bricks, promoting the complete dissolution of the MgO aggregates by the rich slag in FeO.

The fourth and last variable, SiO_2 percentage of the slag, indirectly indicates the acidity level of the slag. It is a direct consequence of the percentage of silicon in the pig iron and the silica in the scrap reused in the process. The slag rich in silica and initially acidic is highly deleterious to the refractory (basic) structure. In addition, depending on the amount of SiO_2 formed in the process, there are high volumes of slag and longer process times caused by unforeseen stops such as those generated by excessive projections of slag outside the furnace.

4.1.9 Analysis of the refractory wear rate in the east cylinder region (trunnion) of the LD of campaign C by SOM

Figure 65 – SOM analysis, refractory wear rate vs slag MgO percentage and amount of calcined dolomite used. East trunnion of campaign C of the LD converter

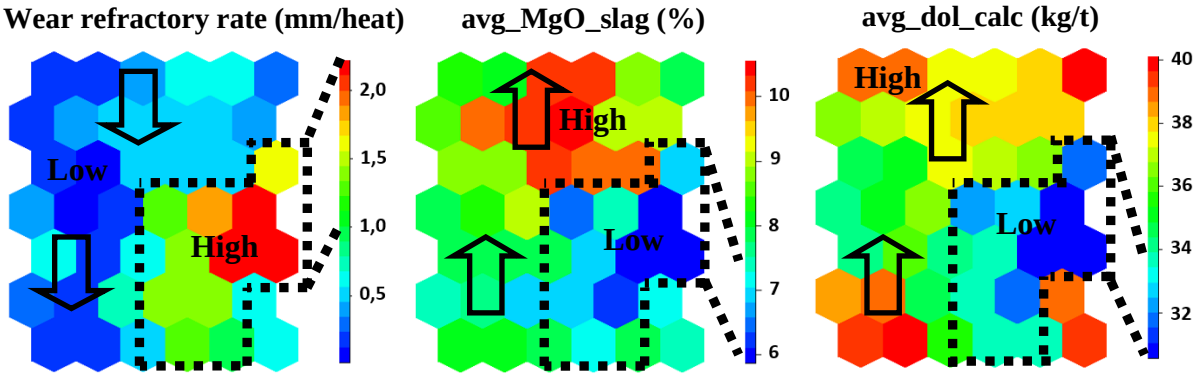

Figure 65 shows the inverse relationship of the refractory wear rate of the LD trunnion with the percentage MgO content of the slag (avg_MgO_slag) and with the amount of calcined dolomite added in the heats (avg_dol_cal). Both results are in according to analyzes obtained from classical statistics previous disccused. In the case of MgO, the inverse relationship with the wear rate is a direct consequence of the chemical constitution of the MgO-C bricks. The more saturated the slag is in

MgO, the smaller the chemical gradient of this compound between the slag and the refractory brick. Therefore, the refractory wear rate is lower. The relationship with the amount of calcined dolomite is a direct consequence, as it is the main source of MgO in the LD. Therefore, it is expected that higher consumption of dolomite per ton of steel produced also represents greater saturation of the slag with MgO. Results above in according with those obtained in previous campaigns A and B.

Figure 66 – SOM analysis, refractory wear rate vs percentage of heats with reblow and oxygen blow in the reblow. East trunnion of campaign C of the LD converter

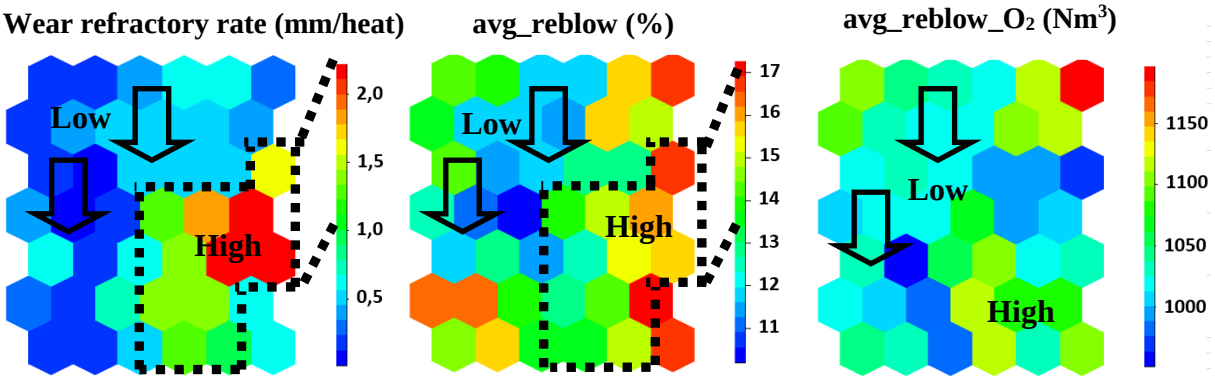

Figure 66 reveal the direct relationships with the refractory wear rate of both variables, reblow (avg_reblow) and volume of oxygen blown into the reblow (avg_reblow). In both cases, the variables are directly related to the oxidation levels of the metallic bath and slag, which makes the process conditions more aggressive to the refractory. The basic explanation has already been disccused in the previuos sections. For these two variables, the SOM results are also in agreement with the statistical analyzes presented and with the results found for campaigns A and B.

Figure 67 – SOM analysis, refractory wear rate vs oxidation of the metallic bath in the end of blow and the carbon end blow. East trunnion of campaign C of LD converter

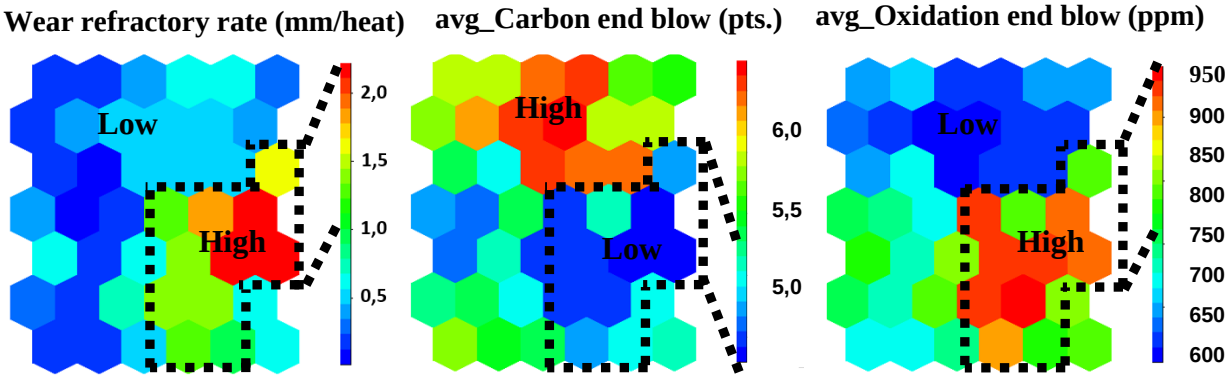

Figure 67 shows the inverse correlation of the carbon in mettalic bath in the end of blow (avg_Carbon end blow) with refractory wear rate and, consequently, the direct correlation of oxidation of the metal bath at end of blow (avg_Oxidation end blow) with wear rate.

In the first case, the higher is the carbon end blow, the lower the oxidation level of the heat and, consequently, the lower the wear rate. In the second case, for higher levels of oxidation of the metallic bath and slag at the end of the blow, the more intense the oxidation reactions of the carbon in the refractories bricks and of the MgO refractory matrix will be.

A relevant contributing factor in the case of higher levels of oxidation is the greater fluidity of the slag, which would lead to greater penetration into the pores of the bricks, causing higher levels of wear. Therefore such results above are also metallurgical and ceramic coherent. Both variables were also highlighted at the serial statistical analysis and agreement with campaign A and B.

Figure 68 – SOM analysis, refractory wear rate vs metallic bath temperature at the end of blow and the binary basicity of slag. East trunnion of the campaign C of LD converter

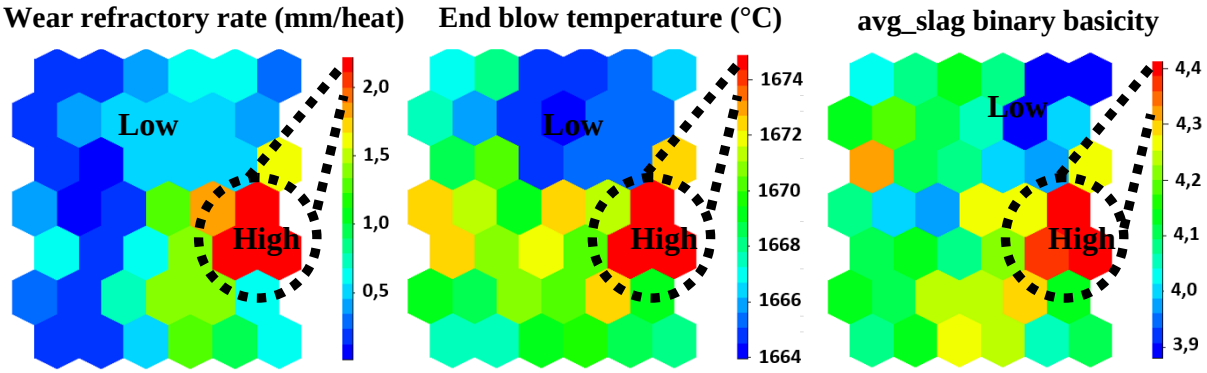

Figure 68 indicates the direct correlation between End blow temperature and refractory wear rate. Higher end blow temperatures, greater the speeds reaction between slag and refractory brick, in addition, expected a greater fluidity of this slag, which would lead to penetration into the pores of the bricks, causing higher levels of wear. Therefore, the results obtained in relation to the final end blow temperature are metallurgical and ceramically consistent.

The variable Slag binary basicity (avg_slag binary basicity), once again, was directly related to the refractory wear rate. Explanations for this unexpected result have already been made previously and may be related to issues of excess CaO in

the slag, which would make the slag “dryer” with a high melting point, making it unsuitable for Slag Splashing and for dissolution and consequently saturation of MgO.

Remembering that the slag binary basicity indicated in the figure 68 is the real basicity obtained by the slag analysis. Therefore, larger additions of CaO outside the predicted model could generate this effect of excess CaO in the slag (consequent dilution of MgO and high real basicity). Such additions are generally related to the greater need for dephosphorization of the steel in the LD, since CaO is the main component of the slag in the retention of the phosphorus element in the form of P_2O_5.

Figure 69 – SOM analysis, refractory wear rate vs process time and amount of material added for Slag Coating and Slag Splashing. East trunnion of campaign C of the LD converter

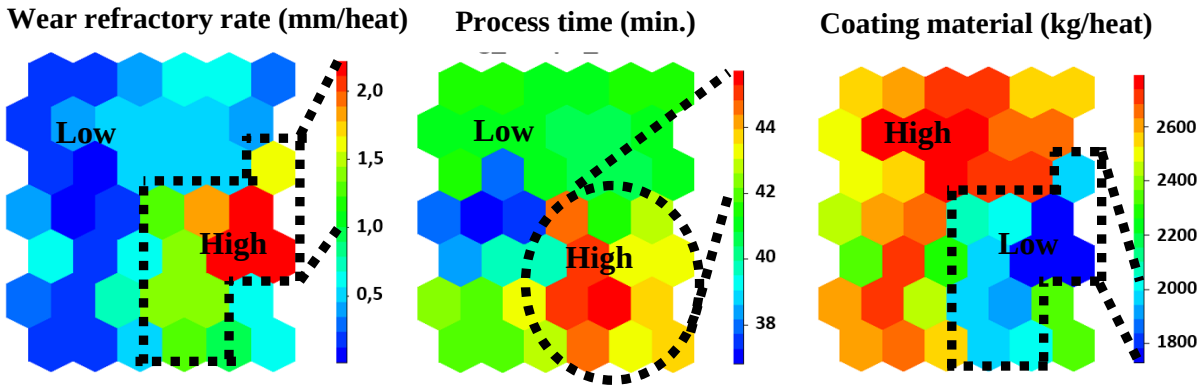

Figure 69 shows the direct relationship between the refractory wear rate and the process time, and the inverse relationship with the amount of material added for Slag Coating/Slag Splashing (Coating material).

In the case of process time, high values promote a longer contact time per heat of the steel/slag with the refractory and consequently increase the wear rate.

In the case of the amount of dolomite (raw or calcined) added to prepare the slag during Slag Splashing or Slag Coating, it is expected that greater amounts up to a certain limit improve the MgO saturation and the viscosity of the slag to the adhesion and fixation of this slag on the refractory surface forming a protective layer and consequently reducing wear rates. Therefore, the results are in agreement with the statistical analyses, literature and operational observations of the factory.

4.1.10 Joint analysis of the refractory wear profile at the east cylinder region (trunnion) in the LD of campaign A, B and C using classic statistical tools

For a joint evaluation of the data from the three campaigns (A, B and C) in order to have an evaluation and a possible single model for all campaigns and, at the same time, a comparative view between campaigns (in addition to verifying the reproducibility of the analyzes in larger samples, in this case three campaigns together) from the influence of the process variables on the average refractory wear rate of the trunnions (inclination of the wear curves shown in figure 40), the data was analyzed jointly and progressively over the campaigns.

In this case, the most relevant variables identified in the previous sections by statistical methods and by SOM for the three campaigns together were considered, in order to have a vision of the evolution of the average rate of refractory wear between and within the campaigns.

Figure 70 – Evolution of the refractory wear rate in the east trunnion of the 3 campaigns (A > 4,000 heats, B ~ 4,000 heats and e C < 4,000 heats), as a function of FeO at the slag in the LD converter process

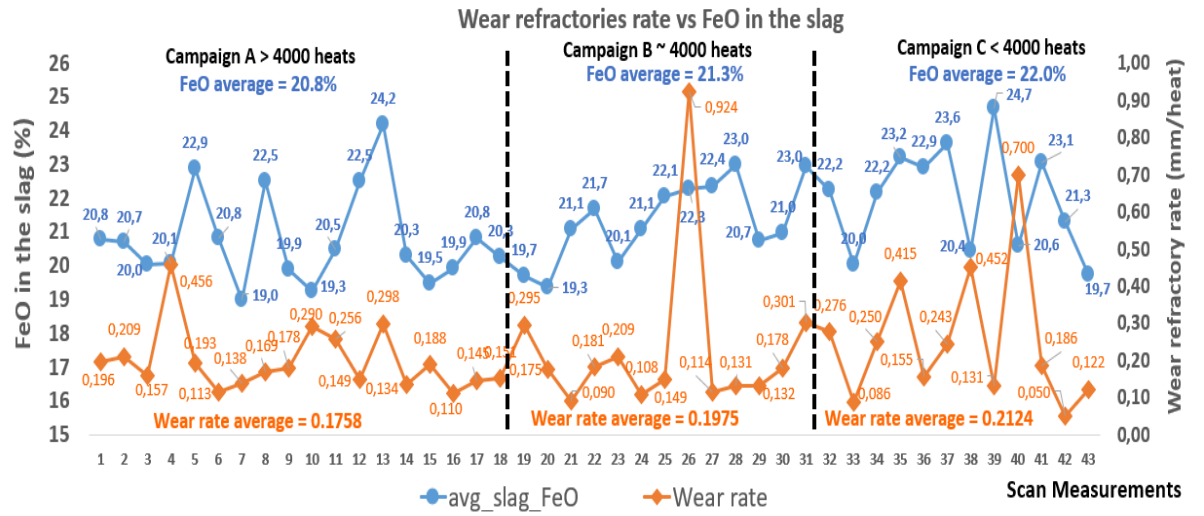

Figure 70 shows the increase in the percentage of FeO in the slag between campaigns. The campaign with highest refractory wear rate have the highest average FeO content in the slag and the campaign with the lowest wear rate have the lowest FeO content.

This result summarizes and agrees with all the individual analyzes made of the campaigns in the previous sections. The evolution of the graphs' peaks and valleys

also shows the upward and downward trend of these two variables in the sense of direct correlation.

As previously mentioned, this variable is directly related to the levels of slag oxidation that impact carbon oxidation in the MgO-C refractory structure of the bricks. The oxidation and, consequently, reduction of the carbon in the refractory matrix increases the wettability of the surface of the refractory bricks by the slag due to the reduction of surface tension and increases the formation of pores in the structure resulting from the formation of $CO_{(g)}$ and $CO_{2(g)}$. This combination, in addition to weakening the refractory and consequently reducing the mechanical resistance, facilitates the entry of slag into the matrix of MgO-C aggregates and, consequently, facilitates the $MgO_{(s)}$ dissolution reactions in the refractory matrix, thus increasing the wear rate. Obviously, this process is cyclical, as matrix degradation implies greater slag penetrations from subsequent heats.

Figure 71 – Evolution of the refractory wear rate in the east trunnion of 3 campaigns (A > 4,000 heats, B ~ 4,000 heats and C < 4,000 heats), as a function of the oxygen volume used in the reblow process in the LD converter heats

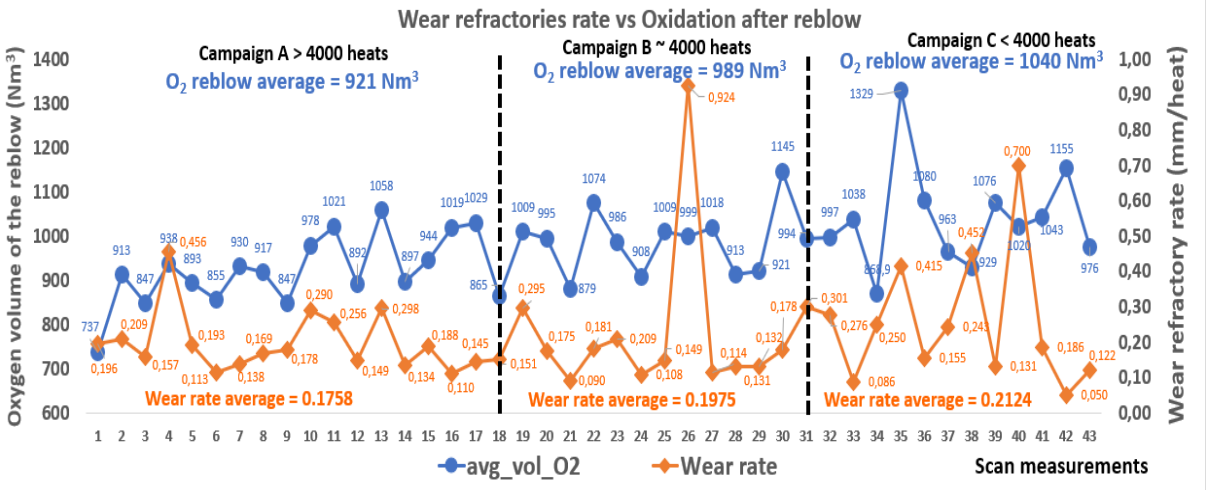

Figure 71 indicates the influence of the volume of oxygen blown in the reblow (avg_vol_O2) of the heats in the increase of the refractory wear rate. The reblow of the heat is a condition in which, after the end of the process, an additional blowing step was required, resulting in a high level of oxidation of the slag and metallic bath. This condition is one of the most aggressive for the refractory, because in addition to the oxidation of the carbon in the bricks, the excess of iron oxides in the slag and the oxygen dissolved in the metallic bath makes the slag very reactive. Therefore, the higher the percentage of heats with reblow, the worse for the refractory.

On the other hand, the volume of oxygen blown in the reblow has a direct influence on the level of aggressiveness of the reblow process. Figure 71 shows the increase in refractory wear rate when this volume of reblow oxygen increases.

A relevant fact of these processes is also the consequent increase in the process time, since the performance of the reblowing entails an extra step in the steel manufacturing phases in the LD, in this case, it would be a process correction step. In this case, longer process times, as already shown in previous sections, increase the contact time of the refractory structure with the environment (slag, steel, gases, etc.), increasing the wear rate per heat.

Figure 72 – Evolution of the refractory wear rate in the east trunnion of 3 campaigns (A > 4,000 heats, B ~ 4,000 heats and C < 4,000 heats), as a function of the percentage of Slag Splashing in the LD converter heats

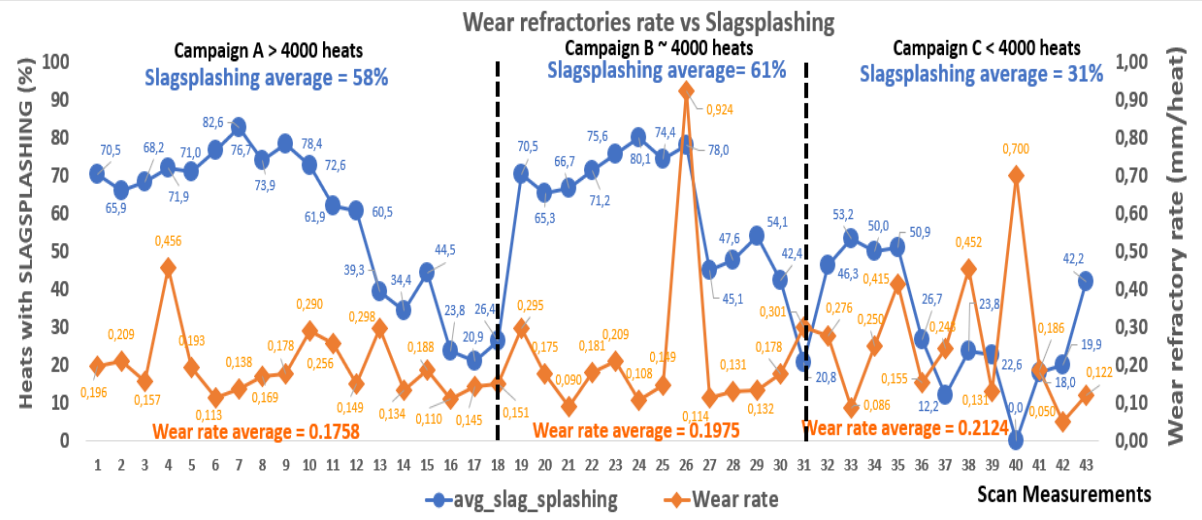

Figure 72 shows the effect of reducing the percentage of heats in which the Slag Splashing process was performed (avg_slag_splashing) and the refractory wear rate between the 3 campaigns. Note that the reduction, mainly in relation to campaign C, was quite high. The explanation comes from the fact that, the more the refractory surface of the trunnions is covered with a suitable slag, the greater the physical barrier between the physical and chemical agents that are deleterious to the refractory (oxygen from the blow, contact with the slag and liquid metal, erosion of solid particles from the process and the refractory, etc.) and the lower the refractory wear rate.

Figure 73 – Evolution of the refractory wear rate in the east trunnion of 3 campaigns (A > 4,000 heats, B ~ 4,000 heats and C < 4,000 heats), as a function of dephosphorization rate of the LD process

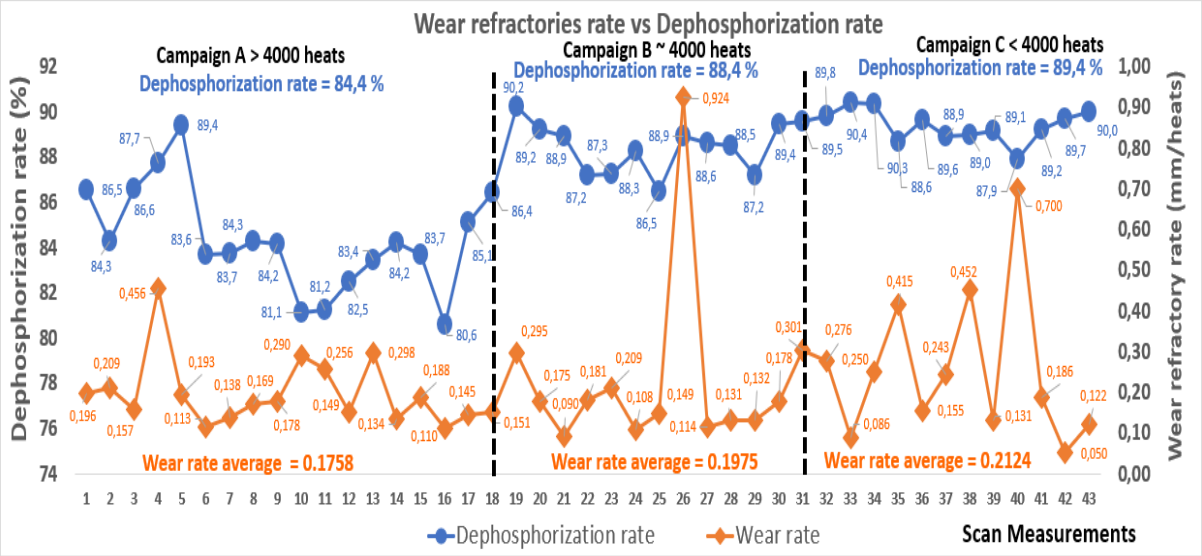

The effect of the dephosphorization rate in the LD campaigns is very evident in the sections indicated in figure 73, the dephosphorization rate was calculated considering the initial phosphorus in the raw materials (pig iron) and the phosphorus of the steel at the end of the blow.

This variable is extremely relevant, as higher levels of oxidation resulting from obtaining a higher rate of dephosphorization in the metallic bath (lower percentages of phosphorus in the final steel) are extremely deleterious for the refractory structure, mainly due to the oxidation of the carbon in the refractory. It can be seen that the higher the steel dephosphorization rate in the LD, the higher the wear rate of the campaigns.

Figure 74 – Evolution of the refractory wear rate in the east trunnion of 3 campaigns (A > 4,000 heats, B ~ 4,000 heats and C < 4,000 heats), as a function of the average oxidation level in the metallic bath at the end of blow in the LD process

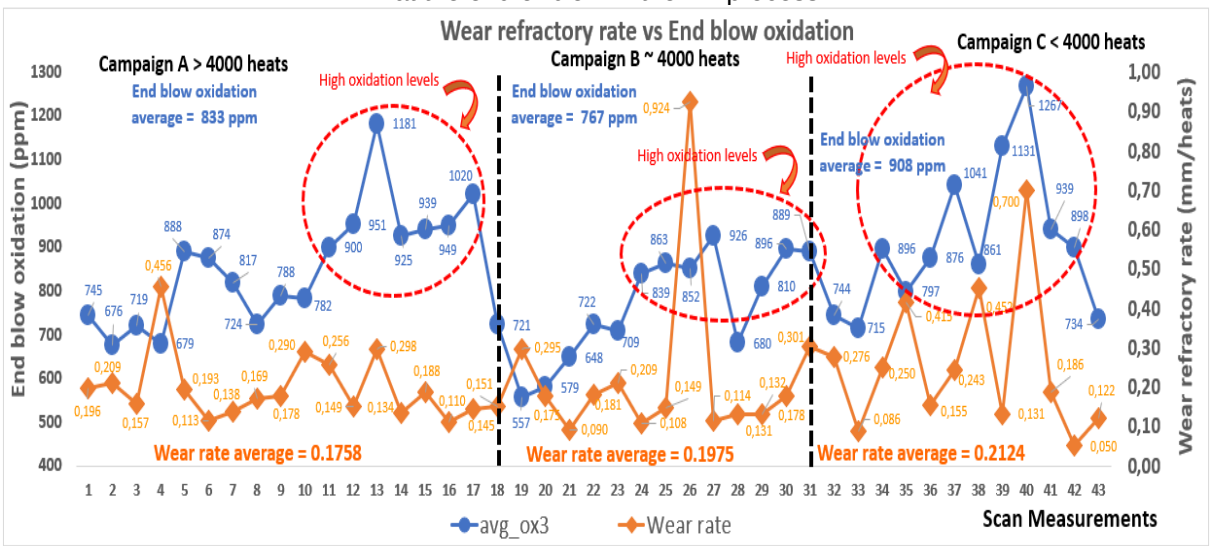

As can be seen from figure 74, the level of oxidation of the metal bath and consequently of the slag at the end of the LD converter blow is directly related to the wear rate of the refractories.

The explanation lead in the possibility of both the oxidation of the carbon in the brick and the dissolution of the MgO aggregates by a slag rich in FeO. From the data in the figure above, the highest average level of oxidation is verified for the campaign with the highest wear rate.

In addition, it is noted that the campaign with the worst refractory performance was the one that operated for a period (relative campaign percentage) with higher levels (above 800 ppm of oxidation), a value considered quite high. This verification can be identified by the size of the highlighted circular area of each campaign against the size (measurement range of each campaign) of the vertically dotted area.

Figure 75 – Evolution of the refractory wear rate in the east trunnionof 3 campaigns (A > 4,000 heats, B ~ 4,000 heats and C < 4,000 heats), as a function of LD converter process time

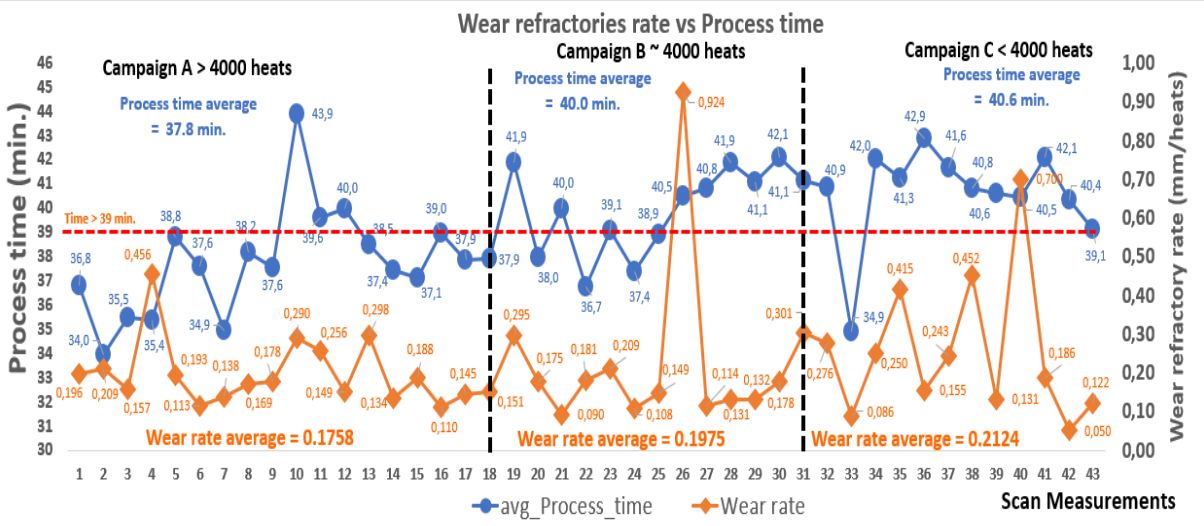

The process time (avg_Process time), shown in figure 75, was representative of the refractory wear rate, it can be seen that the wear rate increases for longer heat times.

Longer process times for the same heat indicate longer contact times between the refractory bricks with the metallic bath and the slag, in addition, of course, to greater exposure to the thermal conditions of the process.

It is noted by the time series data between the campaigns that values above 39 min. significantly impact the wear rate. When analyzing the campaigns, it is verified that the percentage participation of heats with time above 39 min. increases

in the worst performing campaigns. Considering all the necessary steps to manufacture steel in the LD, this would be a maximum time limit or objective to keep the wear rate at acceptable values.

Table 15 was constructed based on the analysis of the figures above, showing the main variables that acted towards increasing and reducing the refractory wear rate over the three analyzed campaigns of the LD converter. Through it, is possible to summarize and jointly verify the effect of process parameters on the attrition rate between campaigns.

Table 15 – Summary of the influence of the main variables that impacted the refractory wear rate in the LD trunnion of 3 campaigns analyzed (A > 4,000 heats, B ~ 4,000 heats and C < 4,000 heats).

Variables	**Campaign A > 4000 heats**	**Campaign B ~ 4000 heats**	**Campaign C < 4000 heats**
Refractory wear rate (mm/heat)	0.1758	0.1975	0.2124
Average process time (minutes)	37.8	40.0	40.6
Average oxidation of steel at the end of blowing (ppm)	833	767	908
Average FeO in the slag (%)	20.8	21.3	22.0
Average of O_2 reblowed (Nm^3)	921	989	1040
LD dephosphorization rate (%)	84.4	88.4	89.4
Heats With *SLAG SPLASHING* (%)	58	61	31

The analysis of table 15 shows that the combination of long process times with high levels of system oxidation and low protection of the trunnion with process slag by Slag Splashing are the main parameters for determining the refractory performance of the trunnion region of the LD converter. When the refractory wear rate is analyzed, there is an increase in this rate (approximately 12%) for the campaign with intermediate life in relation to the best campaign and an increase of 7.5% when comparing the worst campaign with the intermediate one. When

comparing the worst campaign with the best, there was an increase in the wear rate of around 21%.

Regarding the average process times, there is an increase in the wear rate with the increase in process times between campaigns. However, this result is more evident when comparing the campaign with the best performance in relation to the other two campaigns. When comparing the worst campaign with the best, there is an increase of approximately 7% in the average process time (2.8 minutes). For longer process times per heat, longer contact times between the refractory and metal/slag/gases are expected. Therefore, higher wear rates per heat are expected in campaigns with longer process times.

The results of the average oxidation at the end of the blow show that the worst campaign (with the highest wear rate) has values 9% and 18% higher in relation to the campaigns with the highest performance (lower refractory wear rate) and intermediate performance (intermediate wear rate) respectively. An interesting factor is the fact that the intermediate campaign has a lower oxidation value compared to the shorter campaign (the opposite would be expected). However, even with a lower oxidation, there is a longer process time, so that a reduction in oxidation may have been compensated by longer contact times between the refractory and the metal/slag/gases, reflecting a higher rate of wear. This multivariate behavior, in which one variable ends up compensating for the possible effects of others, makes this type of study system (refractory wear in an LD reactor) extremely complex.

Slag FeO values also showed a direct relationship with refractory wear rate. From the data in Table 15, the increase in the average FeO of the slag in the campaigns can be seen in parallel with the increase in the refractory wear rate. There are increases of 2.5% (in relative terms) or 0.5% (in absolute terms) when comparing the intermediary campaign with the best performance and a increase of 3.3% (in relative terms) or 0.7% (in absolute terms) when comparing the campaign with the worst performance in relation to the intermediary campaign. When comparing the worst campaign in relation to the best, the increase in FeO of the slag was 6% (in relative terms) or 1.2% (in absolute terms). These results show once again the deleterious impact of oxidation levels, in this case from the slag and indirectly from the oxidation of the metallic bath, of the system on the refractory wear of the trunnions. The probable oxidation of carbon with consequent increase in porosity of the refractory and penetration of the slag through the pores into the matrix leads to a

structure with lower structural resistance and greater reactivity (greater surface area and penetration of the MgO dissolution reaction by the oxidized slag).

No less important was the variable volume of oxygen blowing during the reblow of the heats. This parameter determines the final level of oxidation of the metallic bath and slag and the consequent evolution of FeO. It is clear from the results shown in Table 15 the direct relationship of this variable with the wear rate. Obviously, for a percentage of reblowing heats, the greater the volume of reblowing oxygen, the greater the wear rate. The consequences and foundations of this parameter are similar to those previously described for oxidation with the aggravating factor of higher bath and slag temperatures generally obtained in these cases.

A prominent factor was the LD dephosphorization rate variable. The values of this variable indicated in table 15 leave no doubt about the relevance of this parameter in the LD refractory wear rate, in which the higher the levels of dephosphorization reached in the LD, the higher the refractory wear rate and the lower the trunnion performance. The observed average fluctuation of this variable was approximately 85% dephosphorization rate in the best campaign (lowest wear rate) to a value around 90% dephosphorization for the worst campaign (highest wear rate). The direct relationship of this variable with the wear rate is explained by the high levels of oxidation in the heats that need to be achieved as the aim is to achieve higher rates of dephosphorization of steel in the LD. In addition, this parameter is also linked to the increases in the percentage of heats with reblowing and the volume of oxygen blown relative to the need to reach increasingly lower levels of phosphorus in the steel at the end of process.

The last indicator in Table 15 was the percentage of heats that were carried out through the Slag Splashing process of each campaign (in relation to the total number of heats produced in the campaign). The worst performing campaign had approximately half the percentage of Slag Splashing heats compared to the other campaigns. While, on average, 60% of the heats were performed with Slag Splashing in the campaigns with good and intermediate performance, the campaign with the worst performance performed only 30% of its heats. The Slag Splashing process is fundamental for covering regions such as the trunnions, because as the LD only has movements in one direction (charging and tapping direction), the region of the trunnions ends up being unprotected by a layer of chemically and physically adjusted slag. This layer works as a physical barrier between the refractory bricks and the

different conditions (process variables), in particular, the oxygen flow in the system and the extremely oxidized slag.

Summarizing table 15, the combination of high levels of oxidation of the metallic bath and slag together with long process times and low protection of the surface of the refractory bricks of the trunnion seem to determine the general behavior of the refractory wear rate of the trunnion.

This combination is evident in processes that involve high rates of dephosphorization of the metal bath, either due to high phosphorus levels in the pig iron and/or low levels of phosphorus in the final steel. All of this is based on considering the typical structure of MgO-C bricks, which have their point of weakness in the oxidation of carbon in the refractory matrix, with a consequent increase in the porosity of the brick structure and reduction in mechanical strength.

In extreme conditions of oxidation of the slag, its greater fluidization occurs, promoting greater infiltration into the refractory matrix through the pores, which can lead to the dissolution of the MgO aggregates and again to a reduction in the refractory mechanical strength.

In a cyclical situation of these events combined with heating and cooling typical of this type of reactor, the generation of thermomechanical stresses and induction of formation and propagation of cracks and spalling lead to a greater or lesser degree to the process of refractory wear. All this, combined with slags with low levels of MgO and basicity, can be the sequence of steps in the physical, chemical and thermal model of wear on the trunnion of the LD converter.

4.1.11 Multivariate statistical analysis of the refractory wear rate in the east cylinder region (trunnion) at the LD campaigns A, B and C together

Through classic multivariate statistical modeling, a deterministic equation was built in which the refractory wear rate can be estimated as a function of process variables. Equation 19 was obtained using the same database as the previous analyses (campaigns A, B and C together). Acceptance criteria for regression coefficients (p-value < 0.05 and 1 < VIF < 2) and residuals (normality, homoscedasticity and independence see APPENDIX D).

$$\text{Wear rate} = -0.431 + 0.02870 * \text{reblow} + 0.000875 * \text{avg\_vol\_}O_2 - 0.0244 * \text{dol\_calc} - 0.00555 * \text{Slag\_Splashing} - 0.0099 * \text{carbon\_end\_blow} + 0.0151 * \text{avg\_lime} \quad (19)$$

$$R^2 = 47.64 \quad R^2 \text{ (aj)} = 39.78$$

Where:

Wear rate: Average refractory wear rate of bricks (mm/heat);

reblow: Percentage of heats that reblow (%);

avg_vol_O_2: Average volume of oxygen blow in the reblow (Nm^3);

dol_calc: Average value of calcined dolomite for heat (kg/t.$_{steel}$);

Slag_Splashing: Percentage of heats with Slag Splashing (%);

Carbon_end_blow: final carbon in the metallic bath in the end process (pts);

avg_lime: Average value added per heat (kg/t.$_{steel}$).

From equation 19, it can be verified that the refractory wear rate is influenced by the average amounts of calcined dolomite and lime added in the heats, by the average percentage of heats that are reblowed in the LD and by the volume of oxygen blown in the reblow, by the level of oxidation end of the metallic bath (and consequently the slag) which is directly related to the carbon in the bath at the end of the blowing process and the frequency which the Slag Splashing process is carried out in the heats. Therefore, these 6 variables can determine the wear rate of the bricks and consequently the life of the LD.

Starting with the variables reblow and volume of oxygen blown in the reblow, respectively, there is a direct relationship between the refractory wear rate and these variables. As the level of oxidation of the metallic bath and slag increases with these two variables, it makes the environment in contact with the bricks highly corrosive. In addition to the fact of direct oxidation of carbon with jet of oxygen from the lance and the furnace environment. Another impact would be the fact that reblown heats and, in particular, those with high volumes of oxygen, acquire extremely high temperatures, which facilitates the kinetics of the reaction between the environment and the refractory bricks, not to mention the fact that the heating time increases. process to carry out this additional step of the process.

The calcined dolomite variable, according to equation 19, has an inverse relationship with the refractory wear rate. That is, large amounts added per heat reduce the LD wear rate. The basic explanation, based on the literature discussed,

and on factory experience, is the increase in the MgO compound in the process slag, as calcined dolomite is the main source of addition of this compound in the process. As refractory bricks are basic and based on MgO-C, higher saturation of MgO in the slag balances the chemical gradient between slag and refractory, preventing this compound (from the refractory brick) from being dissolved by the process slag.

The fourth variable, percentage of Slag Splashing in the campaign, has an inverse relationship with the refractory wear rate. For, the greater the frequency of carrying out this practice, the greater the probability of having a protective layer of slag on the refractory bricks, forming a physical barrier. This physical barrier reduces the performance of wear agents such as highly oxidized process slag and oxygen from the blow. Obviously, for this layer to function as an effective barrier, it is essential that the slag is adjusted to this practice. Therefore, control of basicity, MgO saturation, viscosity, etc. it is fundamental.

The fifth variable, carbon in the metal bath at the end of the process or, indirectly, the final oxidation level of the metal bath (and consequently the slag) was inversely correlated with the refractory wear rate, as expected. For higher carbon contents at the end of the blowing, the oxidation levels of the metallic bath will be lower and, consequently, the refractory wear will be lower. This variable considers the oxidation levels of the heat and, as a consequence, high levels of refractory wear due to the oxidation of the carbon in the bricks. The loss of carbon and the consequent formation of pores in the refractory structure would facilitate the permeability of the slag inside the bricks, promoting the complete dissolution of the MgO aggregates by the FeO-rich slag.

Finally, the variable amount of added lime indicated a direct correlation with the wear rate. This variable, in addition to the metallurgical functions, has the function of controlling the basicity of the furnace. It is through it that the balance is made due to the formation of SiO_2, but at high levels of addition, the dilution of the slag MgO may occur, bringing a deleterious effect and increasing the wear rate.

Unlike the multivariate equations determined individually for each campaign separately, equation 19 did not show a good coefficient of determination (R^2 or R^2 adjusted), that is, a good fit of the regression to the analyzed data. Statistically, low R^2 does not necessarily mean that there is no correlation between the response variable and the independent variables. A possible cause would be individual effects that stand out in a specific campaign and not in others, for example, quality deviation

in some trunnions brick or large difference presented in the variable percentage of Slag Splashing. When the data are analyzed jointly, these effects could distort the general dynamics of the joint action of the independent variables on the response variable, which would in practice lead to a low regression adjustment. Thus, the separate analysis of each campaign (or by ranges of heats) would be a more viable alternative for modeling the wear phenomenon by multivariate statistics.

It would be as if each campaign (or campaign ranges) had its characteristic dynamics, given that campaigns with similar process variable activity spectrums could be modeled with similar equations, while those with very specific characteristics would have to have specific prediction models. For example, campaigns A and B (considered to have satisfactory performance) could have similar equations, whereas campaign C (considered to have low performance) should have specific modeling due to some highly relevant factor (avg_Slag Splashing) that did not occur in the other two campaigns.

4.1.12 Joint analysis of the refractory wear rate of the east cylinder region (trunnion) of the LD campaigns A, B and C by SOM

Figure 76 – SOM analysis, refractory wear rate vs process time and the percentage of MgO in the slag. East trunnion of the LD campaigns A, B and C

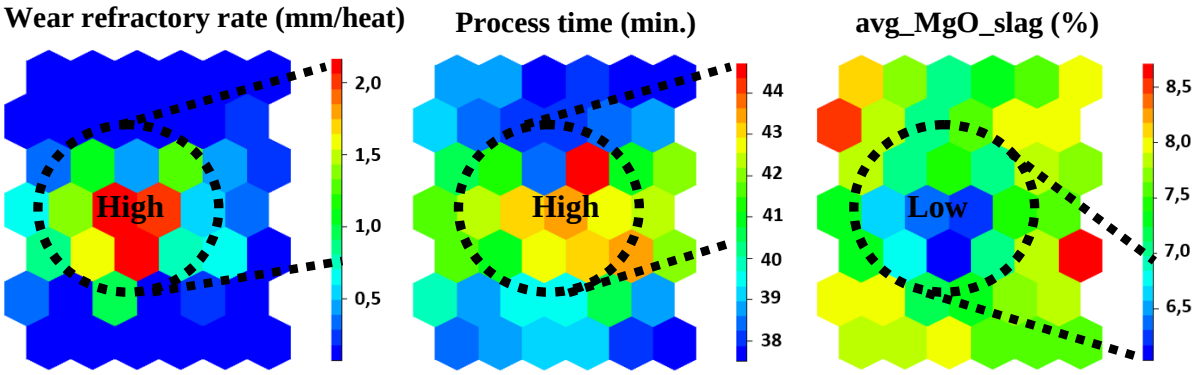

According to figure 76, it appears that longer process times together with lower percentages of MgO in the slag have a decisive impact on the increase in the refractory wear rate. The fundamentals of these variables have already been widely discussed in previous sections and the results of the analyzes by SOM are in line with the results obtained in the statistical analyzes carried out throughout this thesis.

It is noteworthy that this condition of long process times with low percentages of MgO in the slag makes the refractory corrosion as aggressive as possible because its have the two basic conditions for the reaction, high time and chemical potential (MgO gradient). This evidence was found within the analyzes of campaigns and between campaigns.

Figure 77 – SOM analysis, refractory wear rate vs volume of the oxygen blow in the reblow and the percentage of FeO in the slag. East trunnion of LD converter of campaigns A, B and C

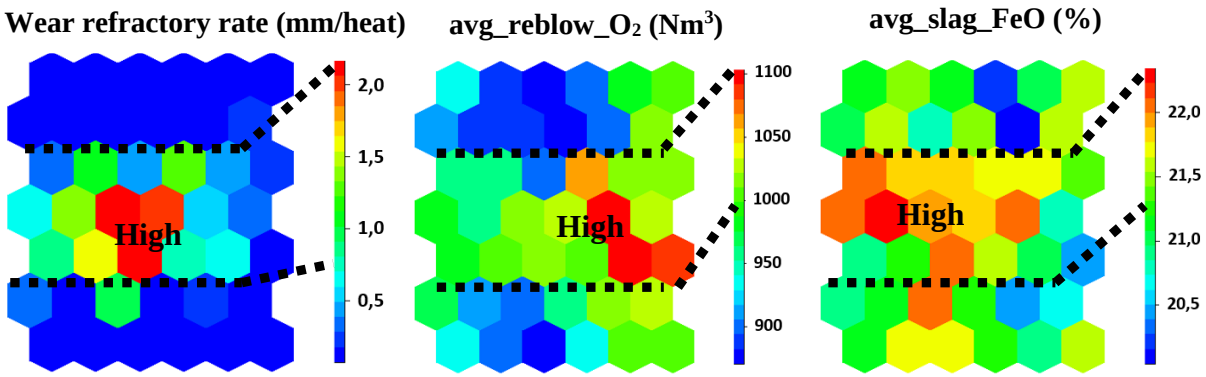

Once again, the effects of the volume of oxygen blown in the reblow, as well as the furnace oxidation levels translated into the percentage of FeO in the slag, indicated that these variables act in the direct direction of refractory wear. Such values are in line with the statistical analyzes carried out in the previous sections and online within and between campaigns. The explanations have also been widely discussed in the previous sections and show that higher levels of oxidation of the metallic bath and slag increase the rate of refractory wear.

Figure 78 – SOM analysis, refractory wear rate vs dephosphorization rate and the percentage of the heats with Slag Splashing. East trunnion of LD converter capaigns A, B and C

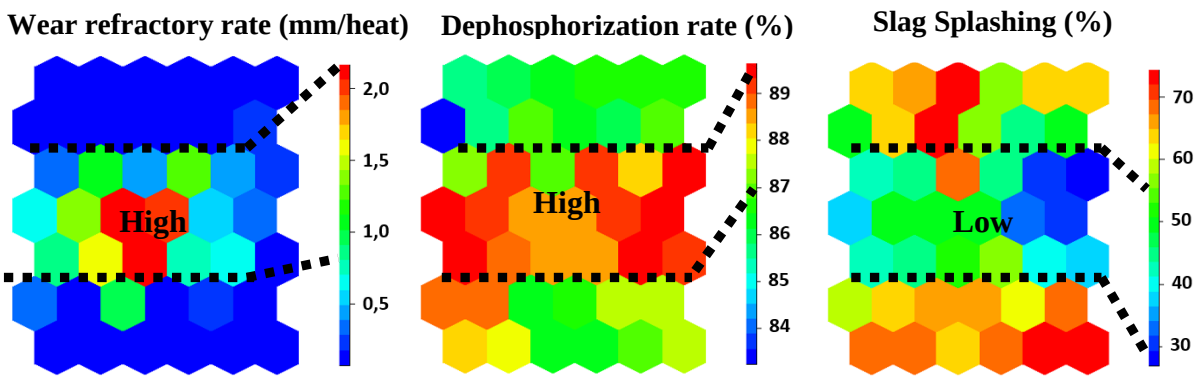

Figure 78 shows the impacts of increasing the dephosphorization rate of the metallic bath on the refractory wear rate. As previously explained, the increase in the dephosphorization rate, sometimes caused by the increase in the phosphorus content in the pig iron and/or by the reduction of phosphorus levels in the final steel, bring deleterious impacts to the refractory wear rate. The causes are the excess oxidation necessary to remove the phosphorus from the metal bath to the slag. Furthermore, the excesses of CaO necessary for this practice end up diluting the MgO in the slag, making it more corrosive to refractories. The SOM analysis indicates that campaigns where the percentage of heats in which the percentage of Slag Splashing was lower there was a higher wear rate. As these results coincide with those of the highest dephosphorization rate, it is suggested that the causes act together in such a way that the effects added up and had a decisive impact on the wear rate. Therefore, the combination of long process times, low levels of MgO in the slag, excessive oxidation of the metallic bath/slag with low percentages of Slag Splashing were the determining factors in the drop in refractory performance and consequently in the increase in the trunnion wear rate accordingly to SOM.

4.2 Post-mortem analysis of the LD converter trunnion bricks from previous, contemporary and post campaign periods analyzed in previous sections

In parallel with the statistical analyzes and the self-organizing maps, post-mortem analyzes were carried out on refractory bricks of trunnions from campaigns that occurred in contemporary periods to the databases analyzed in the previous sections, as well as, from periods subsequent to the analyzed database. In parallel, post-mortem studies carried out by the company in past periods (prior to the analyzed campaigns in this theses) of the trunnion bricks of this LD were rescued. The main objective of this mapping over time is to identify which are the predominant wear mechanisms and phenomena that act in the refractory wear process and, at the same time, to verify if they vary over time and between different suppliers.

In addition, the objective of these analyzes was to substantiate, validate and interrelate the results and models obtained from the analysis of the databases in the previous sections with the physical-chemical and mechanical observations of the bricks after the campaign in order to verify whether the phenomena of real wear observed in the post-mortem analyzes can be explained (or explain) and modeled by

the analyzes and equations obtained previously (statistics and SOM). Initially, post-mortem analyzes were carried out on bricks from the LD studs referring to a contemporary period to the databases analyzed in the previous sections through which all statistical analyzes were carried out and by SOM. The following figure 79 illustrates the trunnion brick of a refractory supplier X after the end of the campaign.

Figure 79 – Photograph of the longitudinal section of one bricks in the region of the LD trunnions after the end of campaign (period contemporaneous with those of the databases and supllier X): hot face of the brick and cracks parallel to the hot face

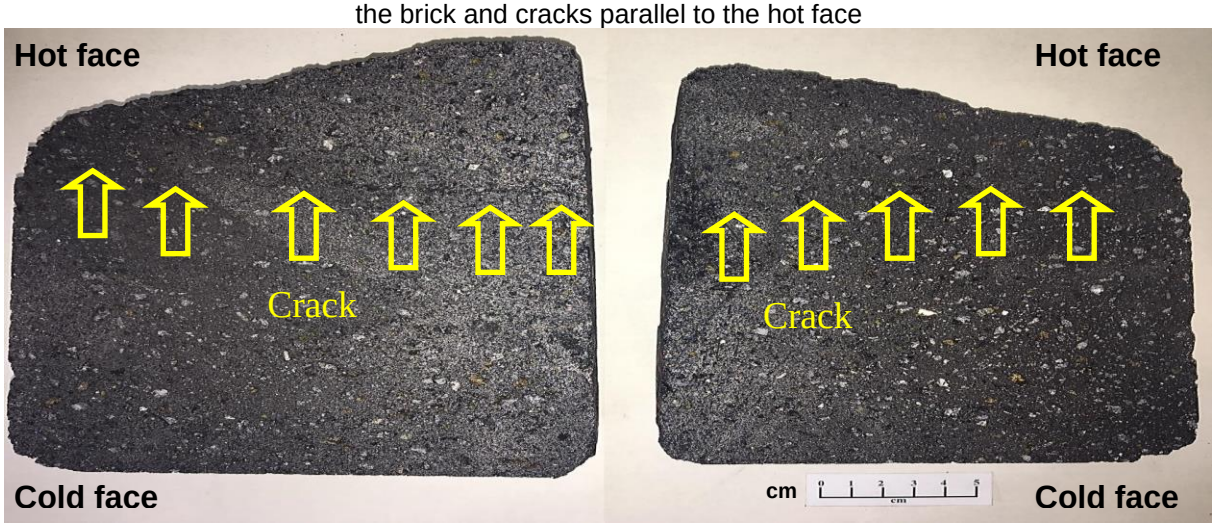

Figure 79 is a longitudinal section of the trunnion brick from supplier X, which reveals the appearance of the refractory section. By visually analyzing figure 79, it is possible to verify occurrences of cracks parallel to the hot face of the refractory (indicated by the arrows in the figure 79). At first, no layer of slag was observed on the surface corresponding to the hot face of the brick.

The cracks observed may be caused by issues related to the operational cycles of the furnace, such as longer intervals and frequency of stoped, problems in post-stop reheating patterns with consequent thermal shocks in the bricks, excess resistance and rigidity of the refractory material, which would lead to a failure to not absorption of thermomechanical tensions generated by the process.

In addition, as the trunnion region is a region subjected to torsional stress (region where the LD rotation motor is located), the issue of excess resistance combined with low flexibility of the bricks can be the main driving force for the wear mechanism by chipping of the refractory bricks of the LD trunnions. Issues related to the final stop of the campaign, such as a very accelerated cooling, could also cause such cracks. The formation of a layer of slag on the surface, in the case of cracks,

could act in the opposite direction, as it would form an insulating layer on the surface of the bricks, reducing thermal gradients along the thickness.

The following figure 80, made from post-mortem studies of trunnion bricks from this same LD (and same supplier X), but in campaigns prior to those relating to the studies referred to by the databases of this thesis, reveals the aspect of the longitudinal section of this structure refractory.

Figure 80 – Photograph of the longitudinal section of the one of the bricks in the region of the LD trunnion after end of the campaign (period prior to the databases): hot face of the brick indicating a thin layer of slag (FQ), crack parallel to the hot face (1) and crack perpendicular to the hot face (2)

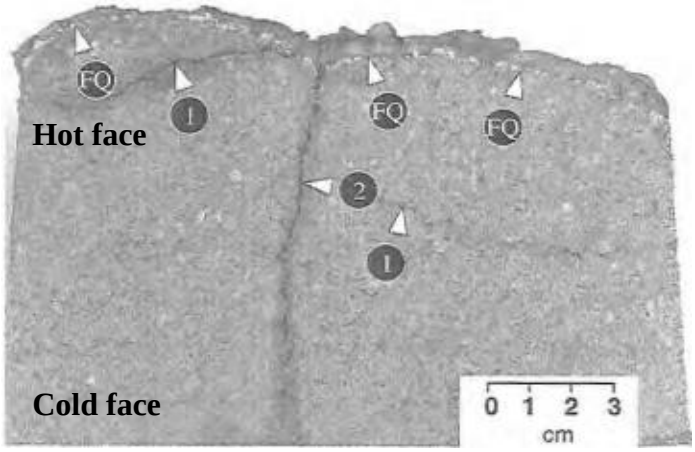

Source: Usiminas Research and Development Center

It is possible to verify, in addition to cracks parallel to the hot face, perpendicular cracks. In addition, a thin layer of slag is observed on the surface corresponding to the hot face of the brick.

The cracks observed in the brick in figure 80 leads to think that the phenomena and mechanisms for generating these cracks are not specific to a given campaign (such as those shown in figure 79 relative to the contemporary campaign of this thesis), but occurring with certain frequency over time and in different campaigns.

In addition to the cracks, the formation of a thin layer of slag can be observed on the hot face of the brick. This indicates that the formation of thin layer thicknesses of slag (structure with lower heat transfer capacity compared to refractory bricks), at first, does not work as an insulating layer in the sense of reducing thermal gradients in the bricks capable of reducing the generation of cracks (thermal conductivity of the slag is about 10 times lower than that of the refractory brick).

This possible function of thermal insulation of the slag layer on the hot face of the bricks, based on the principle that the slag layer, depending on the thickness and chemical composition, has a lower heat transfer capacity than that of the refractory bricks, would be serving as a thermal insulator in order to reduce the temperature gradient between the cold face and the hot face of the bricks, generating a more equalized stress distribution in the refractory structure. In these cases, during the reheating of the LD in the stop returns, the heating of the bricks would occur in a more balanced and soft way. At stops or between heats, the cooling of the bricks would be slower. In both cases, we would have a more balanced distribution and generation of thermomechanical stresses and less impact on the process of generating cracks and spalling, contributing to a reduction in the wear rate of refractories.

The combination of cracks together with the small or no thickness of the slag layer observed on the hot face of the bricks in both cases (figures 79 and 80) leads us to reflect on the possibility of a combination of the phenomenon of spalling and erosion. In this case, it is possible to assume that the lack of a thick layer of slag on the refractory bricks could be the result of intense agitation of the fluids (metal/slag/gases) in the furnace during blowing with the oxygen lance (high flow rates, higher than 35,000 Nm^3/h) which would lead to continuous removal of weakened surface layers (by cracks and high oxidation) of the refractory followed by infiltration of slag and oxygen through the cracks and pores formed. This could lead to a process of chemical corrosion followed by carbon oxidation in this region of the coating. Issues like this, understood by the lack of coverage efficiency in the trunnion region, may be related to low frequency and efficiency in performing Slag Splashing combined with FeO rich slag acting for prolonged process times (see statistical and SOM analyzes of previous sections).

With regard to the process of carbon oxidation (decarburization) of the refractory structure of bricks, carbon content of the hot face to the cold face (figure 81) of bricks from supplier X (same sample in figure 79) and from a second supplier Y (different refractory projects figure 82) with the intention of verifying the possible bricks oxidation. Typical carbon values at the beginning of a campaign, together with the values measured at the end of campaign, are shown in Tables 16 and 17 below.

Figure 81 – Photograph of the longitudinal section of one of the bricks in the region of LD trunnion after the end campaign (period contemporaneous with databases) of suplier X: Points 1 to 3 were the places of measuring the carbon content

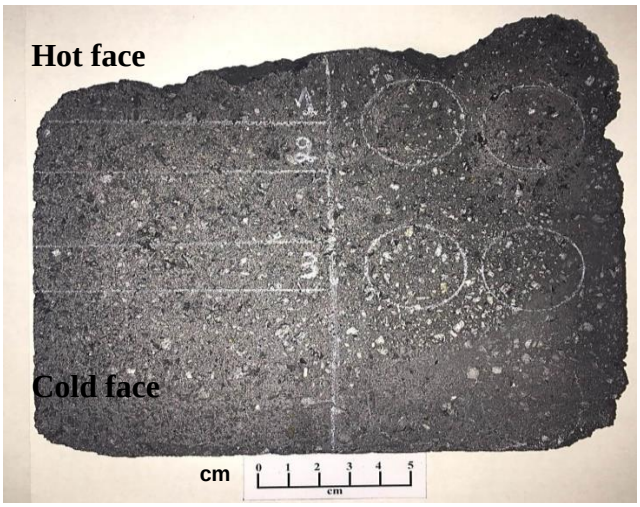

Source: Usiminas Research and Development Center.

Table 16 – Percentage carbon contents in the 3 regions of brick from supplier X, points 1, 2 and 3.

Regions 1, 2 and 3	Carbon content
Hot face (point 1)	12.2 %
Intermediate face (point 2)	14.3 %
Cold face (point 3)	13.6 %
Average value at the beginning of the campaign (original)	~ 14 %

Figure 82 – Photograph of the longitudinal section of one of the bricks in the region of the LD trunnion after the end of campaign (post-database period) of supplier Y: Brick average carbon

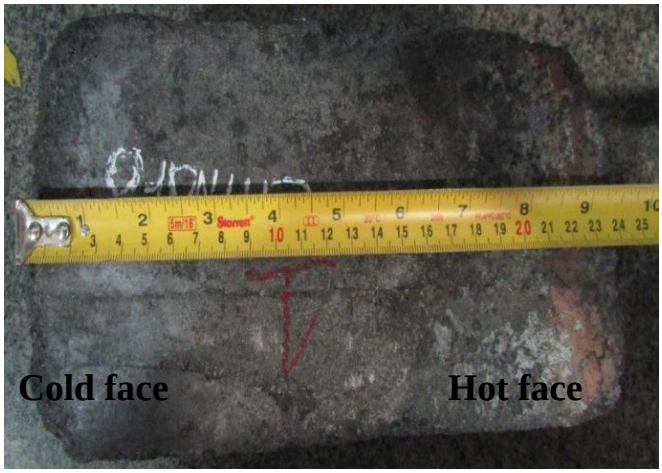

Source: Supplier Y Research and Development Center.

Table 17 – Chemical analysis of the refractory brick from supplier Y after end of campaign.

Compounds	Content
MgO	76.1 %
Carbon	15.1 %
Others	8.8 %
Presense of Corundum	No
Presense of Brucite	No
Average value at the beginning of the campaign (original)	~ 15 %

The analysis of the carbon content in both cases (X and Y) revealed that there were not, in relation to the original values, considerable reductions in the carbon content of the bricks, neither along the thickness nor in average terms (only a slight reduction at point 1 of supplier X's brick). That is, at first, the decarburization process would not be occurring significantly as expected and indicated in the literature. This fact, quite intriguing in view of the results indicated by the statistical analyzes and by SOM, could be explained considering that the carbon oxidation process (decarburization of the bricks) could be occurring only superficially, in small thicknesses of the bricks (as slightly indicated in point 1 from supplier X).

After the oxidation process, the decarburized surface layer would have low structural strength (many pores and voids) and would be pulled out by the movement of process fluids inside the LD converter. Therefore, the post-mortem analysis of the bricks would not indicate this decarburization because this surface layer would no longer be in the brick samples. This pullout dynamic would occur very quickly and would make its identification difficult to measure.

Another possible explanation for the non-decarburization would be the possible efficiency of action of the antioxidants in the brick. In this case, the percentage and the activation system of these compounds seem to be adequate to the type of process that was in force at the time. On the other hand, the generation of previously evidenced cracks can generate surfaces with low mechanical resistance so that the erosion process generated by the turbulence of fluid movement and the successive chipping generate the detachment of the surface layers of the bricks.

These could be strongly deboned by surface oxidation. In this case, the loss of carbon would further weaken the surface, as well as generate a subsequent porous structure on the surface of the bricks. Therefore, it would be difficult to measure the phenomenon of dishonesty since it would be of a very superficial type.

Seeking to know the microstructure of the bricks after use in the LD, X-ray diffraction analyzes were performed on samples from supplier X (figure 83 and table 18) and supplier Y (figures 84 and table 19), revealing the mineralogical composition along the thickness of these bricks.

Figure 83 – Photograph of the longitudinal section of one of the bricks in the LD trunnion region of the supplier X after end of campaign (period contemporaneous with databases) showing the distribution of the refractory brick micro-constituents along the thickess of the brick (HF-Hot face and CF-cold face)

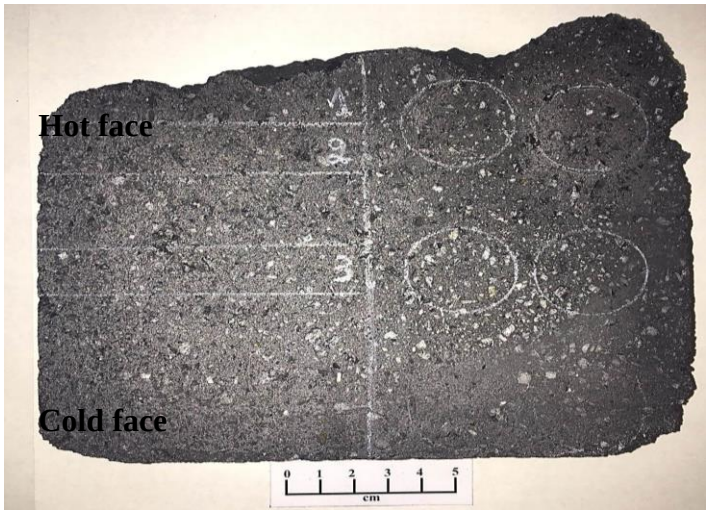

Source: Usiminas Research and Development Center.

Table 18 – Crystalline phases presente in the brick sample from supplier X after end campaign.

Crystalline Phases	MgO (Periclasium)	C (Carbon)	$MgAl_2O_4$ (Spinel)	$Ca_3Mg(SiO_4)_2$ (Mervinite)
Hot Face	***	**	*	*
Intermediate Face	***	***	*	*
Cold Face	***	**	*	*

Content: High***, medium** and low*

The sample from supplier X revealed the presence of periclasium (MgO) and spinel ($MgAl_2O_4$) phases throughout the entire length of the brick, showing the stability of the structure until the end of the LD campaign. Furthermore, the formation

of the spinel indicates the reaction of the antioxidants with the refractory structure as expected and with a consequent increase in the resistance of the material. Carbon, as already mentioned, was also found throughout the brick showing normal structure. Mervinite was also found, a silicate of magnesium that can come both from the raw materials used in the manufacture of bricks or/and from possible reactions involving the LD slag, rich in CaO and SiO_2, with the MgO in the brick.

In the case of Mervinite formation, it is important to use a purer MgO sinter during the manufacturing process of these bricks, avoiding the formation of this type of compound, which has a lower melting point and lower mechanical resistance and which could compromise the structure and refractory performance.

Figure 84 – Photograph of the longitudinal section of one of the bricks in the region of the LD trunnion of supplier Y after the end of campaign (period contemporaneous with databases) showing average distribution of the brick microconstituents

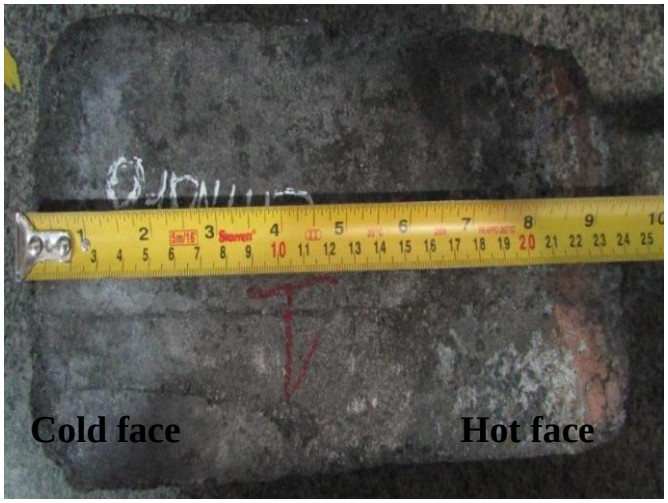

Source: Supplier Y Research and Development Center.

Table 19 – Crystalline phases present in the brick sample from supplier Y after end campaign.

Crystalline phases	MgO (Periclasium)	C (Carbon)	Others	Al_2O_3 (Corindon)	$Mg(OH)_2$ (Brucita)
Contents (%)	76.1	15.1	8.8	0.0	0.0

The sample from supplier Y revealed the presence of periclasium phases (MgO) and carbon contents compatible with brick values at the beginning of the campaign, indicating stability of the refractory microstructure. The presence of spinel ($MgAl_2O_4$) is in the column “Others” of table 19. This cannot be identified due to restrictions of this supplier's analysis equipment. However, it is possible to induce the

presence of spinel due to the high mechanical resistance (resistance to compression) of the post campaign brick indicated in table 20 below.

Table 20 – Mechanical Properties of brick sample from supplier Y after campaign

Mechanical properties	Density (g/cm^3)	Porosity (%)	Compressive strength (MPa)
Values obtained	2.92	6.07	42.3
Typical values from different refractory suppliers	2.6 a 3.2	3 to 5	20 to 60

Furthermore, the possibility of spinel formation indicates the reaction of the antioxidants with the refractory structure as expected and with a consequent increase in the resistance of the material. This analysis highlights the increase in porosity of the brick after application. For reference values for trunnion bricks around 3 to 5%, an increase of more than 50% is observed (considering the value of 4% as an average reference). This increase in porosity is explained by volatile materials typical of the refractory structure (resins) and by possible carbon oxidation reactions and corrosion of the refractory matrix by process slag rich in FeO. This fact reminds of the importance of antioxidants used in the manufacture of bricks, because with the expected increase in porosity (and consequent decrease in mechanical resistance), there must be a compensator in the refractory system, which, in this case, are the reactions of antioxidants with MgO forming spinels with greater mechanical resistance. Hence the explanation for the high mechanical resistance at the end of the some campaign even with the increase in porosity. It is even believed that spinels contribute to a reduction in pores, that is, in filling them.

For supplier X, an increase in porosity was also verified in relation to the initial conditions of this parameter in new bricks. However, the increase was greater in relation to supplier Y. The final values found for the parameter porosity in supplier X was around 10% (increase of 150% considering the same reference of 4% of the average porosity value). The explanations for the increase in porosity are the same as previously indicated. However, this difference in the porosity value between supplier X (10%) and supplier Y (6%) may be related to the different percentages of antioxidants between them. Supplier Y uses a higher percentage than supplier X. Antioxidants play a fundamental role in the refractory system, as in addition to reducing the carbon oxidation process and consequent reducing in porosity, they are

responsible for the formation of spinels and carbides that exert a role in increasing mechanical strength and a possible closure of pores, as described in the literature review.

Regarding the average pore size (Figure 85 and Table 21) along the brick from supplier X, no significant values and variations were found.

Figure 85 – Average pore size on hot face and intermediate face of brick from supplier X

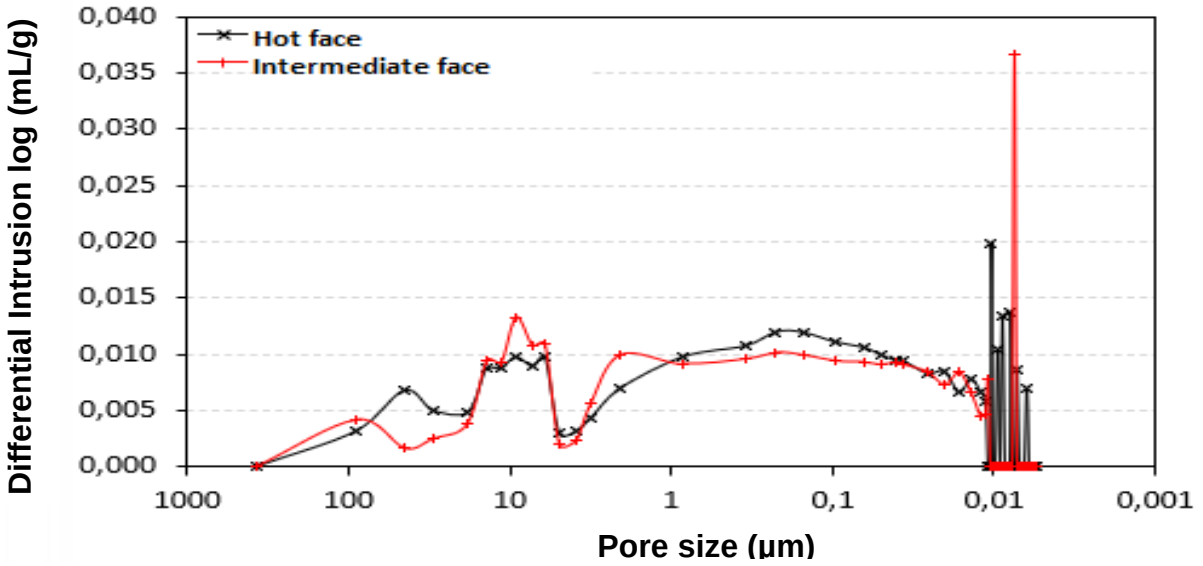

Table 21 – Average pore diameter and porosity along the length of samples of refractory bricks from supplier X taken at the end of campaign, from the hot face of the brick

Sample	Average pore diameter (µm)	Porosity (%)
Hot face	0.5197	10.46
Intermediate face	0.6247	9.64

For purposes of comparison and benchmarking over time, some microstructural analyzes of bricks from the converter were retrieved from reports from past periods (prior to the data analyzed in this thesis) from the Usiminas Research Center.Table 22 shows the results. X-ray diffraction analyzes were carried out on the samples, revealing the mineralogical composition along the thickness of the brick at the end of the campaign.

The X-ray diffraction results indicated in Table 22 shows that there was no considerable change in the mineralogical composition along the brick. The presence

of $MgFe_2O_4$ on the hot face of the brick stands out, probably arising from surface reactions between the process slag (rich in FeO) and the refractory.

.

Table 22 – Mineralogical composition along the length of the refractory brick samples taken at the end of the LD campaign, from the hot face of the brick

Crystalline phases	MgO	C	$MgAl_2O_4$	Al_4C_3	$MgFe_2O_4$	Si	$Ca_3Mg(SiO_4)_2$
0 a 7.6mm *	P	P	P	P	T		T
9.8 to 13.1mm	P	P	P	P			
16.7 to 21.1mm	P	P	P	P			
25.0 to 29.3mm	P	P	P	P			
32.8 to 37mm	P	P	P	P			
40.2 to 44mm	P	P	P	P		P	
47.5 to 52.7mm	P	P	P	P			
56.1 to 61.3mm	P	P	P	P			
66.5 to 71.8mm	P	P	P	P			
75.1 to 80.1mm	P	P	P	P			
188.1 to 193.4mm	P	P	P	P			T
299.0 to 305.2mm	P	P	P	P			T
308.6 to 314.7mm	P	P	P	P			T
317.8 to 328.7mm**	P	P	P				T

P: Present phase, T: Traces, * hot face, ** cold face

Source: Usiminas Research and Development Center.

The compound $Ca_3Mg(SiO_4)_2$, known as mervinite, was identified in different regions of the brick, especially near the cold face. This phase is expected to be associated with periclase or some type of reaction with the slag. As most of it was identified in the deeper regions of the brick, it probably comes from the structure of the manufactured bricks.

The presence of $MgAl_2O_4$ and Al_4C_3 is explained by the typical reactions of this type of refractory system, in which the antioxidants react with the refractory compounds forming spinels and carbides, compounds that in most cases bring benefits to the material in terms of mechanical resistance and non-oxidation of carbon.

Once again mervinite was identified. Seeking to verify and prove the existence of this compound, a diffraction analysis was performed on samples from supplier Y (from another campaign). Figures 86 and 87 illustrate and prove the probable presence of this compound.

Figure 86 – Field photomicrograph of the longitudinal section of one of the bricks in the trunnions region of supplier Y's LD after the end of campaign, showing the probable presence of mervinite in the MgO grain boundaries (EDG Spot 1)

Source: Polytechnic School of USP (Department of Metallurgy and Materials).

Figure 87 – Field microanalysis of MgO particle boudary by possible mervinita (EDG Spot 1)

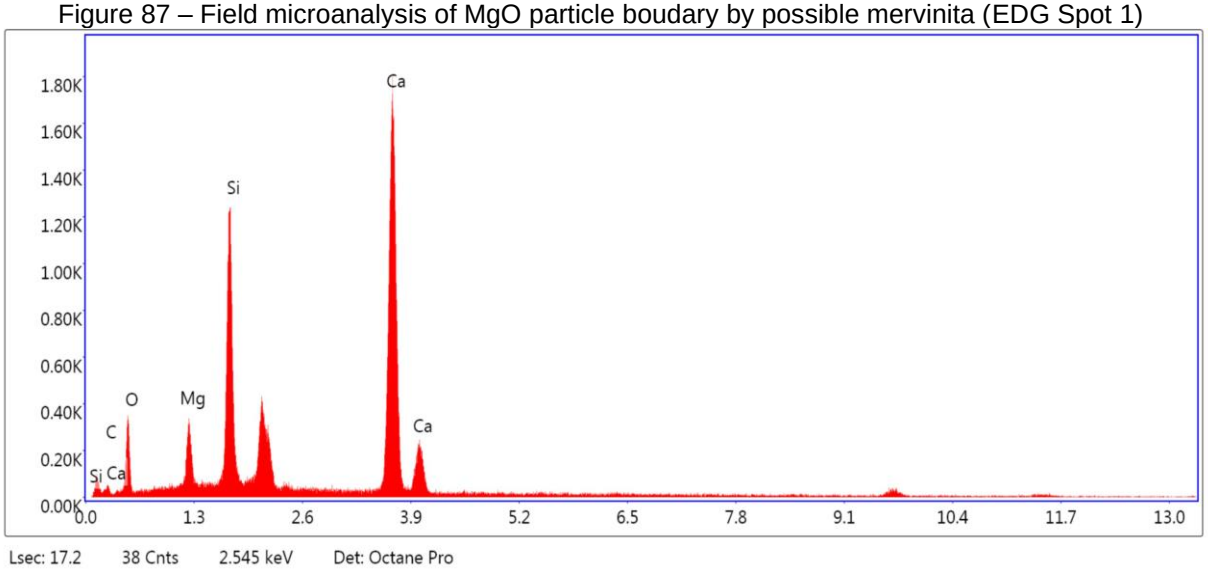

Source: Polytechnic School of USP (Department of Metallurgy and Materials).

Seeking evidence of the possible oxidation of carbon in the refractory structure and the possible wear mechanisms of the refractory trunnions, the microstructural analysis of the brick from supplier Y mentioned above was deepened (figure 88) showing the fronts of reactions that occur on the surface of the bricks.

Figure 88 – Field photomicrograph of the longitudinal section (hot face) of one of the bricks in the region of the LD trunnions after the end of the campaign showing the interaction between the refractory matrix, slag from the LD process and steel. The figure identifies steel (Area 1), high density MgO particle (Area 2), slag region (Spot 1, 2 and Area 3). Y supplier

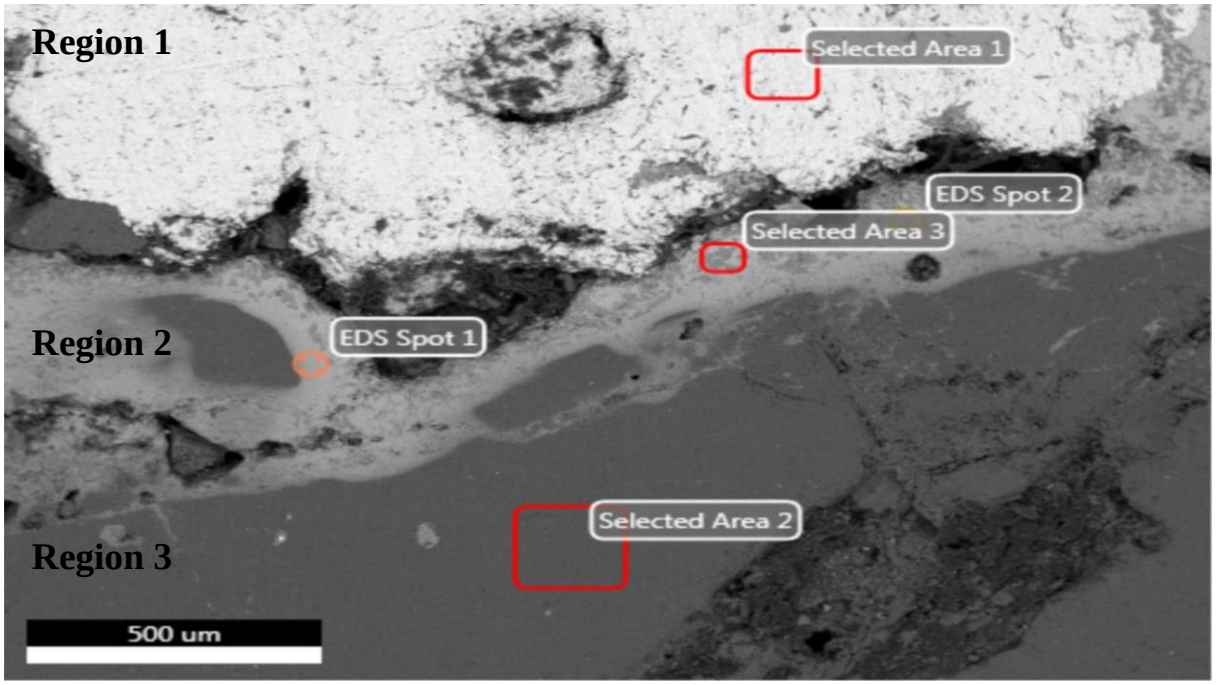

Source: Polytechnic School of USP (Department of Metallurgy and Materials).

In general, regions 1, 2 and 3 represent, respectively, a superficial layer of steel and slag, a transition region with LD slag and MgO grains being dissolved by the slag, and a region of well-preserved MgO grains. Figures 89, 90 and 91 are the respective field microanalyses of these regions confirming their compositions.

Region 1, in addition to not forming a physical protective structure, practically dissolved the refractory grains of the bricks.

In region 2, the process of corrosion and dissolution of the refractory matrix occurred intensely, especially in smaller grains (larger surface area) and generally of lower purity. The possibility of the presence of gaseous phases formed by reactions involving the carbon in the refractory matrix is visible due to the presence of pores and voids found in these two regions.

On the other hand, in region 3, the larger MgO crystals, probably of higher purity (Area 2) were little affected by the slag.

Figure 89 – Field microanalysis in the Area 1 of figure 88 (probable steel)

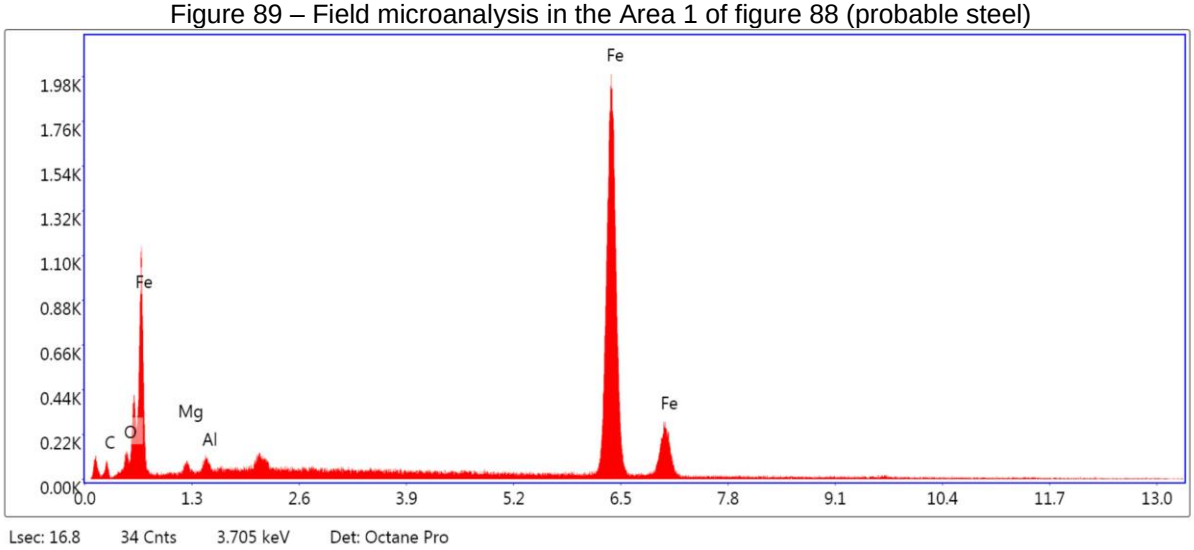

Source: Polytechnic School of USP (Department of Metallurgy and Materials).

Figure 90 – Field microanalysis in the Area 3 of figure 88 (probable LD slag)

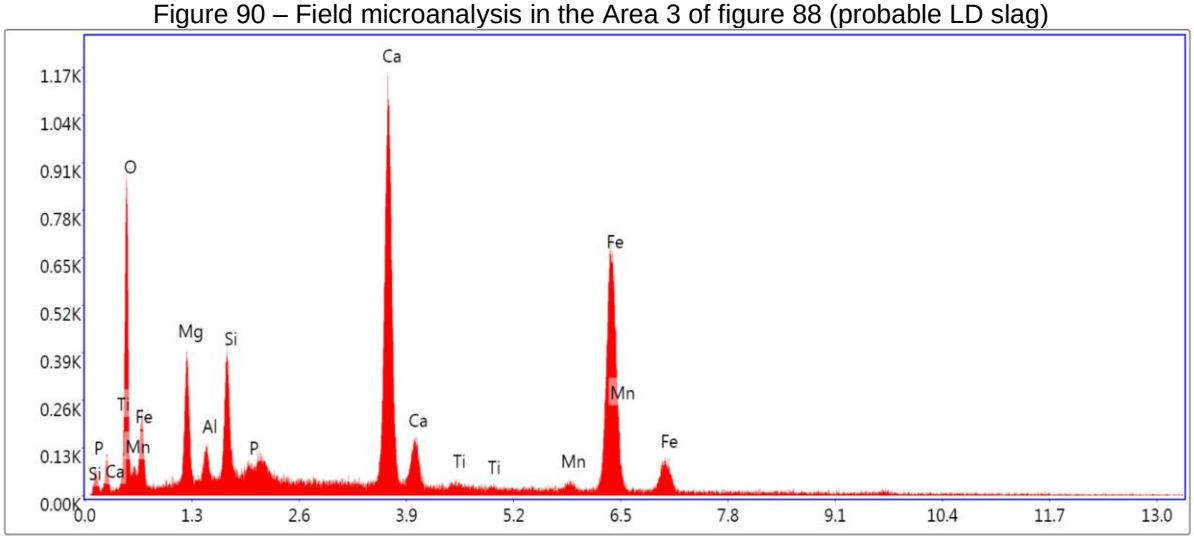

Source: Polytechnic School of USP (Department of Metallurgy and Materials).

Figure 91 – Field microanalysis in the Area 2 of figure 88 (MgO refractory grain)

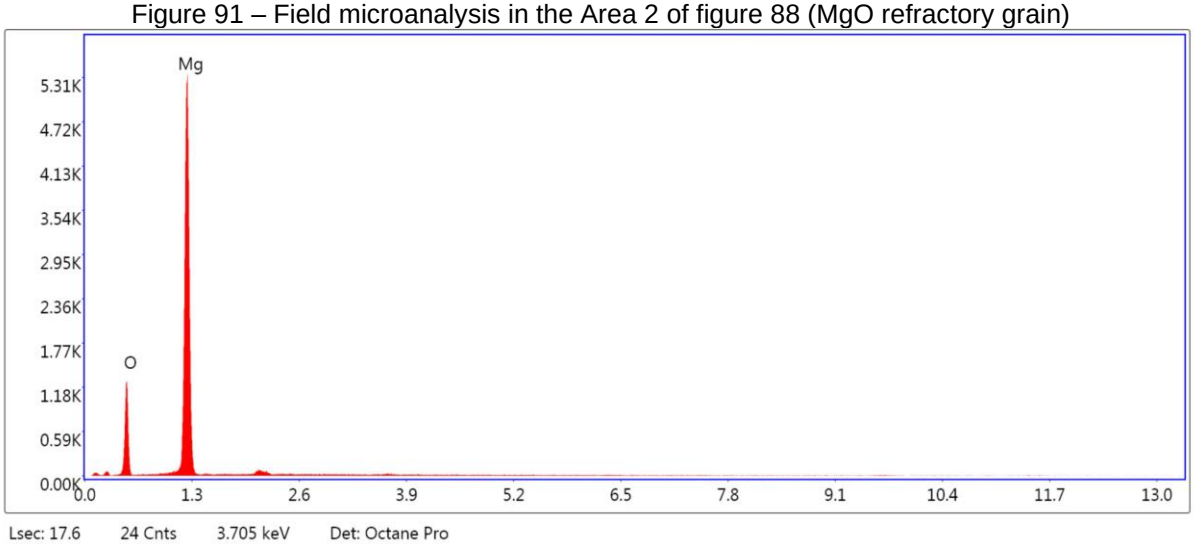

Source: Polytechnic School of USP (Department of Metallurgy and Materials).

It appears that the main characteristics of region 2 were the presence of pores, penetration of typical LD slag and refractory matrix corrosion, and the absence or small amount of graphite lamellae. Such mechanisms corroborate the statistical and SOM analyses, since to maintain low refractory wear rates as indicated in previous analyzes (statistics and SOM) it is important to maintain considerable levels of MgO saturation and slag viscosity (low levels of slag fluidizers), low levels of slag oxidation/reblowing and FeO, short process times and consequent interaction between refractories and slag, high percentages of Slag Splashing (covering the bricks with thick layers of slag saturated in MgO).

Furthermore, the non-observation of graphite lamellae in the superficial region of the hot face corroborate the previous hypothesis that oxidation occurs on the surface of the bricks, in a way that the movement of fluids ends up tearing the surface layers of the refractory weakened by decarburizing and increasing porosity and, consequently, making it difficult to identify the decarburization of the refractory surface. To prove this hypothesis, an analysis of the intermediate region (figures 92, 93 and 94) of the same brick sample from supplier Y was carried out (region before the hot face previously analyzed).

Figure 92 – Field photomicrograph of the longitudinal section (intermediate region) of one of the bricks in the LD trunnion region after the end of the campaign, showing probable graphite lamellae (Area 1 and Spot 3) in the refractory matrix. Supplier Y

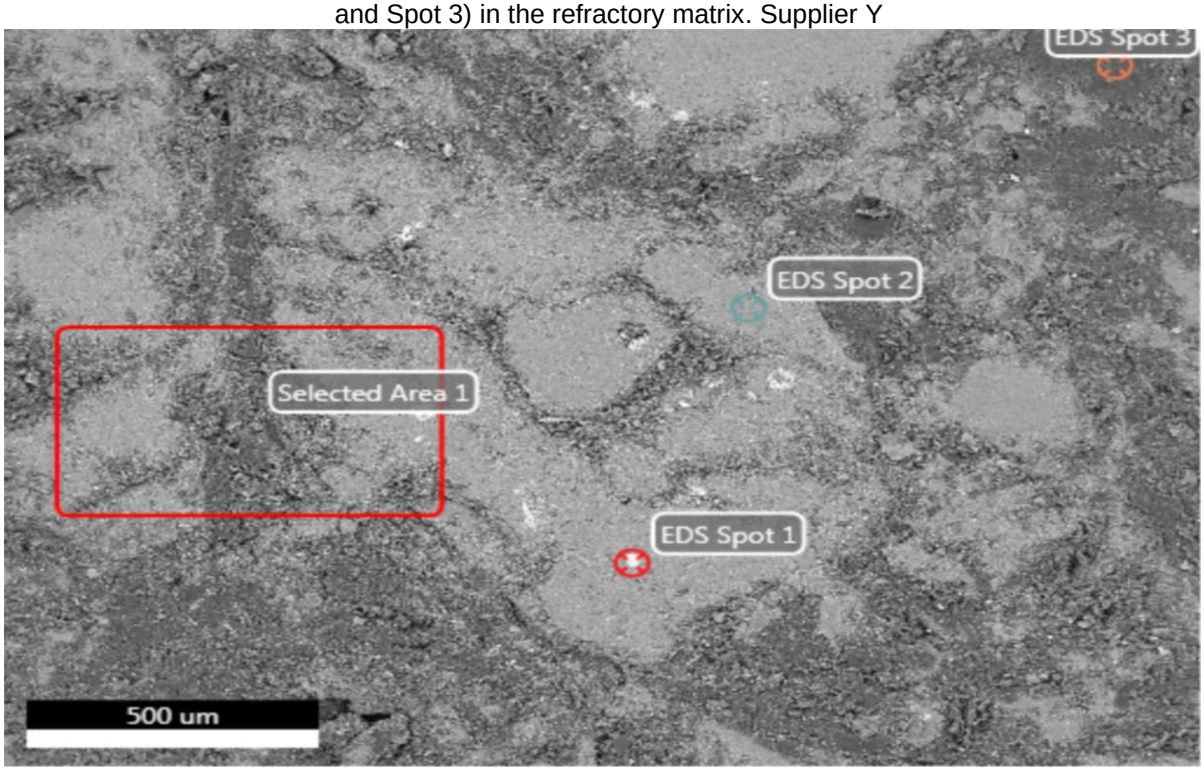

Source: Polytechnic School of USP (Department of Metallurgy and Materials).

Figure 93 – Field microanalysis of the Spot 3 region in the figure 92 (graphite lamella)

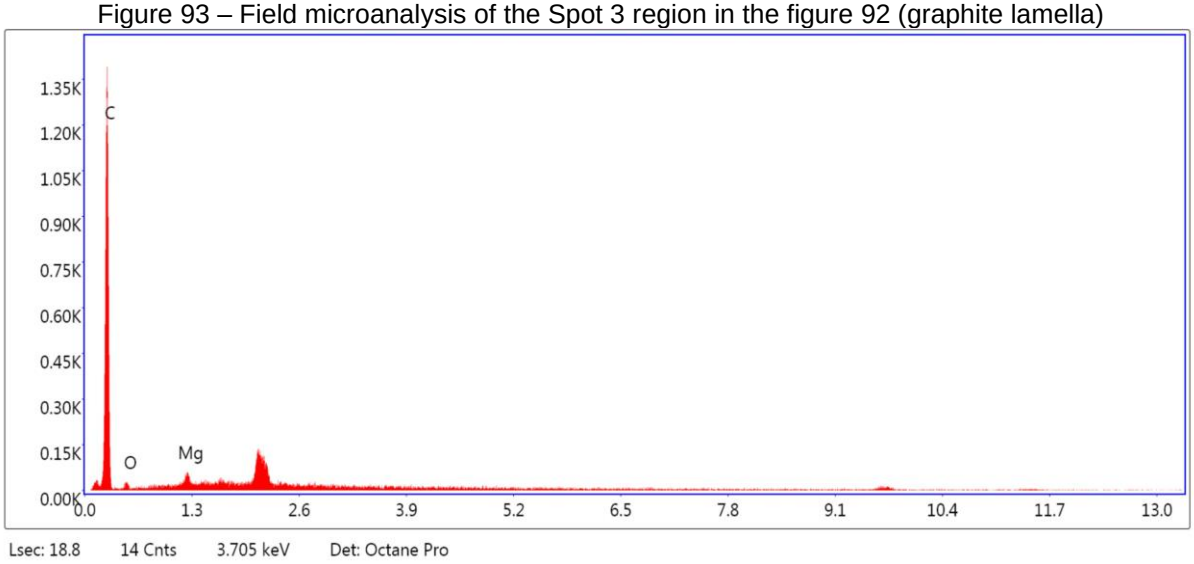

Source: Polytechnic School of USP (Department of Metallurgy and Materials).

Figure 94 – Field microanalysis of the Area 1 region in the figure 92 (MgO-C refractory matrix)

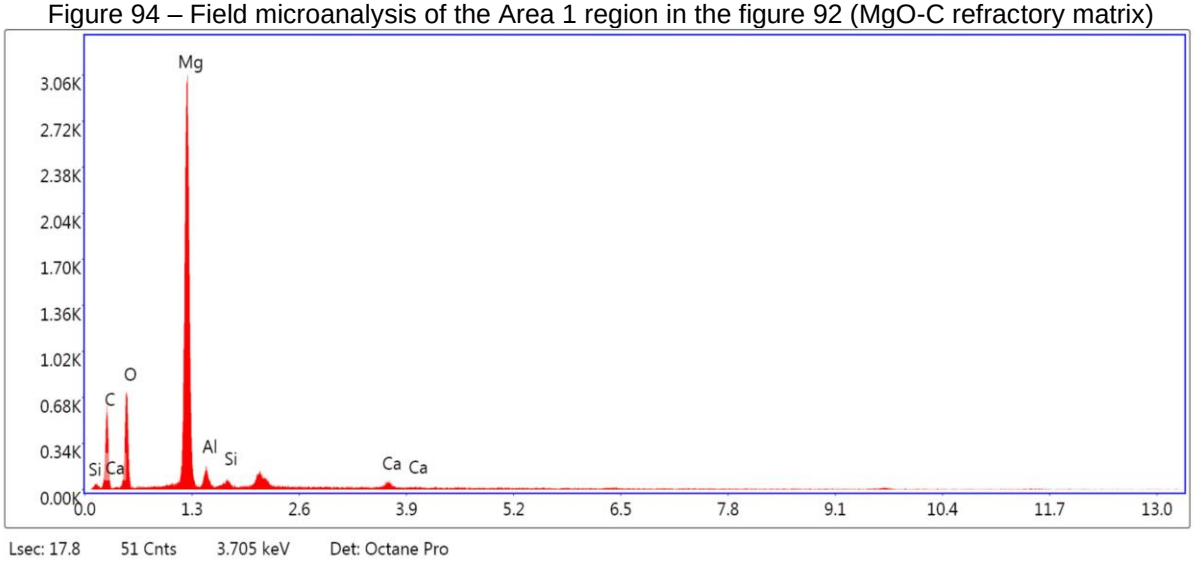

Source: Polytechnic School of USP (Department of Metallurgy and Materials).

In the intermediate region of the brick (figure 92), contrary to the superficial region, the presence of preserved graphite lamellae can be observed, leading to the hypothesis that this type of wear of the MgO-C bricks comes, in part, from the oxidation of the carbon in the surface layers of the brick, leading to changes in the surface (increased wettability and open porosity) in order to facilitate the penetration of slag and consequent corrosion and internal weakening of the refractory matrix. With the turbulence of the metallic bath during the oxygen blowing in the LD and the high temperatures, the already affected surface layer easily dissociates into the steel and slag, causing the internal surrounding aggregates to undergo the same process and, then, triggering the whole process of weathering the bricks.

This sequence of steps and wear mechanisms can be accelerated depending on the prevailing conditions and thermal cycles, that is, depending on the operating condition of stoppages and production pace of the LD furnace, the generation of thermomechanical cracks and consequent chipping of the bricks could accelerate or delay the cycle and wear steps described above.

The microanalysis of the transition regions of the hot face (figures 95, 96, 97 and 98) indicates the chemical gradient of the element magnesium and, consequently, of the compound MgO between these regions, indicating the possibility that it is one of the driving forces of the degradation process of the brick's MgO matrix (difference in MgO percentages between brick and LD process slag). This corroborates with the statistical and SOM analyzes in which the slag MgO saturation would be one of the most important variables in controlling the rate of wear of the bricks.

Figure 95 – Field photomicrograph of the longitudinal section (hot face) of one of the bricks in the region of the LD trunnions after the end of the campaign showing the interaction between the refractory matrix, slag from the LD process and steel. The figure identifies steel (Area 1), high density MgO particle (Area 2), slag region (Spot 1, 2 and Area 3). Supplier Y

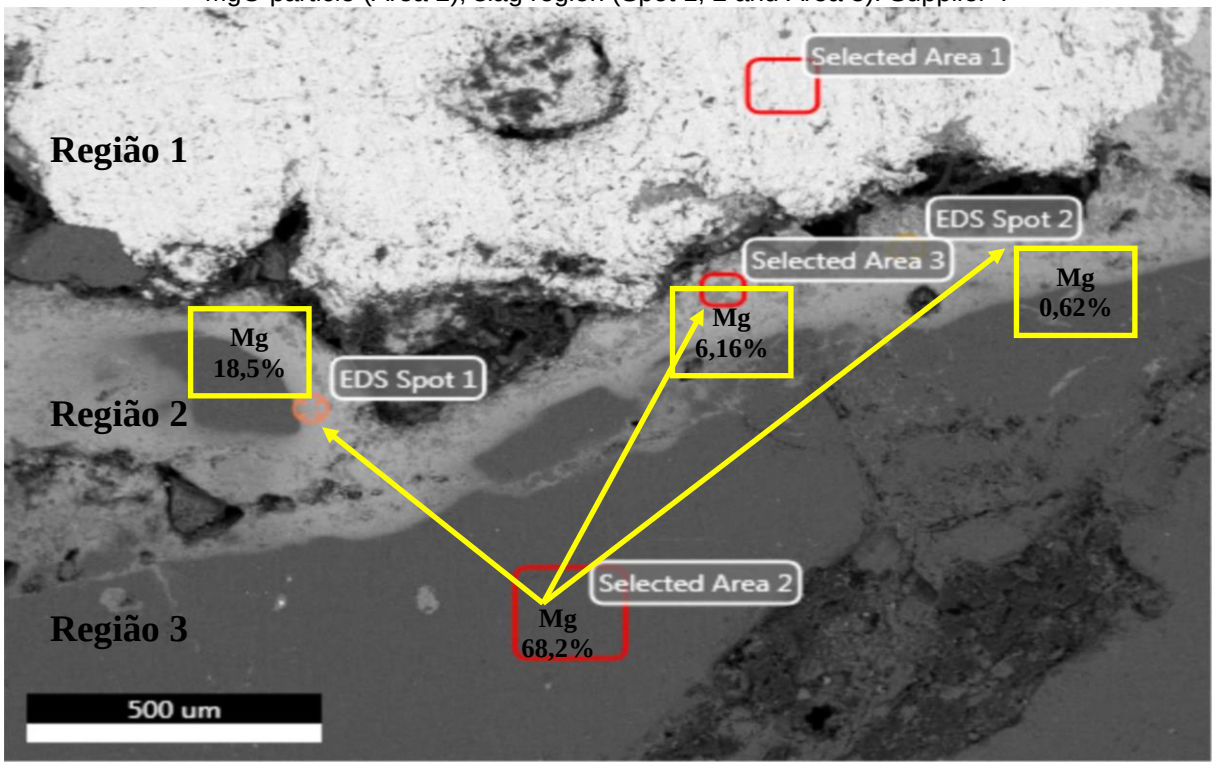

Source: Polytechnic School of USP (Department of Metallurgy and Materials).

The direct implication of these chemical gradients in the refractory wear process also corroborates with the SOM indications and the statistical analyzes of the highest consumption of MgO sources in the reduction and control of refractory wear.

Figure 96 – Field microanalysis of the Area 2 region in the figure 95 (MgO refractory particle)

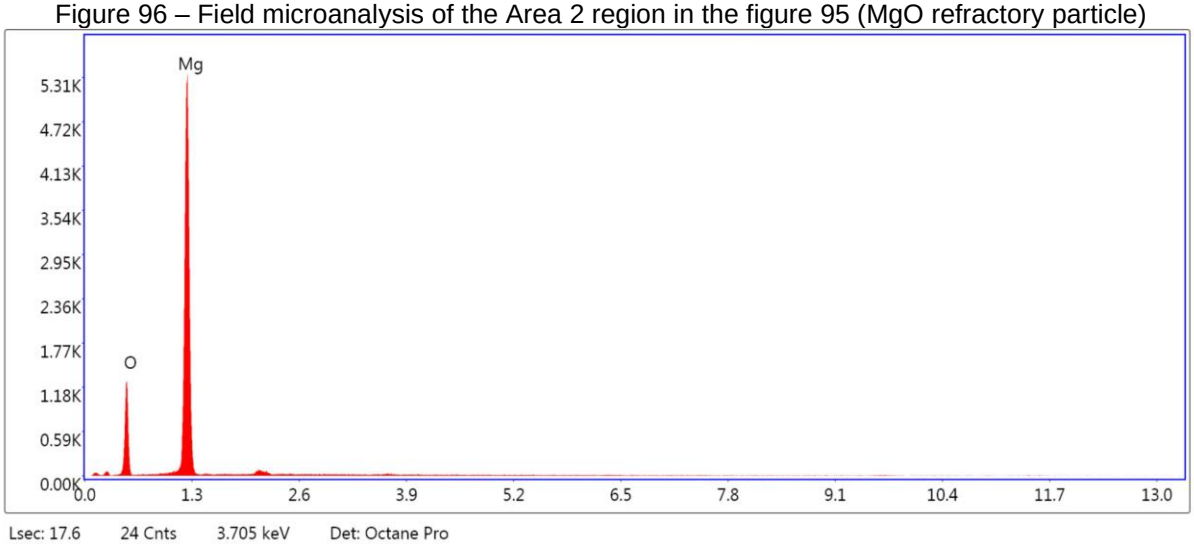

Source: Polytechnic School of USP (Department of Metallurgy and Materials).

Figure 97 – Field microanalysis of the Spot 1 region in the figure 95 (slag + steel + refractory)

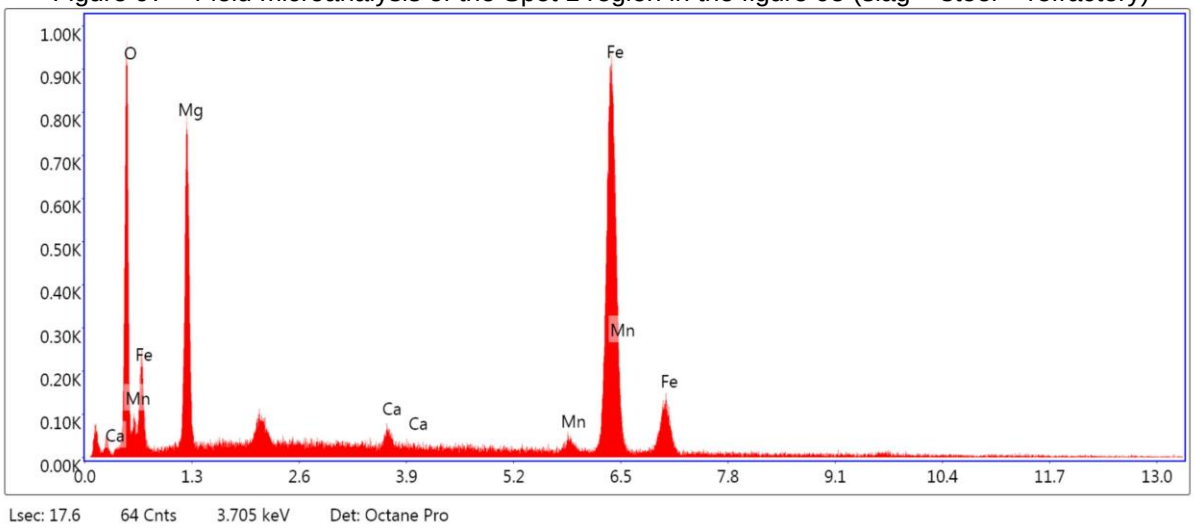

Source: Polytechnic School of USP (Department of Metallurgy and Materials).

Figure 98 – Field microanalysis of the Area 3 in the figure 95 (probable LD slag)

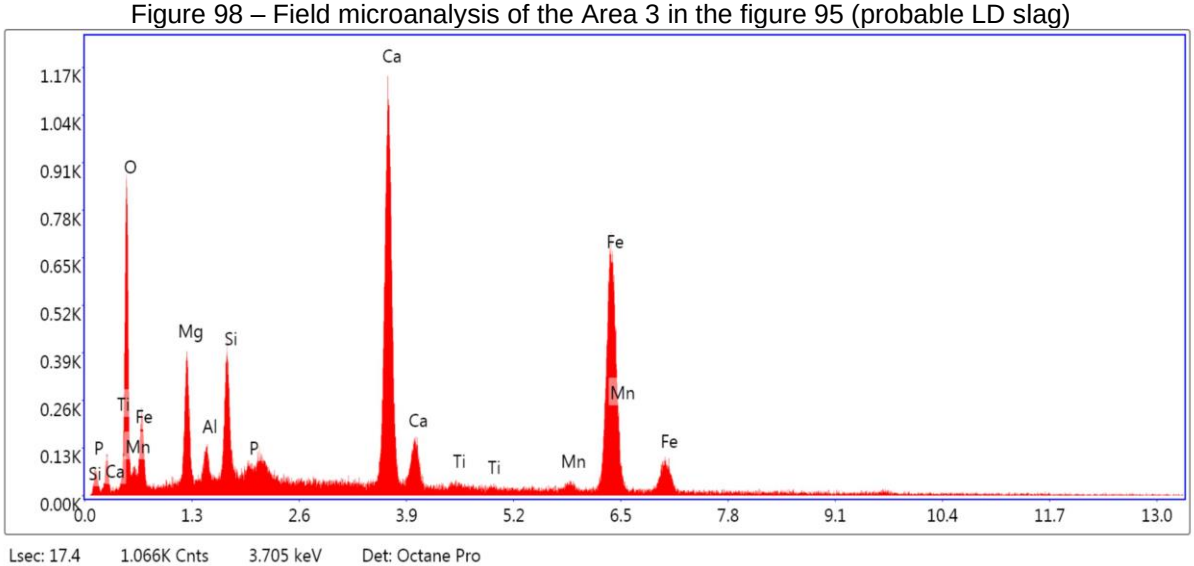

Source: Polytechnic School of USP (Department of Metallurgy and Materials).

The microanalyses performed above that indicated the presence of compounds from LD slag (Ca, Si, Fe, Mn, Mg, O, P) allow inferring the possibility of the presence of spinel iron ($MgFe_2O_4$). According to the literature, the compounds Al_2O_3, Cr_2O_3 and Fe_2O_3 are partially soluble in MgO at high temperatures, for example above 1000 °C. Once again, the results of the microanalyses corroborate the results of the static and SOM analyses, in which it is observed that the increase in Fe oxides in the slag, as a result of processes with high levels of oxidation, reblowing and dephosphorization, increase the refractory wear rate.

Therefore, it is possible to conclude that the periphery of the MgO particles is characterized by having a complex chemical composition so that it is possible to dissociate iron spinel (magnesium-ferrite: $MgFe_2O_4$) in a phase of low refractoriness composed of Ca, Si, Fe, Mn, Mg, O_2 and P.

Another important verification was the fact that in the superficial regions of the hot face, the presence of graphite lamellae was not observed. This may be an indication that carbon oxidation is intense in the surface layers of the brick, generating an increase in the porosity and wettability of the bricks. This would deteriorate the bond between the MgO aggregates and imply more intense corrosion of the refractory matrix, which together with the agitation of the metal bath would cause the dragging of the more superficial MgO particles. As the corrosive process occurs with greater intensity in smaller particles (greater surface area) and lower density (greater amount of pores), it is to be expected that issues related to the manufacture of refractory bricks can have a strong impact on the wear process, as these properties are achieved when working with raw materials of high purity and grain size.

The presence of the element Fe in metallic form close to the MgO grains also reinforces the hypothesis of the possibility of reduction of iron oxide in the slag by the carbon in the brick, which represents an important mechanism of corrosion by oxidation. Failure to observe graphite lamellae in regions close to the hot face and the formation of pores with possible gaseous phases lead to the hypothesis of carbon oxidation and formation of gases such as $CO_{(g)}$.

For the same brick sample from supplier Y indicated above, the analysis of the cold face region (figures 99, 100, 101 and 102) was carried out, in which precipitation was identified in the grain boundaries of MgO, the metals calcium (Ca), Aluminum (Al), silicon (Si) and iron (Fe) corroborating the hypothesis of the reduction of CaO

and SiO_2 by the carbon in the refractory structure, once again demonstrating the desirable use of high purity MgO aggregates with large grain size and high density to reduce refractory wear rate.

Figure 99 – Field photomicrograph of the longitudinal section (cold face) of one of the bricks in the region of the LD trunnions after the end of the campaign, showing the composition and different phases of the refractory matrix of the bricks. The figure identifies MgO particles (Areas 1 and 3), graphite lamella (Area 2), regions composed of a mixture of different components such as Ca, Si, Fe (Spots 1, 2, 3 and 4)

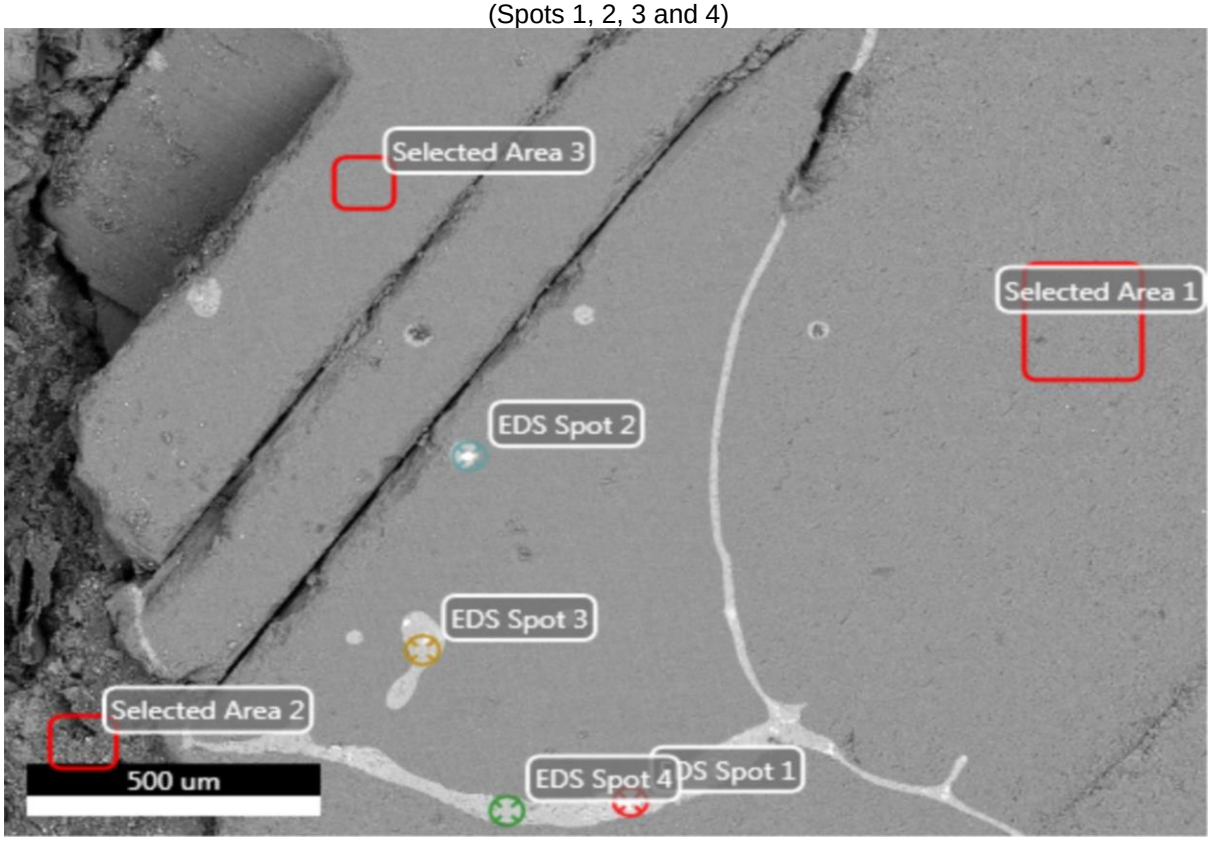

Source: Polytechnic School of USP (Department of Metallurgy and Materials).

Another hypothesis would be that precipitation may be accompanied by the formation of pores and voids due to reactions with carbon with formation of gaseous phases at the grain boundaries. In figure 99, it is possible to identify a cord (Spot 1 and 4) of this mixture of compounds in the grain boundaries of the MgO particles, weakening the refractory structure.

In addition, a probable graphite lamella was identified, which once again corroborates the thesis of carbon oxidation in the surface region of the hot face of the bricks, as opposed to their preservation in the internal regions of the bricks.

Figure 100 – Field microanalysis of the Area 1 in the figure 99 (MgO refractory grain)

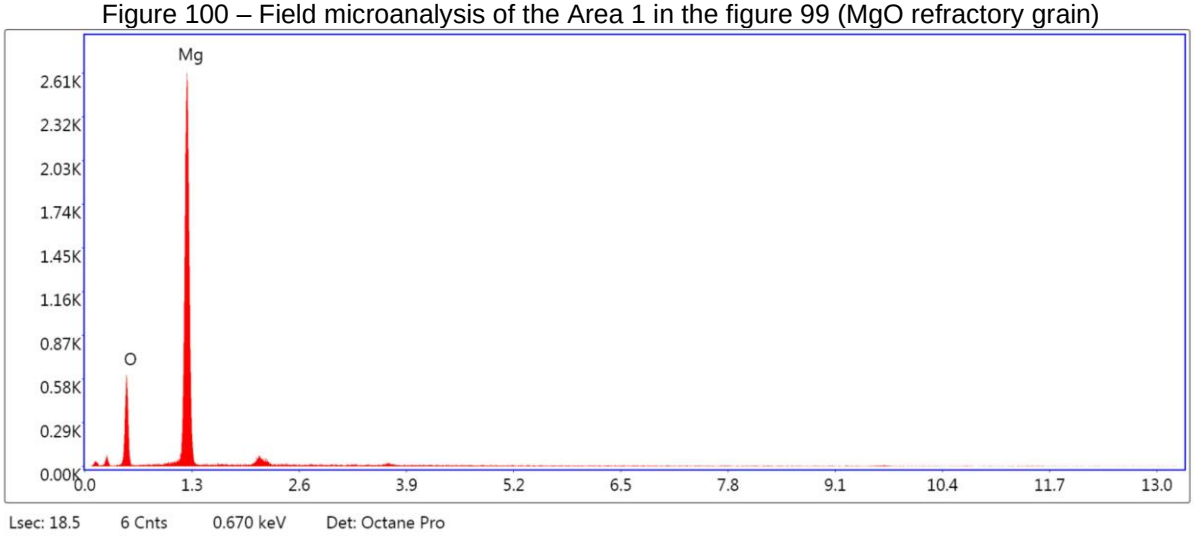

Source: Polytechnic School of USP (Department of Metallurgy and Materials).

Figure 101 – Field microanalysis of the Area 2 in the figure 99 (grafita + MgO grain + antioxidants)

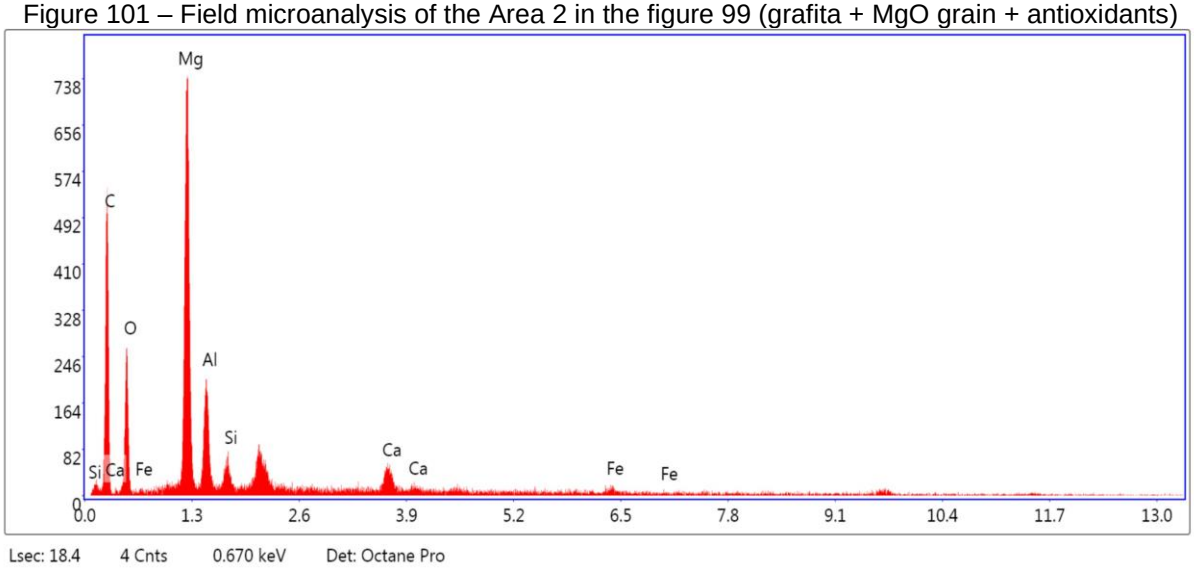

Source: Polytechnic School of USP (Department of Metallurgy and Materials).

Figure 102 – Field microanalysis of the boudaries/Spot 4 in the figure 99 (complex mix of Ca, Si, C)

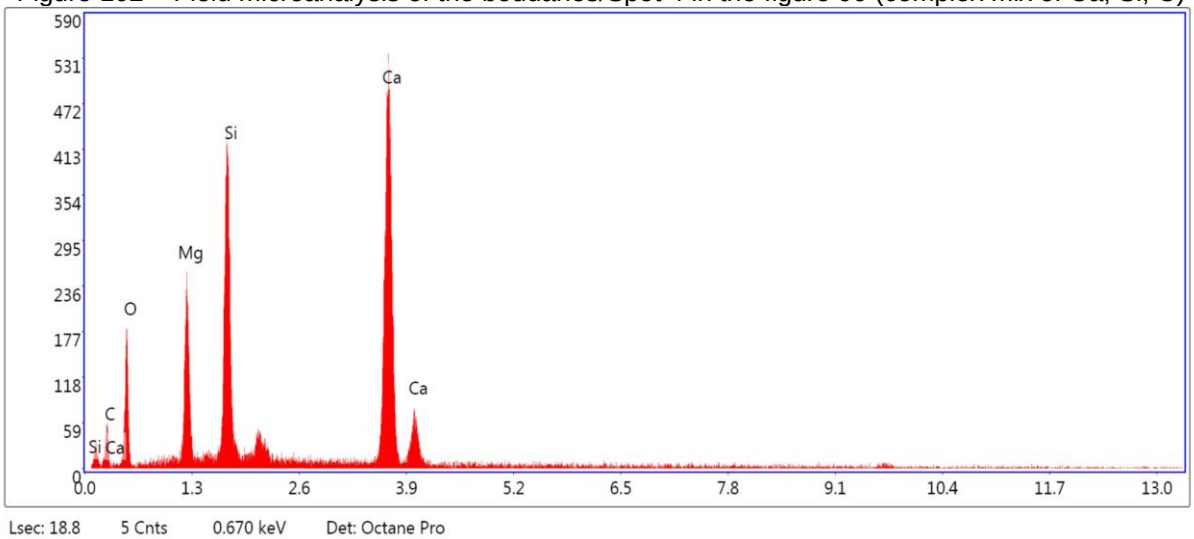

Source: Polytechnic School of USP (Department of Metallurgy and Materials).

Therefore, it appears that the results obtained from the post-mortem tests support and are consistent with the results obtained by statistical analysis and the SOM technique, which underlies the models proposed in the previous sections of this thesis. In addition, a possible descriptive model of the steps and phenomena that predominantly occur in the refractory wear of trunnions bricks can be described as follows:

1. Oxidation of carbon on the surface of the refractory brick (mainly by FeO from the slag, although those caused by other oxides such as MnO, by oxygen in the air in the furnace atmosphere, by oxygen from the blast lance and liquid steel are not excluded);
2. Increased wettability of the refractory surface (carbon oxidation with consequent change in surface tension) by slag, increased porosity and reduced mechanical strength of the refractory brick as a result of surface decarburization;
3. Penetration of slag and steel into the pores and grain boundaries of the refractory and consequent dissolution/corrosion of the refractory matrix (to a lesser or greater degree depending on the saturation of this slag in MgO and the levels of dissolved oxides);
4. Formation of phases of low refractoriness in the refractory matrix with consequent erosion of this affected zone due to the intense movement of fluids during the oxygen blow. In addition to matrix erosion, surrounding MgO particles are also stripped away by fluids.
5. All the steps above can be enhanced to a greater or lesser extent depending on fluctuations in process variables and thermomechanical cycles resulting from the various stops of the LD converter.

5 CONCLUSIONS

From the analyzes obtained by serial statistical analysis, multivariate statistics and SOM, it is concluded that it is possible to model the wear of the cylindrical region (trunnions) of the LD converter through these tools, and a deterministic model for predicting the wear rate refractory (and consequently the life of the LD converter), together with a proposal for a preponderant wear model and its stages, can be built and adjusted according to the analysis of process data and post-mortem of the bricks in the region considered. In addition, the comparative analysis of the results indicated that the SOM analysis technique can be used in the analysis of this type of system, being a more versatile and faster form of analysis for large volumes of data.

It can be concluded that the percentage contents of MgO, CaO and FeO in the process slag, the average amount of nepheline added in the heats, the amount of scrap charged in the metallic charge, the percentage of reblown heats and the volume of oxygen in the reblow, binary basicity, oxidation and temperature levels, process times and the rate of dephosphorization of the heats, as well as the percentage of heats with the Slag Splashing process performed were the most relevant process variables for the determination of the wear rate of the refractory bricks of the LD converter trunnion.

With regard to the SOM, it was verified the total possibility of applying this data analysis tool in the modeling of the refractory wear rate of the LD converters. The use of this tool brings flexibility and agility to systems that involve a large number of process and data variables. In addition, one notes the complementarity in the use of SOM in relation to classic statistical tools, being a way of evaluating systems in which only classic statistics would not be able to bring all the answers.

The deterministic multivariate equation of the refractory wear rate showed a way of acting and controlling the wear rate of the converter trunnion. Thus, it is possible to carry out a better operational management of the performance of the LD (scheduling of operational stoppages, refractory maintenance and production scheduling) and maintain greater operational safety through the predictability of refractory wear rate values. Campaign planning issues can also be better managed, such as budget construction, cost control, inventory management and refractory purchase, as it is possible to make more assertive forecasts regarding the life of the furnace.

Through post-mortem analyses, it was possible to propose a sequence of steps that describe the most likely behavior of the wear dynamics of the trunnions. Basically, the wear stage starts in refractory bricks with low slag coverage. These bricks are attacked by highly oxidized slag and steel, as well as oxygen from the LD furnace environment. In these cases, the carbon in the refractory structure is oxidized, forming gases and pores in the structure. The reduction of carbon increases the wettability of the refractory by the slag, causing penetration into the refractory matrix, where the MgO grains are dissolved by a slag rich in FeO. If the process times are high, the dissolution will be more intense. The increase in porosity, together with the dissolution of the MgO matrix, reduces the mechanical strength of the bricks. All this, together with the various situations of thermal cycling arising from the stages between charging and maintenance stops, generate the various wear phenomena such as erosion, dissolution, spalling, promoting the collapse of the refractory structure of the trunnion.

6 SUGGESTIONS FOR FUTURE WORKS

As a suggestion for future work in order to deepen studies and developments both in the subject of refractory wear in LD converters, and in the application of the SOM analysis tool in steelmaking shops, the following items are suggested:

1. Apply the SOM analysis to the other regions of the converter and check whether the refractory wear variables and phenomena are similar or different in relation to the trunnion;
2. Deepen the oxidation analysis of the surface carbon of the refractory bricks and understand the speed of erosion of the decarburized surface layer;
3. Evaluate how to degree the fluctuations of the process variables imply the speed of degradation of the refractory matrix and carbon oxidation;
4. Evaluate for different refractory designs the influence of these process variables on the wear rate;
5. Evaluate the degree of complementarity between classical statistical analysis and SOM in refractory wear analysis.

BIBLIOGRAPHIC REFERENCES[1]

ALAHAKOON, D.; HALGAMUGE, S. K.; SRINIVASAN, B. “Dynamic Self Organising Maps with Controlled Growth for Knowledge Discovery**”**. **IEEE transactions on Neural Networks**, v. 11, n. 3, p. 601-614, 2000.

ARAS *et al*. “The Kohonen network incorporating explicit statistics and its application to the travelling salesman problem”. **Neural Networks**, n. 12, p. 1273-1284, 1999.

ARAÚJO, L. A. **Manual de Siderurgia**. 2ª Edição, Brasil: Editora Arte e Ciência, v.1, 2009.

AUAD, M. V.; **Desenvolvimento de modelo para cálculo de adições no processo de slag splashing e slag coating de um basic oxygen furnace (BOF)**. 2018. 115 f. Brasil, Universidade Federal de Minas Gerais, Dissertação apresentada ao Programa de Pós-Graduação em Engenharia Metalúrgica, Materiais e Minas, 2018.

AUSTUDILLO, C. A.; OOMEEN, B. J. Imposing tree-based topologies onto self organizing maps. **Information Sciences**, v. 181, p. 3798–3815, 2011.

BARÃO, C. D. et. al. **Aciaria a Oxigênio**. Brasil, Associação Brasileira de Metalurgia e Materiais, Curso intitulado Aciaria a Oxigênio, 2011.

BARRON, M. A. et al. Influence of the slag density on the splashing process in a steelmaking converter. **ISRN Metallurgy**, Mexico, p. 1-6, 2014.

BARRON, M. A.; HILERIO, I. Computer simulation of slag splasing in a steelmaking conversor. **Proceedings of the World Congress in Computer Science**. Las Vegas: Computer Engeneering and Applied Computing. 2011.

BIERLEIN et al. Advanced methodologies for the analysis of databases of mineral deposits and major faults. **Australian Journal of Earth Sciences**, v. 55, p. 79–99, 2008.

BILGIÇ, M. Parameters effecting lifetime of refractory in steelmaking**.** Sweden, Department of Material Science and Engineering, 2005. 21 p.

BISHOP, C. M. “Neural Networks for Patters Recognition” Oxford University Press, 1995.

BLACKMORE, J.; MIILLULAINEN, R. “Visualizing High-Dimensional Structure with the Incremental Grid Growing Neural Network”. In: A. Prieditis and S. Russell (editors), Machine Learning: **Proceedings of the 12th International Conference** (ICML 95, Tahoe City, CA), San Francisco: Kaufmann, p. 55-63, 1995.

[1] De acordo com a Associação Brasileira de Normas Técnicas. NBR 6023.

BORGES, R. A. A. **Otimização do carregamento dos fornos de produção de aço (convetedores LD) minimizando o custo.** Monografia apresentada ao Curso de Especialização em Otimização de Sistemas Industriais do Departamento de Ciência da Computação do Instituto de Ciências Exatas da Universidade Federal de Minas Gerais, 2016. 92f.

BORZOV, D.; ULBRICHT, J.; SCHULLE, W. Technological and environrnental cornparison of different carbon-binders for MgO-C refractories. In.: **INTERNATIONAL COLLOQUIM ON REFRACTORIES**, Acchen, Germany, p. 50-52, 2001.

BUCHEBNER, R.; NEUBOECK, S. G. Carbon-bonding: A new rnilestone on low emission rnagnesia-carbon bricks. In.: Unified International Technical Conference on Refractories, 2001, **BIENNIAL WORLDWIDE CONGRESS**, 7, 2001, Unitecr'ol, 2001, Cancún. Proceedings of Mexico: Alafar, 2001. 1 CD-ROM.

BRIQUEU et al. Traitement des disgraphies a l'aide d'un reseau de neurons du type <carte auto-organizatrice> In: application a l'etude lithogique de la couche silteuse de Marcoule (Gard France), **C R Geoscience**, v. 334, p. 31-337, 2002.

BROWN, A. J.; WHITE, J. New generation refractory materials: Ceramic-Carbon Composites, **Met. Mater. (Inst. Met.)**, 1986, n.10, p. 632-639, 1986.

CARNEIRO et al. Semiautomated geologic mapping using self-organizing maps and airborne geophysics in the Brazilian Amazon**. Geophysics**, v.77, n.4, p.17–24, 2012.

CHAVES, A. J. M. **Avaliaçâo do desempenho operacional de um convertedor LD através do desenvolvimento do processo de sopro com lança de quatro furos.** Dissertação (mestrado) – Departamento de Engenharia Metalúrgica e de Minas, Universidade Federal de Minas Gerais, Belo Horizonte, 2006, 123 f.

CHENG, Y. "Convergence and Ordering of Kohone's Batch Map" **Neural Computation 9**, p. 1667-1676, 1997.

CHESTERS, J. H. Refractories production and properties. **London: The Institute of Materials**, 1993, 553 p.

CHIAVERINI, V. **Aços e ferros fundidos.** 7ª Edição. São Paulo: Associação Brasileira de Metalurgia e Materiais, 2005, 599 p.

CHO, D. S. **Otimizaçâo dos processos sinterização, alto forno, aciária LD através da programação linear.** Dissertação (mestrado) – Departamento de Engenharia elétrica, Universidade Estadual de Campinas, Campinas, 1982.

CHO, D. S. "Self-Organizing Map with Dynamical Node Spliting: Application to Handwritten Digit Recognition". **Neural Computation 9**, p. 1345-1355, 1997.

COSTA, J. A. F. **"Classificação Automática e Análise de Dados por Redes Neurais Auto-Organizaveis".** Tese de Doutorado. Universidade Estadual de Campinas (UNICAMP), Faculdade de Engenharia Elétrica e Computação, 1999.

COOPER, C. F. Graphite containing refractories. **Refract. J.**, v.55, n.6, p.11-21, 1980.

DENG, T. F.; DU, S. C. Dissolution mechanism of dolomite in converter slag at 1873 K. 2012. **Institute of Material, Minerals and Mining**. London: Maney. 2014. p. 123-129.

DUDA, R. O., HART, P. E., STORK, D. G., "Pattern Classification". 2nd edition, **Wiley Interscience**, 2000.

Erwin et al. "Self-Organizing Maps: Ordering, Convergence Properties and Energy Functions". **Biological Cybernetics 67**, p. 47-55, 1992.

EVERETTI, B. "Cluster Analysis" 3td Edition. London. **Edward Arnould**; New York: John Wiley, 1993.

EUROPEAN REFRACTORIES PRODUCERS' FEDERATION, **Refractory Ceramics and Industrial Minerals are Critical for European Industry.** Bruxelles, May. 2009.

FRASER, S. J.; DICKSON, B. L. A new method for data integration and integrated data interpretation: Self Organising Maps**.** In **"Proceedings of Exploration 07**: Fifth Decennial International Conference on Mineral Exploration" edited by B. Milkereit, p. 907-910,2007.

FREITAS, C. M. M.; **Caracterização e desenvolvimento de microestrutura de matrizes de concretos refratários de baixo teor de cimento.** Dissertação de Mestrado Apresentada ao Curso de Pós-graduação em Engenharia Metalúrgica e de Minas da Universidade Federal de Minas Gerais. Belo Horizonte. 1993.

FRITZKE, B. "Unsupervised Clustering Growing Cell Structures". In: **Proceedings of the International Joint-Conference on Neural Networks**, Seattle, 1991.

GARCIA-BERRO, E.; SANTIAGO TORRES, S.; ISERN, J. Using selforganizing maps to identify potential halo white dwarfs, **Neural Networks**, v.16, p.405-410, 2003.

GARDZIELLA, A.; SUREN, J. Phenolic resins as irnpregnating agents for refractories - present state of developrnent. In.: **Proceeding of International Technical Conference on Refractories**, 1997, New Orleans, EUA, p. 975-998.

GONÇALVEZ, W. M. **Adequação do processo de fabricação de aço LD, utilizando ferro-gusa líquido com baixo teor de silício.** Dissertação (mestrado) – Departamento de Engenharia Metalúrgica e de Minas, Universidade Federal de Minas Gerais, Belo Horizonte, 2005, 87 f.

HAN, J; KAMBER, M.; PEI, J. Data Mining: Concepts and Techniques. 3ª Edição, USA: Elsevier, 2012.

HULLE, M. M. V. "Faithful Representation and Topographic Maps: from Distortion to Information-Based Self-Organization" **John Wiley & Sons**, 2000.

JAIN, A. K.; DUBES, R. C. “Algorithms for Clusters Data” **Printice Hall**. Englewwod Cliffs, NJ, 1988.

JAIN at al. “Data Clustering: A Review”. In: **ACM Computing Surveys**, v. 31, n. 3, p. 264-323, 1999.

JANSEN, H. GROßE DALDRUP, H., Refractory Wear in Steelmaking Processes, **Proc. AISTech 2005 Iron & Steel Technology Conference and Exposition**, Charlotte, NC, USA, p. 9-12, 2005.

JANSEN, H.; DALDRUP, H. G. Developments of refractory linings for basic oxygen fumace in Germany. **ISSTech 2003 Conference Proceedings**, p. 307-319, 2003.

Japão. **The Technical Association of Refractories**, Refractories Handbook. 10th ed.:1998. (ISBN 4-925133-01-2).

ICHIKAWA, K.; NISHIO, H.; HOSHIYAMA, Y. Oxidation test of MgO-C bricks. **Taikabutsu Overseas**, v. 14, n. 1, p. 13-24, 1994.

ICHIKAWA, K.; NISHIO, H.; NOMURA, O.; HOSHIYAMA, Y. Suppression effects of aluminurn on oxidation of MgO-C bricks. **Taikabutsu Overseas**, v. 15, n. 2, p. 21-24,1995.

KANG, Y.; MORITA, K. Thermal conductivity of the CaO-Al_2O_3-SiO_2 system. ISU International, v. 46, p. 420-426, 2006.

KANNO K.; KIKE N.; KORAI Y.; MOCHIDA 1.; KAMATSU M. Mesophase pitch andphenolic resin blend as binders for rnagnesia-graphite bricks. **Carbon**, v.37, p. 195-201,1999.

KAWASHIMA, H.; ANEZAKI, S.; YAGI, S.; TAKEHARA, S.; MIYOSHI, S.; FUSHII, Y.; MATSUDA, M. Brick structure of BOF and stress analysis. **Shinagawa Technical Report**, v. 33, p. 103-122,1990.

KASKI, S.; KANGAS, J.; KOHONEN, T. Bibliography of selforganizing map (SOM) papers: 1981-1997, **Neural Computing Surveys**, v.1, p.102-350, 1998.

KASKI, S.; KRISTA, L. “Comparing Self-Organizing Maps”. **Proceedings of International Conference on Artificial Neural Networks (ICANN’96)**. Lecture notes in Computer Science v.1112, Springer, Berlin, p. 809-814, 1996.

KOHONEN, T. Self-organizing maps, third extended edition, springer series. In: **Information Sciences**, Springer: Berlin, Heidelberg, New York, v. 30, 2001.

KOHONEN, T. “Self-organizing maps**”, Series in Information Sciences**, v. 30, 2nd Edition. Springer-Verlag, Heiderbelg, 1997.

KOHONEN, T. “Analysis of a Simple Self-Organizing Process”. **Biological Cybernetics 44**, p. 135-140, 1982

LENZ e SILVA, G. F. B. **Introdução à siderurgia, cap. 9 – refratários para siderurgia**. ABM Associação Brasileira de Metalurgia, Materiais e Mineração, 2007. 428 p. Org. por Marcelo B. Mourão.

LEE, W. E. Theory, Experiment and Practice of Slag Attack of Refractories. Tehran International Conference on Refractories. Tehran: Departament of Materials, University of Sheffield, UK, p. 13-27, 2004.

LI, X.; RIGAUD, M.; PALCO, S. Oxidation kinetics of graphite phase in magnesia-carbon refractories. **J. Am. Ceram. Soe**., v. 78, n. 4, p. 965-971, 1995.

MARTINETZ, T.; SCHULTEN, K. "A Neural Gas Network Learns Topologies". **Elsevier Science Publishers**, Amsterdam, p. 397-402, 1991.

MAIA, B. T. **Efeito da configuraçâo do bico da lança na interaçâo jato-banho metàlico em convertedor LD**. Dissertação (mestrado) – Departamento de Engenharia Metalúrgica e de Minas, Universidade Federal de Minas Gerais, Belo Horizonte, 2007.

MALYNOWSKYJ, A. Altura:19.05cm. Largura:14.14cm. 1 desenho, color. Figura apresentada no Curso de Fabricação de Aço em Forno Básico a Oxigênio. 2004.

MALYNOWSKY, A.; MAIA, B. T.; LIMA, H. Desafios para melhorar a produtividade no convertedor LD. In: **WORKSHOP DESAFIOS PARA MELHORAR A PRODUTIVIDADE NO CONVERTEDOR LD,** Belo Horizonte, Brasil, 2022.

MERJA, O., SAMUEL, K., TEUVO K., Bibliography of self-organizing map (SOM) papers: 1998–2001 addendum, Neural Computing Surveys 3 (2003) 1–156.

MICHALSK, R. S. et al. "Machine Learning and Data Mining. Methods and Applications". John Wiley & Sons 1998

MILLS, K. C. et al. A Review of Slag Splashing. **Iron and Steel Institute of Japan**, Tokyo, v. 45, n. 5, p. 619-633, January 2005.

MONTGOMERY, D. C. Design and Analysis of Experiments. 4th Ed. John Wiley & Sons, New York, 1997.

MONTGOMERY, D. C.; RUNGER, G.C. Applied Statistics and Probability for Engineers. 5th Ed. John Wiley & Sons, New York, 2011.

MUNDIM, M. J., Introdução. In: ETRUSCO, G. S. P., SIGWALT, J. F. G., MUNDIM, M. J., CHAVES, C. A., **Curso sobre Aciaria LD**. São Paulo. Associação Brasileira de Metais, 1991, Cap. 1.

NGUYEN, T. T. *et al*. Clustering spatio–seasonal hydrogeochemical data using self-organizing maps for groundwater quality assessment in the Red River Delta, Vietnam. **Journal of Hydrology** 522, p. 661-673, 2015.

PENN, B.S. Using Self-Organizing maps to visualize highdimensional data. **Computers and Geosciences**, v.31, p.531-544, 2005.

POLLA, M.; HONKELA, T.; KOHONEN, T. Bibliography of self-organizing map (SOM) papers: 2002–2005 addendum, **Neural Computing Surveys**, forthcoming, 2007.

PRETORIUS, E. B.; CARLISLE, R. C. Foamy Slag Fundamentals and their Practical Application to Electric Furnace Steelmaking. 1998 Eletric Arc Furnace Conference. New Orleans: Iron and Steelmaker, p. 79-88, 1999.

PRUDENTE, R; FERA, S.; V ALENTINI, R. Influence of slag composition on K-OBM lining life: the case of high $Ti0_2$. In.: 5th Eurpean Oxygen Steelmaking Conference, 2006, EOSC 2006, 2006, Aachen. **Proceedings of Aachen**: 2006. p. 242-246.

QUINTELA, M. A.; **Caracterização de cerâmicas refratárias para panela de aço.** Brasil, Universidade Federal de São Carlos, Dissertação apresentada ao Programa de Pós-Graduação em Ciência e Engenharia de Materiais, 2003.

QUINTELA, M. A; SANTOS, F. D.; PESSOA, C. A.; RODRIGUES, J. A.;PANDOLFELLI, V. C. Refractories selection for steel ladles. In.: **Unified International Technical Conference on Refractories**, 2005.

QUINTELA, M. A.; PESSOA, C. A.; SALGADO, A. P. Análise de desagaste para convertedor. **Tecnol. Mater. Miner**., São Paulo, v. 6, n.1, p. 36 – 40, 2009.

QUINTELA, M. A; PESSOA, C. A; RODRIGUES, J. A.; PANDOLFELLI, V. C.,RODRIGUES, J. A Refratários para panelas de aço - Caracterísiticas e tendências. IH Encontro de Refrataristas e Usuários de Refratários - ABC, Belo Horizonte, p. 3-16, 2003.

RAAD, H. J.; **Influência das condições de mistura e moldagem na permeabilidade de concretos refratários aluminosos.** Brasil, Universidade Federal de Minas Gerais, Dissertação apresentada ao Programa de Pós-Graduação em Construção Civil, 2008.

RIAZ, S.; MILLS, K. C.; BAIN, K. Experimental examination of slag/refractory interface. **ISIJ International**, v. 29, n. 2, p. 107-113, June 2002.

RIGAUD, M.; BOMBARD, P.; XIANGMIN, L.; BERTRAND, G. Phase evolution in various carbon-bonded basic refractories. In.: Unified International Technical Conference on Refractories, 1993, Biennial Worldwide Congress, 3,1993, Unitecr'93, 1993, São Paulo. **Proceedings of Brazil**: Alafar, 1993. p. 360-371.

ROUTSCHKA, G. (Ed.). **Pocket manual refractory materials**. 2nd Ed. Germany, 2004. 512 p.

SAKANO, Y.; TAKAHASHI, H. **Outlook for the refractories industry in Japan**, Bull. Am. Ceram. Soc., 1988, v.67, n.7, p. 1164 -1175.

SARKAR, R. **Refractory technology: Fundamentals and applications**. 1. ed. CRC Press, 2016. 314 p. ISBN 9781315368054. Disponıvel em: ⟨https://doi.org/10.1201/9781315368054⟩.

SVENSÉN, J. F. M. **GTM: The generative topographic mapping**. PhD Thesis, Aston University, April 1998.

STRECKER, U.; UDEN, R. Data mining of poststack seismic attribute volumes using Kohonen self-organizing maps, **The Leading Edge**, p.1032-1036, October, 2002.

TAFFIN, C.; POIRIER, J. The behaviour of metal additives in MgO-C and Al_20_3-C refractories. **Interceram**, v. 43, n. 5, p. 354-358, 1994.

TAKANAGA, S. Wear of magnesia-carbon bricks in BOF. **Taikabutsu Overseas**, v. 13, n.4, p. 8-14, 1993.

TAKEDA, K.; NONOBE, K.; TAKANAGA, S.; TAKAHASHI. Corrosion mechanism of magnesia-carbon brick by CaO-Si02-Fe203 slag. **Journal of the Technical Association of Refractories**, v. 21, n. 1, p. 51-56, 2001.

TAKEUCHI, K.; YOSHIDA, S.; TSUBOI, S. Gas phase oxidation of MgO-C bricks. **Journal of the Technical Association of Refractories**, v. 23, n. 4, p. 276-279, 2003.

TORITANI, H; KAWAKAMI, T.; TAKAHASHI, H.; TSUCHIYA, L; ISHII, H. Effect of metallic additives on the oxidation-reduction reaction of magnesia-carbon brick. **Taikabutsu Overseas**, v. 5, n. 1, p. 21-27, 1985.

TROIANO, M. et al. Wall effects in entrained particle-laden flows: The role of particle stickness on solid segregation and built-up of wall deposits. **Powder Technology**, v. 266, p. 282-291, June 2014.

TRIOLA, M. F. Introdução à Estatística. 7ª Ed. LTC – Livros Técnicos e Científicos S.A. Rio de Janeiro, 1999.

TURKDOGAN, E. T.; FRUEHAN, R. J. Fundamentals of Iron and Steelmaking-Chapter 2. In: FRUEHAN, R. J. Book the Making Shaping and Treating of Steel 11th Edition. Pittsburg: **The AISE Steel Funadation**, v. 1, p. 13-157,1999.

ULTSCH, A. U-matrix: A tool to visualize clusters in high dimensional data: University of Marburg, Department of Computer Science, **Technical Report**, v.36, n.12, 1993.

ULTSCH, A; SIEMON, H. “Exploratory Data Analysis: Using Kohonen’s Networks on Transputers”. **Technical Report** 329, University of Dortmund, Dortmund, Germany, 1989.

ULTSCH, A.; VETTER, C. Self-organising feature maps versus statistical clustering a benchmark: Technical Report, Dept. of Mathematics and Computer Science, University of Marburg, Germany, 1994, n.9.

VATANEN, T. *at al.* Self-Organization and missing values in SON and GMT. Neurocomputing 147, p. 60-70, 2015.

ZHANG, S.; MARRIOTT, N. J.; LEE, W. E. Thermochemistry and microstructure of MgO-C refractories containing various antioxidants. **Journal of the European Ceramic Society**,21, p.l037-1047,2001.

ZHANG, S.; MARRIOTT, N. J.; LEE, W. E. Influence of additives on corrosion resistance and corroded microstructures of MgO-C refractories. **Journal of the European Ceramic Society**, 21, p. 2393-2405, 2001.

ZUCHINI, M. H. **Aplicações de Mapas Auto-Organizáveis em Mineração de Dados e Recuperação de Informação.** Brasil, Universidade Estadual de Campinas, Dissertação apresentada ao Programa de Pós-Graduação da Faculdade de Engenharia Elétrica e Computação, 2003.

YAMAGUCHI, A. Consideration on improving corrosion-resistance of refractories. **Taikabutsu Overseas**, v. 13, n. 4, p. 3-7, 1993.

YAMAGUCHI, A. Consideration on improving corrosion-resistance of refractories. **Taikabutsu Overseas**, v. 4, n. 1, p. 32-37,1984.

YAMAGUCHI, A. Thermochemical analysis for reaction processes of aluminium and aluminium-compounds in carbon-containing refractories. **Taikabutsu Overseas**, v. 7, n. 2, p. 11-16, 1987.

YAMAGUCHI, A. Studies of new refractory components. **Shinagawa Technical Report**, v. 49, p. 1-12, 2006.

YAMAGUCHI, A; NAKANO, Y.; WANG, T. The effect and behaviour of AI-B-C system antioxidants added to MgO-C refractories. **Canadian Metallurgical Quarterly**, 39, p. 381-386, 2000.

YAMAGUCHI, A.; ZANG, S. Behaviours of various kinds of carbon in carbon-containing refractories. In: **International Symposiun on Advances in Refractories for the Metallurgical Industries II**, Quebec, Canada, p. 59-71, 1996.

YAMAGUCHI, A.; KUN, Y. J. Formation and expansion of open pore in carbon-containing refractories and their prevention. **Taikabutsu Overseas**, v. 14, n. 1, p. 20-25, 1994.

YAMAMURA, T.; NOMURA, O.; TADA, H.; TORIGOE, A Lower carbon containing MgO-C bricks with spalling resistance. **Shinagawa Technical Report**, v.39, p. 57-64,1996.

YUAN, Z. et al. Wettability between Molten Slags and MgO-C Refractories fo the Slag Splashing Process**. ISIJ International**, v. 53, n. 4, p. 598-602, January 2013.

WATANABE, A; TAKAHASm, H.; TAKANAGA, S.; GOTO, N.; ANAN, K.; UCHIDA, M. Behavior of different metaIs added to MgO-C bricks. **Taikabutsu Overseas**, v. 7, n. 2, p. 17-23, 1987.

WILLIAMS P.; TAYLOR D.; LEONI, H. Advanced phenolic resin binder systerns for rnagnesia-carbon refractories. In.: **Proceeding of International Technical Conference on Refractories**, São Paulo, Brazil, p. 347-359, 1993.

YAMAGUCHI, A.; ZANG, S. Behaviours of various kinds of carbon in carbon-containing refractories. In: **International Symposiun on Advances in Refractories for the Metallurgical Industries II**, Quebec, Canada, p. 59-71, 1996.

APPENDIX A – Criteria for normality, homoscedasticity and Independence of the residual of equation 16

Figure 103 – Tests for analysis of confirmation of normality, homoscedasticity and Independence of the residues of equation 16

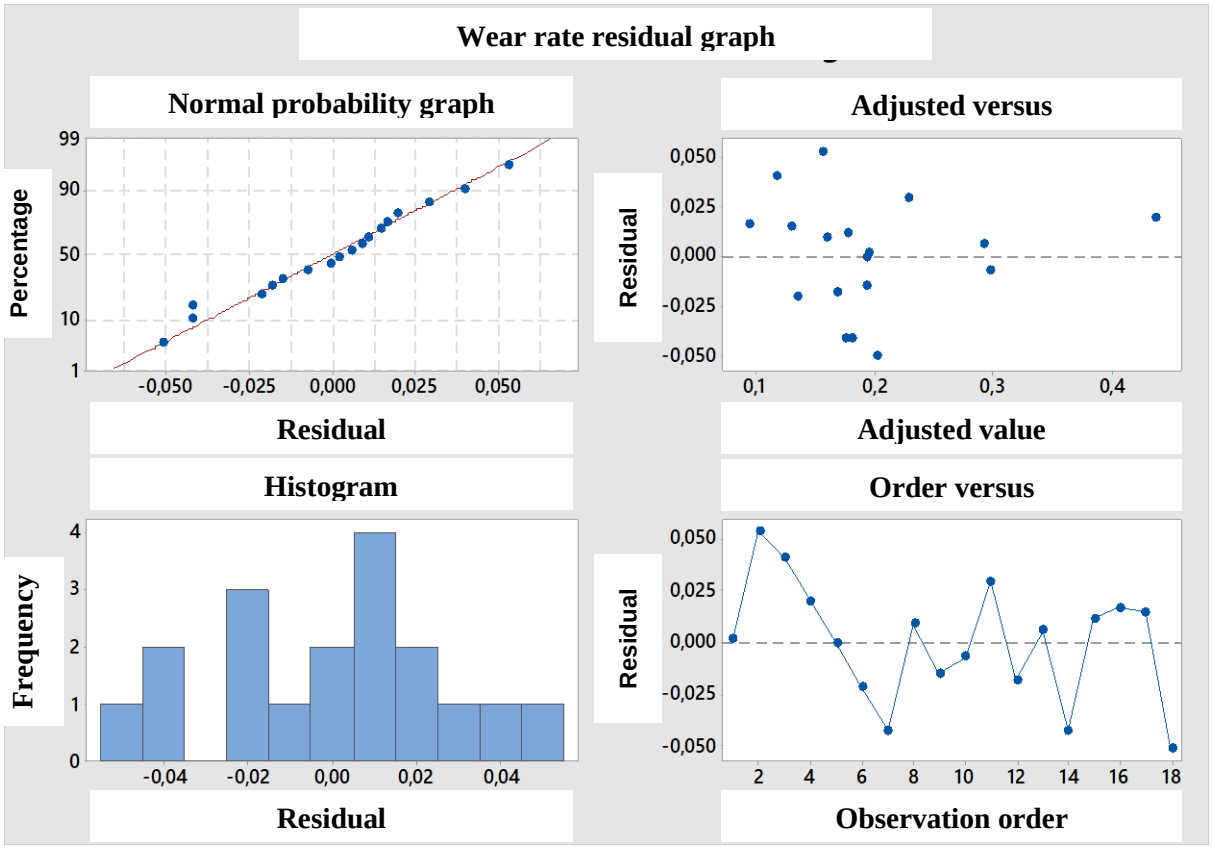

APPENDIX B – Criteria for normality, homoscedasticity and Independence of the residual for equation 17

Figure 104 – Tests for analysis of confirmation of normality, homoscedasticity and Independence of the residues of equation 17

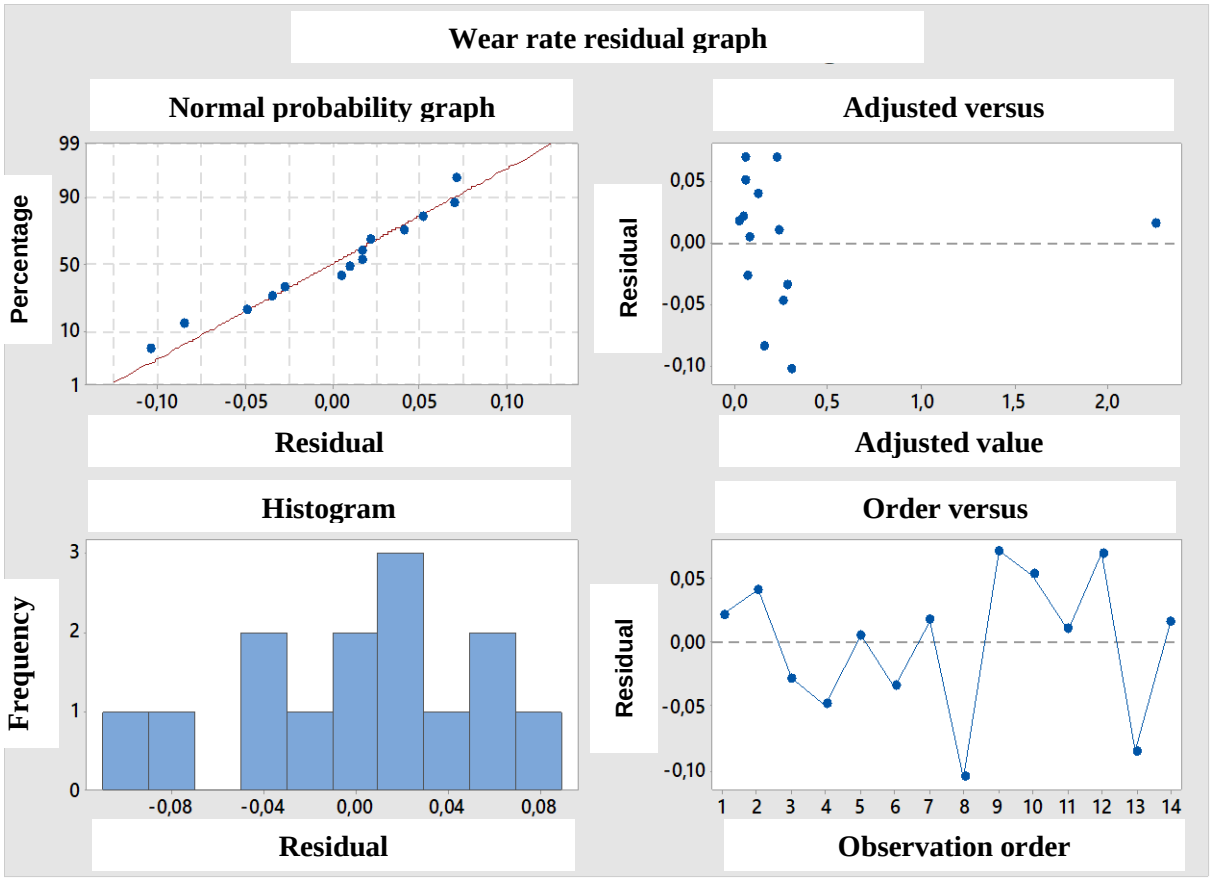

APPENDIX C – Criteria for normality, homoscedasticity and independence of the residual equation 18

Figura 105 – Tests for analysis of confirmation of normality, homoscedasticity and Independence of the residues of equation 18

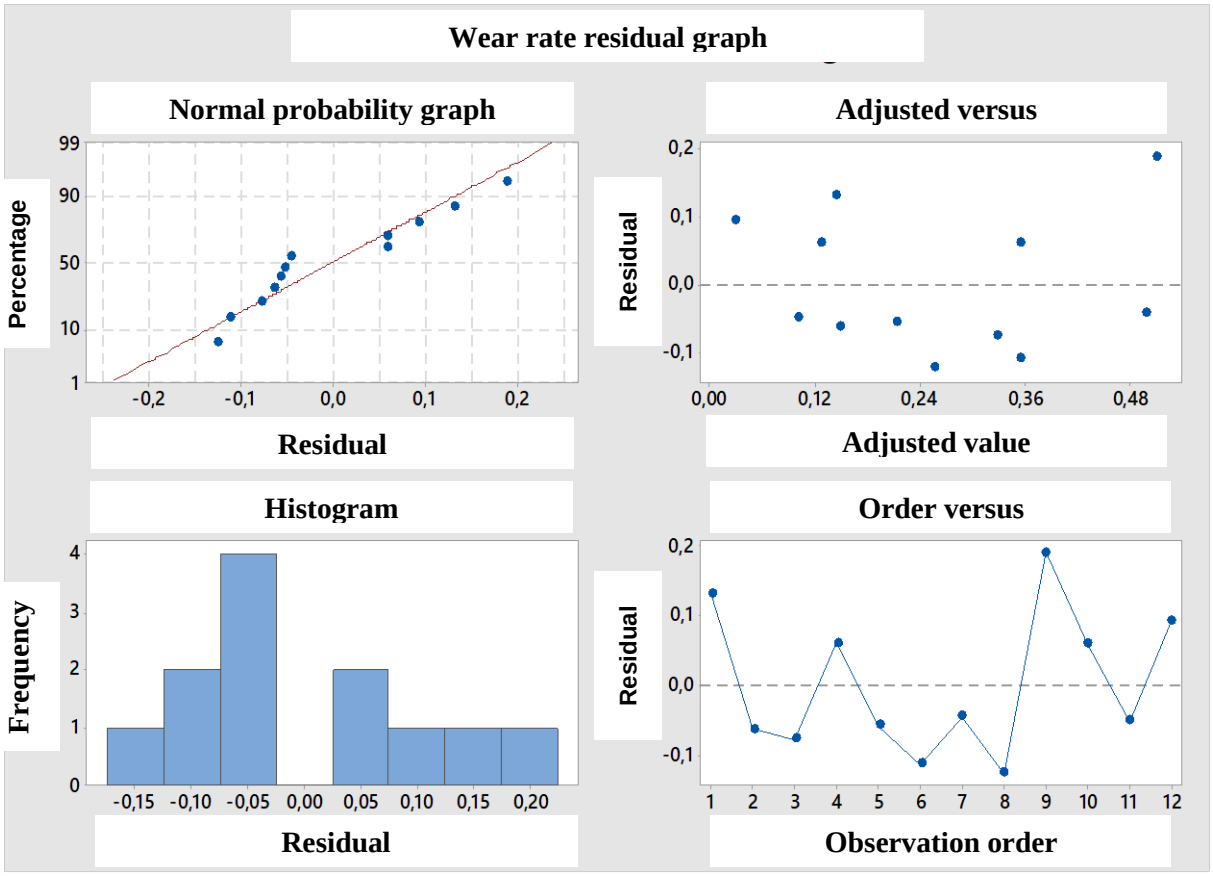

APPENDIX D – Criteria for normality, homoscedasticity and independence of the residual equation 19

Figure 106 – Tests for analysis of confirmation of normality, homoscedasticity and Independence of the residues of equation 19

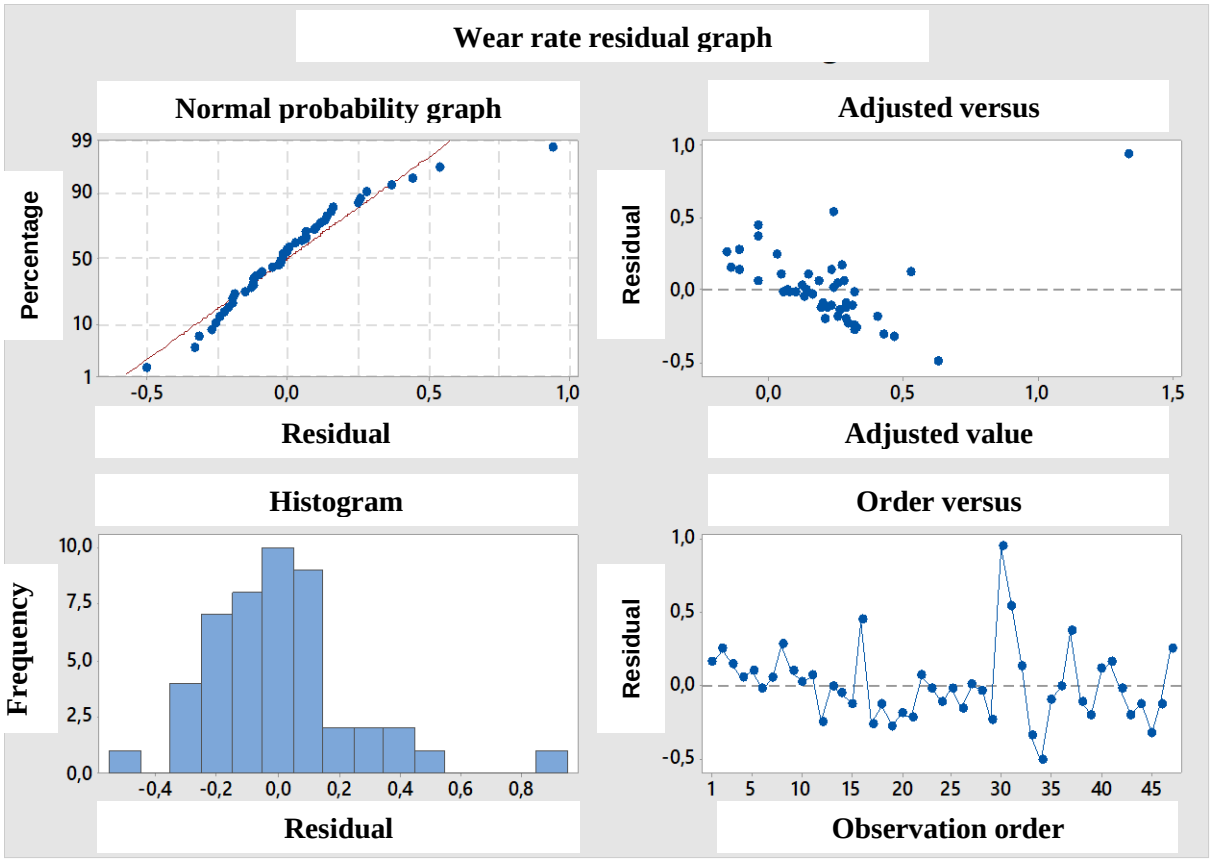

APPENDIX E – Process variables analyzed and Criteria for choosing

Table 23 – Variables analyzed

Variable	Unid.	Variable	Unid.
Lime	Kg/t.steel	Carbon end blow	Pts.
Calcined dolomite	Kg/t.steel	Temperature end blow	°C
Raw dolomite	Kg/t.steel	Oxidation end blow	ppm
Nepheline	Kg/t.steel	Slag MgO	%
Quartz	Kg/t.steel	Slag FeO	%
Sinter FeO	Kg/t.steel	Slag CaO	%
Scrap charged	%	Slag SiO_2	%
Pig iron charged	%	Binary Basicity	-
Steel returned	%	Reblow	%
Silicon in pig iron	Pts.	Slag Splashing	%
Heats with Manganese > 100 pts.	(%) %	Slag Coating	%
Process time	min.	Slag Splashing/Coating material	Kg/t.steel
Tapping time	min.	Ultra low carbon heats	%
Steel average tapping	t.	Dephosphorization rate	%
Steel type	-	Oxygen of the reblow	Nm^3

Souce: Own Authorship.

Table 24 – Criteria and tests for choosing the main relevant process variables with the refractory wear rate for the models described in this thesis

Criteria and tests
Pearson Correlation
Correlation Matrix
Time Series
Stepwise estimation, Forward addition and backward elimination

Souce: Own Authorship.